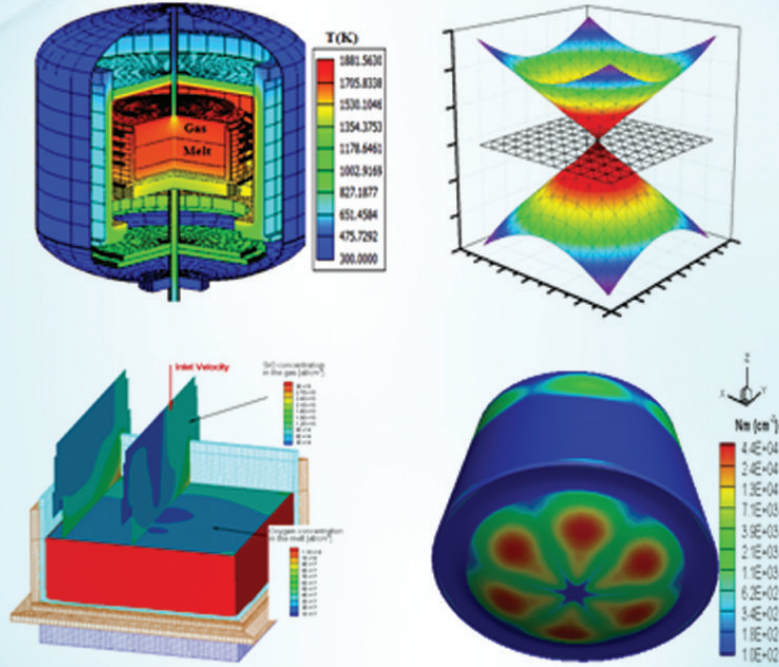


International Symposium on Modeling of Crystal Growth Processes and Devices

பழக வளர்ச்சி நிகழ்வுகள், சாதனங்கள் மீதான
மாதிரி உருவாக்கம் பற்றிய பன்னாட்டு கருத்தரங்கம்

[MCGPD - 2019]
26-28, February, 2019

SSN



Organized by

SSN Research Centre

SSN College of Engineering, SSN Institutions
Kalavakkam, Chennai – 603110, Tamil Nadu, India

In association with

**Indian Association for Crystal Growth, Indian Science and Technology Association
International Organization for Crystal Growth**



INTERNATIONAL SYMPOSIUM ON
Modeling of Crystal Growth Processes and Devices

படிக வளர்ச்சி நிகழ்வுகள், சாதனங்கள் மீதான மாதிரி உருவாக்கம்
பற்றிய பன்னாட்டு கருத்தரங்கம்

[MCGPD - 2019]

26-28, February, 2019



எண்ணித் துணிக கருமம் துணிந்தபின்
எண்ணுவம் என்பது இடிக்கு

(குறள்: 467)

Organized by

SSN Research Centre
SSN College of Engineering, SSN Institutions
Kalavakkam, Chennai – 603110, Tamil Nadu, India

In association with

Indian Association for Crystal Growth, Indian Science and Technology Association
International Organization for Crystal Growth





Ms. Kala Vijayakumar

President, SSN Institutions

Message

I am immensely pleased to know that the SSN Research Centre, SSN Institutions in association with the International organization for crystal growth, Indian association for crystal growth and Indian science and technology association is organizing the International Symposium on “**Modeling of Crystal Growth Processes and Devices (MCGPD-2019)**” during February 26-28, 2019.

A computer solution of a problem gives detailed and complete information. It can provide the values of all the relevant variables throughout the domain of interest. In a theoretical calculation, realistic conditions can be simulated. For a computer program, there is little difficulty in having very large or very small dimensions, in treating very low or very high temperatures, in handling toxic or flammable substances, or in following very fast or very slow processes.

This three day International Symposium is highly beneficial for the researchers who are working in the field of modeling and simulation of various crystal growth processes, semiconductor devices, NLO and Piezoelectric devices. The ultimate goal of the symposium is to give a basic understanding for the young researchers to explore the advance developments of modeling on crystal growth processes and devices, to evolve guidelines for their further research. The symposium includes Keynote/ Invited lectures by eminent experts from foreign and Indian institutions, poster and oral presentations from the researchers.

I would like to congratulate the Chairman of symposium **Prof. P. Ramasamy**, Convener **Dr. M. Srinivasan** and organizing committee of MCGPD-2019. I am sure all the delegates will find the programme immensely useful.

I wish the Symposium a grand success.



Dr. S. Salivahanan
Principal, SSN College of Engineering
salivahanans@ssn.edu.in

MESSAGE

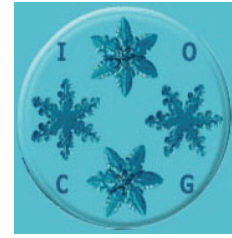
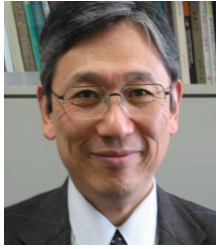
I am delighted that SSN Research Centre of our college is organizing an International Symposium on Modeling of Crystal Growth Processes and Devices (MCGPD-2019) during February 26-28, 2019.

This symposium will establish an effective platform for researchers, students from various institutions and industries from national and international laboratories to share their ideas and to present their latest achievements in the field. This activity is attracting great attention in the field of science and engineering due to ever increasing demand for materials with improved operational capabilities applicable in the fields of energy, defence, space, consumer electronics etc. I hope that the outcome of this symposium will constitute a significant contribution to the knowledge in these areas.

I thank DST-SERB and CSIR, Government of India for granting financial support. I congratulate the Convener, International and National Advisory Board Members and the local organizing committee for their excellent arrangements in conducting the symposium successfully.

I extend my cordial welcome to all the distinguished invitees, plenary speakers, invited speakers and the delegates and wish them a very fruitful time and pleasant stay at SSN College of Engineering.

I wish the symposium a grand success.



Prof. Koichi Kakimoto

President

International Organization for Crystal Growth

Feb. 15 2019

On behalf of the International Organization for Crystal Growth (IOCG), I am honored to share the knowledge and idea regarding crystal growth based on modeling at the International Symposium on Modeling of Crystal Growth Processes and Devices to be held at SSN Research center, SSN College of Engineering of Chennai, India from 26 to 28 February 2019.

Activity of crystal growth in India is really remarkable. One of the most active centers in India and worldwide is Anna University where Prof. Dr. P. Ramasamy's group is performing an excellent activity on crystal growth. Nowadays, the modeling is going to open up a new world of crystal growth. The performance of numerical modeling is going to be much more attractive to experimentalists of crystal growth since the accuracy is increasing and the model can predict some phenomena, quantitatively. Therefore, it is worth to organize the International Symposium on Modeling of Crystal Growth Processes and Devices which will provide sessions for presentation and discussion regarding recent research and development activities in all aspects of crystal growth. The symposium will provide a nice chance to exchange idea and knowledge on modeling of crystal growth processes and devices

Finally, I really appreciate the members of organizing committee for their enthusiastic support on the conference. I believe all of the participants should enjoy the symposium.

Sincerely yours,

A black rectangular box containing a white, handwritten signature that reads "K. Kakimoto". The signature is written in a cursive, flowing style.

Koichi KAKIMOTO



Prof.P.RAMASAMY
President

Indian Association for Crystal Growth (IACG)

Office: Dean (Research)
SSN College of Engineering
Chennai-603110, Tamilnadu, INDIA
Telephone : +91-9283105760
Fax : +91-044-27475166
Email: ramasamp@ssn.edu.in

Prof. P. RAMASAMY
Former Vice Chancellor, Alagappa University,
Karaikudi, Tamilnadu
Founder Director, Crystal Growth Centre, Anna University
Chennai, Tamilnadu



MESSAGE

I am happy that SSN Research Centre, SSN Institutions, Chennai is organizing an International Symposium on “**Modeling of Crystal Growth Processes and Devices (MCGPD-2019)**” during February 26-28, 2019. This symposium would involve active participation and healthy discussions among pioneering researchers, in the field of modeling and simulation in material science. I am sure the eminent resource persons with their wide experience will be able to provide a new impetus to the budding researchers. I am confident that this would give them a good platform for exchange of ideas.

To be a successful lifetime researcher one must ensure, all the time, an updated knowledge of the current developments in their chosen field. This necessitates, among other things, participation in serious Scientific Conferences. Physical participation in conferences creates lasting interests, impressions and new bonds of friendship and networking which potentially are stronger and are likely to last longer. I understand that there are various lectures and contributed papers from international and national researchers. Though organizing a symposium of this nature is a huge task, the rich experience of organizers will certainly ensure successful conduct of the programme.

I congratulate the Convener of this symposium **Dr. M. Srinivasan**, and organizing committee of **MCGPD-2019** for their dedicated work in making this event a great success. Several distinguished speakers from various countries are attending this symposium and I am sure all the delegates will be benefitted by the deliberations in the symposium. I wish the MCGPD-2019 a grand success. **Dr. M. Srinivasan** is planning to organize **MCGPD** as a regular event in the future years. I wish him good luck.

P.RAMASAMY



Prof. R. Jayavel

President

Indian Science and Technology Association

MESSAGE

Modeling on Material science is a diverse field of research in modern science and technology which plays an important role in various fields like Electronics, Medicine, Biotechnology, Energy, Crystallography, Spectroscopy, Information and Communication Technology. Especially, the modeling of various crystal growth process and devices are the current emerging fields and it is believed that it will bring a wave of radical innovation and will spark new industrial revolution in various application areas.

I am very happy to know that SSN Research Centre, SSN Institutions is organizing an **International Symposium on Modeling of Crystal Growth Processes and Devices (MCGPD-2019)** during February 26-28, 2019. The aim of organizing such a symposium will provide a platform for knowledge dissemination and knowledge sharing. I hope the participants would be very much benefited out of this event by getting the details of recent developments in the field of modeling on crystal growth.

I congratulate the convener **Dr. M. Srinivasan** and organizing committee for the untiring work to organize the symposium in a successful manner. Also I would like to thank the management motivation and cooperation to organize the symposium in a grand manner.

Prof. R. Jayavel

President



Dr. M. Srinivasan

Convener, MCGPD-2019

Message

Warm Greeting!

I am very glad that our SSN Research Centre is organizing an **International Symposium on Modeling of Crystal Growth Processes and Devices (MCGPD-2019) during 26-28, February 2019**. Our research centre has recorded consistent improvement in research activities by publishing research work of various fields in highly reputed international journals and obtaining grants from various funding agencies to carry out research. We took initiative to start the modeling activities on silicon growth and DSSC's years ago in SSN Research centre. Modeling and experimental mc-Si growth lab are established with good facilities in SSN RC. Several Ph.D. scholars and scientists are currently working in the field of modeling mc-Si growth process and are getting good results

The main motive of the symposium is to bring together eminent researchers across the world to share their ideas and recent developments in the field of modeling on Crystal Growth, Material Science, Nanoscience and Technology.

I would like to thank Scientific and Technical Committee for their untiring support for conducting this symposium. I convey my sincere thanks to IACG, IOCG, ISTA and STR group for their support and I would also like to thank DST-SERB and CSIR, Government of India, for sanction of financial support. I thank International and National Advisory Board Members and our local organizing committee for their excellent arrangements in conducting the symposium.

I specially thank my great Guru, **Prof. P. Ramasamy**, President, IACG for his extraordinary support for developing modeling activities in the field of crystal growth and material science in our country. I warmly thank **Prof. Kochi Kakimoto**, President IOCG for his guidance to build the overall international organizing committee and for associating IOCG with us. Finally, I would like to thank in special way **Mrs. Kala Vijayakumar**, President and **Dr. S. Salivahanan**, Principal, SSN Institutions for all the cooperation to organize the symposium in a smooth manner.

I am sure that all the distinguished invitees, delegates and scholars will definitely benefit from the academic deliberations with tremendous ideas and visions during this three day symposium. I hope you all will enjoy the visit and I am sure that you all will have a pleasant stay with us.

Organizing Committee	Scientific Advisory Committee
<p><u>Chief Patron</u> Dr. Shiv Nadar, <i>HCL Technologies</i></p> <p><u>Patron</u> Mrs. Kala Vijayakumar, <i>President, SSN Institutions</i></p> <p>Dr. S. Salivahanan, <i>Principal, SSN Institutions</i></p> <p><u>Chairman</u> Dr. P. Ramasamy, <i>Dean(Research), SSN Institutions</i></p> <p><u>Convener</u> Dr. M. Srinivasan</p> <p><u>Organizing Secretaries</u> Dr. P. Balaji Bhargav Dr. Muthu Senthil Pandian Dr. K. Aravinth Dr. R. Govindaraj Dr. S. Kotteswaran Mr. Nafis Ahmed Mr. C. Balaji</p> <p><u>Organizing Members</u> Dr. A. Rajalakshmi Dr. R. Srinivasan Dr. B. S. Sreeja Dr. Prita Nair Mr. S. Singaravadivelu Dr. S.M.M. Kennedy Dr. N.P. Rajesh Dr. Julie Charles Dr. G. Anandhababu Dr. P. Rajesh Dr. A. Chandrasekaran Dr. P. Nagapandi Selvi</p>	<p>Dr. Koichi Kakimoto, Kyushu University, Japan Dr. Jeffrey J. Derby, University of Minnesota, USA Dr. Noritaka Usami, Nagoya University, Japan Dr. T. Duffar, Universite Grenoble - Alpes INP, France Dr. Mathis Plapp, Ecole Polytechnique, France Dr. Daniel Vizman, West University of Timisoara, Romania Dr. Jyh- Chen Chen, National Central University, Taiwan Dr. Vladimir Kalaev, STR Group, Inc. Russia Dr. Kolandaivel, Periyar University, Salem Dr. M. Kurt, Ahi Evran University, Turkey Dr. Liliana Braescu, Matelligence Inc., Canada Dr. Wolfram Miller, IKZ, Germany Dr. Robert Menzal, IKZ, Germany Dr. Yasuhiro Hayakawa, Suizuoka University, Japan Dr. A. K. Barua, IEST, India Dr. M. H. Tavakoli, Bu-Ali Sina University, Iran Dr. A.V. Kulik, STR Group, Inc. Russia Dr. Vikram Kumar, IIT Delhi, India Dr. Roberto Fornari, University of Parma, Italy Dr. Kentaro Kutsukake, Nagoya University, Japan Dr. Kensaku Maeda, Tohoku University, Japan Dr. K. Kalyanasundaram, SFIT, Switzerland Dr. R. K. Bhandari, IUAC, India Dr. R. Jayavel, Anna University, India Dr. Jiban Podder, BUET, Bangladesh Dr. Prapun Manyum, Suranaree Uni & Tech, Thailand Dr. Ajayan Vinu, University of South Australia, Australia Dr. Anupam Diwan, IIT Delhi, India Dr. John V. Kennedy, MacDiarmid Institute, New Zealand Dr. S. Gunasekaran, St. Peter's University, India Dr. S. Ganesamoorthy, IGCAR, India Dr. RV. Mangalaraja, University of Concepcion, Chile Dr. Sharat Chandra, IGCAR, Kalpakkam, India Dr. R. Sumathi, Ludwig-Maximilians-University, Germany Dr. R. Vidya, Anna University, Chennai Dr. Palash Kumar Mollick, BARC, India Dr. D. Velmurugan, University of Madras, Chennai Dr. Rita John, University of Madras, Chennai Dr. D. Mohit Tyagi, BARC, Mumbai Dr. Anurag Srivastava, ABV-IITM, Gwalior Dr. M. Arivanandhan, Anna University, Chennai Dr. P. Ravindran, CUTN, Thiruvarur Dr. A. Shashwati Sen, BARC, Mumbai Dr. P. Murugan, CSIR-CECRI, Karaikudi Dr. N. Vijayan, National Physical Laboratory, New Delhi Dr. Ashraf Ali, NIT Surathkal, India</p>

"Lifetime Achievement Award-2018"

(by ISTA-Elavenil)

Awardees



Prof. P. T. Manoharan

DST Ramana Fellow
Founder and Head
SAIF, IIT Madras, Chennai-25
(Former Vice Chancellor
University of Madras)



Prof. V. Devanathan

Founder and Head
Department of Nuclear Physics
University of Madras, Chennai-25
(Former President
The Academy of Sciences, Chennai)

Hearty Congratulations!

PROGRAMME SCHEDULE

International Symposium on Modeling of Crystal Growth Processes and Devices

26 - 28 February 2019

SSN Research Centre, SSN College of Engineering, SSN Institutions (Autonomous)

[Venue - Main Auditorium]

Registration: 8.30 am to 9.30 am

Day - 1 (26.02.2019)

Talk	Time	Speakers name	Institution
Inaugural function		9.30 am to 10.45 am	
Tea Break		10.45 am to 11.00 am	
Chair Person: Prof. Daniel Vizman, West University of Timisoara, Romania			
Keynote lecture-1	11.00 am to 12.00 noon	Prof. Koichi Kakimoto	Kyushu University, Japan
Plenary lecture-1	12.00 noon to 12.50 pm	Prof. Mathis Plapp	Ecole Polytechnique , France
Plenary lecture-2	12.50 pm to 1.40 pm	Prof. P. Ramasamy	SSN Institutions, Chennai, India
Lunch		1.40pm to 2.30 pm	
Chair Person: Prof. R. Jayavel, Anna University, Chennai, India			
Invited lecture-1	2.30 pm to 03.10 pm	Dr. Asharaf Ali	NIT Surathkal, India
Invited lecture-2	3.10 pm to 3.50 pm	Dr. Vladimir Kalaev	STR Group, Inc. Russia
Tea Break		3. 50 pm to 4.10 pm	
Chair Person: Prof. Rita John, University of Madras, Chennai, India			
Invited lecture-3	4.10 pm to 4.50 pm	Dr. Madhav Ranganathan	IIT Kanpur, India
Invited lecture-4	4.50 pm to 5.30pm	Prof. Binay Kumar	University of Delhi, New Delhi, India
Poster Presentation (PP-01 to PP-139)		5.30 pm to 06.30 pm	
Oral presentation (OP-1to OP-5)		06.30 pm to 07.00 pm	
Cultural Programme		7.00 pm to 8.00 pm	
Dinner		08.00 pm to 09.00 pm	

Day - 2 (27.02.2019)

Venue: Mini Auditorium

Talk	Time	Speakers name	Institution
Oral Presentation - 08.30 am to 09.30 am (OP 05 to OP-10)			
Chair Person: Prof. Koichi Kakimoto, Japan			
Plenary lecture-3	9.30 am to 10.20 am	Prof. Jyh- Chen Chen	National Central University, Taiwan
Plenary lecture-4	10.20 am to 11.10 am	Prof. Daniel Vizman	West University of Timisoara, Romania
Tea Break		11.10 am to 11.30 am	
Chair Person: Prof. Mathis Plapp, <i>Ecole Polytechnique</i> , France			
Invited lecture-5	11.30 am to 12.10 am	Dr. A.V. Kulik	STR Group, Inc. Russia
Invited lecture-6	12.10 pm to 12.50 pm	Prof. Rita John	University of Madras, Chennai, India
Invited lecture-7	12.50 pm to 1.30 pm	Dr. Kentaro Kutsukake	RIKEN, Japan
Lunch		1.30pm to 2.15 pm	
Chair Person: Prof. Jyh- Chen Chen, National Central University, Taiwan			
Invited lecture-8	2.10 pm to 2.50 pm	Prof. P. Ravindran	CUTN, Thiruvavur, India
Invited lecture-9	2.50 pm to 03.30 pm	Dr. Robert Menzal	IKZ, Germany
Invited lecture-10	3.30 pm to 4.10 pm	Dr. R. Vidya	Anna University, Chennai, India
Tea Break		04.10 pm to 4.20 pm	
Chair Person: Dr. K. Gunasekaran, University of Madras, Chennai, India			
Invited lecture-11	4.20 pm to 5.00 pm	Dr. Sharat Chandra	IGCAR, Kalpakkam, India
Invited lecture-12	5.00 pm to 5.40 pm	Dr. Anandh Subramanian	IIT Kanpur, India
Invited lecture-13	5.40 pm to 6.15 pm	Dr. R. Navamadhavan	VIT Institutions, Chennai, India
Oral Presentation(OP-11 to OP-25)			06.15pm to 8.00pm
Dinner 08.00 pm to 09.00 pm			

Day - 3 (28.02.2019)

Venue: Mini Auditorium

Talk	Time	Speakers name	Institution
Chair Person: Prof. P. Ramasamy, SSN Institutions, Chennai, India			
Plenary lecture-5	9.00 am to 9.50 am	Dr. K. Gunasekaran	University of Madras, Chennai, India
Invited lecture-14	9.50 am to 10.30 am	Dr. Kesaku Maeda	Tohoku University, Japan
Tea Break		10.30 am to 10.50 am	
Chair Person: Dr. M. Arivanadhan, Anna University, Chennai, India			
Invited lecture-15	10.50 am to 11.30 am	Dr. Palash Kumar Mollick	BARC, Mumbai, India
Invited lecture-16	11.30 am to 12.10 pm	Dr. P. Murugan	CSIR-CECRI, Karaikudi, India
Invited lecture-17	12.10 pm to 12.50 pm	Dr. C. Meganathan	CIPET, Chennai India
Oral Presentation (OP-26 to OP-30) 12.50 pm to 01.30 pm			
Lunch		1.30 pm to 2.15 pm	
Chair Person: Dr. R. Srinivasan, SSN Institutions, Chennai, India			
Invited lecture-18	2.15 pm to 2.45 pm	Dr. P. Srinivasan	CNC, Erode, India
Invited lecture-19	2.45 pm to 3.15 pm	Dr. M. Prasath	PG Ex., Centre, Periyar Univ., India
Plenary lecture-6	3.15 pm to 4.15 pm	Dr. V. Subaramaniyan	CSIR-CLRI, Chennai, India
Tea Break		4.15 pm to 4.30pm	
VALEDICTORY FUNCTION			

S.No.	Keynote Lecture	Page. No
KL-1	Collaboration of Numerical and Experimental studies on Crystal Growth Processes <i>Koichi Kakimoto</i>	1
	Plenary Lectures	
PL-1	Modeling of Solidification and Microstructure Evolution Using the Phase-Field Method <i>Mathis Plapp</i>	3
PL-2	Computational and Experimental Investigation of mc-Si Crystal Growth for PV applications <i>M. Srinivasan & P. Ramasamy</i>	5
PL-3	Numerical Simulation of the Oxygen Concentration Distribution in the Silicon Melt During Czochralski Crystal Growth <i>Jyh-Chen Chen, Thi Hoai Thu Nguyen</i>	8
PL-4	Three Dimensional Modeling of Melt Convection in Solar Silicon Grown By Czochralski and Direct Solidification Methods <i>Vizman Daniel</i>	11
PL-5	Molecular Dynamics Simulation (Cost and Time Effective drug development strategy) <i>Krishnasamy Gunasekaran</i>	14
PL-6	Computational Studies on the Design and Development of Carbon based Novel Two-Dimensional Dirac Materials <i>Dr. V. Subramanian</i>	16
	Invited Lectures	
IT-1	Numerical Investigation of Hydrodynamics and Crystal Growth in a Pilot-Scale Batch Crystallizer <i>Dr. B. Ashraf Ali</i>	17
IT-2	Turbulent Heat and Mass Transfer during Cz & Ds Si Crystal Growth for Solar Cells <i>V. Kalaev, V. Artemyev, D. Borisov, A. Vorob'ev, A. Kuliev, E. Bystrova, S. Smirnov</i>	23
IT-3	Quantum Dot Formation in Silicon-Germanium Thin Films on Patterned Silicon substrates <i>Gopal Krishna Dixit, Monika Dhankhar and Madhav Ranganathan</i>	28
IT-4	New Geometrical Modeling for Crystal Morphology <i>Prof. Binay Kumar</i>	30
IT-5	Modeling of Vapor-Phase Growth of Wide Bandgap Bulk Crystals and Epilayers <i>A.V. Kulik</i>	31
IT-6	Quaternary Heusler alloys for Spintronic Applications – A first principle study <i>Rita John and Namitha Anna Koshi</i>	36
IT-7	Generation and Propagation of Dislocations In Multicrystalline Silicon for Solar Cell <i>Kentaro Kutsukake, Yusuke Hayama, Tetsuya Matsumoto, Hiroaki Kudo, Tatsuya Yokoi, Yutaka Ohno, and Noritaka Usami</i>	38
IT-8	Develop Functional Materials for Energy Harvesting From Ab Initio Calculations <i>P.Ravindran</i>	40
IT-9	Numerical Simulation of the Float Zone Process for Silicon: Comparison of Modeling Approaches In COMSOL Multiphysics <i>Robert Menzel, and Kaspars Dadzis</i>	46
IT-10	Theoretical Prediction of Materials for Bio-Implant Applications <i>Dr. R. Vidya</i>	50
IT-11	Development of Interatomic Potentials for Molecular Dynamics Simulations Using Density Functional Theory <i>Sharat Chandra</i>	52
IT-12	Liquid like Nucleation in Nanoscale Thin Films <i>Pooja Rani, Arun Kumar, B. Vishwanadh, Kawsar Ali, A. Arya, R. Tewari and Anandh Subramaniam</i>	54
IT-13	Nanomechanical Properties of Wide Bandgap Semiconductors: Experimental and Theoretical Perspective <i>R. Navamathavan</i>	27
IT-14	Formation mechanism of twin boundary and fabrication of periodically-twinned structure in borate crystal <i>Kensaku Maeda, Kozo Fujiwara, Satoshi Uda</i>	59
IT-15	Role of Thermal Hydraulics on the Crystal Growth by Chemical Vapor Deposition <i>P. K. Mollick and M. Krishnan</i>	61

IT-16	Understanding Structural Stability and Electronic Properties of Carbon Based Nanocomposites for Lithium Ion Battery Applications by First Principles Density Functional Calculations <i>P. Murugan</i>	64
IT-17	Single Crystal, Spectral and Electronic Transition Studies on (E)-N-(3-Ethoxy-4-Hydroxybenzylidene)-4-Nitrobenzohydrazide <i>C Meganathan S. Subaschandrabose</i>	66
IT-18	Modelling for Organic Solids via <i>Ab Initio</i> Crystal Structure Predication and Quantum Chemical Methods <i>P. Srinivasan and A. David stephen</i>	67
IT-19	Designing Potent Inhibitors of Influenza a Virus - A Quantum Chemical and Spectroscopic Study <i>M. Prasath</i>	69

Oral Presentations

S. No.	Title & Authors	Page No.
OP-1	Surface Stress and Surface Reconstruction: an Abinitio Study on the Polar Gan (0001) Surface <i>Razia and Madhav Ranganathan</i>	71
OP-2	Influence of additional Heat Exchanger Block on Directional Solidification System for growing Good Quality multi-crystalline Silicon Ingot – A Simulation Investigation <i>Nagarajan S G, Srinivasan M and Ramasamy P</i>	72
OP-3	Coupled Growth of Tin-Zinc Eutectic Crystals during Directional Solidification and Influence of Solid-Solid Interface Anisotropy in Morphological Evolution <i>Aramanda Shanmukha Kiran, Salapaka Sai Kiran, Kamano Chattopadhyay and Abhik Choudhury</i>	72
OP-4	Heteroepitaxial Quantum Dots on Patterned Substrates <i>Monika Dhankhar and Madhav Ranganathan</i>	73
OP-5	Phase Field Modeling of Microstructure Evolution in Sn-Zn Eutectic Alloy under Directional Solidification Conditions <i>Sumeet Khanna, Abhik Choudhury</i>	74
OP-6	Growth and Characterization of L-Tartaric Acid Lead Acetate Single Crystals <i>Jagadeesh M. R, Suresh Kumar H. M</i>	75
OP-7	Synthesis, Theoretical And Docking Studies, Antibacterial Activities Of Hydrazone Derivative <i>K. Ananthi, Dr. H. Anandalakshmi Dr. S. Senthilkumar</i>	75
OP-8	Investigation of Electron Density, Impact Sensitivity and Electrostatic Properties of Highly Energetic Benzoxadiazol Derivatives via DFT and AIM Analysis <i>L. Sathya, P. Srinivasan, B. Gnanavel and A. David Stephen</i>	76
OP-9	Effect of Crucible Dimension in the Directional Solidification Process <i>G. Aravindan, M. Srinivasan and P. Ramasamy</i>	76
OP-10	Quantum Chemical and Docking Studies on Piperidine Derivatives via DFT and Autodock Methods <i>P. Periyanna¹, P. Srinivasan, A. David Stephen and K. Ravichandran</i>	77
OP-11	Atoms in Molecule Analysis and Third-Order Nonlinear Optical Absorption Properties of Guanidinium 4-nitrobenzoate <i>Sasikala V., D. Sajan</i>	78
OP-12	The Electrical Conductivity of Methylene-Methyliminomethyl Formamidine Molecular Nanowire via DFT and QTAIM Theory <i>S. Palanisamy, P. Jayalakshmi, P. Srinivasan, A. David Stephen and K. Selvaraju</i>	79
OP-13	Theoretical Investigation of Electrical and Optical Properties of Sodium Succinate Hexahydrate (B Phase) Single Crystal: A Potential Third Order NLO Material <i>S. Anitha, P. S. Latha Mageshwari, R. Priya</i>	80
OP-14	Performance Analysis of Hybrid Bulk Junctionless Transistors Using Numerical Simulation <i>A. Nisha Justeena and R. Srinivasan</i>	81
OP-15	Band Gap Engineering of Cu₂-II-IV-VI₄ Quaternary Semiconductors Using PBE-GGA, TB-mBJ and mBJ+U Potentials. <i>J. Bhavani, Rita John</i>	82
OP-16	Engineering Sub Wavelength Scale 3D Focal Structures Using Annular Walsh Filter <i>D. Thiruarul, K. B. Rajesh</i>	82

OP-17	Effect of Heat Exchanger Block Thickness on Grown Multi-Crystalline Silicon Ingot by Directional Solidification Process <i>M. Thiyagarajan, S.G. Nagarajan, M.Srinivasan, and P. Ramasamy</i>	83
OP-18	First Principles Calculation on the Electronic and Optical Properties of AA-Stacked Two-Dimensional Graphene, Silicene, Germanene, and Stanene <i>Benita Merlin and Rita John</i>	84
OP-19	Liquid like Nucleation in Nanoscale Thin Films <i>Pooja Rani , Arun Kumar , B. Vishwanadh , Kawsar Ali , A. Arya , R. Tewari and Anandh Subramaniam</i>	84
OP-20	Effect of Zinc Sulphate on Growth, Characterisation and Applications of L Lysine Single Crystals <i>P. Sagunthala, P.Yasotha</i>	86
OP-21	Structural and Spectroscopic (Ft-Ir, ¹³c and ¹h Nmr) Investigation, Molecular Orbital Calculation and Nlo Properties of Novel Piperidine Derivative By Quantum Chemical Calculation <i>Akumtoshi Aier,P. Samuel Asirvatham, M. Krishna Priya, T. Ramila, B. K. Revathi</i>	86
OP-22	Spectral Investigations (FT-IR, FT-Raman, UV-Visible), NBO, NLO, Molecular geometry, Mulliken charges, HOMO-LUMO, MEP calculations of 1-[(2R, 4S, 5S)-4-azido-5-(hydroxyl methyl) oxolan-2-yl]-5-methylpyrimidine-2, 4-dione [1] by DFT method <i>Thanmayalaxmi. D, Suvitha. A, Ravishankar. K,</i>	87
OP-23	Modification on Coumarin Based Groups toward for Highly Efficient organic Dye-Sensitized Solar Cells: A DFT Study <i>A. Arunkumar and P. M. Anbarasan</i>	88
OP-24	Single-Crystal Neutron Diffraction Study of the Strong O-H...O Hydrogen Bond in 2-picolinic perchloric acid <i>R.S. Arun Raj, D.Sajan, Rajul Ranjan Choudhury and R. Chitra</i>	88
OP-25	Effect of Spin-Orbit Coupling in Topological Insulator Bi2se3 Using Dft as a Tool <i>Umamaheshwari M & Rita John</i>	89
OP-26	Experimental and Theoretical Investigation of Structural and Magnetic Properties of YbFe₂As₂ Crystal <i>S. Santhosh Raj, P. Iyyappa Rajan, Nilotpal Ghosh, S. Mahalakshmi, R. Navamathavan</i>	89
OP-27	Population Balance Modelling of Crystal Growth Behaviour in A Batch Crystallizer <i>Lister H Falleiro, B. Ashraf Ali</i>	91
OP-28	Vibrational (FTIR & FT-Raman spectra), electronic (UV-vis) analysis and molecular docking evaluation of Mangiferin in neuraminidase enzyme using DFT stimulations <i>B. Sathya and M. Prasath</i>	92
OP-29	Intermolecular interaction, charge density distribution and electrostatic properties of Kaempferol in the active site of AChE via docking and quantum chemical calculations. <i>Azhagesan, Dr. Kumaradhas Poomani</i>	93
OP-30	Optical and Spectral Characterization of Tartaric Acid Doped Lsmh Crystal <i>Anithalakshmi M, Robert R</i>	93

Poster Presentations

PP-1	Heater Modification on Directional Solidification System by Numerical Investigation <i>G. Anbu, M. Srinivasan and P. Ramasamy</i>	95
PP-2	Physical properties of tin chalcogenide crystals for solar cell applications <i>A G Kunjomana and Bibin John</i>	95
PP-3	Exploring the Structure, Electron density and HOMO-LUMO analysis of Tetrathiafulvalene (TTF) molecule (Superconducting) via DFT and AIM analysis <i>P. Gnanamozi, V. Pandiyan, A. David Stephen and P. Srinivasan</i>	96
PP-4	Effect of shock waves on dielectric properties of KDP crystal <i>A.Sivakumar, S.A.Martin Britto Dhas</i>	97
PP-5	Applications of Nanofluids in Heat Pipe Solar Collector - A Review <i>N. Jayanthi, M. Venkatesh and R. Suresh Kumar</i>	97
PP-6	Growth and Characterization of a Promising NLO 2,4- dinitrophenylhydrazone Crystal <i>R. Gnanadeepam A. Senthil</i>	98
PP-7	Experimental and theoretical investigation on piperazinium hexachloro stannous trihydrate single crystal for second harmonic generation applications <i>Radhakrishnan Anbarasan and Jeyaperumal Kalyana Sundar</i>	98

PP-8	Theoretical with Experimental Comparison of Optical and Electrochemical Properties on Ethyl-2-Cyano 3-(4-(Dimethylamino) Phenyl) Acrylate Single Crystal <i>S. Kotteswaran and P. Ramasamy</i>	99
PP-9	Synthesis and Characterization of Cds Quantum Dots (Qds) Using Fruit Extract As an Organic Capping Agent <i>K. Kandasamy, M. Venkatesh, S.P. Rajasingh</i>	99
PP-10	Growth and Characterisation of Pure and L-Methionine doped Sulphamic Acid single crystal <i>M.Selvapandiyan and J.Arumugam</i>	100
PP-11	Numerical Investigation on mc-silicon Growth Process for Photovoltaic Applications <i>V. Kesavan, M. Srinivasan and P. Ramasamy</i>	101
PP-12	Numerical Simulation of Reduction in thermal Stress Maxima of CZ Grown Silicon Crystal <i>M. Avinash Kumar, M. Srinivasan, P. Ramasamy</i>	101
PP-13	Structural, Optical and Dielectrical Properties of Chalcone Derivative Crystal Grown by VASR Technique. <i>N.Madhavan, S.A. Martin Britto Dhas</i>	102
PP-14	The Structural and Magnetic Properties of Gadolinium Doped Of Nickel Nanoferrite Using Microwave Combustion Method <i>K. Poovarasu, M. Vanitha Sri and M. Venkatesh</i>	103
PP-15	Microwave Assisted Combustion Synthesis and Characterization of Nickel Ferrite Nanoplatelets Doped Effects on Rare-Earth Ions <i>D. Koushika, M. Vanitha Sri and M. Venkatesh</i>	103
PP-16	Growth and Characterization of L Lysine Added Single Crystals <i>P.Yasothea, P.Sagunthala</i>	104
PP-17	Reduction of Oxygen Impurities by Titanium Carbide heat exchanger block and retort in mc-Silicon: Numerical modelling <i>M. Vishnuwaran, M. Srinivasan, V. Kesavan, and P.Ramasamy</i>	105
PP-18	Photocatalytic Performance of the Biologically Synthesized Titanium dioxide (TiO₂) Nanoparticles using Lemon Leaf Extract <i>Vishali D, Manikandan B, K R Murali and Rita John</i>	105
PP-19	Role of Copper Chloride on the Growth, Optical and Antibacterial Properties of Γ-Glycine Single Crystal <i>V.Vijayalakshmi and P.Dhanasekaran</i>	106
PP-20	Vibrational Spectroscopy (FT-IR and FT-R) Investigation and Computational (DFT) Analysis on the Structure of 2,7 dihydroxy Naphthalene <i>M. Vennila, R. Rathikha, S. Muthu, A. Senthil</i>	106
PP-21	Spectroscopic investigation, FT-IR, FT-Raman, HOMO -LUMO and natural bond orbital analysis on 4-(2-Hydroxyethyl)morpholine <i>K. venkateswaran, M. Karnan and R. Muthukumar, K. venkateswaran</i>	107
PP-22	Defects Investigation Probed by Powder X – Ray Diffraction Technique on Pure and Doped Transition Metal Vanadate <i>P. Vasantha Kumar and S. Rajashabala</i>	107
PP-23	Molecular engineering on carbazole donor based metal-free organic dyes for dye sensitized solar cells <i>V. Mohankumar, P. Pounraj, M. Senthil Pandian, P. Ramasamy</i>	108
PP-24	Synthesis, Growth, Structural and Optical Characterization of the Organic Nonlinear Optical Thiosemicarbazide 5- Sulfosalicylate (T5ss) Single Crystals <i>R.Usha, D.Jayalakshmi</i>	109
PP-25	Generation of Ultra-Long Pure Magnetization Needle by Azimuthally Polarized Beam with a Ternary Optical Element <i>M.Udhayakumar, K.Prabakaran, K.B. Rajesh,</i>	109
PP-26	An Investigation on Thermal Diffusivity and Dielectrical Properties of Sulfanilic Acid Nonlinear Optical Single Crystal <i>J. Thirupathy, S.A. Martin Britto Dhas</i>	110
PP-27	Crystallographic and Computational Studies on N-Acetylglycine Single Crystal <i>V.J.Thanigaiarasu, N.Kanagathara, M.K.Marchewka</i>	110
PP-28	Heterogeneous Nucleation and Vapor Growth of Antimony Telluride Crystals <i>Thankamma George, Ajayakumar C J and A G Kunjomana</i>	111
PP-29	Synthesis of Perfect Cusnzr Cubic Thin Film by Simple Successive Ionic Layer Adsorption and Reaction Method <i>M. Balaji, T.R.K. Priyadarzini, R. Daphine</i>	111

PP-30	Structural and Optical Characterization of Potassium Bromide Doped L-Histidine Single Crystal <i>Sweatha.L, Robert. R</i>	112
PP-31	X-Ray and NMR Spectral Investigation, DFT Calculations, Molecular Dynamics, Physicochemical Descriptors, ADME Parameters, Pharmacokinetic Bioactivity Report On 1-[(2R, 4S, 5S)-4-Azido-5-(Hydroxyl Methyl) Oxolan-2-Yl]-5-Methylpyrimidine-2, 4-Dione [1] <i>Suvitha. A, Thanmayalaxmi. D, Ravishankar. K,</i>	113
PP-32	Controlled Growth of Hydroxyapatite Micro/Nanostructures Using Edta Under Microwave Irradiation <i>G. Suresh Kumar, E.K. Girija</i>	114
PP-33	Spectral Investigation of FT-IR, FT-Raman, UV-Visible and NMR studies of 4-Methoxyphenylboronic acid using DFT method <i>S.Sundari and S.Chandra</i>	115
PP-34	Imine Based Propeller-Shaped Architectural Macrocyclic Synthons. <i>S.Sriam, Suresh Madhu, D.Velmurugan, Gunasekaran G. J. Sanjayan</i>	115
PP-35	Hubbard -U – A correction to DFT A comparative study on the Electronic structure of FeO using LDA and GGA With & without Hubbard- U <i>Singaravelan T R and Rita John</i>	116
PP-36	Investigation on the Synthesis, Growth and Physicochemical Properties of Creatininium Nitrate Single Crystal for Third Order Synthesis and Characterization of Semi-Organic Nonlinear Optical Material: Potassium Doped Sodium Para-Nitrophenolate Crystal <i>Sindhusha S, Padma C M</i>	117
PP-37	Enhancement in SHG, LDT and Thermal Properties Of Zn²⁺ Doped L-Alanine Acetate (LAA) Single Crystals <i>Silviya M, Robert R</i>	117
PP-38	Crystal growth and optical studies on lithium hydrogen oxalate monohydrate single crystal <i>Senthilkumar Chandran P. Ramasamy</i>	118
PP-39	Unidirectional growth of <100> Directed Sodium Di (L-Malato) Borate Single Crystal and Its Characterization <i>A.Senthil, and P. Ramasamy</i>	119
PP-40	Structural Analysis of 1,3 Diamino Propane With Arsenic Acid Complex <i>K.Senthil Kumar, N.Kanagathara, G.Anbalagan, M.K.Marchewka</i>	119
PP-41	Synthesis and Characterization of Semi-Organic Nonlinear Optical Material: Potassium Doped Sodium Para-Nitrophenolate Crystal <i>M. Selvapandiyan and R. Sathyanarayanan</i>	120
PP-42	Different characterizations of silver aluminium oxide thin films by spray pyrolysis technique <i>Dr.P. Saritha</i>	120
PP-43	Morphology and Size Controlled Synthesis of Zinc Oxide Nanostructures <i>T. Saravanan, G. Suresh Kumar, E.K. Girija</i>	121
PP-44	Experimental and Theoretical Investigation of Structural and Magnetic Properties of YbFe₂As₂ Crystal <i>S. Santhosh Raj, P. Iyyappa Rajan, Nilotpal Ghosh, S. Mahalakshmi, R. Navamathavan</i>	122
PP-45	Growth, Optical, Thermal and Third-order Non-linear optical properties of Potassium Trihydrogen Succinate: A potential material with Self-defocusing Applications <i>P.S. Latha Mageshwari, A.Chamundeeswari, S. Jerome Das</i>	123
PP-46	Bio Synthesis and Characterization of CuO NanoParticles using from ulva fasciata algae extract <i>S.Ravi, R.Balasubramanian, B.Rajamannan and R.Selvaraju</i>	124
PP-47	Molecular Docking Studies and Density Functional Theory of Some Novel Ethyl 5-(1-Methyl-1H-Tetrazol-5-Ylthio)-4-Oxo-2,6-Substituted Diphenylpiperidine-3-Carboxylate Derivatives <i>S. Ranjith and P. Sugumar</i>	124
PP-48	Mechanical and Dielectrical Properties of Dyes Doped Kdp Crystals for NLO Applications <i>S.Rajeshkumar, P.Kumaresan</i>	125
PP-49	Studies of Urea Doped 4-Nitrobenzoyl Chloride Single Crystal <i>R. Raja, S. Kanimozhi, S. Sudha, V.K. Mohanapriya, S.Kanimozhi</i>	126
PP-50	Growth and Characterization of Dicoumarole Derivative Crystal <i>S. K. Parmar, H. K. Gohil, A. R. Zinzuvadia, S. D. Hadiyal, P. M. Vyas and A. H. Patel</i>	126
PP-51	Bulk Growth Of 3,4 – Diamino Benzophenone By Micro-Tube Czochralski Method <i>S. Usharani, J.Judes, V. Natarajan, M. Arivanandhan</i>	127

PP-52	Investigation on Growth and Characteristics Glycine Sodium Fluoride (GSF) For Optoelectronic Applications <i>R. Ravisankar, R. Vijayakumar, N.Harikrishnan, G.Senthilkumar D. Rajendiran, J.Chandramohan</i>	128
PP-53	Crystal Growth and Characterization of Glycine Potassium Iodide (GPI) For Nonlinear Optical Applications <i>R. Ravisankar, D. Rajendiran, R. Vijayakumar, P. Jayaprakash, K.M. Freny Joy</i>	128
PP-54	Structure and Intermolecular Interactions of Some Benzodiazepine Derivative Molecules with GABA-A Receptor: A Molecular Docking and Quantum Chemical Analysis <i>M. Prasath , B. Sathya and M. Ramaraj</i>	129
PP-55	Synthesis, Structure Elucidation Of A New Chalcone Derivative <i>T. Ramila, B.K. Revathi, M. Krishna Priya, AkumToshi Aier,P. Samuel Asirvatham</i>	130
PP-56	Observation of Carbon Related New Donors in Cz-Silicon in the Temperature Range 450 °c to 510 °c Based On Ftir <i>Rajeev Singh , P. B. Nagabalsubramanian</i>	130
PP-57	Mechanical Behaviour of Benzimidazole Derivative Single Crystals <i>M. Rajalakshmi and R. Indirajith</i>	131
PP-58	Growth and Characterization of Piperazine Doped Adipic Acid Single Crystal <i>R. Raja , S. Kanimozhi</i>	132
PP-59	Synthesis, Characterization and Application of Nickel Doped Zn Nanocrystals for the Photocatalytic Degradation of Textile Dyeing Effluent <i>P. Logamani, R. Rajeswari, G. Poongodi</i>	132
PP-60	Synthesis, Growth, Spectral and Optical Properties of L-Alaninium P- Hydroxybenzoate Nonlinear Optical Single Crystal <i>G. Parvathy, R. Kaliammal, K. Velsankar, S. Sudhahar</i>	133
PP-61	Synthesis Growth Structural Spectroscopic and Optical Properties of L-Lysine Monohydro Chloride Ammonium Chloride Non Linear Optical Single Crystals <i>R.Ragavendiran, M. Selvapandiyam, C. Govindaraj</i>	134
PP-62	Thermal and Spectroscopic Analysis of Idol Making Rocks <i>R.Jayaprakash, P.Rajkumar, S.Rajesh kumar</i>	134
PP-63	Comparative DFT Study and Vibrational Spectra of Hemiterpenes: A Study on A- And B-Furoic Acid Dimers <i>P.Rajkumar, S.Selvaraj, R.Suganya, D.Velmurugan, S.Gunasekaran, S.Kumaresan</i>	135
PP-64	Organic solids via <i>ab initio</i> crystal structure predication and DFT Investigation <i>P. Srinivasan and A. David stephen</i>	135
PP-65	Computational, Spectral And Structural Studies Of A New Organic NLO Crystal: 2-Amino 5-Methyl Pyridinium Succinate For Nonlinear Optical Applications <i>S. Nithya, B. Chandra Shekar, K.R. Aranganayagam, K. Boopathi</i>	136
PP-66	Sensitivity Enhancement of Copper with the Use of Transition Metal Dichalcogenides (Tmdcs) In Surface Plasmon Resonance Biosensor <i>A. Nisha, P.M. Anbarasan, P.Maheswari, K.B. Rajesh</i>	137
PP-67	Screening Effect Of Various Acceptor Groups In The Perylenemonoimide Based D- Π -A Architecture Of Dye Sensitized Solar Cells: A Theoretical Study <i>M. Prasath and D. Nicksonsebastin</i>	137
PP-68	Synthesis, Growth, Structure, Characterization and Anti Microbial Activities of L-Isoleucinium-P-Toluenesulfonate Monohydrate (Liptsa) <i>Dr. P.Nagapandiselvi and Dr. M. Muralidharan</i>	138
PP-69	Structural, Vibrational, Electronic and Molecular docking dynamics of 2-benzyloxy 3-methoxybenzaldehyde – An experimental and quantum approach <i>P.B.Nagabalasubramanian^d, K. Manivannane T. Prabu, S. Periandy, Rajeev Singh</i>	138
PP-70	Synthesis and Spectroscopic Investigation of 4-(Benzylideneamino) Benzenesulfonamide <i>R.Muthukumar, M. Karnan and K.Venkateswaran, R.Muthukumar</i>	139
PP-71	Growth, Structure and Characterization of NLO Active 4-Methylpyridinium Picrate <i>S. Sivaraman, R. Markkandan, R. Selvaraju and SP. Meenakshisundaram</i>	140
PP-72	Crystal growth, spectral, optical, thermal analysis and DFT study of the organic single crystal <i>M. Manikandan, P. Rajesh, P. Ramasamy</i>	140
PP-73	Growth and Characterization of Alanine Doped Urea Thiourea Magnesium Chloride (Autmc) Single Crystals <i>P.Malliga</i>	141

PP-74	Sensitivity Enhancement Of Surface Plasmon Resonance Optical Biosensor Based On Graphene Structure With Nanocomposite Layer <i>P.Maheswari, V.Ravi, A.Nisha, K.B.Rajesh</i>	142
PP-75	Crystal Growth, Structural, Vibrational, Optical, Thermal and Mechanical Properties of Semi Organic Piperazinium Tetrachlorozincate Monohydrate(PTCZ) Single Crystal <i>M. Magesh, P. Karuppasamy, M. Senthil Pandian, P. Ramasamy</i>	143
PP-76	Structural, Optical and Dielectrical Properties of Chalcone Derivative Crystal Grown by VASR Technique. <i>N.Madhavan, S.A. Martin Britto Dhas</i>	144
PP-77	Correlation between Magnetization and Cell Volume in Mn²⁺ Substituted Copper Ferrite <i>M. Balaji</i>	144
PP-78	Growth of high quality organic single crystal by rotational SR – a novel method <i>P. Karuppasamy, T. Kamalesh, Muthu Senthil Pandian, P. Ramasamy, Sunil Verma</i>	145
PP-79	Structural, Morphological and Mechanical Properties of Doped Chalcogenide Materials <i>Karthikeyan R, Jeffrey Jose, Bibin John and Kunjomana A G</i>	146
PP-80	A Role of Temperature on the Properties of Lanthanum Oxide Nanoparticles by Reflux Routes <i>S. Karthikeyan, M. Selvapandiyan</i>	147
PP-81	Growth, Optical and Laser Damage Threshold Properties Of 4-Dimethylaminopyridinium 4-Nitrophenolate 4-Nitrophenol (Dmapnp) For Nlo Applications <i>T. Kamalesh P. Karuppasamy, Muthu Senthil Pandian, P. Ramasamy, Sunil Verma</i>	147
PP-82	Crystal Growth and Characterization of 2-Amino 6-Methylpyridinium 3,4 Dimethoxybenzoate Organic Nonlinear Optical Single Crystal <i>R.Kaliammal, G.Parvathy, G.Maheswaran, S.Sudhahar</i>	148
PP-83	Vibrational, NBO, Fukui Function, DOS, Thermodynamical and Molecular Docking Analyses of P-Chlorophenacyl Bromide Using Hartree Fock And B3LYP Methods <i>G. John James, Senthilkumar Chandran, M. Arivazhagan</i>	149
PP-84	Synthesis and Characterization of Ni_{0.5-x} Mg_xcu_{0.5} Fe₂o₄ Sintered Spinel Ferrite System <i>J.Jeyabunaveswari, Dr. S.Aravazhi</i>	150
PP-85	N-hexylcarbazole donor substituted triphenylamine compound based sensitizers for dye sensitized solar cells application - theoretical investigation <i>P. Pounraj, V. Mohankumar, M. Senthil Pandian, P. Ramasamy</i>	150
PP-86	Growth, Spectral, Optical, Thermal, Dielectric And Mechanical Studies On Urea Potassium Iodide Single Crystal <i>Hareeshkumar M. R., Jagadeesh M. R., G. J. Shankaramurthy</i>	151
PP-87	Growth and Characterization of Cadmium Doped Zinc Tris Thiourea Sulphate Crystal (Cd-ZTSC) by Gel Growth Technique <i>H. K. Gohil, S. K. Parmar, A. R. Zinzuvadia, P. M. Vyas and A. H. Patel</i>	151
PP-88	Identification of novel NAD (P) H dehydrogenase 1 antagonist using computational approaches <i>Rajendran Selvakumar, Anantha Krishnan Dhanabalan, D.Velmurugan and K.Gunasekaran</i>	152
PP-89	Identification of Novel inhibitors for BACE1 using Pharmacophore based Virtual screening and Molecular Dynamics <i>Anantha Krishnan, Manish Keshrwani, Krishnasamy Gunasekaran Devadasan Velmurugan</i>	153
PP-90	Investigation on 2-Methyl-5-(propan-2-yl) phenol an anticancer drug by Spectroscopic, invivo and Molecular Docking Dstudies <i>M.Govindammal, M.Prasath, S.Kamaraj</i>	154
PP-91	Growth and Characterization of Cadmium Doped Zinc Tris Thiourea Sulphate Crystal (Cd-ZTSC) by Gel Growth Technique <i>H. K. Gohil, S. K. Parmar, A. R. Zinzuvadia, P. M. Vyas and A. H. Patel</i>	155
PP-92	Studies on Growth, Optical and Mechanical Properties of Semi-Organic Crystal – Bis (Thiosemicarbazide-S, N) Zinc (II) Dinitrate <i>Redrothu Hanumantharao, S.Kalainathan</i>	155
PP-93	Synthesis, Spectral, DFT Studies on inorganic-organic hybrid material: Tetrabromo (piperazinium) zincate (II) (TBPZ) <i>K. Boopathi, K. Muthu Krishnan, K.R.Aranganayam, P.Ramsamy</i>	156
PP-94	The Effect of Angle Of Incidence on Photonic Band Gap in Lithium Niobate with Silver Composite Based One Dimensional Photonic Crystal <i>V.Doni Pon, K.S.Joseph Wilson</i>	157
PP-95	Studies on the Growth and Characterization of Organic 2-Amino-5-Nitropyridinium Dichloroacetate Non Linear Optical Single Crystal	158

	<i>David Willington T, Joema S E</i>	
PP-96	Enhanced Sensitivity of Cu-Mn Ferrite Gas Sensor By Incorporating SnO₂ Nanocomposites Towards Carbon Dioxide and Oxygen <i>M. Balaji , R. Daphine , T.R.K. Priyadarzini</i>	158
PP-97	Investigation of Anticorrosive and Antibacterial Efficacy of Copper Substituted Hydroxyapatite/Functionalized Multiwalled Carbon Nanotube Nanocomposite Fabricated 316L Stainless Steel <i>D. Sivaraj and K. Vijayalakshmi</i>	159
PP-98	Growth, Structural, Vibrational Analysis, Hirshfeld Surfaces, Quantum Chemical Studies, Uv-Vis Nir And Photoconductivity Studies Of The P- Toluidine P- Toluenesulfonate Single Crystal <i>S. Chinnasami, M. Manikandan, Senthilkumar Chandran, Rajesh Paulraj, P. Ramasamy</i>	159
PP-99	Structural and Optical Properties of Zn Doped TiO₂ Prepared by Sol-Gel Technique: For Photocatalysis and Dye Sensitized Solar Cell (DSSC) Applications. <i>B. Manikandan, K.R Murali and Rita John</i>	160
PP-100	Suitability of Drinking Ground Water Using Water Quality Index <i>Dr.B.Kavitha and Dr.S.Akilandeswari</i>	161
PP-101	DFT & TD-DFT Studies on 2,2'-Bipyridine-4,4'-Dicarboxylic Acid: Dye Sensitizers Solar Cell <i>B. Amudhavalli, M. Prasath and P. Srinivasan</i>	161
PP-102	Vibrational Spectroscopic Studies and Computational Study of 2,4-diamino-6-methyl-1,3,5-triazin-1-ium levulinate <i>K.Ayisha Begam, N.Kanagathara, G.Anbalagan, M.K.Marchewka</i>	162
PP-103	Growth, spectral, linear and nonlinear optical studies of a new Nitrophenol complex crystal <i>R. Durgadevi and T. Arumanayagam</i>	162
PP-104	Magneto-transport studies on p-type Sb₂Te₂Se Topological Insulators <i>Gopi Govindhan and Anandha babu Govindan</i>	163
PP-105	Unidirectional Growth and Characterization of Triphenylmethane Single Crystals for Scintillator Application <i>V. Govindan, D. Joseph Daniel, H. J. Kim, K. Sankaranarayanan</i>	164
PP-106	Structural, Optical and Thermal Properties Of Organic 4,4'- Dimethylbenzophenone (Dmbp) Single Crystal Grown by Bridgman – Stockbarger Method <i>K. Ramachandran, Arumugam Raja, V. Mohan Kumar, Muthu Senthil Pandian, P. Ramasamy</i>	164
PP-107	Spectroscopic analysis (FT-IR and FT-Raman), NBO analysis, HOMO-LUMO and molecular docking studies on Cetirizine using DFT Simulations <i>N. Mani and M. Prasath</i>	164
PP-108	Structural and Electrical properties of (1-x)Bi_{1/2}Na_{1/2}TiO₃-xBaTiO₃ Single Crystals Across the Morphotropic Phase Boundary by TSSG Method <i>M. William Carry, G. Gopi, G. Anandha Babu</i>	166
PP-109	One-step Synthesis and dual-luminescence Properties of Single Phase Fluoroperovskite KCaF₃:Eu³⁺ Phosphors for White Light Emitting Diode and dosimetry Applications <i>Arumugam Raja, R. Nagaraj, K. Ramachandran, P. Ramasamy</i>	167
PP-110	Synthesis, growth and Characterization of 2-amino-5-nitropyridine 4-chlorobenzoic acid (1:1): a new D-π-A type Organic Single Crystal for Third-order NLO Applications <i>V. Sivasubramani, Muthu Senthil Pandian, P. Ramasamy, G. Vinitha</i>	167
PP-111	Enhancement of the Growth Rate and Crystalline Perfection of Lithium Sulfate Monohydrate: An Efficient Negatively Soluble Piezoelectric Crystal <i>P. Rajesh, P. Ramasamy</i>	168
PP-112	Eu³⁺ Ions doped Boro-Phosphate Glasses for Photonic Applications <i>R. Nagaraj, K.Aravinth, P. Ramasamy, S. Ranjith</i>	169
PP-113	Nucleation kinetics, crystal growth and characterization of ADP: KDP (85:15) mixed crystals for nonlinear optical applications <i>Iyappan Gunasekaran , Rajesh Paulraj, Ramasamy Perumalsamy</i>	170
PP-114	Ceramic/ Polymer Bio-Composite for Load-Bearing Application <i>J. Mobika and M.Raj Kumar</i>	170
PP-115	Bulk Growth Of 3,4 – Diamino Benzophenone By Micro-Tube Czochralski Method <i>S. Usharani, J.Judes, V. Natarajan, M. Arivanandhan</i>	171
PP-116	Antibacterial Efficiency of Chitosan Incorporated HAP nanocomposite Synthesized by Simple Co-precipitation Method <i>L. Noor Ul Haq, K. Vijayalakshmi</i>	172
PP-117	Growth, Physicochemical and Quantum Chemical Investigations on Hexamethylene	172

	tetraminium Di-Malate – An Organic Crystal for Optoelectronic Device Applications <i>M. Saravanakumar and J. Chandrasekaran</i>	
PP-118	Structural and electrical properties of Lead-free (1-x) Na_{0.5} Bi_{0.5} TiO₃- xBaTiO₃ Solid Solutions <i>Rajesh Narayana Perumal , Venkatraj Athikesavan</i>	173
PP-119	Effect of crystallization of Calcium oxalate crystals in the industrial area water on living organisms <i>R.Selvaraju, B.Anitha, K.Anandalakshmi</i>	173
PP-120	First principles study of structural and electronic properties of half Heusler compounds ZrIrX (X= As, Sb and Bi) using GGA and TB-mBJ <i>R. Anubama, Rita John</i>	174
PP-121	Crystallographic, Spectroscopic and Hirshfeld Surface Analysis of Anilinium Arsenate <i>F.Mary Anjalin, N.Kanagathara, G.Anbalagan , M.K.Marchewka</i>	174
PP-122	Molecular Structure, Vibrational, Optical, Molecular Docking and Thermodynamics Properties of N, N-Dimethylnicotinamide <i>M. Arivazhagan, Senthilkumar Chandran</i>	175
PP-123	Crystal growth and characterization of glycine potassium Iodide (GPI) for NLO applications <i>R. Ravisankar, D. Rajendiran, R. Vijayakumar, P. Jayaprakash, K.M. Freny Joy</i>	176
PP-124	Molecular Structure and Electrostatic Properties of High Energetic 2,4,6-Trinitropyridine N-Oxide Molecule Via Quantum Chemical Calculations <i>L. Sathya, B. Gnanavel, A. David Stephen and P. Srinivasan</i>	176
PP-125	Abundant and Multifunctional Materials for the electrochemical storage device application <i>V. Vignesh, S. Bhagyashree, K. Subraman , M. Sathish, R. Navamathavan</i>	177
PP-126	Growth and Physical Investigation of AgIn_{0.5}Ga_{0.5}S₂ single crystal for Mid-IR Applications <i>N. Karunakaran and P. Ramasamy</i>	178
PP-127	Synthesis and characterization of Zn_{1-x}Mg_xO nanocrystals for thermoelectric applications <i>T.M.V.Muruguthiruvalluvan, V.Natarajan, M.Ramesh, S.Pari, R.Chandramohan P.Anandan, M.Arivanandhan,</i>	178
PP-128	Synthesis and Characterisation of Nanostructured Bi_xCo_{1-x}O Material for Thermoelectric Applications <i>S. Alagar Nedunchezian¹, D.Sidharth, N. Yalini Devi, R.Rajkumar, G.Anbalagan, M. Arivanandhan, R. Jayavel</i>	179
PP-129	Growth and Characterization of 4-Amino Benzophenone: A Promising Organic NLO Material <i>V. Natarajan, S. Usharani, M. Arivanandhan, P. Anandan, Y. Hayakawa</i>	180
PP-130	Comparitive Analysis of Synthesis and Electrochemical Characterizations of CeO₂/Rgo and CeO₂/Mos₂ Nanocomposites for Supercapacitor Application <i>M.Mohamed Ismail,P.Saraswathi devi, Prisilla Juliet, D.Mani, M. Arivanandhan</i>	180
PP-131	Theoretical, Biological and Insilico Studies of Pendant Armed Heteroleptic Nickel(Ii) Phenolate Complexes <i>P. Arthi, A. Kalilur Rahiman</i>	181
PP-132	Kinetic Studies on the Phase Transfer Catalysed Free Radical Polymerization of Alkyl Methacrylate <i>Yoganand. K. S,</i>	182
PP-133	Theoretical Investigations and Biological Studies of 4-Bromo-3-[N-(N-3,4dimethoxyphenyl)ethy l-N-methylsulfamoyl]-5-methyl benzoic acid monohydrate <i>R.Kavipriya, Helen P. Kavitha, C.Suneel Manohar Babu, Jasmine P.Vennila</i>	182
PP-134	Growth and Characterization with Molecular Modeling Studies of Benzotriazole Salicylic Acid <i>P.Sathya</i>	183
PP-135	An unconventional spin-glass transition in ordered hexagonal DyMnO₃ single crystals <i>P. Aravinth Kumar, G. Anandha Babu, S. Ganesamoorthy and P. Ramasamy</i>	184
PP-136	Crystal and Electronic Structure Studies on Transparent Conducting Nitrides A₃N₂ (A= Mg, Zn and Sn) and Sn₃N₄ <i>T. Premkumar and R. Vidya</i>	185
PP-137	Numerical Investigation on grown mc-Si Ingot for PV Applications <i>S. Sanmugavel, P. Ramasamy</i>	186
PP-138	Growth and Characterization of Xylenol orange tetrasodium salt added KAP single crystal <i>G. Babu Rao, P. Rajesh and P. Ramasamy,</i>	186
PP-139	Growth of 1D ZnO Nanorods on Flexible Substrate and their heterojunction properties <i>Ganesh Kumar K, Arokiyadoss Rayerfrancis, Balaji C, Nafis A, Balaji Bhargav P</i>	187

Keynote, Plenary and Invited Lectures

KL-1

Collaboration of Numerical and Experimental studies on Crystal Growth Processes

Koichi Kakimoto

Research Institute for Applied Mechanics, Kyushu University

*E-mail: kakimoto@riam.kyushu-u.ac.jp

Collaboration of numerical and experimental studies is opening up a new world to investigate the process of crystal growth, for example optimization of furnace structure and/or quantitative prediction of defect density in semiconductors. This lecture focuses on some examples on the communication between numerical and experimental studies on impurity transfer in silicon CZ process and dislocation density in SiC crystals in physical vapor transport (PVT) process.

Single-crystalline silicon (Si) obtained via Czochralski (CZ) crystal growth is the most widely used material for electronic and photovoltaic wafers owing to large-scale fabrication. Si crystals with long carrier lifetime are required for high-performance power devices and high-conversion-efficiency solar cells. The lifetime of CZ-Si crystal is affected by oxygen (O) precipitates and O- and/or C-related defects. Carbon (C) contamination had been reported to promote the O precipitates as the nucleation sites. C contamination could also degrade the characteristics of Si wafers via the formation of C-induced defects. Therefore, controlling C transport and reducing C contamination during the growth of Si crystals is important for the fabrication of wafers and various associated devices.

When the temperature of the quartz approaches the melting point of Si (1685 K), the quartz begins to soften and deform. In addition, because of a load of molten Si in the crucible, the crucible comes almost entirely into close contact with the inner shape of the susceptor supporting the crucible from the outside. Contact reactions between the crucible and the susceptor occur at high temperatures via the contact reaction process schematically shown in Fig. 1.

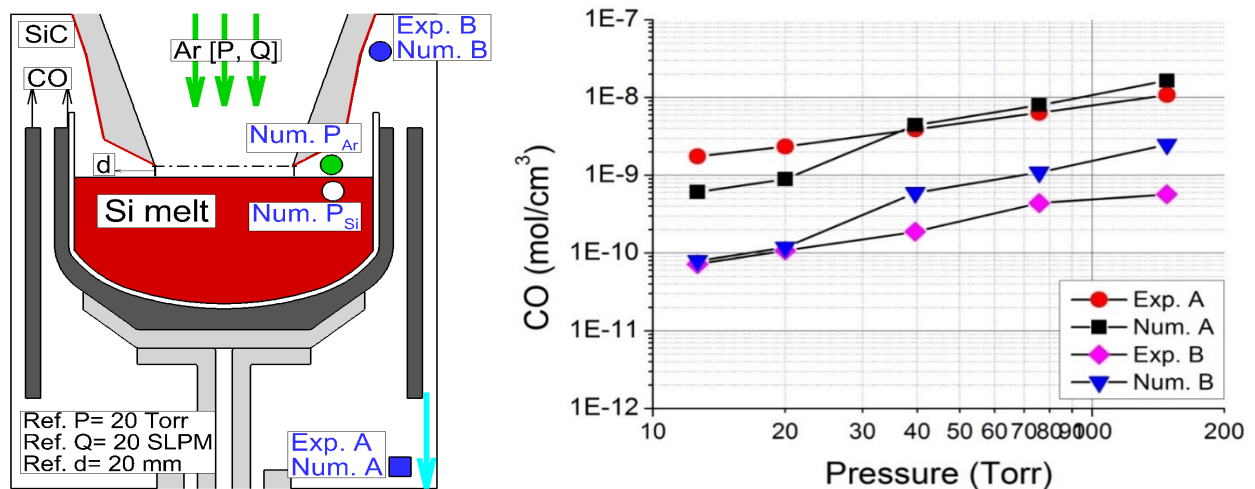


Fig. 1. Contact reaction between quartz crucible and graphite holder. Fig.2. CO conc. vs. pressure in a furnace.

The effect of furnace pressure on CO concentrations at different locations was investigated numerically and experimentally. A series of simulation and in-situ measurements in pressure ranges from 15 to 140 Torr was performed at a fixed flow rate of 20 SLPM and a fixed gap-width of 20mm. The concentrations of CO at the monitor A and B are plotted as a function of pressure in Fig. 2 for measurements and predictions.

Wide-bandgap silicon carbide (SiC) is a promising semiconductor material for electronic and optoelectronic devices involving high power, high temperature, high frequency, and intense radiation owing to its stable chemical and thermal properties. Bulk SiC crystals are commonly grown by the physical vapor transport (PVT) method. In bulk SiC crystal growth, significant progress has been achieved in reducing the most damaging defects: micropipes. From 2010 to 2013, researchers at Cree Inc. reduced the micropipe density (MPD) by 90% in 150-mm substrates.³ As the density of micropipes in SiC crystals has been suppressed to a technologically tolerable level, the quality improvement focus has shifted to less severely damaging defects such as dislocations.

The 3D BPD density at room temperature for the 10 h cooling time is shown in Figure 3. The crystal grows from the top to the bottom. The surface of the bottom of the crystal is slightly convex. The order of the BPD density at the bottom of the crystal is 10^4 cm^{-2} , and it shows 6-fold symmetry on the basal plane, which is consistent with the experimental data.

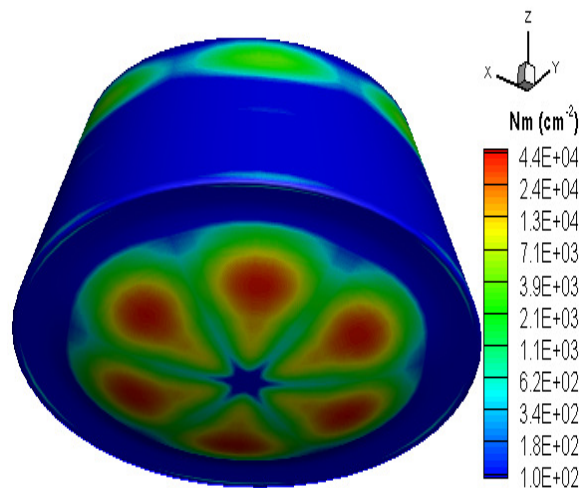


Fig. 3. 3D view of the BPD distribution at room temperature for 10 h cooling time.

PL-1

Modeling Of Solidification and Microstructure Evolution Using the Phase-Field Method

Mathis Plapp

Laboratoire de physique de la matière condensée, Ecole Polytechnique, CNRS, 91128 Palaiseau, France

*E-mail: mathis.plapp@polytechnique.fr,

The properties of a material are often largely influenced by its microstructure. Therefore, the prediction of the microstructure as a function of the processing conditions is an important task. Microstructures are generally formed out of equilibrium and result from spontaneous self-organization processes that involve moving interfaces and grain boundaries. A complete understanding of microstructure formation therefore requires to follow this complex interface dynamics and the resulting structure evolution. In recent years, the phase-field method has emerged as a method of choice for the numerical modelling of microstructure formation. It is based on phenomenological equations of out-of-equilibrium thermodynamics that are combined with free-energy functionals of Ginzburg-Landau type; interfaces are represented implicitly by profiles of suitable order parameters. Using relatively simple codes, microstructure evolution can be simulated qualitatively, and for some cases even quantitatively.

For metals and their alloys, the solid-liquid interfaces are usually microscopically rough. As a consequence, solidification microstructures are smooth and rounded, unlike the strongly faceted morphologies seen in many minerals and organic crystals. Nevertheless, the crystalline structure comes into play through the interfacial anisotropies that it induces. Although often small, this anisotropy plays an important role in many pattern formation processes during solidification. The phase-field method is ideally suited to capture and study such phenomena in numerical simulations.

In this presentation, I will first give an introduction to the principles of the phase-field method, taking as an example the dendritic crystallization of a pure melt, and then discuss several cases of alloy solidification in which the interfacial anisotropy plays a subtle but important role. In directional solidification of a dilute binary alloy, for processing parameters that put the crystallization front slightly above the threshold for morphological instability, arrays of smooth cells are formed. It is shown that the stability of such arrays crucially depends on the presence of crystalline anisotropy. The simulation results are in agreement with earlier calculations in two dimensions using the boundary-integral method, and with recent in situ experiments on transparent organic alloys. In directional solidification of eutectic alloys, a two-phase composite is formed through coupled growth. The morphologies that are most frequently observed are alternating lamellae (platelets) of the two phases, or rods of the minority phase inside a continuous matrix of the majority phase. Since more than fifty years, the Jackson-Hunt theory is the standard guide to the physics of such microstructures. However, if the underlying free-boundary problem with isotropic interfaces is numerically simulated, regular lamellar patterns never spontaneously arise. Moreover, other observations made in many experiments, such as the fact that lamellae often grow tilted with respect to the direction of the applied temperature gradient, are not explained by theories and models with isotropic interfaces. It was found in recent years that the anisotropy of the solid-solid (interphase) boundaries is decisive for the explanation of these phenomena. Although it comes into play only at the trijunction lines between the liquid and the two solid phases during solidification, it can govern the

organization of the entire pattern. This is directly demonstrated by three-dimensional phase-field simulations of directional solidification of eutectic alloys.

Finally, I will also discuss the possibility of modelling the growth of faceted crystals with the phase-field method. Facetting usually is created by strong interface anisotropies, often accompanied by singularities (cusps) in the surface free energy as a function of orientation. I will comment on several methods to include and regularize such singularities. In the particular case of molecular beam epitaxy in the step-flow regime, the moving steps can be treated with the help of the same mathematical tools as the moving interfaces and grain boundaries in solidification. This is demonstrated by phase-field simulations of spiral surface growth and meandering instabilities.

PL-2

Computational and Experimental Investigation of mc-Silicon Crystal Growth for PV Applications

M. Srinivasan & P. Ramasamy

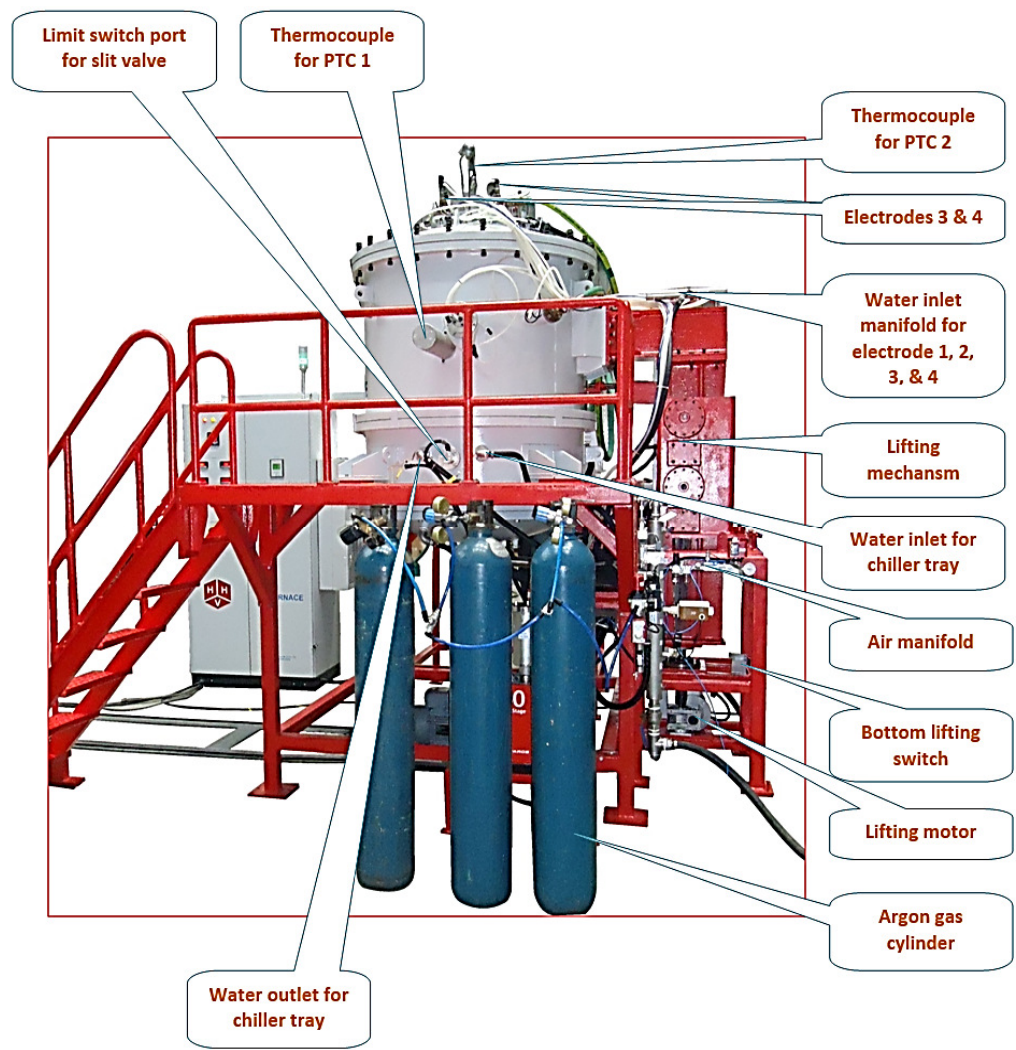
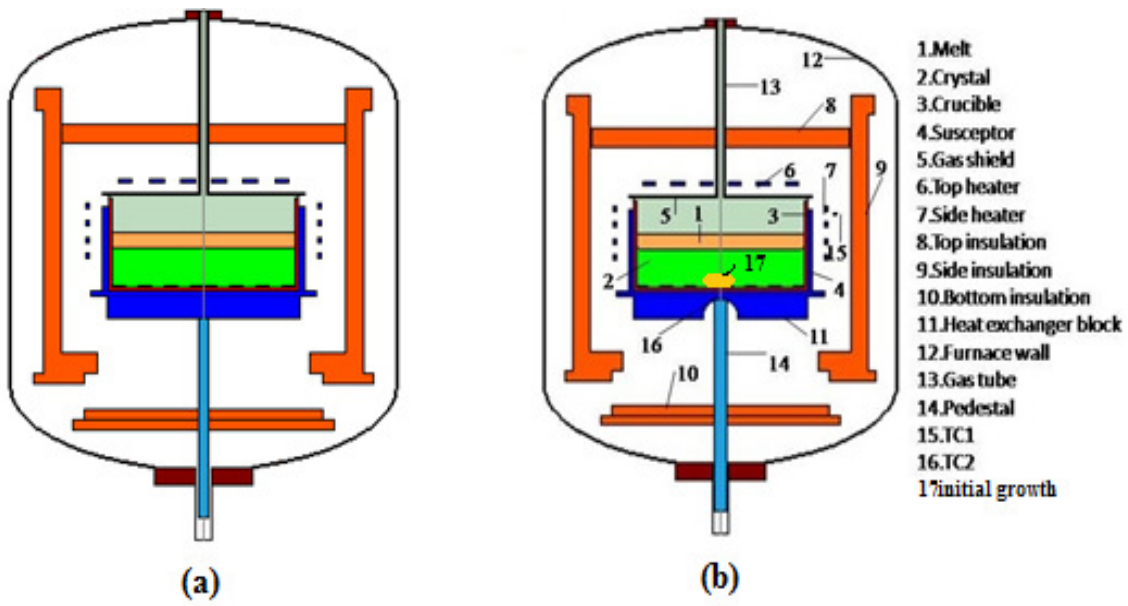
SSN Research centre, SSN College of engineering, Chennai-603110.

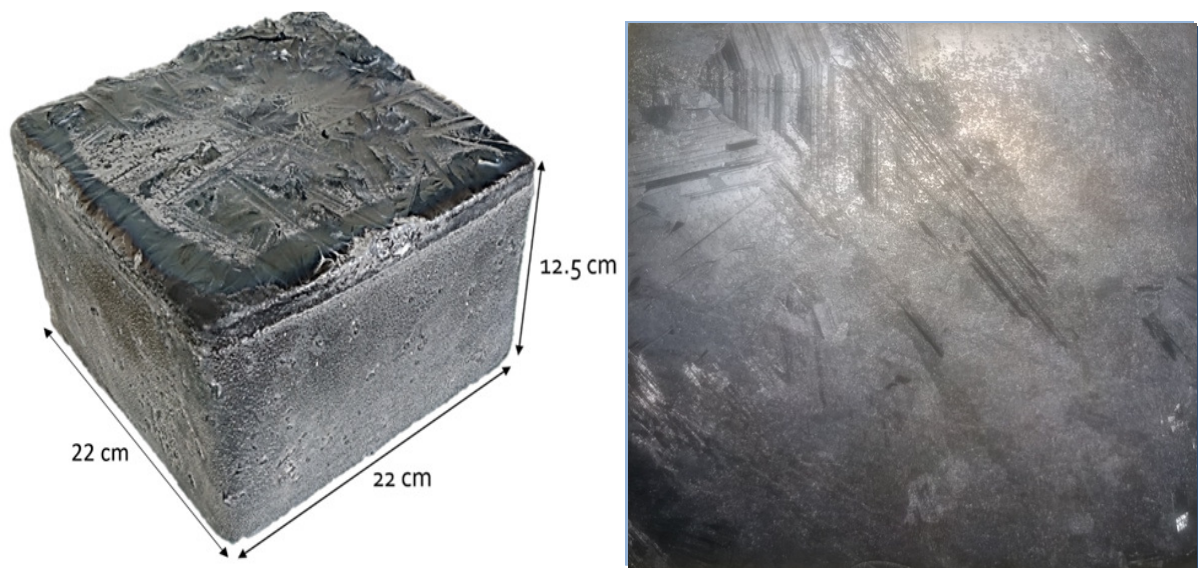
*Email :ramasamyp@ssn.edu.in

Among all the renewable energy sources, PV solar cell plays a major role[1]. Single crystal and multi- crystalline solar cells are considered as first generation solar cells. Thin film based solar cells are considered as second generation solar cells. Nano-crystalline based solar cells, dye-sensitized solar cells and concentrated solar cells are considered as third generation solar cells. There is lot of crystal growth in several of these solar cells.

Unlike silicon crystals used in the electronics industry, purity, crystal perfection and homogeneity need not necessarily be highest on the list of desirable attributes for crystalline silicon incorporated into commercial PV modules. The majority of PV solar cells are fabricated from bulk silicon crystals, which may be either single-crystalline or multi-crystalline. A market share of mono- and multi-crystalline silicon (mc-Si) are more than 90% at present and will be so in the foreseeable future[2]. Indian solar cell industries import silicon wafers and cells and convert them into solar modules. Today 98% of the silicon wafers imported into country are mc-silicon wafers and 2% wafers are single crystalline wafers. Single-crystalline wafers typically have better material parameters but are also more expensive which is grown by Czochralski(Cz) growth process. CZ wafers contain a large amount of oxygen in the silicon wafer. Oxygen impurities reduce the minority carrier lifetime in the solar cell, thus reducing the voltage, current and efficiency. In addition, the oxygen and complexes of the oxygen with other elements may become active at higher temperatures, making the wafers sensitive to high temperature processing. To overcome these problems, Float Zone(FZ) wafers may be used. Due to the difficulty in growing large diameter ingots and the often higher cost, FZ wafers are typically only used for laboratory cells and are less common in commercial production.

Multi-crystalline silicon (mc-Si) is an important material with advantages of low-production cost and high conversion efficiency. It has a market share of more than 60% in all photovoltaic materials. Directional solidification (DS) method has become the leading technique for producing mc-Si because of its better feedstock tolerance, higher throughput and easier operation. Solar cell efficiency is decreased by impurities, precipitates, and structural defects in the mc-Si ingots [2]. The generation and distribution of these are investigated using numerical analyses in this paper. Simulation of heat and mass transfer in bulk growth has become an indispensable tool for an efficient, time and cost saving optimization procedure. A global modelling of heat transfer was performed to study the generation of creep stress and formation of dislocations in multi-crystalline silicon at the various growth stages for the various modified DS system. The aim is to increase average grain size in silicon multi-crystals and reduce the impurities distribution and dislocation density. We have found suitable dimensionless numbers, bottom groove DS block and suitable insulation speed.





We took initiative to start the modeling activities on silicon growth eight years ago in SSN Research centre, and experimental activity two year ago with the support of MNRE, Government of India. Modeling and experimental mc-Si growth lab are established well in SSN RC. Several Ph.D. scholars and scientists are currently working in the field of mc-Si growth process and are getting good results.

References:

1. B. K. Sahu, *Renewable and Sustainable Energy Reviews*, **59**, 927-939 (2015).
2. J. Friedrich et al. *Journal of Crystal Growth*, **447**, 18–26 (2016).

PL-3

Numerical Simulation of the Oxygen Concentration Distribution in the Silicon Melt During Czochralski Crystal Growth

Jyh-Chen Chen,* Thi Hoai Thu Nguyen

Department of Mechanical Engineering, National Central University, Zhongli 320, Taiwan, R.O.C.

*E-mail: jcchen@ncu.edu.tw,

Oxygen impurities are incorporated into the silicon crystal during the Czochralski (CZ) manufacturing process. It has been recognized that there is a need for lower oxygen concentration silicon wafers, since the oxygen impurities contained in silicon wafers lead to degeneration in the performance of ultra-large-scale integration devices, power electronics, and solar cells. The previous studies of the CZ growth have mainly focused on the crystal-crucible counter-rotation. The oxygen transport in the melt is significantly affected by the rotation of the crystal and the crucible. The melt flow in crucible is governed by the interaction of several driving forces: buoyancy, thermo-capillary, and forced convection due to crystal and crucible rotation. Under this counter-rotation condition, it is very difficult to obtain a uniform radial distribution of impurities along the crystal-melt interface. The effect of crystal-crucible iso-rotation on the thermal and flow fields as well as impurity transport during the growth process has not been studied intensively.

In this study, a series of quasi-steady numerical simulations has been carried to study the oxygen concentration distribution in the silicon melt during the CZ growth of 8 inch diameter silicon crystal. The effects of different rotational combinations between the crystal and the crucible on the flow, heat and mass transfer in the melt are investigated. Both crystal-crucible counter and iso-rotations for a crystal length of 200 mm are discussed: $(n_s;n_c) = (13;-10); (10;-10); (5;-10); (5;10); (10;10); (13;10); (17;10); (20;10);$ and $(23;10)$. Here, n_s and n_c indicate the crystal and crucible rotation rates (rpm), respectively. The notation (-) indicates that the direction of rotation of the crucible is against that of the crystal rotation. As can be seen, in these cases, the difference in rotation rate between crystal and crucible ($n_s - n_c$) is reduced and then increased again with iso-rotation. Fig. 1 shows the flow pattern and oxygen distribution inside the silicon melt. Fig. 2 shows the distribution of the melt velocity. Fig. 3 compares the oxygen concentration along the c-m interface. The results show that the oxygen concentration along the crystal-melt interface is determined by competition between the mechanisms of convection and diffusion. When the differences in rotation between the crystal and crucible are low during iso-rotation, the melt velocity is significantly weakened and the effect of the diffusion process on oxygen transport in the melt becomes stronger than the effect of convection. The distribution of oxygen atoms and the temperature of the melt are more significantly affected by the flow pattern in cases of counter-rotation than iso-rotation. A lower concentration and more uniform radial distribution of oxygen can be obtained by using the iso-rotation conditions. Fig. 4 shows the growth parameter V_{cr}/G_c along the c-m interface, where V_{cr} represents the crystallization rate and G_c denotes the crystal temperature gradient normal to the c-m interface. It is clear that V_{cr}/G_c gets lower in the central region of the ingot and more uniform in the radial direction for iso-rotation cases. This indicates that a lower defect density and a flatter defect transition can be obtained by using iso-rotation. The lower V_{cr}/G_c for iso-rotation cases is mainly due to the enhancement in the temperature gradient G_c . This allows faster pulling of the crystals during growth.

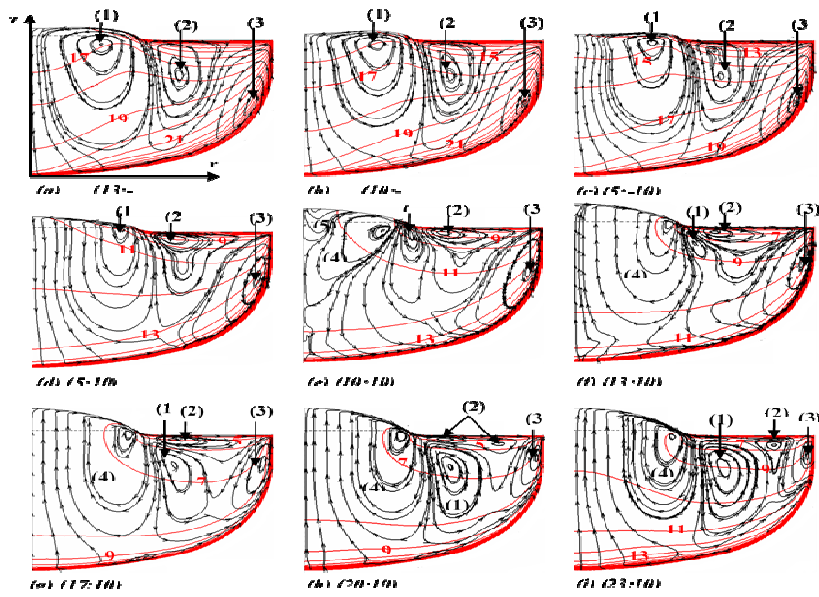


Figure 1. Distribution of flow patterns and oxygen concentrations (red, $\Delta C_O=1$ ppm) for crystal-crucible counter- and iso-rotations at different crystal rotation rates

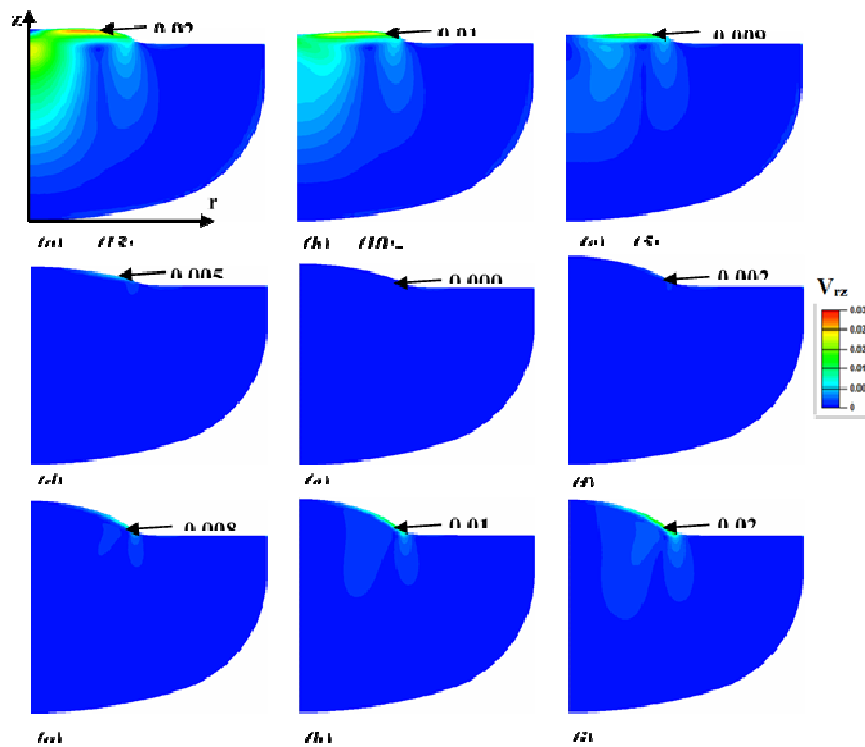


Figure 2. Comparison of the planar melt velocity V_{rz} ($V_{rz} = \sqrt{V_r^2 + V_z^2}$) in the melt for crystal-crucible counter- and iso-rotations at different crystal rotation rates

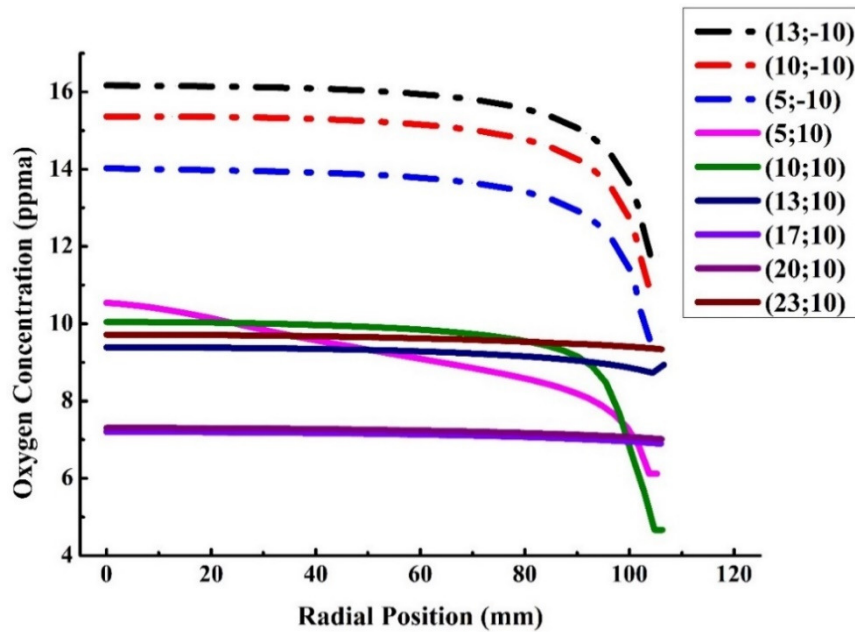


Figure 3. Comparison of oxygen concentrations along the c-m interface for crystal-crucible counter- (*dash curves*) and iso-rotations (*solid curves*) at different crystal rotation rates

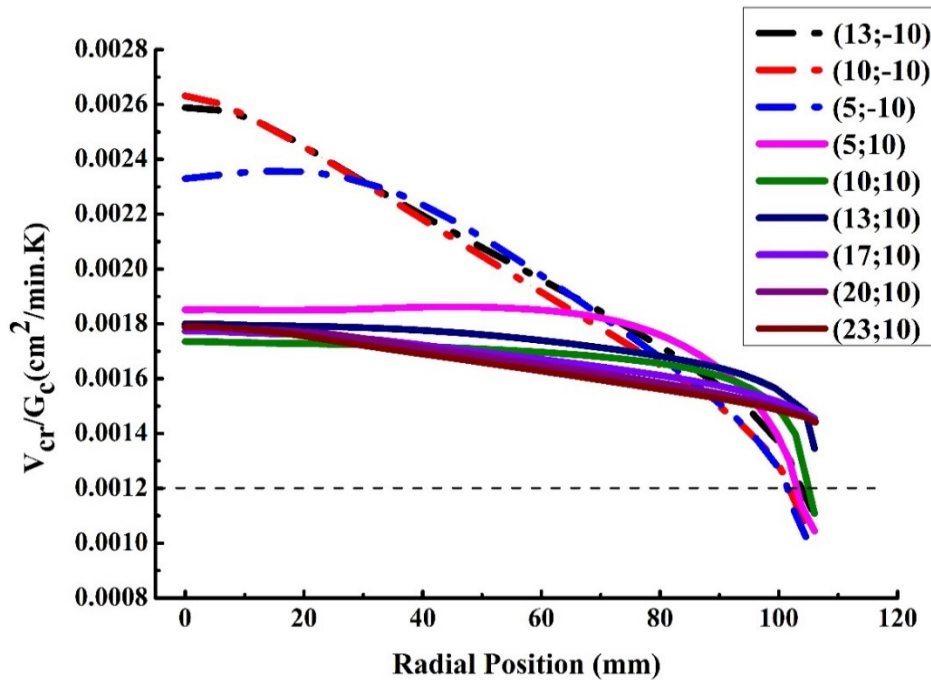


Figure 4. Comparison of the growth parameter V_{cr}/G_c between crystal-crucible counter- (*dash curves*) and iso-rotations (*solid curves*) at different crystal rotation rates

PL-4

Three Dimensional Modeling of Melt Convection in Solar Silicon Grown By Czochralski and Direct Solidification Methods

Vizman Daniel

Faculty of Physics, West University of Timisoara, Bd. V. Parvan 4, 300223, Timisoara, Romania

*E-mail: daniel.vizman@e-uvv.ro

The solar cell efficiencies achieved by the different techniques correlate directly with the material quality, i.e. higher efficiency is achieved the less crystal defects and impurities are present in the material. Therefore, in order to increase the efficiency, a deep understanding of the underlying chemo-physical phenomena occurring during the crystallization process and their influence on the material properties is of utmost importance. There are today two dominating crystallization techniques:

The growth of mono-crystalline Si by the Czochralski (Cz) technique delivers high performance solar cells with efficiencies as high as 21% and more. Directionally solidified (DS) multi-crystalline ingots in Si₃N₄ coated silica crucibles results in solar cells with efficiencies in the range of 18% [Green, M.A., et al. (2009), Prog. Photovolt: Res. Appl.,17: 320–326].

Melt convection is acknowledged to be a very important factor in the field of crystal growth: Convective flows contribute to heat transfer and thus control the rate of solidification; The resulting temperature field in the vicinity of the solid-liquid interface affects its shape and therefore the generation of thermal stress and the formation of dislocations; Convection controls the species/impurity transport in the melt; It affects the dissolution rate of crucible materials, the entry and evaporation of impurities from, respectively to, the gas phase via the melt surface; It determines the extension of the stagnant boundary layer above the solid-liquid interface where impurity transport is diffusion limited, and thus the effectiveness of the segregation of impurities from the crystal to the melt; It affects the formation and transport of particles in the melt; Furthermore, in a complex interaction of both heat and species transport, convection strongly influences the morphology and stability of the solid-liquid interface.

The aim of this paper was to show the potential of numerical simulation(using STHAMAS3D software) in determination of melt convection characteristics, which have a significant influence on the crystal properties.

Melt convection in Cz method is one of the most complex convection among the growth methods from the melt. The crucible is heated by a heater which surrounds it and the crystal is pulled up from the melt surface. Therefore a strong buoyancy force occurs, which is expected to flow the melt upward near the crucible wall and downward below the crystal. In reality the flow is more complex due to the superposition of buoyancy and centrifugal forces (usually, the crucible, as well as the growing crystal are counter-rotated) and in a lesser extent to the Marangoni forces which act at the melt free surface. Temperature fluctuations in the melt and especially under the solid-liquid interface are an important issue in the optimization of Cz method.

Since the silicon is melted in a quartz crucible, the ingot contains significant levels of oxygen due to dissolution of the crucible. Oxygen-related defects that can act as recombination centres include thermal donors; oxide precipitates and associated crystal defects. Solar cell manufactures attempting to limit negative impact of oxygen and related defects will ask for much lower oxygen levels in future. A numerical study of the influence of iso and counter rotation of crucible and crystal on the temperature and oxygen distribution will be presented for a 200mm Cz-configuration. Fig.1 show the temperature and oxygen distribution in a vertical section and fig.2 show the temperature and oxygen fluctuations in a monitor point under the S-L interface.

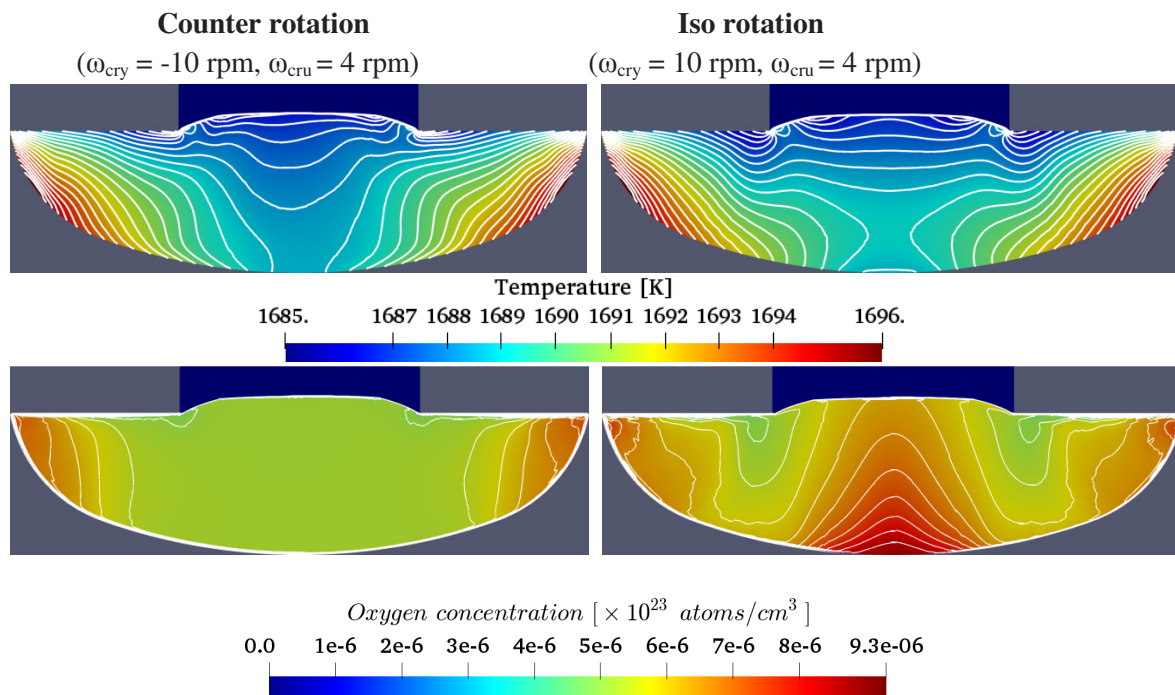


Fig.1 Temperature distribution in a vertical section

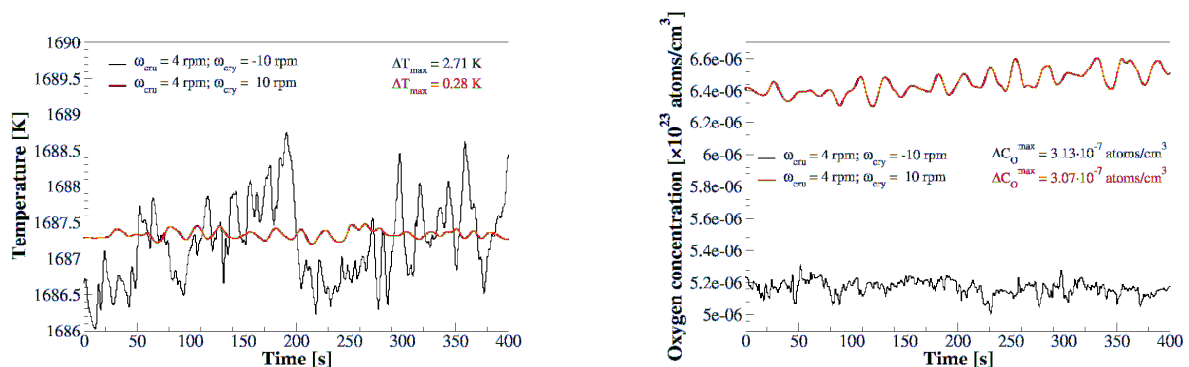


Fig.2. Temperature and oxygen fluctuation in a monitor point under the S-L interface

It can be observed that on one side the iso rotation damp the temperature fluctuations, but on the other side increase the oxygen level. The characteristics of temperature and impurities fluctuations will be compared with the striation fluctuations along the crystal obtained by Lateral Photovoltaic Scanning (LPS). The

frequency range (obtained by FFT) are in good agreement with the numerical simulations, which show a good correlation between patterns in doping gradients with temperature and impurities concentration fluctuations in the melt.

In the case of DS method, the increase in ingot size and the use of a feedstock material of lesser purity could lead to potential problems such as the detrimental curvature of the solid-liquid interface, the accumulation of more impurities during the longer growth time needed for larger ingots or from the lesser purity feedstock leading to the morphological destabilization of the growth interface or to their precipitation after the solubility limit is reached. The solution for this problems would consist in controlling the melt flow structure. A complete homogenization is required in order to have the optimal distribution of impurities, as this will reduce the impurity diffusion boundary layer thickness at the growth interface and lead to optimal axial segregation profiles. Due to the fact that in the method of DS the temperature is hotter at the top than at the bottom of the crucible, as the solidification starts from the bottom, a strong buoyant convection which could lead to a better melt mixing cannot be obtained. This requires the employment of a forced convection. The present paper will present how the use of magnetic fields (travelling magnetic field and electromagnetic stirring) can influence the melt convection and impurities distribution in the crucible.

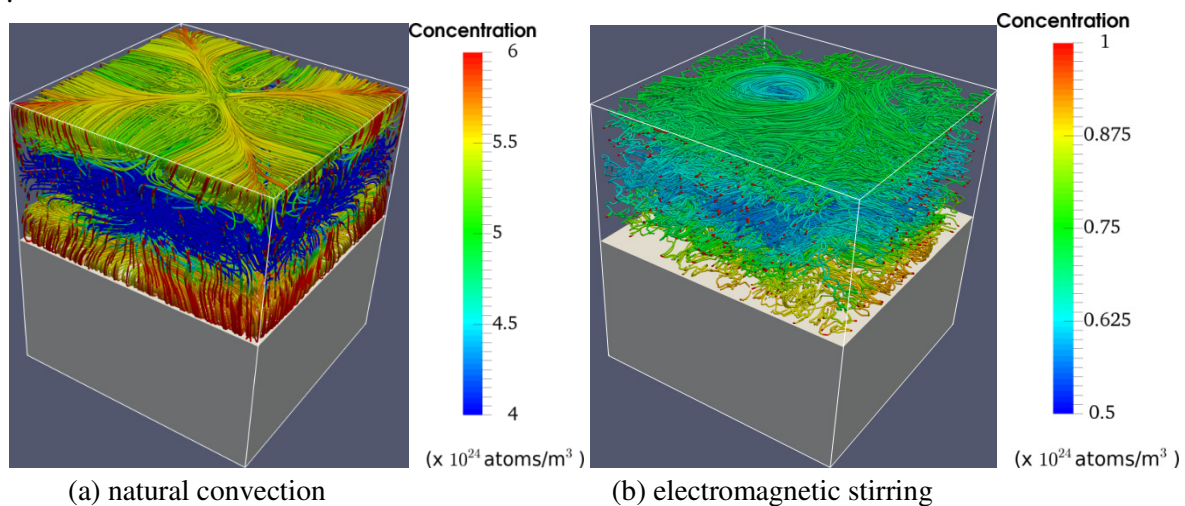


Fig.3 Melt convection in a DS configuration without (a) and with (b) electromagnetic stirring after 100s.

Fig. 3(a) show the impurities distribution in a configuration without forced convection. It can be observed that, because of the melt flow particularities, the impurities are trapped near S-L interface and at the free melt surface. An electromagnetic stirring can homogenize very fast (hundreds of seconds) the impurity distribution in the whole melt (Fig. 3b). It will be highlighted how numerical simulations can contribute to the development of new ideas in order to improve the crystal growth processes, having in mind that numerical experiment is much cheaper than a real crystal growth one.

PL-5

Molecular Dynamics Simulation (Cost and Time Effective drug development strategy)

K. Gunasekaran

CAS in Crystallography and Biophysics University of Madras, Guindy Campus, Chennai – 25

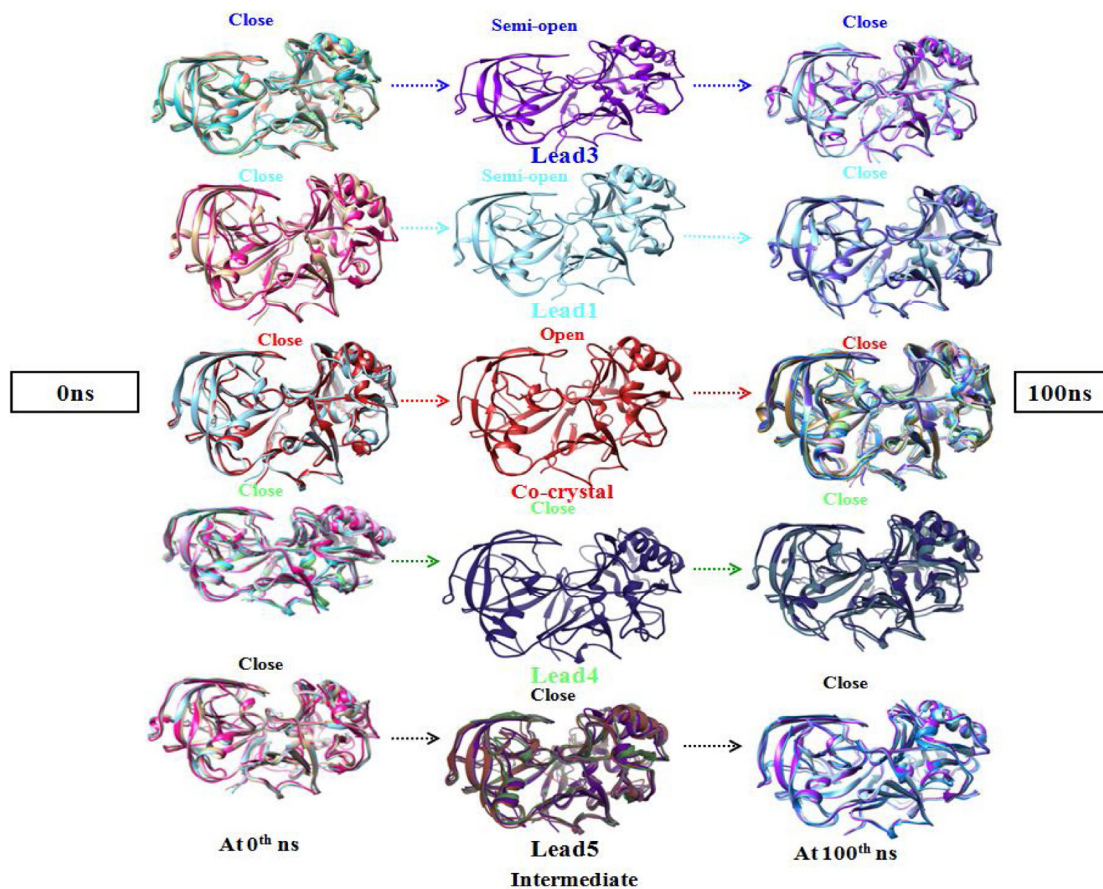
In Nature, structure of an object dictates the function. Similarly, in molecules also, the 3D structure i.e the spatial arrangement of atoms in the molecule makes the molecule functional. In biological systems, proteins not only act as the building blocks but also responsible for biochemical reactions in-turn responsible for energy production, cell division, immunity and even free radical scavenging. Immune pathway, blood clotting, signal transduction, oxygen and nutrient transport and many other events are possible only because of action of proteins. As already mentioned, these proteins should be in a desired 3D structure which is termed as active form for successful life processes. Sometimes, switching between active and inactive forms also needed. Proteins generally are fragile, flexible so sensitive to many factors to exist in active structure. Also, it is very true that malfunctioning of proteins (by getting denatured or over active), cause (or becomes reasons for) many diseases. In case of infectious diseases, the pathogen (bacteria, virus, parasites, etc.) also uses protein machinery for infection and invasion.

Now it can be understood, by establishing structures proteins (drug targets) of interest, one can design a small molecule that can fit in the active site for arresting the activity (or even enhancing) of the protein. In traditional way of finding suitable small molecule, biochemical assay are carried out with thousands of compounds one by one which is expensive both in cost and equipment time and human hour.

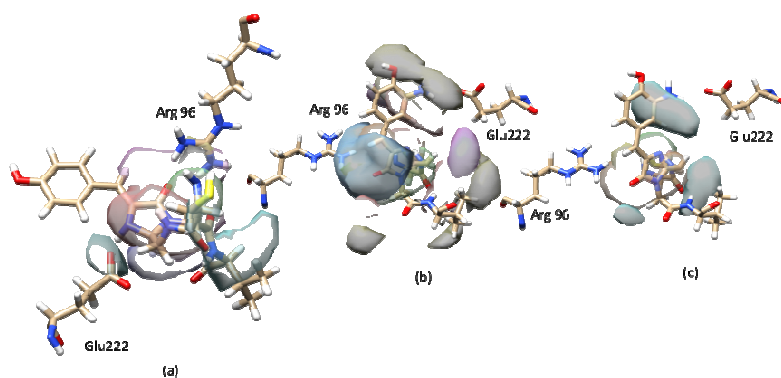
Since 3D structures are known (or can be modeled), then protein – ligand interactions can be assessed by fitting small molecular structures at the active site architecture of the protein structure. This way, thousands of compounds either from synthetic data bases (collection of synthetic compounds) or natural data bases (collection of pyto compounds, microbial compounds) can be evaluated for their binding with the protein in less than a day. Also further structure optimizations can be incorporated to have better desirable binding. This procedure is called “virtual Screening” and the fitting strategies are referred as “Molecular Docking”.

Though it is cost and time effective, sometimes we find the selected compounds fails during drug development for many reasons. One of the main reasons could be the lability of binding due to real physiological environment. One particular strategy to overcome this issue is “Molecular Dynamics Simulation”. By understanding dynamics of binding, the stability of interactions, so the effectiveness and druggability of the compound can be validated.

Dynamics simulation for this purpose is normally done using classical mechanics principles. The equilibrated system with periodic boundary condition was used to perform constant temperature and pressure simulation for 50 ns with 1 fs integration time step using the leapfrog integrator AMBER12 simulation program. Simulation trajectory was saved on 1 ps of simulation time and used for further structural analysis such as root mean square deviation of overall protein (RMSD), residue-wise root mean square fluctuation (RMSF) and radius of gyration (RGYR) as well as hydrogen bonding. Hydrophobic occupancies were calculated between inhibitors and target protein. Equilibration and simulation processes were validated as a function of the potential energy of the system. The hydrogen bonding (N-H · · O) and hydrophobic interactions occupancies were also will be calculated between inhibitors and protein active site. Some of recent efforts in MD will be presented.



Our MD simulation on BACE1 enzyme – Alzheimer’s target.



Comprehending intermolecular occupancy and interactions in GFP.

PL-6

Computational Studies on the Design and Development of Carbon based Novel Two-Dimensional Dirac Materials

Dr. V. Subramanian

Inorganic & Physical Chemistry Department, CSIR-Central Leather Research Institute, Adyar, Chennai 600020, India

In this study, we have proposed a series of novel 2D Dirac carbon allotropes with the aid of density functional theory-based first-principle calculations. The presentation gives a brief account on the different carbon allotropes, two-dimensional (2D) materials, Dirac materials^{1,2} and their electronic prospects. Further, I will also discuss about the structural and electronic properties of some of the novel 2D Dirac materials which mainly include α -2 graphyne,³ β -graphyne analogues, butterfly-graphyne, corographene, circumcoro-graphyne,⁴ *cp*-graphyne,⁵ and sulflower based quasi-planar 2D porous networks. In particular, the energetics of proposed 2D materials, structural properties, dynamical and thermal stabilities, mechanical stability, energetic favorability for the experimental synthesis, effect of the nanoconfinement, strain, doping and extremal electric field on the Dirac electronic dispersion will be addressed.

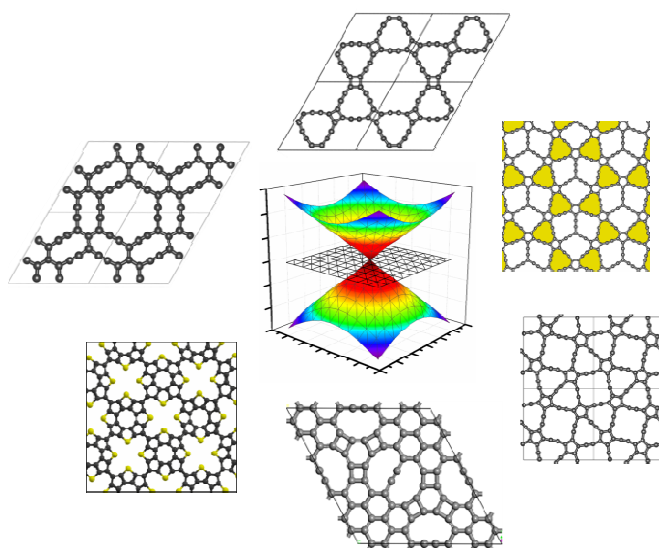


Figure 1. The geometrical and electronic features of different 2D materials

References:

- Wehling, T. O.; Black-Schaffer, A. M.; Balatsky, A. V. Dirac Materials *Adv. Phys.* **2014**, 63, 1–76.
- Wang, J.; Deng, S.; Liu, Z.; Liu, Z. The Rare Two-Dimensional Materials with Dirac Cones *Natl. Sci. Rev.* **2015**, 2, 22–39.
- Nulakani, N. V. R.; Subramanian, V. A Theoretical Study on the Design, Structure, and Electronic Properties of Novel Forms of Graphynes *J. Phys. Chem. C* **2016**, 120, 15153–15161.
- Nulakani, N. V. R.; Kamaraj, M.; Subramanian, V. Coro-graphene and Circumcoro-graphyne: Novel Two-Dimensional Materials with Exciting Electronic Properties *RSC Adv.*, **2015**, 5, 78910-78916.
- Nulakani, N. V. R.; Subramanian, V. Cp-Graphyne: A Low-Energy Graphyne Polymorph with Double Distorted Dirac Points *ACS Omega* **2017**, 2, 6822–6830.

IT-1

Numerical Investigation of Hydrodynamics and Crystal Growth in a Pilot-Scale Batch Crystallizer

Dr. B. Ashraf Ali

Department of Chemical Engineering, National Institute of Technology, Karnataka (India)

*E-mail: ashrafmchem@gmail.com

In this work, hydrodynamics and crystal growth in a draft tube batch crystallizer is investigated using Computational Fluid Dynamics (CFD) coupled with the Discrete Element Model (DEM). The flow generated by the rotating impeller interacts with baffles and generates a complex, unsteady, three-dimensional turbulent flow with large-scale recirculations. To predict liquid phase turbulence, standard k- ϵ model is used. At first, CFD model is used to investigate the flow field and find an optimum liquid volume in the batch crystallizer. Later, CFD is coupled with Discrete Element Model (DEM) to describe crystal dynamics and indirectly crystal growth in a batch crystallizer. Such a coupled approach is important since particle dynamics depend directly on mixing and hydrodynamic conditions. From the CFD-DEM simulation, it was found that the driving force controlling crystal growth can be obtained quantitatively. This delivers essential data for process improvement. By varying the most important crystallization process parameters, it was found optimal conditions for a liquid phase volume in the crystallizer of 24 L, for an initial seed crystal size of 0.5 mm.

Key words : Batch crystallizer, Hydrodynamics, CFD, Crystal Growth, DEM

Introduction :

Crystallization is a major manufacturing process in chemical and pharmaceutical industries. The crystallization processes is affected by hydrodynamics (turbulent flow, stirring and mixing) and particle dynamics (nucleation, growth, suspension, sedimentation, aggregation, breakage). For the practical analysis of crystallization processes, macroscopic models are mostly used. They treat the whole crystallizer as well-mixed and do not consider inhomogeneities within the vessel. Though very practical for a first assessment, neglecting local differences in composition, temperature and crystal number density may lead to an oversimplified representation of the situation in a real crystallizer, preventing the process optimization [1].

In order to obtain a more accurate description, it becomes increasingly important to introduce models resolved in space and time, which is called differential modelling. These models take into account local, instantaneous fields inside the crystallizer (e.g. for concentration, velocity and turbulence intensity) and are able to consider the impact of such distributions on nucleation, crystal growth, aggregation and breakage [2]. Recently, Computational Fluid Dynamics (CFD) has progressed significantly and is now becoming an effective tool for differential modelling of real crystallization processes.

Schematic of batch crystallizer

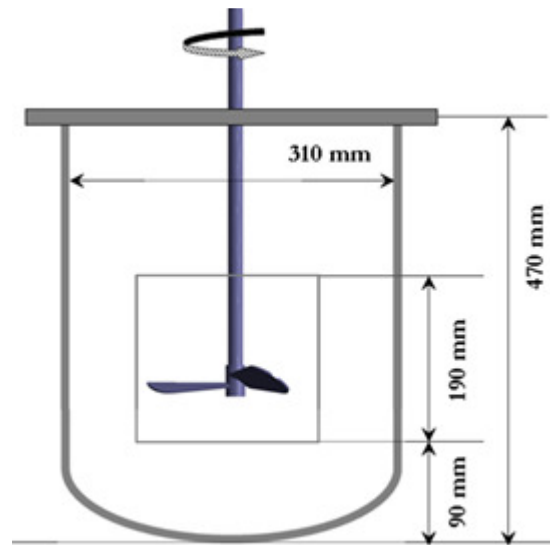


Fig. 1. Geometry of the draft tube batch crystallizer

Fig. 1 shows the geometry of the batch crystallizer. The total vessel volume is 35 L. The considered draft tube crystallizer is equipped with a propeller on a centrally mounted shaft. The inner diameter of the crystallizer is 310 mm, while the diameter of the impeller is 180 mm. An installed stationary baffle (draft tube) begins 90 mm above the bottom of the reactor and extends vertically over 190 mm. All computations in this paper consider a rotational impeller speed of 300 rpm.

Simulation methodology

To simulate the crystallizer, a Multiple Reference Frame approach (also called inner-outer approach) was first used [3,4]. Here, the flow characteristics of the inner region are solved using a rotating framework. These results provide the boundary conditions for the outer region, which is solved in a stationary framework. Hereby, the solution for the outer region provides the boundary conditions for the inner region. These steps are repeated in an iterative manner until a converged solution is obtained. Once a converged solution has been obtained in this manner, more realistic simulations can be carried out in transient conditions using the Sliding Mesh (SM) approach [5,6]. Here, the grid surrounding the rotating components really moves during the solution procedure. One (outer) grid zone is attached to the stationary baffles and reactor wall while the other (inner region) is attached to the rotating impeller and moves with it. The impeller blades are modelled as solid rotating walls. No-slip boundary conditions are imposed at all the walls. For turbulence modelling, standard wall functions are employed. The top surface of the liquid is modelled as a horizontal surface at a fixed level (slip conditions).

Results and discussions

To investigate the flow field in the crystallizer, at first contours of velocity magnitude is analysed and it is shown in Fig 2. Fig. 2(a) shows instantaneous isocontours of velocity magnitudes for liquid phase volume of 35 L predicted by CFD. The resulting flow pattern is predominantly vertical (following the tank axis), since the blades are pitched at a 60° angle.

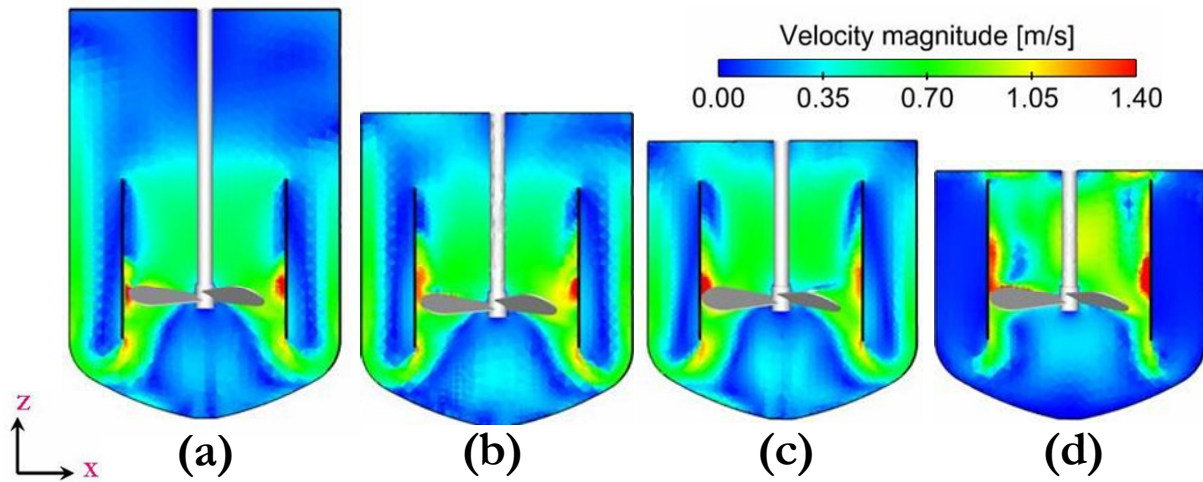


Fig 2. Comparison of velocity magnitude along the vertical plane for various liquid phase volume (a) 35 L, (b) 30 L, (c) 24 L, and (d) 22 L.

Further, to find optimum liquid phase volume in such batch crystallizer, CFD simulations are performed for various bulk volume of the liquid such as 30, 24 and 22 L [Fig 2(b-d)]. It is observed that the main liquid loop (downward motion below the impeller, upward motion near the external reactor wall) that supports the mass exchange between the impeller region and the outer flow region, is qualitatively unchanged when the volume decreases from 35 to 24 L [Figs. 2 (a-c)]. On the other hand, for the smallest volume of 22 L [Fig 2(d)], this circulation breaks down because the liquid level above the baffles becomes too small, preventing sufficient exchange of mass and momentum between inner and outer regions. This reveals that a volume of 22 L is clearly insufficient to support the crystallization process; it will therefore not be considered further.

CFD-DEM Coupling

Further, an Eulerian-Lagrangian coupling method is used to couple the particle dynamics (DEM) with the fluid flow (CFD). In the coupling between the discrete and the continuous phase, the mutual interactions are accounted for.

The CFD is first performed as a single-phase, transient calculation that is iterated until convergence for a specific time step. A drag force is then calculated by taking into account the current position of the DEM particles using the fluid velocity in the mesh cell within which each particle is located. While freezing the flow solution, the DEM software then takes sole control of the simulation and performs iterations on its side. In most cases, the DEM

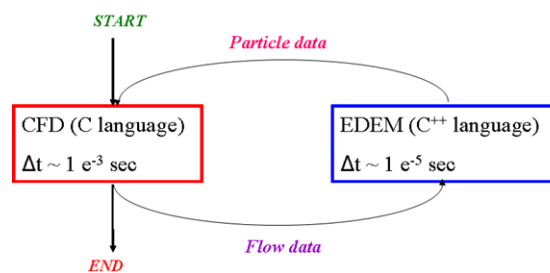


Fig 3. Coupled calculation methodology adopted to investigate crystal dynamics.

time step is noticeably smaller than the employed CFD time step [7]. After the DEM finishes its own iteration process, control is passed back to the CFD. A momentum sink term is then added to each of the CFD mesh cells containing particles in order to take into account transfer from the fluid to the particles [8]. This double iteration process in time is schematically depicted in Fig 3.

Connection between hydrodynamics and crystal growth

Crystal growth requires both transport and surface integration. First, the solute molecules need to be transported from the bulk of the solution through a boundary layer to the crystal surface by diffusion before they can be attached to the surface. These processes are driven by specific local concentration differences. For the purpose of this study, it is instructive to exploit the simplifying assumption that both processes are linear and that the rates of mass transfer and surface integration are equal. Then, a total (overall) growth rate constant, k_{tot} can be obtained by ,

$$k_{tot} = \frac{1}{\frac{1}{k_{dif}} + \frac{1}{k_{sur}}} \text{ with } k_{dif} = \frac{D}{\delta} \quad (1)$$

In the eq 1, k_{dif} is the transport rate constant, k_{sur} is the surface integration rate constant, D is the component diffusivity in the fluid phase, and δ is the boundary layer thickness. This thickness is strongly influenced by the hydrodynamics in the two-phase system, in particular by the local slip velocities [3]. Higher slip velocities decreases the layer thickness δ . According to eq 1, this increases k_{dif} and k_{tot} and, thus, favours crystal growth.

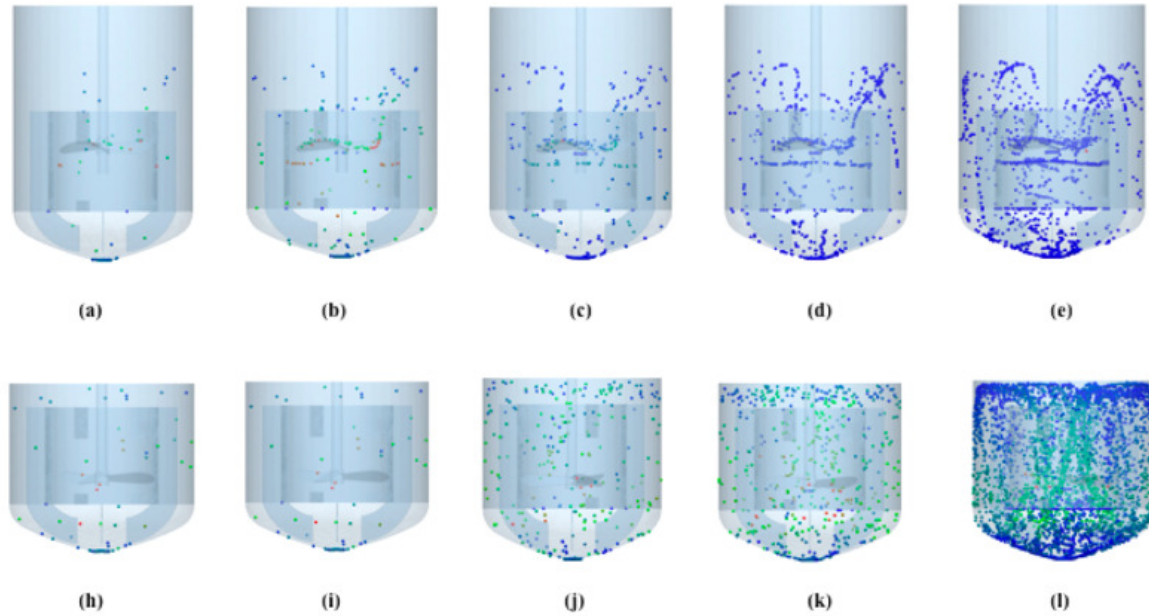


Fig 4. Crystal dynamics in crystallizer for a liquid volume of 35 L (a-e, top row) or 24 L (h-l, bottom row), considering an increasing number of crystals, from 100 to 10000 from left to right (100, a, h; 500, b, i; 1000, c, j; 2500, d, k; 10000, e, l). The results shown correspond to the end of the simulation, and crystals are colored by instantaneous velocity magnitude.

To predict crystal growth, Pottasimum di hydrogen phosphate (KDP) of 0.5 mm considered in batch crystallizer, the number of crystals injected in the CFD-DEM simulation is progressively increased from 100 up to 10000, considering again liquid volumes of 35 and 24 L. The instantaneous position of the crystals is shown in Fig 4 at the end of the CFD-DEM simulation. In the present case, a homogeneous

injection has been implemented, implying that the initial crystal position is initiated randomly within the liquid volume when beginning the coupled simulation, corresponding initially to a perfectly mixed state. Here, many crystals are temporarily trapped by the rotating impeller when a crystallizer volume of 35 L is used (top row of Figure 4); however this phenomenon does not appear at a reduced liquid volume (24 L, bottom row). Hence, the liquid volume of 24 L once again appears to be superior for practical purposes. It is also clear from the top row of Figure 4 that the upper part of the crystallizer does not participate in the process for a liquid volume of 35 L, since no crystals are found there at all.

$$ASV = \frac{1}{\text{No of injected crystal}} \sum_{i=1}^{\text{No of injected crystal}} \frac{1}{T} \int_0^T \Delta V_i(t) dt \quad (2)$$

In order to quantify crystal growth, the average slip velocity between the crystal and fluid is calculated again using eq 2. Table 1 depicts the calculated average slip velocity (ASV), as well as the relative velocities (RV) observed when crystals collide with the impeller. All data confirms the advantage of the reduced liquid volume, 24 L.

The calculated slip velocity (ASV) is found to be systematically higher for the 24 L reactor, 40% higher when averaging over 10000 crystals, indicating a similar difference in crystal growth rate. At the same time, the relative velocity during collisions is much smaller with a liquid volume of 24 L, typically by a factor 20. This is because, as aforementioned, crystal dynamics and particle velocity distribution are completely different in the 24 L and in the 35 L reactor; the crystals moving in the latter do so at a much slower speed. Consequently, crystal attrition and secondary nucleation are expected to be much higher for a liquid volume of 35L.

Seeding crystal numbers	ASV (35 L) (m/s)	ASV (24 L) (m/s)	RV (35 L) (m/s)	RV (24 L) (m/s)
1	0.0203	0.0205	1.20	0.26
100	0.0238	0.0326	1.50	0.42
500	0.0233	0.0329	16.81	0.55
1000	0.0241	0.0338	20.02	1.04
2500	0.0255	0.0358	21.04	1.16
10000	0.0286	0.0401	25.23	1.24

Table 1. Average Slip Velocity (ASV, see eq 2) in liquid as well as Average Relative Velocity (RV) When Crystals Collide with the Impeller for Liquid Volumes of 35 and 24 L

When a small number of particles are considered, a large proportion of those appear to be trapped within the plane of the impeller, in particular for a liquid volume of 35 L. When 500 crystals or more are considered, this effect becomes progressively less important. This is partly due to increased interactions ejecting the crystals outside of the impeller plane.

In conclusion, the crystal growth is found to be faster when a liquid volume of 24 L is used. The relative velocity of those, are considerably lower for 24 L. Therefore, the CFD-DEM simulation indicates that a 24 L liquid volume is highly advantageous in every respect

Summary and conclusions

Hydrodynamic conditions have been investigated quantitatively in a draft tube crystallizer. For this purpose, Computational Fluid Dynamics has been combined with a Sliding Mesh is used. Many advantages are observed when reducing the liquid phase volume in the draft tube crystallizer studied from 35 L down to 24 L, in particular more homogeneous hydrodynamic conditions. However, reducing the bulk volume further to 22 L modifies completely the hydrodynamic conditions in an unacceptable way for the process. A volume of 24 L was identified in this theoretical study to be most suitable. Further, four-way coupling (using the Discrete Element Model) is used in simulations where DEM coupled with CFD in which larger quantities of crystals [KH_2PO_4 (KDP)] are injected into the flow. Up to 10000 individual crystals have been considered in the simulation. The impact of various process parameters on crystal growth has been quantified by analysing the average slip velocity, relative velocity. One notable discovery is that a liquid volume of 24 L is solely advantageous compared with a larger liquid volume of 35 L.

References

- [1] B. Wan. "CFD simulation of Crystallization Process-Verifications of Fluent's population balance modelling". Ph.D. Thesis, University of Utah(2005).
- [2] B. Wan, T.A. Ring. "Verification of SMOM and QMOM population balance modelling in CFD code using analytical solutions for batch particulate processes". *China Particuology* 4 (2006) 243-249
- [3] E. Marshall, A. Haidari, S.Subbiah. AICHE Annual Meeting, Chicago(1996).
- [4] A. Brucato, M. Ciofalo, F. Grisafi, G. Micale. "Complete numerical simulations of flow fields in baffled stirred vessels: the inner-outer approach". *ICHEME Symposium Series* 136, (1994)155.
- [5] C.K. Harris, D. Roekaerts, F.J.J. Rosendal, F.G.J. Buitendijk, P.H. Daskopoulos, A.J.N. Vreenegoor, H. Wang. "Computational fluid dynamics for chemical reactor engineering", *Chemical Engineering Science*. 51 (1996) 1569-1594.
- [6] V.V. Ranade, Y. Tayaliya, D. Choudhury. "Modelling of flow in stirred vessels: comparison of snapshot, multiple reference frame and sliding mesh approaches". 16th NAMF Meeting, Williamsberg, 1997
- [7] Deen, N. G.; Van Sint Annaland, M.; Van der Hoef, M. A.; Kuipers, J. A. M. "Review of discrete particle modeling of fluidized beds". *Chemical Engineering Science*. 62(2007), 28-44.
- [8] EDEM2.1: Theory and Reference guide; DEM solutions Ltd, Edinburgh, 2010

IT-2

Turbulent Heat and Mass Transfer during Cz & Ds Si Crystal Growth for Solar Cells
V. Kalaev, V. Artemyev, D. Borisov, A. Vorob'ev, A. Kuliev, E. Bystrova, S. Smirnov
STR Group, Inc., 64 Bolshoi Sampsonievskii pr., Build. "E", St. Petersburg, 194044, Russian Federation

E-mail: vladimir.kalaev@str-soft.com

We discuss modeling of turbulent heat and mass transfer during Czochralski (CZ) and direct solidification (DS) silicon crystal growth for solar cells. Two most important electronic characteristics of a silicon as a material for solar cells are resistivity and the minority carrier lifetime. Degradation is characterized by decreasing of the minority carrier lifetime, which could be related to silicon crystal defects, including grown-in point defects and impurities. The major impurities are oxygen, carbon, nitrogen and metals. We have focused on approaches to limit degradation in silicon solar cells by decreasing oxygen and carbon content in Si melt and crystal. Computer modeling is a useful tool for investigation and improvement of heat and mass transfer in crystal growth. Complicated turbulent convective mass transport governs the impurity and dopant distributions in the melt because of the low molecular diffusivity. As of special importance in day-by-day engineering applications, we have focused on the development of modified RANS (Reynolds-averaged Navier-Stokes equations) approach for simulation of turbulent heat and mass transfer in the melt, using advanced 3D unsteady DNS (Direct Numerical Simulation) data and available experimental measurements for validation and critical analysis.

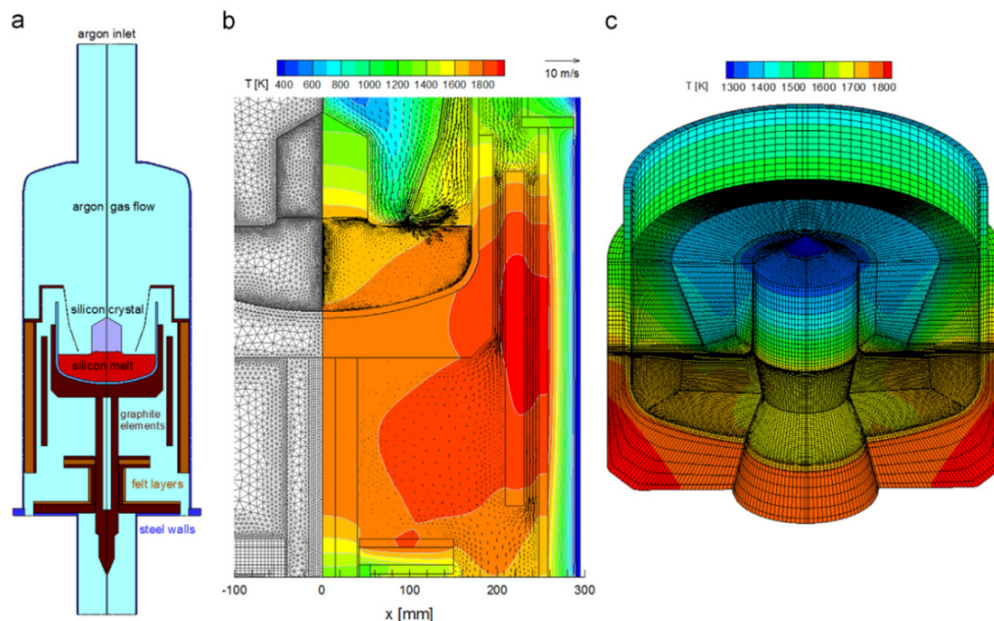


Fig. 1. Schematic view of Cz Si growth system (a), global heat transfer modeling and fluid flow (b), and 3D local model and temperature distribution (c) [2].

As a modeling example of CZ Si growth, there is a schematic view of EKZ 1300 system [1] demonstrated on Fig. 1. Our modeling strategy for Cz and DS crystal growth technologies is first to perform 2D axisymmetric global heat transfer modeling by basic CGSim software with the account of radiation and heat conduction, as well coupled with RANS modeling of melt convection and gas flow (see

Fig.1a-b). Second, 3D Flow Module of CGSim can be used for advanced DNS or LES (Large Eddy Simulation) of the flow, heat and mass transport (see example of Cz 3D domain on Fig.1c).

Till today RANS is the most popular approach to solve conservation equations for the turbulent kinetic energy and its (specific) dissipation rate [2], as the basis for further calculation of turbulent heat & mass fluxes via the isotropic turbulent effective viscosity and gradients of quantities within the Boussinesq hypothesis. However, fundamental physics of generation and dissipations of the turbulent kinetic energy is still poorly understood for Cz and DS Si flows because of their complexity. Generation of turbulence is known as a result of the mean melt velocity stresses, P (see Fig.2, left), flow instabilities owing to buoyancy, G (see Fig.2, right), and, as we have recently revealed, a contribution of the Marangoni (Ma) convection caused by a certain distribution of the temperature along the melt free surface.

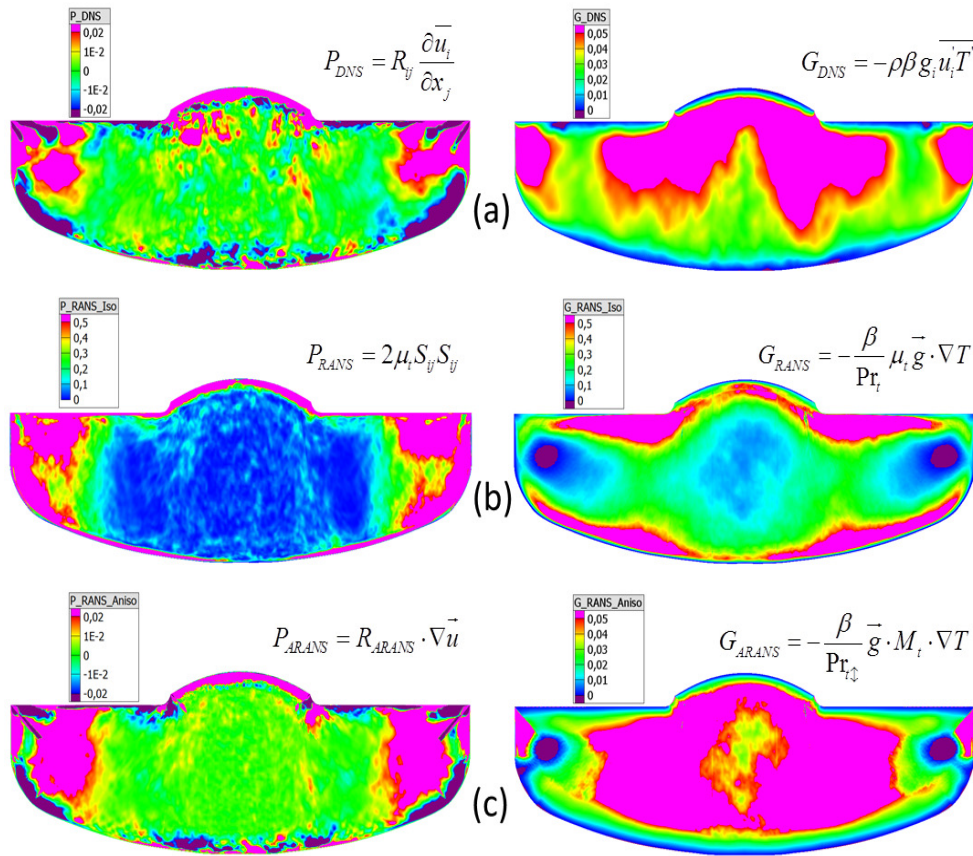


Fig. 2. Turbulence generation due to the mean flow P (left) and owing to buoyancy G (right), calculated using DNS data (a), within standard RANS approximation (b), and within ARANS (c).

DNS data illustrated in Fig.2 are obtained using a detailed computational grid of about 17 000 000 computational cells with the time step of 0.02 second, allowing us to resolve small scale turbulence with the length scale smaller than 1 mm in near wall regions. A comparison of P and G , as a reference calculated directly from DNS data (Fig.2a), to their standard RANS approximations (Fif.2b) has demonstrated that the standard RANS approach overpredicts turbulent generation with a huge discrepancy (more than one order of magnitude) and does not predict negative values of P . This stimulated us to develop a special anisotropic RANS approach (A-RANS) to predict turbulence generation much better, as demonstrated on Fig.2c, using a novel approximation with the tensor of anisotropic turbulent viscosity M_t , instead of the scalar μ_t .

The Ma thermocapillary convection effect is especially important because of evaporation of impurities through the melt free surface to the gas, limited by turbulent mass exchange near the surface. It is well known that the Ma surface tension is used in the boundary condition for momentum exchange through the melt free surface. However, the direct contribution of the Ma effect on turbulence generation probably has not been studied yet. We suggest a novel boundary condition for the turbulent kinetic energy balance through the melt free surface. Without Ma effect (see Fig.3 left), the standard boundary condition is always valid and the kinetic energy on the free surface is of the same values as inside the melt. However, for real growth cases with the Ma effect, the novel boundary condition results in additional turbulence generation with the free surface kinetic energy several times higher than that inside the melt (see Fig.3 right), which is confirmed theoretically and by a comparison to reference DNS data.

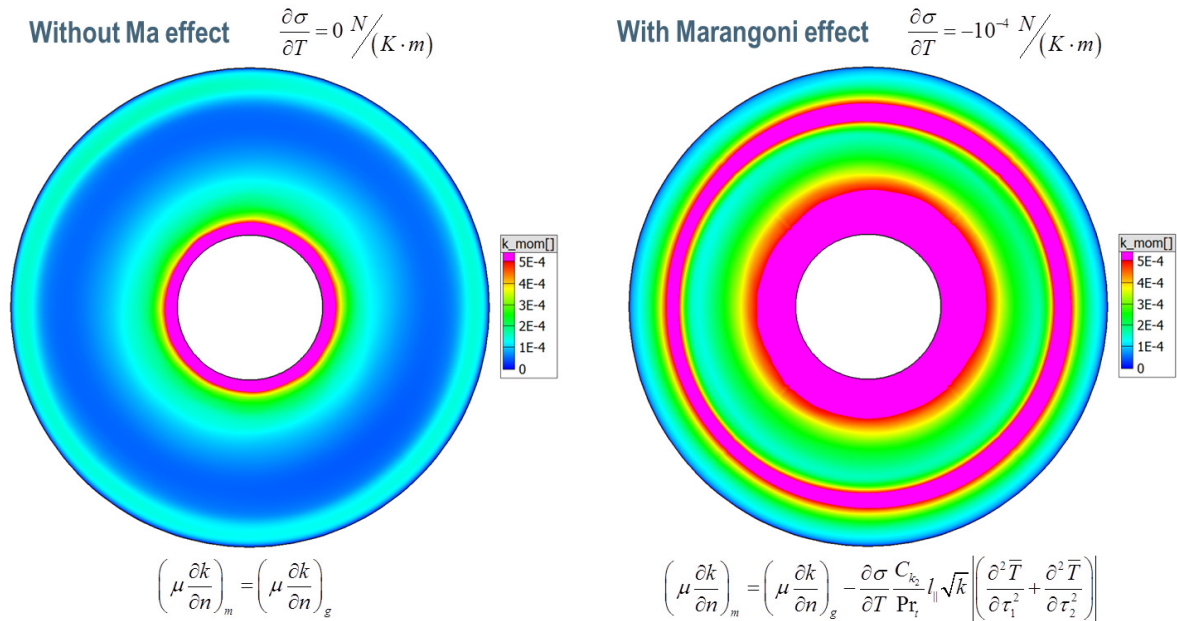


Fig. 3. Turbulent kinetic energy distributions over the melt free surface, calculated by detailed DNS without Ma effect (left) and with Ma effect (right).

Improvements in turbulence modeling greatly contribute to the development of predictive models of mass transport, including chemical reactions with phase transitions during Cz and DS Si crystallization [3]. Conventional turbulence models usually fail to predict oxygen concentration in the melt mainly because turbulence anisotropy is not considered under the melt free surface and turbulent oxygen mass flux through the surface is dramatically overestimated. This results in overestimation of SiO evaporation and excessive CO generation on graphite walls. To predict oxygen and carbon concentrations in Si crystal and melt, one needs to account for turbulence anisotropy in the melt flow, which is taken into account in our modifications of available turbulence models. Fig. 4 illustrates the difference in predictions of standard isotropic turbulence models (RANS) and modified models with anisotropic effects (ARANS). It is well seen that the modified model predicts experimental oxygen concentration in the crystal [4,5] much better with respect to general trends and absolute values.

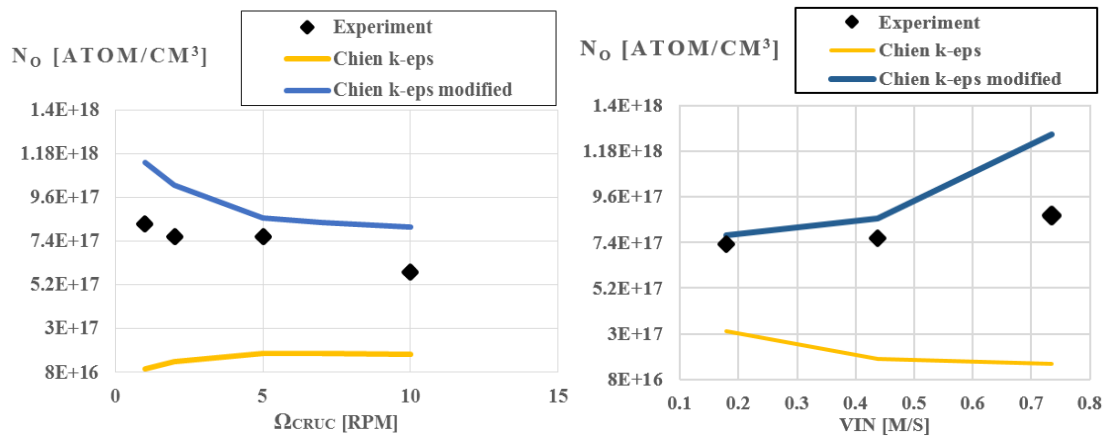


Fig. 4. Oxygen concentration in the crystal as a function of the crucible rotation rate (left) and as a function of the argon flow velocity (right).

Correct modeling of oxygen evaporation as SiO from the melt free surface and heterogeneous reactions on graphite surfaces [3] contributes to fairly good predictions on CO concentration in the argon gas flow and carbon concentration in the melt. Fig. 5 illustrates a comparison of predictions by CGSim software and experimental data published in [6] with respect to measurements of CO concentration in Ar gas flow in two points (A,B) inside a Cz configuration with varying Ar pressure and flowrate. In the case of DS of Si crystals (See Fig.6), 3D computer modeling may also include the effect of the Lonentz force (LF), generated by alternating current powering the resistive heaters and the effect of asymmetric gas outlet positions resulting in inhomogeneous SiO and CO concentrations over the melt free surface (Fig.6 left). As a result of the LF effect on DS Si melt flow, the crystallization front shape has quite complicated geometry providing inhomogeneous impurity segregation, and generation of dislocations.

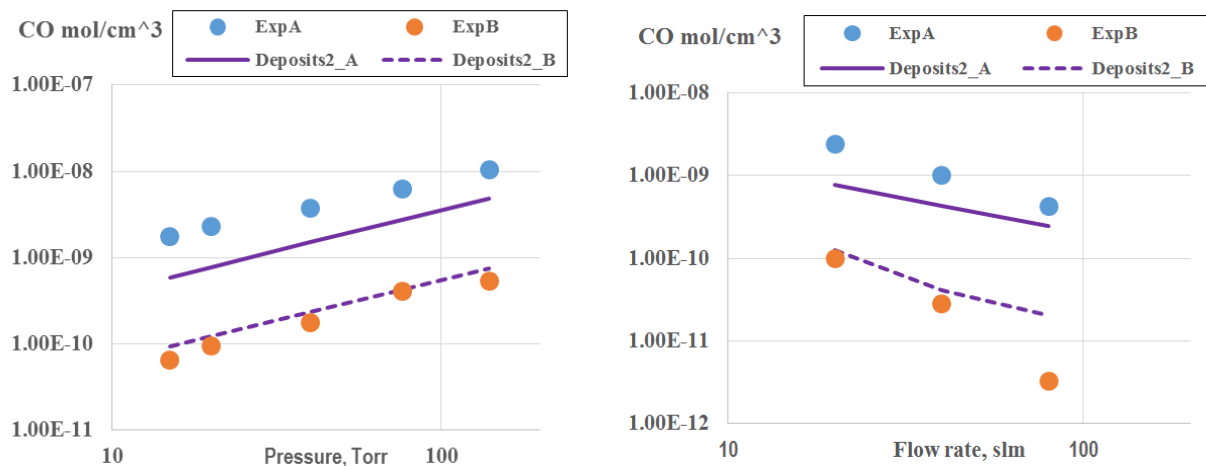


Fig. 5. CO concentration in Ar gas as a function of the gas pressure (left) and of the gas flowrate (right).

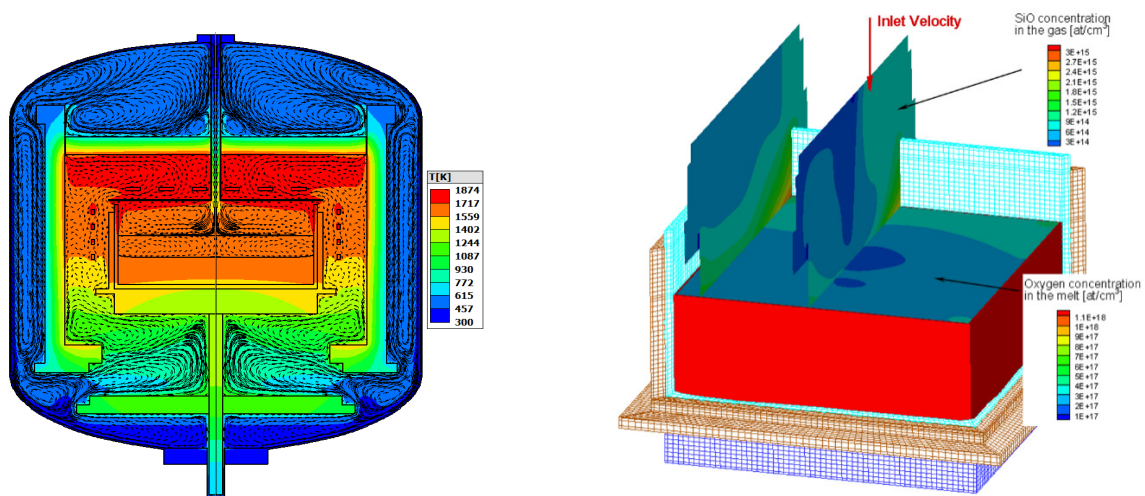


Fig. 6. Modeling of global heat transfer modeling and fluid flow in schematic DS Si growth system (left), and 3D local model of flows and impurity transport in the melt and gas (right).

This work was supported by the Foundation for Assistance to Small Innovative Enterprises (FASIE, Russia) within ERA.Net RUS Plus Project, grant number ERA-RUS-41114 0042017.

References:

- [1] V. Kalaev, A. Sattler, L. Kadinski, Journal of Crystal Growth 413 (2015) 12–16
- [2] A.N. Kolmogorov, Izvestia Academy of Sciences, USSR; Physics, 6, 1-2 (1942) 56-58
- [3] A.N. Vorobev, A.P. Sidko, V.V. Kalaev, Journal of Crystal Growth 386 (2014) 226–234
- [4] K.V. Khodosevitch, et al., 4th IWMCG, Abstracts, p.148-149, Nov. 5-7, 2003, Fukuoka, Japan
- [5] I.Yu. Evstratov, et al., 3rd IWMCG, Abstracts, p.49-50, Oct. 18-20, 2000, Hauppauge, NY, USA
- [6] X. Liu, et al., J. of Crystal Growth, V. 499, 8-12, 2018

IT-3

Quantum Dot Formation in Silicon-Germanium Thin Films on Patterned Silicon substrates

Gopal Krishna Dixit¹, Monika Dhankhar¹ and Madhav Ranganathan^{1}*

Department of Chemistry, Indian Institute of Technology Kanpur, Kanpur 208016, India.

*Email: madhavr@iitk.ac.in

Silicon-Germanium thin films grown epitaxially on a silicon substrate spontaneously form quantum dots when grown above a certain thickness [1]. This offers an exciting route for spontaneous self-organized quantum dots, which have enhanced transport properties. However, a major drawback of this approach is the lack of precise control over the quantum dots. Indeed, though the quantum dots are of a typical size, there is significant variation in their spatial locations and their sizes, which makes them unsuitable for potential applications. Substrate patterning is a popular way to control the size and positional homogeneity of spontaneously formed quantum dots [2]. In this approach, the substrate on which the films are grown is pre-patterned using lithographic techniques. It is expected that this pre-patterning of the substrate will direct the location of quantum dot formation.

Towards this goal, patterns such as stripes and pits have been used and shown to partially localize the formation of the quantum dots [3-5]. However, the choice of the size of the pattern features affects the localization of the quantum dots. Theoretical modeling of quantum dot formation in strained heteroepitaxy has been extended to study growth on patterned substrates[6,7]. Following this work, we model the formation and evolution of quantum dots in strained silicon-germanium systems using continuum modeling[8,9]. The surface is described by a scalar height field which evolves due to deposition and surface diffusion, which is governed by surface and elastic energy. The resulting evolution are successively to different orders in the surface slope, using methods developed in our group. Significant progress can be achieved by studying the behavior in the linear regime, i.e. the very small slope regime. Such behavior shows the onset of instabilities that eventually lead to quantum dots. A major milestone in this area was the identification of competing length scales between the pattern wavelength and the typical size of the quantum dots[6]. This typical size is characterized by the wavelength of the Asaro-Tiller-Grinfeld (ATG) instability. It is, in fact, this instability in biaxially strained films that is the cause of the quantum dot formation. The competition between length scales leads to regimes where the quantum dots form in the valleys of the patterns and regimes where they form on the tops of the pattern.

We have extended the earlier studies on heteroepitaxial growth to include the cubic elastic nature of the silicon-germanium system. This leads to a preferred alignment of quantum dots along the elastically soft crystallographic directions. Interestingly, this preference is seen in the linear regime itself indicating that the alignment effects are rather strong. In the case of patterned substrate heteroepitaxy, there is an additional competition between the pattern orientation and the elastically soft directions. This results in a further localization of the quantum dots to specific positions on the tops of the patterns. Our results are directly compared with experiments carried out on Gaussian like pit-patterned substrates. In these experiments, the patterns appear Gaussian pit-like for small opening widths and quasi-sinusoidal for large widths [5]. Thus, there is, in addition to the pattern wavelength, an additional parameter, namely the pit width that controls the localization of quantum dots. Experiments revealed a phase diagram where the quantum dots are observed to mostly form in the pits, except for a small range of wavelengths and widths.

Further, the exact location of these quantum dots when they form on the top of the pattern was found to be *saddle* positions, i.e. positions directly between two pits as opposed to a center of a square pit array [10].

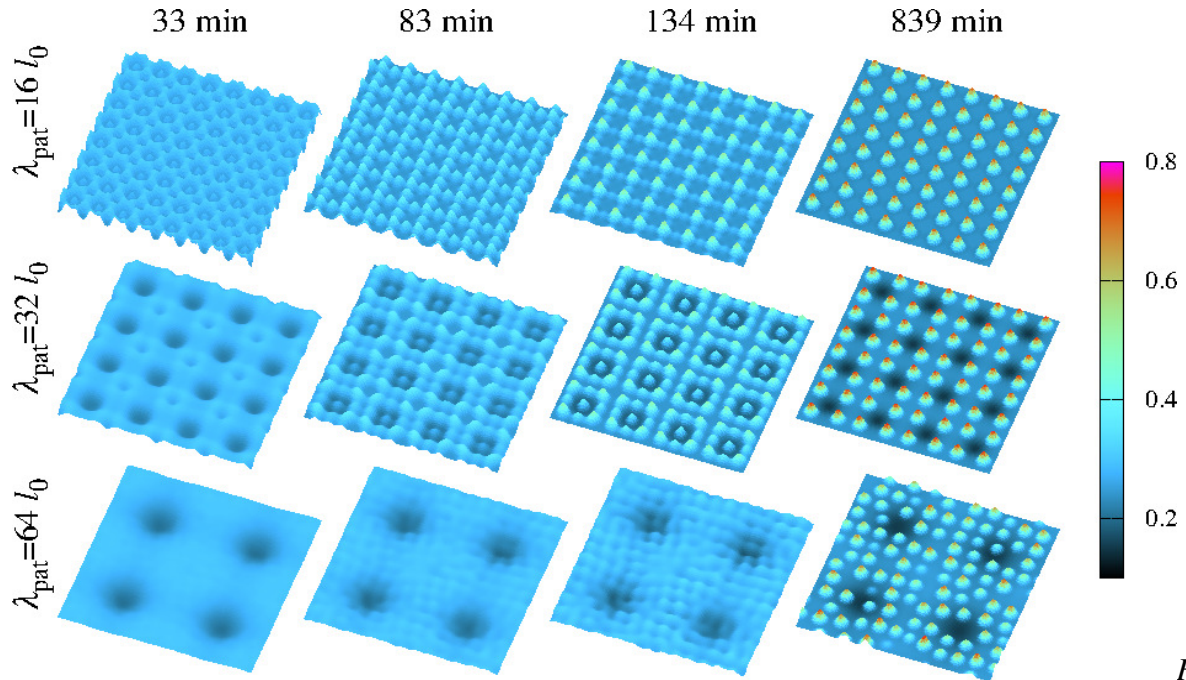


Fig 1: Time evolution of surfaces starting with different pattern wavelengths (λ_{pat}) indicated. The color bar refers to the height of the film in units of the l_0 which works out to 32 nm. The system size is 128 X128 in units of l_0 and the initial thickness of the film above the patterned substrate is 12 ML or 1.62 nm.

We examined the higher order numerical solutions on the model. The numerical methods developed in our group were significant advances where the anisotropic elasticity equations were solved order by order using the patterned substrate as boundary conditions. Through our work, we have shown that the elastic anisotropy due to the cubic nature of the film is a crucial effect necessary to explain the localization of quantum dots. Indeed, we found that using elastic anisotropy causes the quantum dots to form at the experimentally observed *saddle* positions whereas ignoring them leads to formation at the *crown* positions (See Fig. 1).

References:

- [1] J.-N. Aqua, I. Berbezier, L. Favre, T. Frisch, A. Ronda, Phys. Rep., **522**, 59 (2013).
- [2] M. Brehm, M. Grydlik, Nanotechnology, **28**, 392001 (2017).
- [3] M. Grydlik, G. Langer, T. Fromherz, F. Schäffler, M. Brehm, Nanotechnology, **24**, 105601 (2013).
- [4] M. Bollani, D. Chrastina, A. Fedorov, R. Sordan, A. Picco, E. Bonera, Nanotechnology, **21**, 475302 (2010).
- [5] J.M. Amatya and J.A. Floro, Appl. Phys. Lett., **109**, 193112 (2016).
- [6] J.-N. Aqua, X. Xu, Phys. Rev. E, **90**, 030402 (2014).
- [7] X. Xu and J.-N. Aqua, Surf. Sci., **639**, 20 (2015).
- [8] G.K. Dixit and M. Ranganathan, J. Phys. Condens. Matter, **29**, 375001, (2017).
- [9] G.K. Dixit and M. Ranganathan, Nanotechnology, **29**, 365305 (2018).
- [10] G.K. Dixit, M. Dhankhar and M. Ranganathan, *in preparation*.

IT-4

New Geometrical Modeling for Crystal Morphology

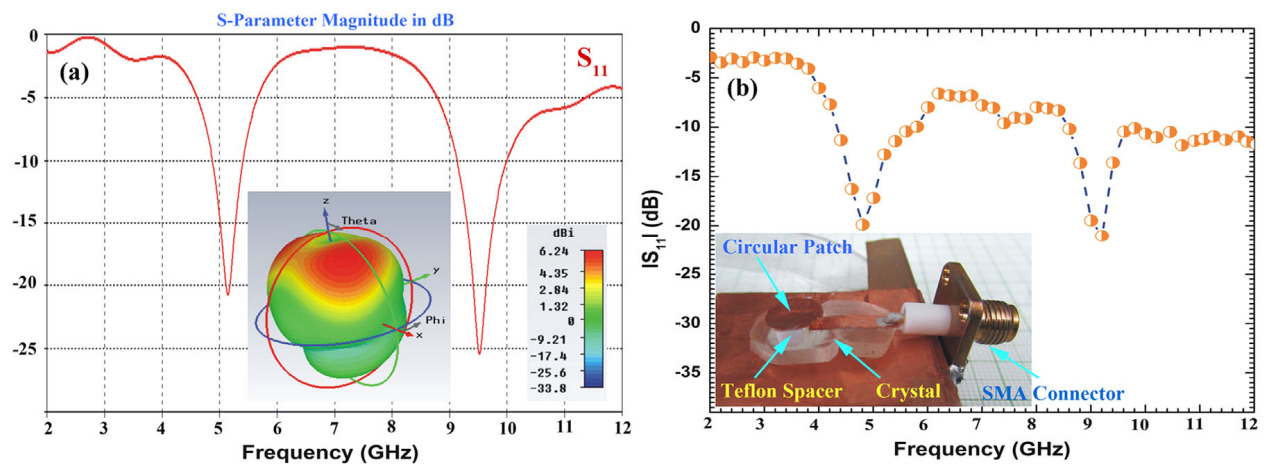
Binay Kumar

Crystal Lab, Department of Physics & Astrophysics, University of Delhi, Delhi-110007, India

*Email: b3kumar69@gmail.com

The morphology of grown crystal reflects the relative rate of growth in different crystallographic directions which is important for the industrial crystallization process and device applications. The precise prediction of the crystal morphology helps to save time and reduce technical troubleshooting processes. Various laws viz. Bravais–Friedel–Donnay–Harker (BFDH) law, Hartman–Perdok (HP) law, etc. have been proposed from time to time which are helpful in explaining observed morphology of various crystals at different success levels.

We have developed a new geometrical model in which crystal morphology is predicted from the propagation vector of center of mass of the molecular basis in the crystal lattice [1]. In this novel approach, the dependence of growth rate of different crystal planes on the bond strength between molecules of the crystal is inherently preserved. The development of the HNB propagation vector is described in detail and is used to predict the morphology of different crystals grown by solution technique. The derived morphology is compared with the morphology predicted from other laws to explain the experimentally actual morphology exhibited by grown crystals [2]. These concepts have been successfully used to explain various other systems like ZnO nanocrystals which are synthesized in different morphologies like rods, pencil-shape, 2D sheet, etc. The explanation of different morphologies of ZnO was useful to understand extraordinary piezoelectric behaviour in ZnO [3]. Further the role of simulation in designing and fabrication of GHz patch antenna using Cz grown organic crystals will also be presented [4].



In the present talk, different situations like synthesis of new ferroelectric system for enhanced piezoelectric properties, fabrication of new crystal growth system [5] etc. will be presented in which we need simulation.

IT-5

Modeling of Vapor-Phase Growth of Wide Bandgap Bulk Crystals and Epilayers

A.V. Kulik

STR Group, Inc. – Soft-Impact, Ltd., St. Petersburg, Russian Federation

E-mail: alexey.kulik@str-soft.com

Wide bandgap semiconductors, such as SiC and group-III nitrides, are advanced materials widely used for production of electronic and optoelectronic devices. Ever-increasing demand for improvement of performance of the devices and reduction of their degradation requires production of high-quality substrates and epitaxial layers. Experimental study of technologies for production of bulk crystals and epilayers of wide bandgap semiconductors is very expensive and time-consuming. For the last decades, numerical modeling has proved to be a tool assisting development, scaling and optimization of vapor-phase growth technologies. Use of modeling provides better understanding of physical mechanisms underlying the processes and, thus, facilitates optimization of both growth system design and the operating conditions. This work reviews basic principles of modeling of vapor-phase growth of wide bandgap bulk crystals and epilayers and the most significant physical effects which must be considered in simulations.

Modeling of bulk crystal growth

The most promising technique for growth of bulk crystals of SiC and group-III nitrides is Physical Vapor Transport (PVT) method also known as sublimation method. The sublimation growth is quite complex process involving many physical and chemical phenomena: conjugated heat transfer, gas mixture flow and species mass transport coupled with physical-chemical processes associated with the source sublimation and the crystal growth, flow through reacting porous medium, formation of parasitic deposits, thermoelastic stress, and defect generation. To accurately analyze the PVT process, all these phenomena should be taken into account.

One of the key aspects of PVT technique is temperature distribution in the growth system. Thermal field governs most of the physicochemical phenomena occurring in the growth of wide-bandgap crystals. Temperature determines heterogeneous chemical processes and, therefore, the growth rate and the shape of the crystal, source operation behavior and secondary phase formation. Temperature gradients in the crystal cause thermoelastic stress, which is one of the major reasons for generation of dislocations. Thus, accurate computation of thermal field is the primary problem in simulation of PVT. There are three basic mechanisms of heat exchange: conduction, convection and radiation. Each of them may be essential for temperature distribution depending on the growth conditions and, hence, must be accounted in the model of heat transfer. Additionally, heat exchange must be coupled with electromagnetic field in case of radio-frequency heating of the reactor. Fig. 1 shows results of computation of temperature distribution in RF-heated reactor for growth of bulk SiC crystals by PVT.

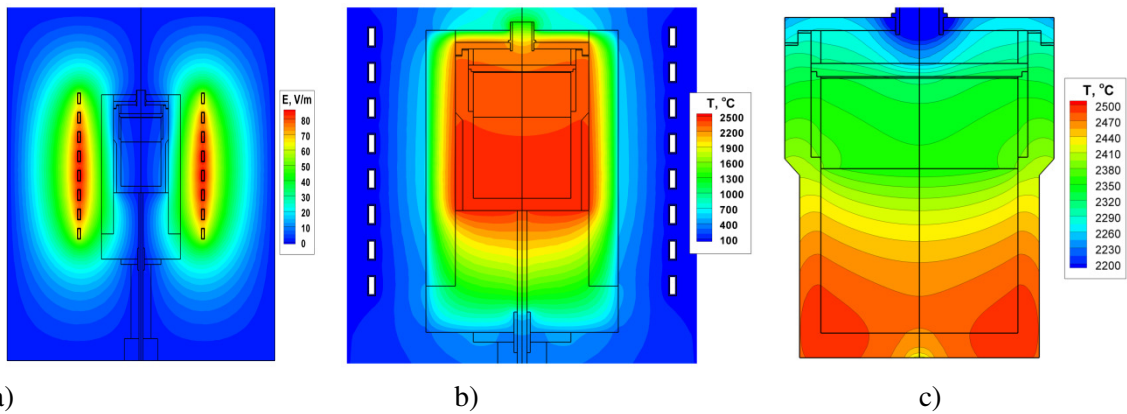


Fig. 1. Prediction of thermal field in RF-heated reactor for growth of bulk SiC crystals by PVT. (a) Distribution of the electric field. (b) Temperature distribution in the whole reactor. (c) Detailed temperature distribution in the growth crucible

Computation of temperature is very important but insufficient for complete and detailed understanding of the growth process. Mass transport in the growth system must be analyzed to predict the growth rate and the shape of the crystal, generation of secondary phase inclusions, formation of parasitic deposits, and efficiency of the source operation.

The vapor phase in sublimation growth is a multicomponent gas mixture. The reactive species are produced during the source material sublimation and then are transported to the seed surface where they condense giving rise to the crystal growth. Fig. 2a presents distribution in the growth chamber of mass fraction of one of the species (SiC_2) formed as a result of SiC sublimation. Mass transport involves both diffusion and convection. Intensive phase transitions (sublimation and condensation) generate a macroscopic directional flow from the source to the crystal, known as Stefan flow (Fig. 2).

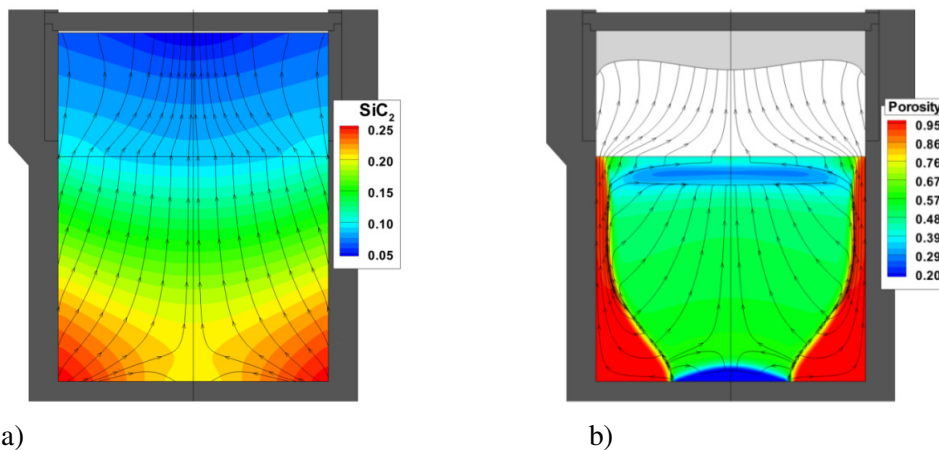


Fig. 2. (a) Distribution of SiC_2 mass fraction and flow pattern in the growth chamber at the beginning of the process. (b) Porosity distribution in the powder source and flow pattern in the growth chamber after 72 hours

Common practice in PVT is to use powder as a source material. Physical and chemical processes occurring in the powder charge during the growth affect the heat and mass transport in the growth chamber and, consequently, the growth rate and quality of the crystal. Also of practical interest are

questions of source utilization efficiency and its operation stability. The processes in the powder are very complex, especially in the case of SiC growth. Sublimation of source material is accompanied by its graphitization, leading to the formation of low-density graphite foam in the hottest regions of the chamber. The evaporated gas mixture is infiltrated through the porous medium of the powder and chemically interacts with the granules. Generally, condensation of the vapor on the granules is observed in colder zones of the source – near the powder top and sometimes in the bottom part of the powder. Because of this secondary crystallization, dense SiC disks are formed at the source top and bottom (Fig. 2b).

All sublimation-condensation processes occurring in PVT including crystal growth are the result of heterogeneous chemical reactions. The reactions take place at surfaces of the source, crystal, and also at the crucible walls. Interaction of vapor with crucible is especially significant in the case of SiC growth where graphite is primarily used as a crucible material. The surface chemistry at graphite walls generally leads to the graphite etching. This provides additional mass supply to the gas phase and, therefore, changes the gas composition and influences the growth rate and the crystal shape. To account for heterogeneous chemistry, quasi-thermodynamic model is used (for details refer to [A.S. Segal, et al., *Mater. Sci. Eng. B* 61–62 (1999) 40] and [S.Yu. Karpov, et al., *MRS J. Nitride Semicond. Res.* 4 (1999) 4]). This model provides a unified description of the surface chemistry and is applicable to various materials and growth techniques. Solution of surface chemistry problem is coupled with computation of mass transport in the gas, providing distributions of species concentrations and fluxes at the surfaces of the growth chamber. This information allows evaluation of the growth rate profile along the crystal surface.

There is a specific feature of sublimation technique which should be considered in modeling – the pressure in the growth chamber is not known a priori and must be found as a result of the computation. The pressure in the growth cell depends on external pressure outside the chamber, temperature distribution, and on the regime of mass exchange between the growth chamber and its ambient through the openings or porous material of the crucible.

Sublimation growth is essentially unsteady process. During a long-term operation, the crystal grows and the powder source changes its structure. Besides, process conditions, such as pressure, heating power, and inductor coil position, can be varied by growth engineers. All this leads to changing in heat and mass transport phenomena. Therefore, simulation of a long-term growth process accounting for evolution of the crystal shape and the source structure is a complex procedure governed by many factors. Fig.2b shows the growth chamber after 72 hours of growth. Evolution of the crystal shape during growth is presented in Fig. 3.

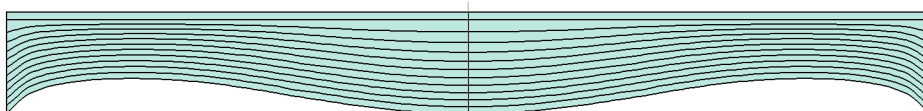


Fig. 3. Evolution of the crystal shape during growth. The lines represent the crystal shape at different instants. Time step between the instants is 5 hours. The total duration of the growth process is 55 hours

A matter of high importance is how the density and distribution of defects in the grown crystal are related to the growth conditions. Thermal stresses are commonly considered to be one of the main reasons for defect formation. Shear stress is a driving force for nucleation and multiplication of the basal-plane

dislocations which are known to be the primary structure defects limiting the material performance. High tensile stress can result in material cracking, completely destroying the whole crystal. The stress in the bulk crystals depends on the shape and size of the crystal, temperature distribution in the growth system and on mechanical interaction of the crystal with the crucible. The intensity of the effect the crucible has on the stress in the crystal depends on the crucible design, the way the crystal is bonded to the crucible, and on the crucible material. Fig. 4 shows distribution of the shear stress in AlN crystal and the crucible for the cases of BN and TaC crucibles.

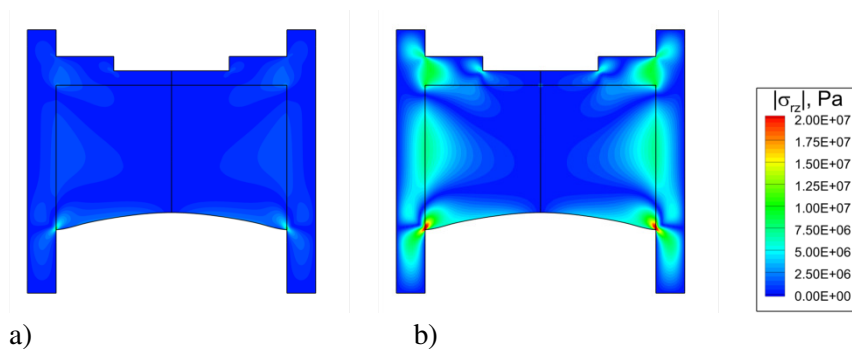


Fig. 4. Distribution of absolute value of shear stress σ_{rz} in AlN crystal grown by PVT method. Stress is shown in the crystal and the crucible. (a) Growth in BN crucible. (b) Growth in TaC crucible

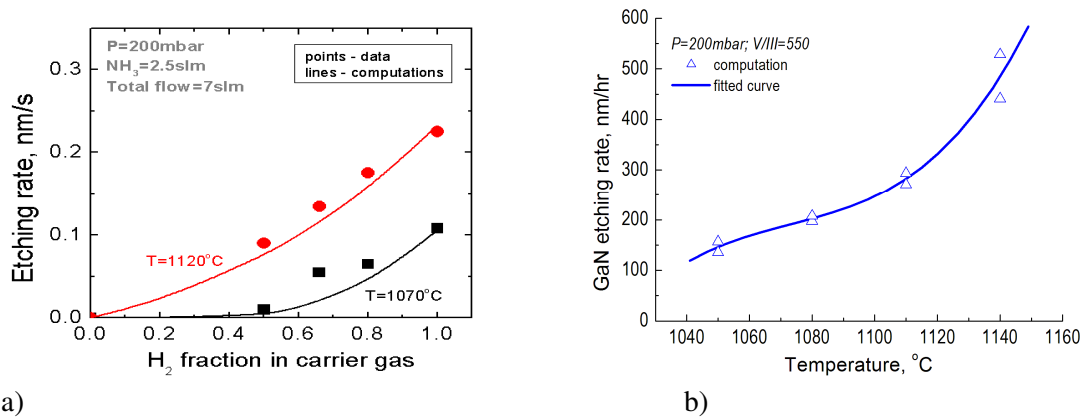
Modeling of epitaxial growth of thin films

Metal Organic Vapor Chemical Vapor Deposition (MOCVD) is the conventional technique for the growth of III-nitride epitaxial layers and device heterostructures. Elaboration of the process window and adjustment of the thickness and composition uniformity in epitaxy of III-nitride compounds should be considered in view of complex gas-phase and surface chemistry specific for these materials. Numerical modeling of MOCVD processes is now actively explored by both manufacturers and users of epitaxial reactors. To provide process conditions with high uniformity and efficient precursor utilization, one should account for gas-phase chemistry, including nucleation of nanoparticles at elevated pressures and long residence times in the reactors, surface chemical mechanisms, dramatically affected by growth temperature and carrier gas composition, and parasitic deposition, including low-temperature condensation of reaction products.

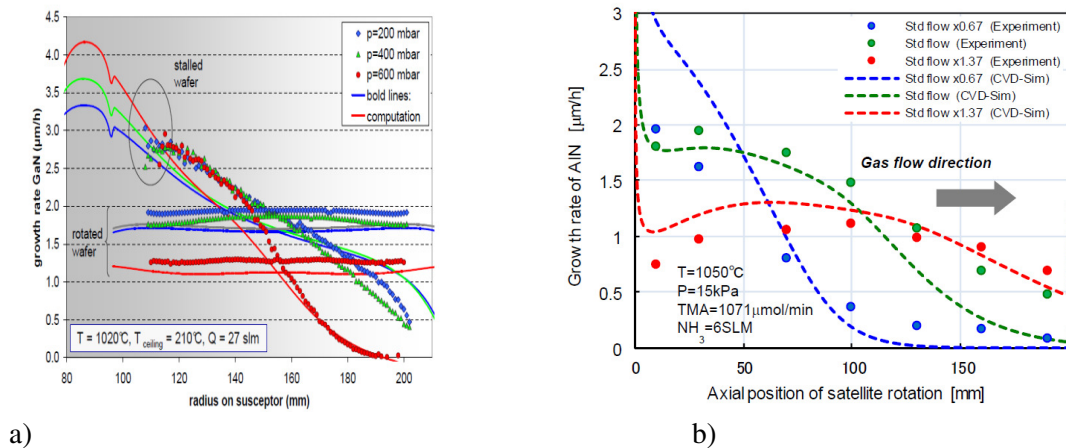
Unlike the case of arsenides and phosphides, hydrogen, typically used as the carrier gas in MOCVD, is strongly involved in the gas-phase and surface chemical processes during the growth of III-nitrides, having a strong impact on the growth rates and layer composition. In particular, interactions of (Al)GaN with hydrogen result in the etching of the GaN constituent of the alloy and, therefore, reduction of the growth rate and increase in the Al content. GaN etching rate as a function of the carrier gas composition and temperature are plotted in Fig. 5. Reduction of the H_2 fraction as well as of the temperature lowers the etching rate, but such conditions are normally unfavorable with regard to the material quality. This means that one should take etching into account when selecting process conditions, especially for thin layers requiring precise control of the composition.

Formation of nanoparticles in the gas-phase is another important aspect of the MOCVD technology. The particles are transported out of the reactor by the gas flow, thus not contributing to the growth and serving as a source of material losses. Reactor pressure, gas residence time (total flow), and

temperature are among the operating parameters that strongly affect particle generation. Fig. 6a illustrates the influence of the growth pressure on the GaN growth rate measured for stalled wafers in a planetary reactor. Up to the pressure of 400 mbar, the depletion curve is not affected by the pressure, which suggests a weak contribution of particle formation to the overall process. Further pressure increase results in a pronounced decrease of the growth rate in the downstream part of the wafer due to intensive gas-phase nucleation and respective material losses. A similar study was performed for AlN growth (Fig. 6b) in a large production-scale reactor equipped with 8" wafers: reduction of the total flow, compared to some standard conditions, increases the gas residence time and accelerates particle nucleation. As a result, the growth rate drops to almost zero around the center of the wafer.



a) Fig. 5. (a) GaN etching rate as a function of the carrier gas composition. (b) GaN etching rate versus temperature.



a) Fig. 6. (a) Pressure effect on the GaN growth rate in the Aixtron 8x4" Planetary Reactor. (b) AlN growth rate versus the total flow in the UR26K 6x8" Reactor by Taiyo Nippon Sanso.

It can be clearly seen that growth of bulk crystals and epitaxy are complex multi-physics, multi-scale processes. Physical and chemical phenomena underlying the growth are strongly coupled with each other. This requires a global model accounting for all the effects mentioned above. In this work, software package Virtual Reactor (www.str-soft.com) was used to perform modeling.

IT-6

Quaternary Heusler alloys for Spintronic Applications – A first principle study

Rita John and Namitha Anna Koshi

Department of Theoretical Physics, University of Madras, Chennai, India

*E-mail:ritajohn.r@gmail.com

Heusler alloys are attracting research importance due to their multifunctional nature i.e. a combination of functions (properties) within the same compound. These alloys are named after Fritz Heusler, 19th-century German mining engineer and chemist. Heusler alloys are intermetallic compounds made up of four interpenetrating fcc sublattices. Co-based Heusler compounds have gained considerable attention in the recent past due to their high Curie temperature, high spin polarization and tunable electronic structure with possible applications in spintronics. They have the general composition X_2YZ where X and Y are transition metals and Z is a sp element. Quaternary Heusler alloys (QHA) are formed when one of the X atoms is replaced by a third transition metal. The positions of Heusler, Half Heusler, Quaternary Heusler and Inverse Heusler Alloys are shown in figure 1.

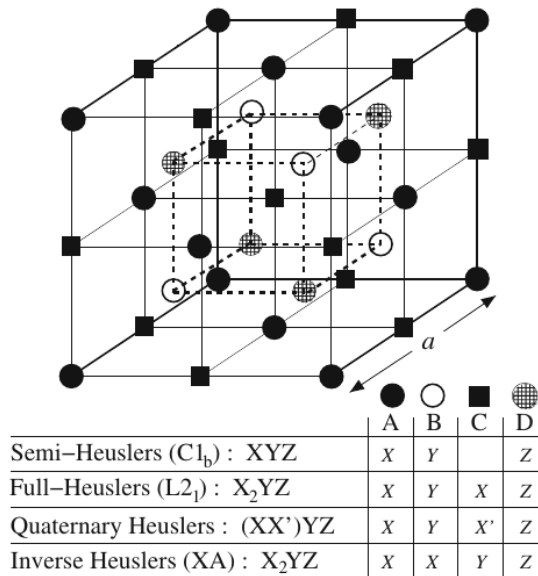


Figure1 Positions of atoms of Heusler Alloys

In this study, the structural, electronic, magnetic and transport properties of $CoFeNbZ$ ($Z = Al, Si$ and In) quaternary Heusler compounds are investigated employing the full potential linearized augmented plane wave (FP-LAPW) method implemented in WIEN2k code within the density functional theory prescription. The exchange and correlation effects are treated by using generalized gradient approximation (GGA). From the electronic and magnetic properties, it is found that $CoFeNbAl$ is a half-metal (Figure 2) with a spin flip gap of 0.33 eV and satisfies the $M_t = Z_t - 24$ Slater Pauling rule.

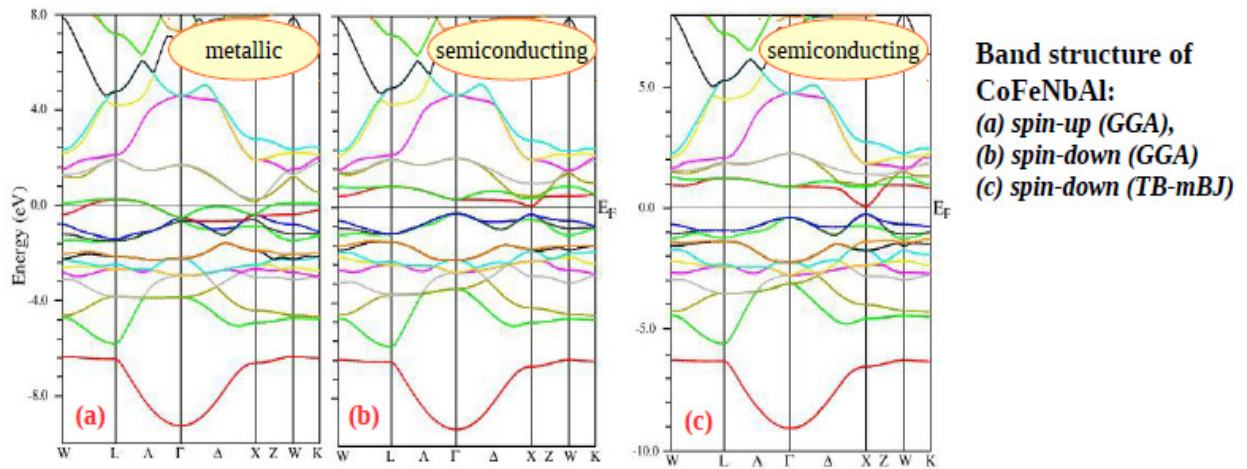


Figure 2: Band structure of CoFeNbAl (a) spin-up (GGA), (b) spin-down (GGA) (c) spin-down (TB-mBJ)

It is known that GGA underestimates the band gaps of semiconductors and insulators. Here, the Tran and Blaha modified Becke Johnson potential (TB-mBJ) is used to obtain reasonably accurate band gaps. The spin flip gap increases to 0.34 eV with the use of TB-mBJ and the nature of gap changes from indirect to direct. The half-metallic gap in CoFeNbAl arises due to the complex hybridization between the d-states of transition metals Co, Fe and Nb. CoFeNbIn has metallic behaviour in both spin channels. CoFeNbSi is a near half-metal with a near integer magnetic moment. The effect of hydrostatic strain on the magnetic and half-metallic properties of CoFeNbAl is determined. In the spin up channel, electrical conductivity decreases as a function of temperature whereas it increases in the spin down channel for CoFeNbAl. This affirms the metallic behaviour in the spin up channel and the semiconducting behaviour in the spin down channel. The high spin polarization and robustness of half-metallicity against hydrostatic strain makes CoFeNbAl a potential candidate for spintronic applications.

IT-7

Generation and Propagation of Dislocations In Multicrystalline Silicon for Solar Cell

Kentaro Kutsukake^{1*}, Yusuke Hayama², Tetsuya Matsumoto³, Hiroaki Kudo³, Tatsuya Yokoi², Yutaka Ohno⁴, and Noritaka Usami²

¹ Center for Advanced Intelligence Project, RIKEN, 1-4-1 Nihonbashi, Chuo-ku, Tokyo 103-0027, Japan

² Graduate School of Engineering, Nagoya University, Furocho, Chikusa-ku, Nagoya 464-8603, Japan

³ Graduate School of Informatics, Nagoya University, Furocho, Chikusa-ku, Nagoya 464-8601, Japan

⁴ Institute for Materials Research, Tohoku University, 2-1-1 Katahira, Aoba-ku, Sendai 980-8577, Japan

*E-mail: kentaro.kutsukake@riken.jp

Dislocations are the most harmful crystallographic defects in multicrystalline silicon for solar cells. They act as recombination sites for photogenerated carriers and decrease the solar cell performances. Numerous observations of etch pits distribution and photoluminescence images on ingot cross-sections have showed that dislocations are generated from grain boundaries and propagate in the growth direction of the ingot accompanied by increase of their density. Therefore, control of generation and propagation of dislocations during crystal growth processes is one of important issues to improve the performance of solar cells using multicrystalline silicon wafers. In this paper, generation mechanism of dislocations will be discussed, in particular in terms of influence of grain boundary structures. In addition, a new research approach that is three-dimensional imaging of configuration of dislocation clusters in an ingot will be presented.

Figure 1 shows schematic illustration of influence of grain boundary structure on dislocation generation. Stress, which is driving force of dislocation generation, is induced by crystal growth phenomena, such as temperature gradient, difference of thermal expansion coefficient, and volume expansion at solidification. Grain boundary structure is expected to influence on the stress that generates dislocations through two parameters: critical stress and stress concentration [1]. The critical stress of dislocation generation depends on microstructure of grain boundaries. In particular, in the case of coincidence site lattice (CSL) grain boundaries and small angle boundaries, their microstructure is very sensitive to misorientation angle and its components. Therefore, small difference of the angle and components of misorientation results in a large difference of the amount of generated dislocations [2]. On the other hand, the microstructure of random grain boundaries is insensitive to small changes in the misorientation angle and its components. Thus, difference of amount of generated dislocations from random grain boundaries in an ingot originates from difference of stress concentration [3]. This means that stress changes with crystal orientation while the strain induced by crystal growth is the same. In addition, in some cases of crystal orientation combination of the grains, discontinuous change of elastic constant across a grain boundary produces stress concentration around the grain boundary. For these reasons, amount of dislocations from random grain boundaries depends on their macroscopic structure i.e. large angle change of misorientation.

The above story considered simple multicrystalline structure and has been demonstrated in crystal growth experiments of mono-like silicon with straight and few numbers of artificial grain boundaries. However, in the case of practical ingot growth of multicrystalline silicon, multicrystalline structure is

much complicated: random crystal orientation, various size of grains, curved grain boundaries, and formation and annihilation of grains. Therefore, to reveal the generation mechanism of dislocations in practical multicrystalline silicon ingots, understanding of the complicated three-dimensional configuration of crystal grains and dislocation clusters is the first step. For this issue, we tried to visualize dislocation clusters inside the ingots [4]. Figure 2 shows an example of three-dimensional visualization of configuration of a dislocation cluster reconstructed by stacking of photoluminescence images of adjacent wafers in an ingot. To analyze a number of wafers, we developed automatic program to extract dislocation area from the images and three-dimensionally construct the clusters using various image process techniques. Using this program, generation, propagation, and annihilation of a dislocation cluster in a multicrystalline ingot was clearly visualized. This technique will be useful for revealing defects generation mechanism in the growth of practical multicrystalline silicon ingots.

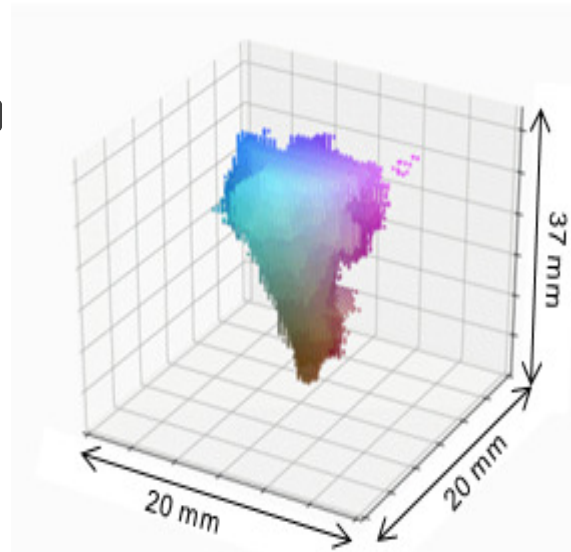
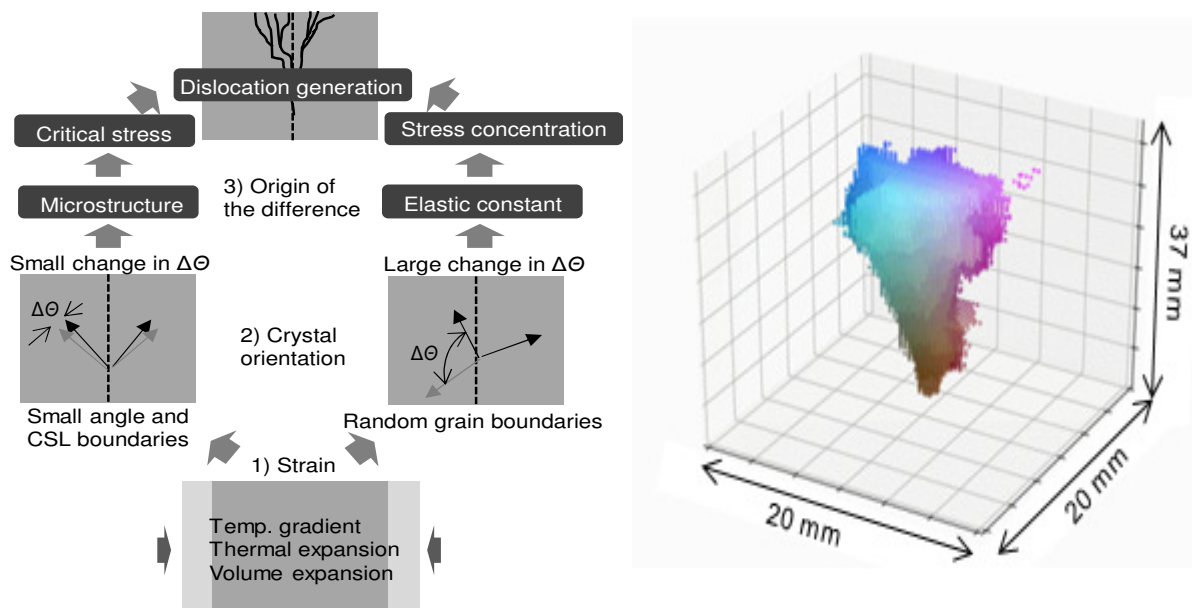


Fig. 1 Schematic illustration of mechanism of dislocation generation from grain boundaries, Fig. 2 A dislocation cluster three-dimensionally visualized by the automatic program.

Acknowledgment

This work was partly supported by JST/CREST, Grant No. JPMJCR17J1 (2017-2023) and JSPS KAKENHI Grant (No. 16H03856).

REFERENCES

- [1] K. Kutsukake, Chap. Growth of Crystalline Silicon for Solar Cells: Mono-Like Method, in Handbook of Photovoltaic Silicon edited by D. Yang, (Springer-Verlag GmbH, Germany, 2018).
- [2] K. E. Ekstrøm, G. Stokkan, R. Søndena, H. Dalaker, T. Lehmann, L. Arnberg, M. Di Sabation, Phys. Status Solidi A 212, 2278 (2015).
- [3] I. Takahashi, N. Usami, K. Kutsukake, G. Stokkan, K. Morishita, K. Nakajima, J. Cryst. Growth 312, 897 (2010).
- [4] Y. Hayama, T. Matsumoto, T. Muramatsu, K. Kutsukake, H. Kudo, and N. Usami, Sol. Energ. Mat. Sol. Cells 189, 239 (2019).

IT-8

Develop Functional Materials for Energy Harvesting From Ab Initio Calculations

P.Ravindran

¹*Department of Physics, Central University of Tamil Nadu, Thiruvarur, Tamil Nadu, 610005, India*

²*Simulation Center for Atomic and Nanoscale MATerials (SCANMAT), Central University of Tamil Nadu, Thiruvarur, Tamil Nadu, 610005, India*

Identifying advanced functional materials with efficiency higher than current level is one of the key areas of research. Studying materials with multiple functionalities attract much attention in recent years to resolve important issues such as energy crisis, environmental degradation etc. Also, by controlling various order parameters involved in magnetic, electric and lattice coupling one can tune the properties of functional materials to the desired level. So, using state-of-the-art ab initio methods we have studied magnetic, electric, optical, magnetoelectric, magneto-optic, photoelectric, photocatalytic, thermoelectric, and electro-chemical properties of materials useful for energy and environmental technologies.

Converting solar energy into fuel via photocatalytic water splitting to generate hydrogen is an attractive scientific and technological goal to address the increasing global energy demand. Converting solar energy into fuel via photocatalytic water splitting to generate hydrogen is an attractive scientific and technological goal to address the increasing global energy demand. It is to be noted that solar water splitting no doubt represents a promising and sustainable method for energy production. But its relatively low-energy conversion efficiency limits its practical applications. Hence, there is an urgent demand to put in greater efforts to design/fabricate or search for new potential photocatalytic materials with improved efficiency. Recently, two dimensional (2D) materials drawn great attention in the field of photocatalytic water splitting because of the fast migration of charge carriers to the reactive sites, large surface area, and reduced recombination rate. Other than transition-metal dichalcogenides, phosphorene, Group III–VI monochalcogenides, and MXene, Carbon-nitride based nanostructures attract research community due to their suitability as photocatalyst for water splitting. Its unique structure and exotic properties created interest among the researchers to search for other 2D carbon nitrides such as g-CN, C₂N, g-C₄N₃, C₃N, C₄N, and so on and so forth. C₂N and g-CN are new to carbon nitride family and they show interesting properties for photocatalytic water splitting applications. This talk will focus in detail on modelling and tailoring the band gaps and band edge positions of carbon nitrides suitable for water splitting applications. Specifically, the influence of isoelectronic substitutions/molecular adsorption on photocatalytic water splitting activity will be discussed.

In order to understand the role of W-site substitution on mechanical properties of cubic tungsten carbide (β -WC), we have investigated the structural, mechanical, and electronic properties of WXC₂ (X = Si, Sc, Ti, V, Cr, Ge, Y, Zr, Nb, Mo, Ru, Rh, Pd, Ag, Cd, Sn, Hf, Ta, Re, Os, Ir, Pt, Th, U) using first principles calculations based on density functional theory, within generalized gradient approximation. The structural optimization has been carried out for all these compounds using force as well as stress minimization. The optimized structural parameters for experimentally known compounds are in good agreement with the available X-ray diffraction measurements and structural parameters for nineteen WXC₂ compounds are newly predicted. The W-site substitution of the above-listed elements into β -WC reduces the symmetry of the crystal from cubic to tetragonal. The heat of formation (ΔH_f) and the

mechanical stability studies are carried out to investigate the stability of these systems. Based on the results, we have found that IrWC₂, PtWC₂, and OsWC₂ are mechanically unstable phases. The single-crystal elastic constants C_{ij} elastic moduli of the polycrystalline aggregates, anisotropy in elastic constants and related properties of the WXC₂ materials are calculated and discussed in detail. The hardness of the above materials is predicted using two different criteria, based on the softest elastic mode as well as the Pugh's modulus ratio. There is a correlation in the hardness predicted from these two approaches except in the case of β -WC and AgWC₂. The chemical bonding interaction between the constituents is analysed using the density of states, crystal orbital Hamiltonian population, and charge density for selected systems. All these compounds are predicted to be metal and our calculations suggest that W-site substitutions do not improve the hardness of β -WC. However, from the heat of formation studies, we have identified five new stable compounds such as CrWC₂, NbWC₂, ScWC₂, YWC₂, and UWC₂ with reasonably good hardness and those need experimental verifications.

In solids, crystal structure describes the orderly arrangement of constituent atoms. Knowing the crystal structure is absolutely mandatory for any further theoretical investigation of a material. Predicting the crystal structure of an unknown material from first principles, even before it is synthesized is still one of the most challenging and interesting issue in materials research and development. Here, we present the results from ab-initio calculations based on density functional theory on a series of ternary antiperovskite compounds: Be₃PN, Mg₃PN, Ca₃PN, Sr₃PN, Ba₃PN and Zn₃PN. We have predicted the equilibrium crystal structures of these compounds using structural optimization with stress and force minimization by considering the potential structures of 32 space groups in to the calculation. The calculations were performed using the Vienna ab-initio Simulation Package (VASP) within the Generalized Gradient Approximation (GGA). We have predicted that the ground state of all the compounds have orthorhombic structure with a space group of *P21ma*, except Be₃PN for which stabilizes in a space group of *Pbmm*. We have done a systematic study on the structural characteristics of the compounds. The electronic properties are also analyzed to explain the bonding characteristics and stability in these compounds. Our results represent a step toward a more complete understanding of the structural and electronic properties of the mentioned compounds. This is the first quantitative theoretical prediction of structural and electronic properties of Be₃PN, Sr₃PN, Ba₃PN and Zn₃PN compounds that require experimental confirmation.

For the last few decades, developing efficient Li-ion battery technology is one of the vibrant fields of research. There are several research groups working on various components of Li-ion batteries such as anode, cathode and electrolyte. In our studies, we mainly focus on developing high efficiency cathode materials for Li-ion batteries. Structural stability and the electronic properties of LiNiBO₃ and LiFe_xNi_(1-x)BO₃ are studied using first principle calculations based on density functional theory. The calculated structural parameters are in good agreement with the available theoretical data. The most stable phases of the Fe substituted systems are predicted from the formation energy hull generated using the cluster expansion method. The bonding mechanisms of the considered systems are discussed based on the density of states (DOS) and charge density plot. The detailed analysis of the stability, electronic structure, and the bonding mechanisms suggests that the systems can be a promising cathode material for Li ion battery applications. Since the presence of multiple Li atoms in this material is one of the open windows to improve the capacity of cathodes in Li-ion batteries. We have also investigated the battery related properties of Li₆FeS₄ and its Mn substituted derivative such as Li₆Mn_{0.5}Fe_{0.5}S₄ and Li₆MnS₄ using ab-initio calculations. The total energy calculations predict the G-type antiferromagnetic insulating ground state for parent and fully substituted system. The 50% Mn substituted system stabilizes with ferrimagnetic insulating ground state due to unequal magnetic moments at the Fe and Mn sites. The calculated enthalpy

of formations using VASP code confirmed the stable nature of these systems. Among these three systems, the 50% Mn substituted one is found to have higher stability. The 300 K voltage profile is plotted using Monte-Carlo techniques as implemented in Cluster Assisted Statistical Method (CASM) code. The average voltage is found to decrease with the increase of Mn content. The density of states analysis shows that there is a covalent hybridization between transition metal d states and sulphur p states.

We have demonstrated the battery-related properties of $\text{Li}_2\text{Fe}(\text{SO}_4)_2$ and its Fe site Ti substituted derivatives ($\text{Li}_2\text{Ti}_{0.5}\text{Fe}_{0.5}(\text{SO}_4)_2$ and $\text{Li}_2\text{Ti}(\text{SO}_4)_2$) using *ab-initio* calculations. The calculated voltage profile of all these systems clearly indicates the increase of voltage with delithiation. Even though the average voltage values of Ti-substituted systems gradually changes with the Ti concentration, they are still in the range of requirement for a good cathode material. In most of the cases, Ti substitutions increase the specific capacity and energy density of $\text{Li}_2\text{Fe}(\text{SO}_4)_2$. The negative enthalpy of formation implies that all the considered systems are thermodynamically stable. These results indicate that Ti-substituted $\text{Li}_2\text{Fe}(\text{SO}_4)_2$ could be a potential cathode material for rechargeable Li-ion batteries.

We have also analysed the thermodynamic properties of the monoclinic NaMnO_2 with density functional theory-based calculations. Cluster expansion methods are used to find the minimum formation energy configurations at different concentrations of Na removal. This material shows a strong Na vacancy ordering during the extraction of Na from the host structure. Several ground state configurations as a function of Na composition are predicted by the cluster expansion method. The thermodynamic intercalation potential of the electrode is calculated using Monte Carlo simulation. The stability of the cathode material at higher temperatures are also analyzed.

Storage of hydrogen in chemical compounds offers a much wider range of possibilities to meet the transportation requirements, but no single material investigated to date exhibits all the necessary properties. In order to identify potential materials for hydrogen storage application worldwide attention has been focused on hydrides with high gravimetric and volumetric capacity. Hydrogen is a unique element that possess positive, negative or neutral oxidation state in solids depending upon the chemical environment. More than 35% of hydrides, hydrogen is in negatively charged state and their equilibrium inter-atomic state is governed by "The 2 Å-rule" which limit the design of new hydrogen storage materials with high volume density. If one can find hydrogen storage materials where hydrogen is present in both negative and positive oxidation state within the same structural frame work then one can accommodate hydrogen with high volume density because of the attractive interaction between oppositely charged hydrogen. Moreover, it is highly unusual to have hydrogen with both positive as well as negative oxidation state in the same structural framework and hence very few such compounds are reported in the literature based on structural study. So, it is fundamentally as well as technologically important to identify compounds in which hydrogen is in amphoteric nature and understand the necessary criteria for its origin. The experimental structural analysis of Cyclotriborazane and Diammonium dodeca hydro-closo-dodecaborate with the chemical formula, $(\text{BH}_2\text{NH}_2)_3$ and $(\text{NH}_4)_2(\text{B}_{12}\text{H}_{12})$, respectively insinuate the presence of partially charged hydrogen with anionic and cationic behavior. The equilibrium structural parameters obtained from structural optimization including force as well as stress minimization with GGA functional deviate from corresponding experimental parameters by more than 5%. So, in order to understand the role of van der Waals (vdW) interactions on structural parameters we have considered 12 difference vdW corrected functional for the structural optimization and found that the optPBE-vdW functional predict the equilibrium structural parameters reliably with less than 0.009 % deviation from experimental result. So, the optPBE-vdW functional is used to calculate charge density, ELF, total as well

as partial density of state, Bader and Born effective charge analysis etc. We have observed that hydrogen is exhibiting amphoteric behavior with H closer to B in the negatively charged state and that neighboring to N is in positively charged state. Due to the presence of finite covalent bonding between the constituents in $(\text{BH}_2\text{NH}_2)_3$ and $(\text{NH}_4)_2(\text{B}_{12}\text{H}_{12})$ the oxidation state of hydrogen is observed to be a non-integer value. The possible origin of amphoteric behavior of hydrogen in $(\text{BH}_2\text{NH}_2)_3$ and $(\text{NH}_4)_2(\text{B}_{12}\text{H}_{12})$ is analyzed. The present demonstration of amphoteric behavior of hydrogen in same structural frame-work has huge implication on designing hydrogen storage materials with high volume density.

Alkaline-earth hydrides (AH_2) are considered as potential hydrogen storage materials owing to their high hydrogen storage capacity, light weight, low cost, and abundance. Due to high decomposition temperature and slow sorption kinetics, these hydrides cannot be used for practical hydrogen storage applications. In our studies, we attempted to destabilize the strong ionic bonding between alkaline earth metal and hydrogen in these hydrides by anionic/cationic substitution. First, we have substituted fluorine at hydrogen site in alkaline earth hydrides. We have analysed the structural stability, electronic structure, and chemical bonding of AH_2 and fluorinated AH_2 ($\text{AH}_{2-x}\text{F}_x$). We found that the enthalpy of formation and H site energy increases with increase of fluorine substitution. Hence, $\text{AH}_{2-x}\text{F}_x$ are relatively more stable than the corresponding pure hydrides. The positive and very low value of enthalpy of mixing for $\text{AH}_{2-x}\text{F}_x$ imply that single-phase of $\text{AH}_{2-x}\text{F}_x$ may form at reasonable temperatures. The electronic structure calculations reveal that $\text{AH}_{2-x}\text{F}_x$ are insulators. The chemical bonding analyses conclude that $\text{AH}_{2-x}\text{F}_x$ are governed mainly by ionic bonding. Our results suggest that hydrogen closer to fluorine can be removed more easily than that far away from fluorine since the fluorination brings disproportionation in the bonding between the constituents.

In our second attempt, we explored how solid solutions involving metastable ZnH_2 with MgH_2 can improve the hydrogen storage properties of MgH_2 . ZnH_2 has been known for many years as a meta-stable compound with white colour that will decompose easily. So, its crystal structure is not yet identified experimentally. By considering 37 different AB_2 type of structural variant into the calculation, we have predicted the ground state crystal structure of ZnH_2 which is found to be $\text{Pna}2_1$ (orthorhombic). Since ZnH_2 is metastable in nature, it cannot be used for practical hydrogen storage applications. We have analysed the structural stability, electronic structure, and chemical bonding of Zn substituted MgH_2 ($\text{Mg}_{1-x}\text{Zn}_x\text{H}_2$). The calculated enthalpy of formation and H site energy calculations suggest that Zn substitution reduces the stability of MgH_2 , thereby it may reduce the decomposition temperature of MgH_2 . The electronic structure calculations show that the $\text{Mg}_{1-x}\text{Zn}_x\text{H}_2$ systems are insulators. The chemical bonding behaviour of $\text{Mg}_{1-x}\text{Zn}_x\text{H}_2$ systems is established as ionic-covalent in nature. Moreover, Zn substitution in MgH_2 induce disproportionate Mg-H bonds which could also contribute the reduction in the decomposition temperature as well as H sorption kinetics. Hence, $\text{Mg}_{1-x}\text{Zn}_x\text{H}_2$ could be a potential materials for hydrogen storage applications.

In another study, we have performed Ti (2+, 3+, and 4+) substituted MgH_2 . Our calculated enthalpy of formation and H site energy implies that Ti substitution in Mg site reduces the stability of MgH_2 which may improve the hydrogen storage properties. Our results reveal that Ti in the +4 oxidation state in MgH_2 :Ti is favorable for H storage applications. The bonding analyses confirm the existence of ionic-covalent nature. Electronic structure obtained from hybrid functional calculations show that intermediate bands (IB) are formed in Ti^{4+} substituted MgH_2 which could improve the solar cell efficiencies due to multiple photon absorption from valence band to conduction band via IBs and converts low energy photons in the solar spectrum also into electricity. Further, our calculated carrier effective

masses and optical absorption spectra show that Ti^{4+} substituted MgH_2 is suitable for higher efficiency photovoltaic applications. Our results suggest that Ti^{4+} substituted MgH_2 can be considered as a promising material for hydrogen storage as well as photovoltaic applications.

With the rise in economy and population in the 21st century world has urge more demand of the energy consumption for everyday work which produces the harmful chemical and gases to the environment and hence increase the global warming. In the present scenario there has been lots of research developed to find the alternative energy technologies to reduce the energy supply gap. Thermoelectric materials (TE) can be the one of the solution to reduce the energy consumption by converting the waste heat energy into useful electrical energy. One of the major challenge for the researchers is to find the low cost, light weight and environment friendly materials for waste heat recovery. Half Huesler (HH) alloys are considered as the good candidates to deliver all the requirements. HH alloys are ternary intermetallic compounds with the general formula XYZ in which X and Y are typically transition metals and Z is a main group element. The efficiency of the TE materials can be calculated as the dimensionless figure of merit $ZT = S^2\sigma T/\kappa$, where S is Seebeck coefficient, σ is electrical conductivity, κ is total thermal conductivity i.e. electronic and thermal conductivity ($\kappa_e + \kappa_l$) HH alloys conserve the semiconducting behavior by transferring the valence electrons from electropositive element X to more electronegative elements Y and Z provide the stable closed shell configuration i.e. a d^{10} for Y and s^2p^6 configuration for Z . HH alloys based on TiCoSb has been investigated extensively over a past decades. Experimentally it has been found that TiCoSb has high power factor. But it also shows high thermal conductivity which decreases the efficiency. One of the successful approach adopted by the researchers to reduce the thermal conductivity is isoelectronic substitutions of different size atom at the sites of Ti , Co and Sb of TiCoSb alloys. Isoelectronic substitutions cause additional phonon scattering centre which reduces the thermal conductivity and hence expected to increase the efficiency of the system. In our previous studies we have reported that the multinary substitution without altering the 18 valance electron count rule (VEC) can increase the phonon scattering center in the system and hence increases the ZT .

In order to improve the thermoelectric performance of TiCoSb we have substituted 50% of Ti equally with Zr and Hf at Ti site and Sb with Sn and Se equally at Sb site. The electronic structure of $\text{Ti}_{0.5}\text{Zr}_{0.25}\text{Hf}_{0.25}\text{CoSn}_{0.5}\text{Se}_{0.5}$ is investigated using the full potential linearized augmented plane wave method and the thermoelectric transport properties are calculated on the basis of semi-classical Boltzmann transport theory. Our band structure calculations show that $\text{Ti}_{0.5}\text{Zr}_{0.25}\text{Hf}_{0.25}\text{CoSn}_{0.5}\text{Se}_{0.5}$ has semiconducting behavior with indirect band gap value of 0.98 eV which follow the empirical rule of 18 valance-electron content to bring semiconductivity in half Heusler compounds, indicating that one can have semiconducting behavior in multinary phase of half Heusler compounds if they full fill the 18 VEC rule and this open-up the possibility of designing thermoelectrics with high figure of merit in half Heusler compounds. We show that at high temperature of around 700K $\text{Ti}_{0.5}\text{Zr}_{0.25}\text{Hf}_{0.25}\text{CoSn}_{0.5}\text{Se}_{0.5}$ has high thermoelectric figure of merit of $ZT = 1.05$ which is higher than that of TiCoSb (~ 0.95) suggesting that by going from ternary to multinary phase system one can enhance the thermoelectric figure of merit at higher temperatures

Materials of multifold functionalities such as ferroelectricity, magnetism^{1,2}, and ferroelasticity have been receiving everlasting attention, driving substantial efforts in miniaturization, integration, and high-density storage technologies of devices/systems are made of these materials^{3,4}. One of the driving forces along these lines is an exploration of multiferroic materials in which multifold ferroic functionalities coexist and inter-coupled, resulting promising potential applications. But the co-existence

of (anti)ferroelectricity and (anti)ferromagnetism is rare. This is because, in usual perovskite-based ferroelectrics like BaTiO₃, the ferroelectric distortion occurs due to the displacement of B-site cation (Ti) with respect to the oxygen octahedral cage. Here the transition metal ion (Ti in BaTiO₃) requires an empty “*d*” shell since the ferroelectric displacement occurs due to the hopping of electrons between Ti “*d*” and O “*p*” atoms. This normally excludes any net magnetic moment because magnetism requires partially filled “*d*” shells. However, partially filled “*d*” shell on the B-site reduces the tendency of perovskites to display ferroelectricity. For the coexistence of magnetism and ferroelectricity (multiferroic), one possible mechanism is lone-pair driven where the A-site drives the displacement and partially filled “*d*” shell on the B-site contributes to the magnetism. Our work is mainly focused on computationally designed new series of multiferroic materials where two mechanisms ($6s^2$ lone-pair electrons, Ti⁴⁺ cations with *d*⁰-ness) for ferroelectricity coexist, such as $x\text{BaTiO}_3-(1-x)\text{BiCoO}_3$ ⁵, $x\text{PbTiO}_3-(1-x)\text{BiCoO}_3$ ⁶, $\text{PbTi}_{1-x}\text{V}_x\text{O}_3$ ⁷, Bi_2XTiO_6 ($X = \text{Mn, Fe, Ni}$)⁸⁻¹⁰. The magnetic cations with *d*^{*n*} configuration take care of the magnetic properties. These compounds are interesting for advanced technological applications because their magnetic properties can be tuned with applied electric field and vice-versa. In extreme cases, an applied electric field can also make a magnetic-to-nonmagnetic transition and similarly a ferroelectric-to-paraelectric phase transition can be obtained by an applied electric field. This kind of coupling between the electric and magnetic order parameters is called giant magnetoelectric coupling. In this presentation, we will discuss about the mechanisms behind such kind of giant coupling. This work also demonstrates that the cooperative effect of strong lattice coupling with different order parameters on the magnetoelectric properties which would be important to develop multifunctional materials for advanced technologies.

References

- M.R. Ashwin Kishore, H. Okamoto, Lokanath Patra, R. Vidya, Anja O. Sjøstad, H. Fjellvåg, P. Ravindran, *Phys. Chem. Chem. Phys.* 18, 27885 (2016)
- Lokanath Patra, M.R. Ashwin Kishore, R. Vidya, Anja O. Sjøstad, H. Fjellvåg, P. Ravindran, *Inorganic Chemistry* 55 (22), 11898-11907 (2016).
- Bibes, Manuel, and Agnès Barthélémy. *Nature materials* 7.6 (2008): 425-426.
- Cheong, Sang-Wook, and Maxim Mostovoy. *Nature materials* 6.1 (2007): 13-20.
- Lokanath Patra, Zhao Pan, Jun Chen, Masaki Azuma, P. Ravindran, *Phys. Chem. Chem. Phys.* (20), 7021-7032. (2018)
- Zhao Pan, Jun Chen, Lokanath Patra, P. Ravindran et. al. *Chemistry of Materials* (in press).
- Lokanath Patra, R. Vidya, H. Fjellvåg, and P. Ravindran, Submitted to *Inorganic Chemistry*.
- Lokanath Patra, P. Ravindran, *AIP Conference Proceedings* 1832 (1), 130053 (2017)
- Lokanath Patra, P. Ravindran, *AIP Conference Proceedings*, 1942 (1), 130054 (2017)
- Lokanath Patra, P. Ravindran, *AIP Conference Proceedings*, 1953 (1), 120039 (2017).

IT-9

Numerical Simulation of the Float Zone Process for Silicon: Comparison of Modeling Approaches in COMSOL Multiphysics

Robert Menzel,*and Kaspars Dadzis

Leibniz-Institut für Kristallzüchtung (IKZ), Max-Born-Str. 2, 12489, Berlin, Germany

*E-mail: robert.menzel@ikz-berlin.de,

Numerical simulation of the Float Zone (FZ) process for growth of ultra-pure silicon remains an essential tool to improve material quality, process yield and reduce production cost. A variety of mathematical model chains for the calculation of electromagnetic (EM), temperature, thermomechanical stress, melt flow and dopant concentration fields have been developed. These models are based on different modeling approaches, assumptions and simplifications for reduction of computational costs. However, the literature on the applicable range for which these assumptions are valid and the modeling error that arises from the negligence or simplification of physical correlations is still scarce. The present work aims to fill this gap and elaborates on some of the most common FZ modeling approaches and their implications on the numerical accuracy. The investigations were carried out using the FZ model chain shown in Fig.1, which was developed in the Finite Element Method (FEM) based multiphysics platform COMSOL [1].

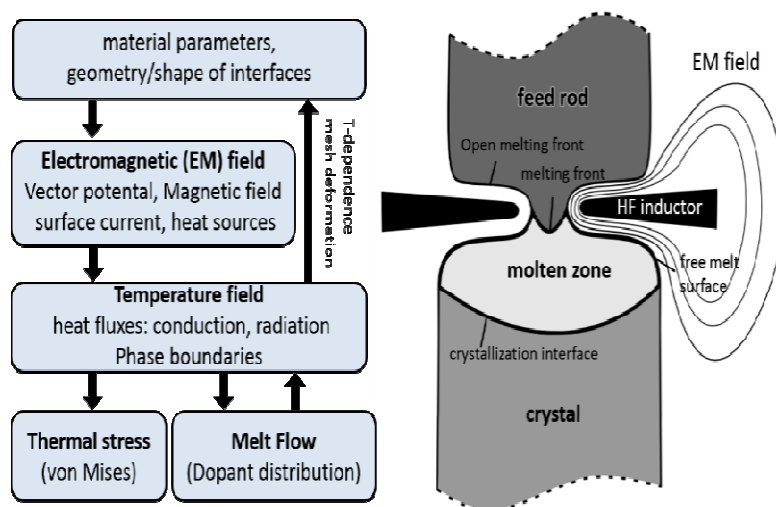


Fig. 1. FZ model chain

A very common modeling approach is assuming axial symmetry of the FZ system. One of the first fully axisymmetric models for calculation of EM, temperature- and stress field as well as fluid flow was presented by Mühlbauer et al. [2,3]. Due to azimuthal homogenization by crystal and feed rod rotation, the assumption of an axisymmetric field distribution is well fulfilled for the temperature. Furthermore, it is valid for the EM field, if high frequency (HF) pancake inductors with simple geometry are considered. However, for growth of FZ crystals with large diameter, more sophisticated HF inductors with distinct 3D characteristics as shown in Fig.2 are used. Here, the non-symmetry of the EM field distribution has impact on temperature and fluid flow [4]. The COMSOL FZ model presented in the current work uses a

combined 3D-2D method, in which the EM quantities are first calculated in 3D and then projected on the boundaries of a 2D FE mesh, for further evaluation of the azimuthal average of the EM result quantities [1]. If in a subsequent case study 3D aspects need to be considered, e.g. for calculation of melt flow or thermal stress, which is inherently three-dimensional in silicon, the 2D temperature solution can be projected back to a 3D mesh again. The differences between the 2D and 3D solutions will be explained.

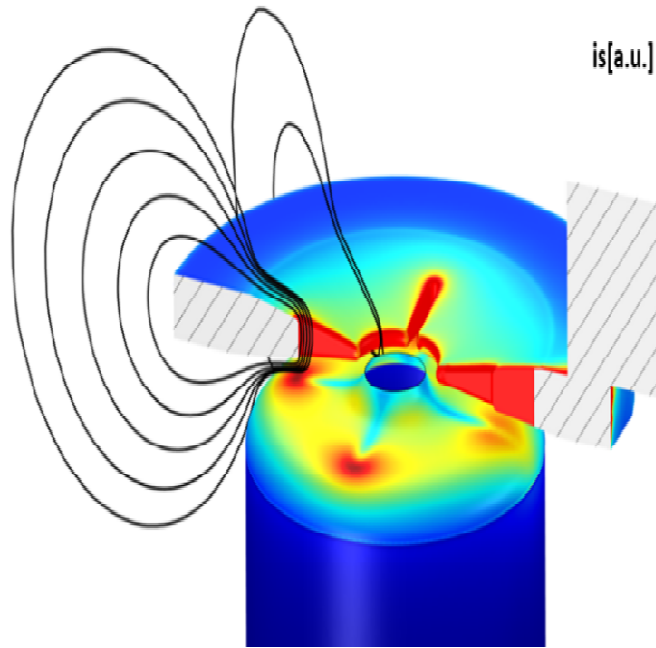


Fig. 2. Surface current distribution generated by a HF inductor during a 4'' FZ process

The high-frequency approximation is a useful approach to efficiently model the HF EM field in the inductively heated FZ process. Due to the distinct skin effect at $f = 3$ MHz, the EM field in the conductors is concentrated in a thin layer near the surface. Resolving the skin layer would require a locally extremely fine FEM mesh. Hence, the Boundary Element Method (BEM) has been applied for FZ process simulation, as it requires solution of the field variables on the domain boundaries only [5]. In the presented FEM-based FZ model, the need to resolve the skin layer is avoided by applying the so called Impedance Boundary Condition (IBC). The IBC relates the components of the electric field and the magnetic field tangential to the surface via a surface impedance:

$$Z = \frac{1 + j}{\sigma \delta},$$

where σ is the electric conductivity and δ is the skin depth. The IBC boundary condition is imposed to model the interfaces between the conductors and the gas atmosphere in the FZ process. Enforcing the IBC allows to remove the conductor domains and, hence, drastically reduces the number of unknowns. The system of equations for the EM field needs to be solved only in the gas domain bounded by the surfaces of the conductors and an exterior bounding surface. The results obtained in COMSOL using the IBC are compared to numerical results, in which ideal conductors are assumed and the penetration depth is zero. Both numerical results are compared to experimental results obtained in a measuring station for the magnetic field generated by HF inductors.

The so called quasi-steady-state (QSS) approach described in [6] is generally applied to avoid a costly transient analysis of a crystal growth process and has been widely used for FZ simulation [1-3,7]. The time-harmonic EM field during FZ growth can generally be considered quasi-stationary, since the

typical size of the puller is much smaller than the wavelength of the field. The heat flux, temperature and other relevant quantities are assumed being independent of time in a delimited section in the laboratory coordinate system. The crystal growth rate is considered as a known input parameter equal to the pull rate, which is treated as a source term at the growth interface in order to consider the impacts of the latent heat of solidification on the heat transport. The QSS approach is valid if the geometry does not change in time, i.e. during the cylindrical crystal growth phase. However, in the development of a crystal growth process, e.g. for larger crystal diameter, the unsteady start cone phase is often of higher interest for the process developers. In the present work, it will be elaborated on the error that arises if the QSS approach is applied for the start cone phase of the FZ process.

The moving grid or deformed mesh approach is usually applied to model the interface shapes during FZ growth [1-4,7,8]. In the moving grid approach, the FEM or BEM mesh is deformed in order to fulfil an equilibrium condition that is imposed on a boundary. For calculation of the crystallization interface shape, commonly the Stefan condition that states the equilibrium of heat fluxes is imposed. In the present COMSOL FZ model, a Lagrange multiplier is incorporated for mesh deformation. An alternative to the moving grid approach is the phase field approach. Here, the mesh is fixed and a phase field variable is introduced that defines the underlying material state. The Fig.3 shows calculation examples for the crystallization interface. The phase field approach requires a finer FE mesh than the moving grid approach. Nevertheless, it can consume less computation time and is more robust. The results of phase field calculations of the crystallization interface shape and the free melt surface shape during FZ growth will be presented and compared to results obtained using the standard approaches.

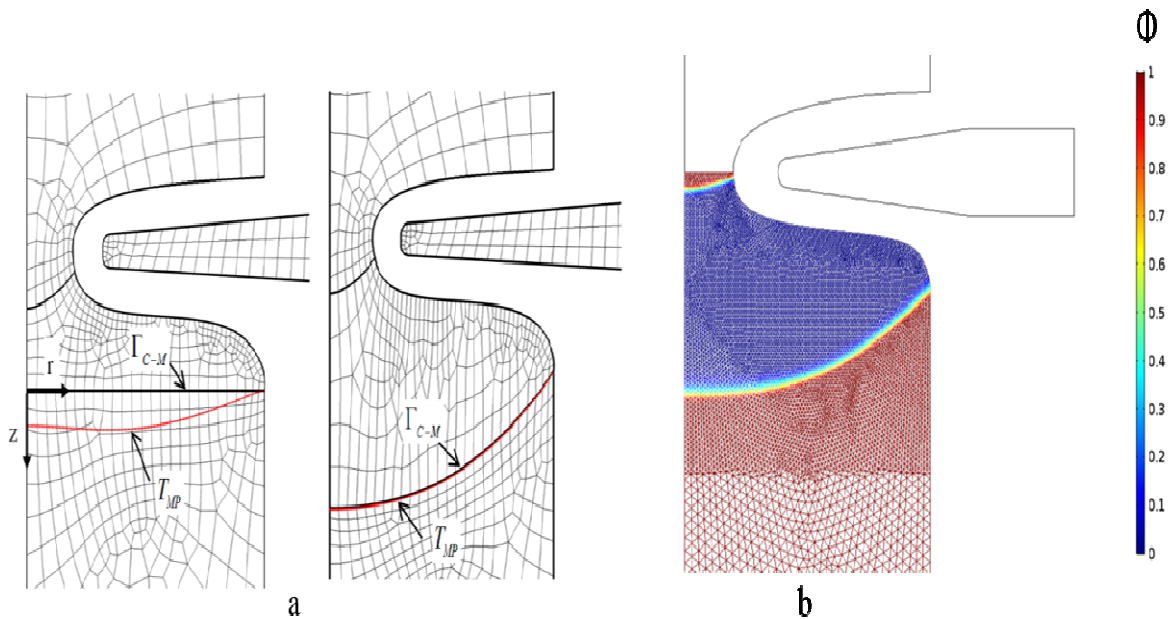


**Fig. 3. Calculated crystallization interface shape during 4" FZ growth
a) using the moving grid approach b) using the phase field approach**

References

- [1] M. Wünscher, R. Menzel, H. Riemann and A. Lüdge, "Combined 3D and 2.5D modeling of the floating zone process with Comsol Multiphysics", *J. Crys. Growth* 385 (2014) 100-105
- [2] A. Mühlbauer, A. Muiznieks, J. Virbulis, A. Lüdge and H. Riemann, "Interface shape, heat transfer and fluid flow in the floating zone growth of large silicon crystals with the needle-eye technique," *J. Crys. Growth* 151 (1995) 66-79

- [3] A. Mühlbauer, A. Muiznieks and G. Raming, "System of Mathematical Models for the Analysis of Industrial FZ-Si-Crystal Growth Process," *Cryst Res. Technol.* 34 (1999) 217–226
- [4] G. Ratnieks et al., "Influence of the three dimensionality of the HF electromagnetic field on resistivity variations in Si single crystals during FZ growth," *J. Crys. Growth* 216 (2000) 204–219
- [5] A. Mühlbauer, A. Muižnieks, A. Jakowitsch, and J. Virbulis, "Berechnung des dreidimensionalen Hochfrequenzfeldes beim Zonenschmelzen von Silizium" *Arch. Elektrotechn.* 76 (1993) 161
- [6] J.J. Derby and R.A. Brown, "On the quasi-steady-state assumption in modeling Czochralski crystal growth", *J. Crys. Growth* 87 (1988) 251-260
- [7] H. Riemann, A. Lüdge and K. Boettcher, "Silicon Floating Zone Process: Numerical Modelling of RF Field, Heat Transfer, Thermal Stress and Experimental Proof for 4 inch Crystals.," *J. Electrochem. Soc.* 142 (1995) 1007–1014
- [8] G. Ratnieks, A. Muiznieks and A. Mühlbauer "Modelling of phase boundaries for large industrial FZ silicon crystal growth with the needle-eye technique," *J. Crys. Growth* 255 (2003) 227–240

IT-10

Theoretical Prediction of Materials for Bio-Implant Applications

Dr. R. Vidya

Department of Medical Physics, Anna University, Sardar Patel Road, Guindy, Chennai – 600 025.

Density-Functional Theory (DFT) based computational methods can provide atomic-scale understanding on properties of materials which constitutes an interesting starting point for the preparation of advanced materials with superior properties. In this work we are showing that, we can predict novel materials for implant applications using advanced DFT calculations.

Recent studies evoked renewed attention towards Titanium Tetrafluoride (TiF_4) in the field of catalysts, optoelectronics, and dentistry. Titanium fluoride exists in its three valence states namely TiF_2 , TiF_3 , and TiF_4 . In the field of H_2 production from metal hydrides, application of constant shear stress on the additives reduces Ti^{4+} into Ti^{3+} and Ti^{2+} during mechano-chemical process. Therefore, polyvalent TiF_4 certainly been a potential precursor, because of its multivalence states. TiF_3 is half metallic known for its spintronic applications in addition to the li-ion battery anode material. TiF_2 is not studied thoroughly because of its stability issue.

Besides, fluorides has long outgrown in the pre-restorative dentistry. For instance, polyvalent metal makes stronger bond with the surrounding tooth structure thereby provides mechanical protection. Among the transition metal fluorides, TiF_4 is attractive because of its compatibility with tooth mineral and it forms a polymer layer which in turn leads to hydrophobicity. Perhaps, the interaction of TiF_4 with the tooth structure creates protective shield against bacterial proliferation and acid erosion and inhibits the leakage of cavity lesion.

Even though TiF_4 ascertains its role in all emerging fields, its mechanical strength has not been studied yet. Hence in the present study we focus on the mechanical property of TiF_n ($n= 4, 3, \text{ and } 2$) and attempt to bring new insight to the material property.

We have used state-of-the-art Density Functional Theory (DFT) to perform the calculation. The stress-strain method implemented in Vienna Ab-initio Simulation Package (VASP) provided with a plane-wave energy cutoff of 550 eV was utilized. The atomic geometry was optimized by force as well as stress minimizations. We evaluated the mechanical stability of all TiF derivatives using Born elastic stability criteria from the elastic stiffness constant matrix. We derived the other mechanical property like Young's modulus (E), bulk modulus (B), shear modulus (E), and poison's ratio (ν) from the elastic tensor of strained crystal.

Titanium can form as binary, ternary and quaternary fluorides, namely TiF_4 , TiF_3 , and TiF_2 and take up cubic, rhombohedral, and orthorhombic lattice type, respectively as shown in Figure 1. Complete structural optimizations were performed for TiF_4 , TiF_3 , and TiF_2 . The equilibrium structural parameters are in good agreement with the experimental lattice parameters. Ti occupies octahedral site in both TiF_4 and TiF_3 , while TiF_2 has flattened octahedral configuration with each Ti is surrounded by eight fluorine ions. TiF_4 has highly distorted octahedra with five different bond lengths. In terms of structural property,

significantly TiF_4 has columnar pillar-like structure grown along b -axis similar to the tooth enamel consisting of hydroxyapatite (HAp).

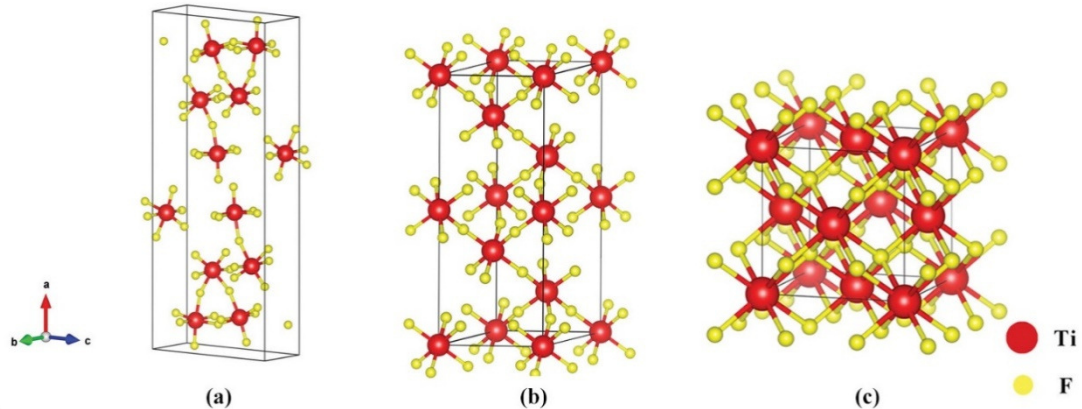


Figure 1. Crystal Structure of (a) TiF_4 , (b) TiF_3 , and (c) TiF_2

The spatial dependence of Young's modulus of TiF_4 , TiF_3 , and TiF_2 is visualized in the corresponding Figure 2a, 2b and 2c, respectively. Significantly, the spatial variance along different axis indicates the unique elastic properties of TiF_4 .

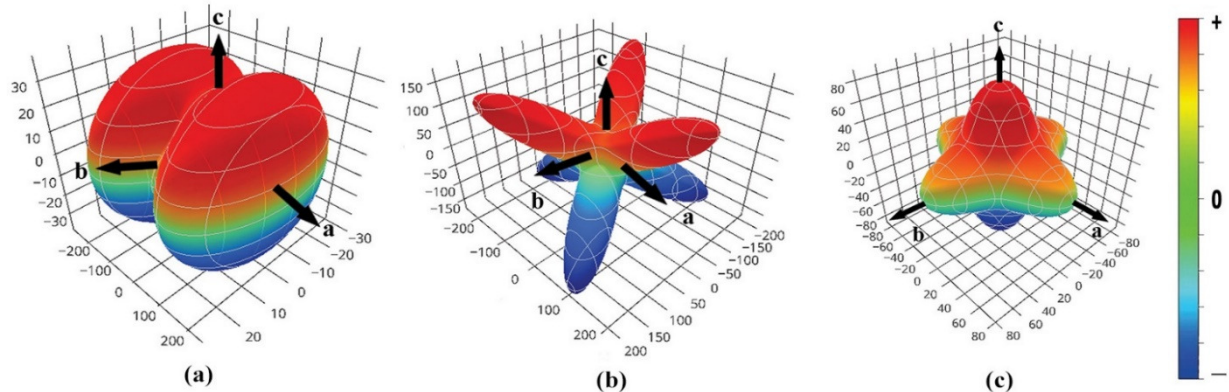


Figure 2. Young's modulus of (a) TiF_4 , (b) TiF_3 , and (c) TiF_2

The average Young's modulus of TiF_4 is 47 GPa which is greater than that of other restorative materials used currently. Since materials with Young's modulus close to bone (20-30 GPa) are intensely searched for implant applications, we propose that TiF_4 can be used for this purpose.

References:

1. R. Mariyal Jebasty and R. Vidya, ACS BioMatSci. Engg. (Accepted; 2019).

IT-11

Development of Interatomic Potentials for Molecular Dynamics Simulations Using Density Functional Theory

*Sharat Chandra**

Materials Science Group, Indira Gandhi Centre for Atomic Research, Kalpakkam 603 102, TN, India

*E-mail:sharat@igcar.gov.in,

Molecular dynamics (MD) simulations have become the norm these days in a wide variety of fields that include bio-physics, chemistry, materials science and physics. The classical MD simulations use Newton's equations to obtain the force, position and velocities of individual units, which can be atoms, or cluster units, as a function of simulation time step. The force calculation requires defining the potential energy of the system under simulation. The potential energy is a consequence of the interatomic or interparticle interactions that control the chemistry of the atoms in the system, which are quantum in nature. For classical MD simulations these interactions have to be described by force-fields or interatomic potentials and the quality of the MD simulations depend intimately of the quality of the potentials used in the simulations.

In this talk we present the methodology for the development of appropriate interatomic potentials for MD simulations. We report on the development of the interatomic potentials for $Y_2Ti_2O_7$ and Y_2TiO_5 crystals which can be used to study the effects of the damage caused in these crystals under self-ion irradiation. The methodology followed for the development of these potentials will be discussed, followed by the tests that are necessary to qualify the appropriateness of the potentials. Finally the displacement cascades characteristics in these crystals will be presented.

$Y_2Ti_2O_7$ and Y_2TiO_5 are very important materials for nuclear applications. So a complete understanding of their radiation response is warranted. This can only be understood when we are able to delineate their physical properties such as thermal expansion, diffusion of different species and the behaviour of the point defects in these systems. We have developed pair-wise interatomic potentials suitable for MD studies of highly energetic processes in Y_2TiO_5 and $Y_2Ti_2O_7$ crystal systems. For developing the interatomic potentials we need to first develop an extensive database which has data from both experimental as well as first principles density functional (DFT) calculations. The data can consist of the lattice parameters as a function of temperature and pressure, elastic constants, phonon modes, formation energies for the various defect types and the total energies of the systems when the system undergoes various static lattice distortions. The useful data can come from IR and Raman measurements, mechanical property measurements, x-ray and neutron diffraction, as well as DFT calculations, resulting in an extensive database that contains the total energies as well as atomistic configurations for the various cases. This database is used to fit to the functional form of the interatomic potential that we are planning to use for our simulations. As the systems are ionic in nature, it is appropriate to use only the two-body potentials. We have used a combination of Coulomb and Buckingham potentials for the purpose as shown in the equations below. Here i and j denote the various atomic species combinations present in the systems. So, for the three atomic species we have six different combinations to delineate (Y-Y, Y-Ti, Y-O, Ti-Ti, Ti-O and O-O).

(Total potential)

$$U_{ij} = U_{ij}^{Coulomb} + U_{ij}^{Buckingham} \quad (1)$$

(Long-ranged)

$$U_{ij}^{Coulomb} = q_i q_j / r_{ij} \quad (2)$$

(Short-ranged)

$$U_{ij}^{Buckingham} = A_{ij} \exp\left(-\frac{r_{ij}}{\rho_{ij}}\right) - C_{ij} / r_{ij}^6 \quad (3)$$

The potentials reproduce melting points of both the systems fairly accurately as shown in Fig.1. The cation antisite pair formation energy is found to be quite less in both the systems, which indicates the tendency of pyrochlores to form cation antisite defects upon irradiation. A study of diffusion coefficients and Zachariasen criteria shows that $Y_2Ti_2O_7$ is more resistant to amorphization than Y_2TiO_5 .

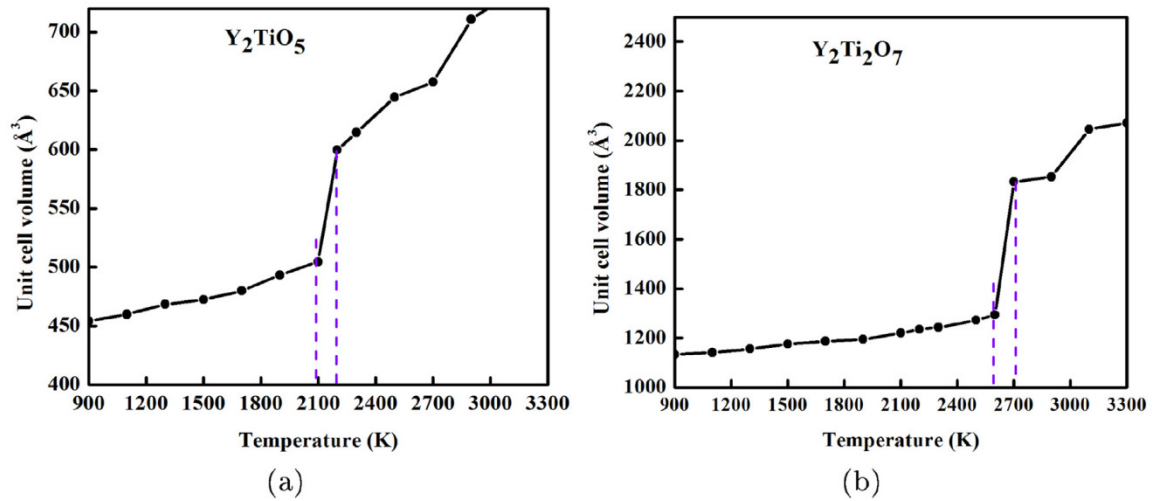


Fig. 1. Unit cell volume vs temperature in NPT ensemble: (a) Y_2TiO_5 ; (b) $Y_2Ti_2O_7$.

References

- Tomas Lazauskas, Steven D. Kenny, Roger Smith, Gurpreet Nagra, Manan Dholakia, M.C. Valsakumar, *J. Nucl. Mater.* **437** (2013) 317-325.
- Manan Dholakia, Sharat Chandra, M.C. Valsakumar, S. Mathi Jaya, *J. Nucl. Mater.* **454** (2014) 96-104.
- P. Jegadeesan, S. Amirthapandian, Gurpreet Kaur, Sharat Chandra, B.K. Panigrahi, *Physica Status Solidi B* **252** (2015) 206-211.
- Manan Dholakia, Sharat Chandra, S. Mathi Jaya, *J. Alloys Compd.* **739** (2018) 1037-1047.
- Manan Dholakia, Sharat Chandra, S. Mathi Jaya, *J. Appl. Phys.* **125** (2019) 025104.

IT-12

Liquid like Nucleation in Nanoscale Thin Films

Pooja Rani¹, Arun Kumar¹, B. Vishwanadh², Kawsar Ali², A. Arya², R. Tewari² and Anandh Subramaniam^{1,*}

¹Materials Science and Engineering, Indian Institute of Technology Kanpur, Kanpur-208016, India.

²Materials Science Division, Bhabha Atomic Research Centre, Trombay, Mumbai-400085, India.

*E-mail: anandh@iitk.ac.in

The concept of critical nucleus size (r^*) is of pivotal importance in phase transformation involving nucleation and growth. Above this size, it is favorable for the product phase to grow; while, 'embryos' smaller than this size tend to revert to the parent phase. The current investigation pertains to crystallization in nanoscale thin films and study of the same using high resolution lattice fringe imaging (HRLFI) and finite element simulations.

The CuZrAl bulk metallic glass (BMG) is used as a model system for this study. This BMG alloy serves as a model system for the study of the phenomena due to the following reasons: (i) homogeneous nucleation is expected to be dominant in the absence of grain boundaries, dislocations and other crystallographic defects; (ii) it is convenient to determine the size of the nuclei via HRLFI as the amorphous matrix does not give lattice fringes; (iii) by keeping the temperature of the transformation low, we can be in the 'nucleation dominant regime' (i.e. practically suppress growth); (iv) the interfacial energy is expected to be reasonably isotropic (and the error introduced by the approximate treatment of the glass matrix as a liquid for the computation of γ is small) and (v) the diffusion is sluggish at room temperature and hence any transformation while performing experiments (like TEM) can be ignored.

For the computation of the value of r^* the following parameters are required: (i) ΔG_V , (ii) γ (ii) E_{strain} . In the approximation that the material is isotropic, to determine E_{strain} we further require the values of the: (i) Young's modulus (Y), (ii) Poisson's ratio (ν) and (iii) misfit (f_m). The values of the moduli for both the glass and crystal are required. A simplifying assumption for the calculation of ΔG_V (glass→crystal) often used is to compute the value for liquid to crystal transformation.¹ For the formation of Cu₁₀Zr₇ crystal (Cmca, oC68, $a = 12.68 \text{ \AA}$, $b = 9.31 \text{ \AA}$, $c = 9.35 \text{ \AA}$ ⁱⁱ) from an amorphous matrix (composition of (Cu₆₄Zr₃₆)₉₆Al₄), the value of ΔG_V can be determined using the prescription of Zhou and Napolitanoⁱⁱ: $(-16133-1.905T)$. Another approach for the computation of ΔG_V is that due to Turnbullⁱⁱⁱ: $\Delta G_V = \Delta H_f (T_m - T) / T_m$, where T_m is the melting temperature. It is noteworthy that in the current case both these approaches give a very similar value of ΔG_V . The values of the parameters are: $\Delta H_f = 1.23 \times 10^4 \text{ J/mole}$, $T_m = 1185 \text{ K}$ and the computed value from Turnbull equation: $\Delta G_V(\text{Turnbull}) = 7.39 \times 10^3 \text{ J/mole}$. The crystal-glass interfacial free energy (γ) is a difficult quantity to compute and often it is observed that the value of crystal-liquid interfacial energy is a good enough approximation and can be computed usingⁱⁱⁱ: $\gamma = \frac{\alpha \Delta H_f}{(N_A V_m^2)^{1/3}}$, where, α is the Turnbull coefficient which depends on the crystal structure, ΔH_f the enthalpy of fusion,

N_A the Avagadro's number and V_m the molar volume of the crystal. The computed value of is: $\gamma = 0.03 \text{ J/m}^2$. The strain energy is computed using approach of Kumar et al.^{iv} and a schematic of the model is shown in Figure 1. The inset to the figures shows the case of a hemi-spherical surface nucleus in an amorphous matrix. SAD pattern (Figure 2a) confirms the formation of the amorphous phase on quenching. HRLFI is used for the measurement of crystallite sizes on nucleation (Figure 2b). The stress state of the system on the formation of the nucleus is shown in Figure 2c.

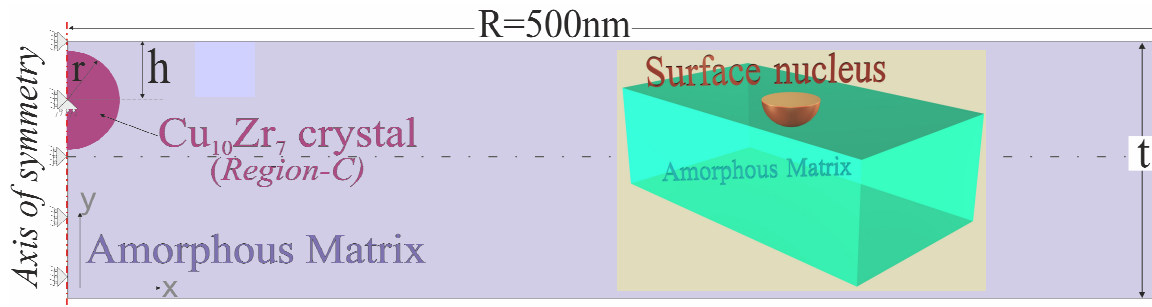
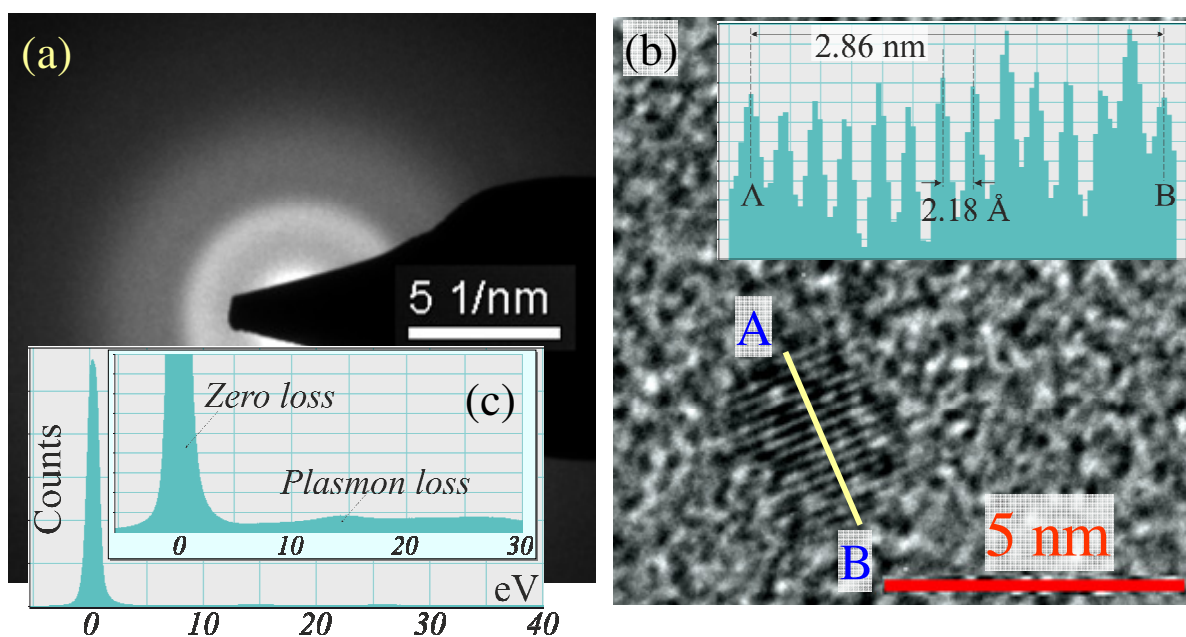


Figure 1. The finite element model used for the computation of strain energy in the presence of a spherical crystal of radius 'r' in a free standing thin film of thickness 't'. The boundary conditions used are also marked in the figure; along with the region (C), where eigenstrains are imposed to simulate the stress state in the presence of a crystal. Inset shows the model used for the case of surface nucleation.

Using the models as outlined before, we demonstrate liquid like nucleation behaviour in thin solid films on heating. The r^* for the formation of the $\text{Cu}_{10}\text{Zr}_7$ phase in thin films of decreasing thickness, approaches

that of the r^* for the formation of the crystal from the liquid (i.e. $r_{thin\ film}^* \rightarrow r_{liquid}^*$) (Figure 3). Working in the nucleation dominant regime, we determine the position of the nuclei (along z-direction) from lattice fringe images— an information which is usually absent in such images. The TEM sample is used as a free-standing thin film, crystallite sizes are measured using HRLFI, thickness of the film is determined by electron energy loss spectroscopy and strain energy of the system is computed using finite element computations.



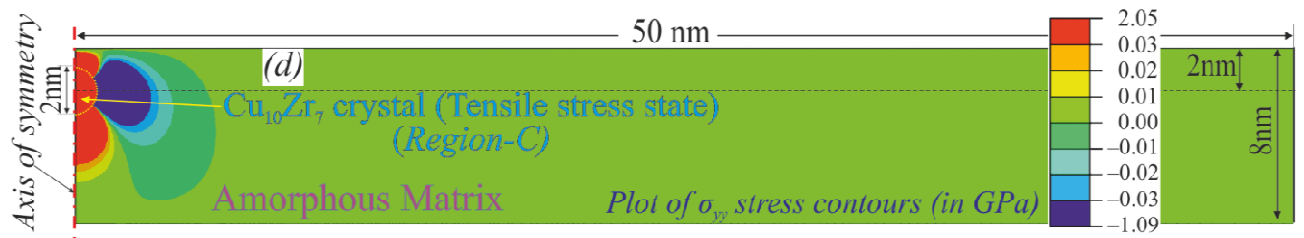


Figure 2. (a) Selected area diffraction (SAD) pattern showing the formation of an amorphous structure on suction casting the $(\text{Cu}_{64}\text{Zr}_{36})_{96}\text{Al}_4$ alloy. (b) HRLFI from a crystallite ($2r = 2.86$ nm) embedded in an amorphous matrix. (c) A typical EELS spectrum acquired from region of diameter 10 nm, which is used in the computation of the thickness of the specimen. (d) FEM simulation of the stress state in the presence of a crystalline in an amorphous matrix.

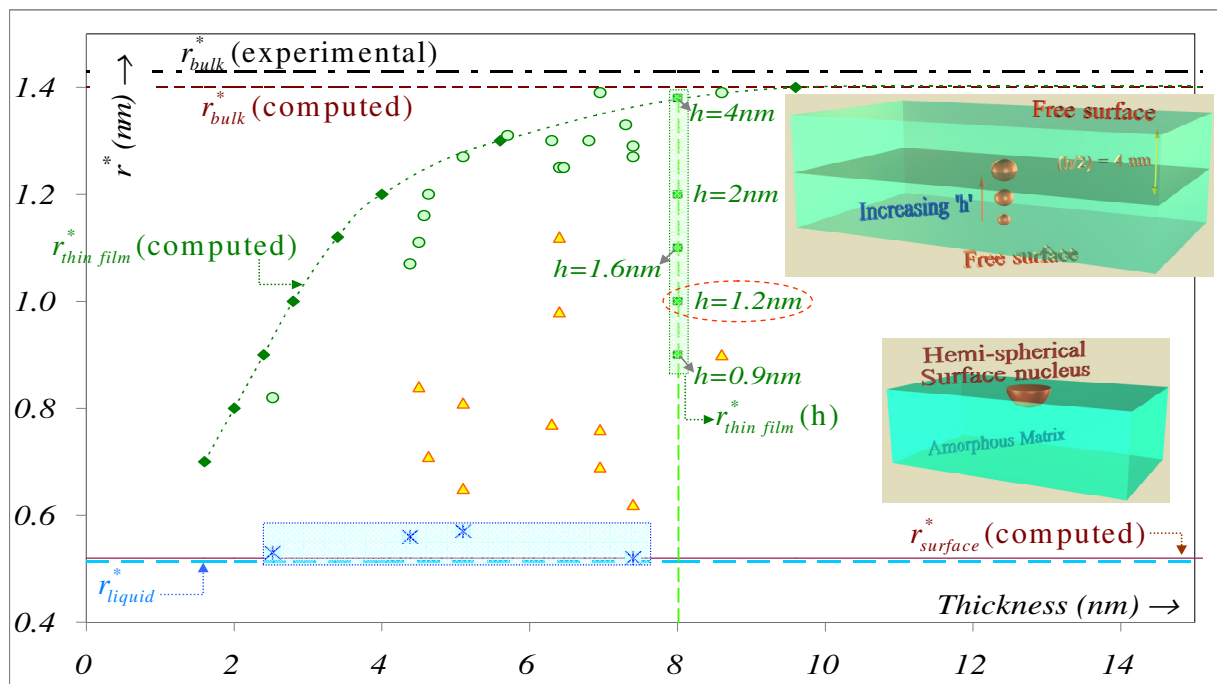


Figure 3. (i) The computed variation of r^* ($r_{thin\ film}^*$ (computed)) with thickness of the sample (curved line). (ii) The horizontal dashed lines correspond to r_{bulk}^* (computed), r_{bulk}^* (experimental) and r_{liquid}^* . (iii) The experimental data for thin films is shown as a scatter of points. (iv) The change in the value of r^* with 'h' (computed $r^*(h)$) for a film of thickness 8 nm (shown for discrete values of $h \in [4.0\ \text{nm}-0.9\ \text{nm}]$), enclosed in a vertical box). Inset to the figure shows a schematic rendition of the variation. (v) The horizontal line (solid) corresponds to $r_{surface}^*$ (computed) for a (100) oriented hemi-spherical surface nucleus. The experimental data points enclosed in horizontal box are expected to be surface nuclei.

References

- ¹ K. Mondal, U. K. Chatterjee and B. S. Murty, *Appl. Phys. Lett.*, 2003, **83**, 671–673.
- ¹ A. Figini Albisetti, C. A. Biffi and A. Tuissi, *J. Alloys Compd.*, 2012, **544**, 42–45.
- ¹ K. Yamaguchi, Y. C. Song, T. Yoshida and K. Itagaki, *J. Alloys Compd.*, 2008, **452**, 73–79.
- ¹ A. Kumar, G. Kaur and A. Subramaniam, *Int. J. Mater. Res.*, 2013, **104**, 1171–1181.

IT-13

Nanomechanical Properties of Wide Bandgap Semiconductors: Experimental and Theoretical Perspective

*R. Navamathavan**

*Division of Physics, School of Advanced Sciences, Vellore Institute of Technology Chennai,
Vandalur - Kelambakkam Road, Chennai 600 127*

*E-mail: navamathavan.r@vit.ac.in

Recently, wide-band gap semiconductors, such as GaN, ZnO and their alloys have been extensively investigated to develop short-wavelength optoelectronics, such as light-emitting diodes, short-wavelength diode lasers and ultraviolet detectors. The successful fabrication of optoelectronic devices based on epitaxial GaN and ZnO thin films requires an understanding of the mechanical properties of this material as well as its optical and electrical properties. The former are of special concern since heteroepitaxy using typical substrates (e.g. sapphire and silicon) involves a high lattice mismatch. Understanding the mechanical properties of materials at the nanoscale is crucial for device applications.

The characterization of epitaxial layers and their surfaces have benefited a lot from the enormous progress of nanomechanical analysis techniques during the last decade. In particular, the dramatic improvement of the structural quality of semiconductor epilayers and heterostructures results from the level of sophistication achieved with such analysis techniques. First of all, micromechanical technique is nondestructive and its sensitivity has been improved to such an extent that nowadays the epilayer analysis can be performed on layers with thicknesses ranging on the atomic scale. This advantage could turn out to be extremely important from a technological point of view, i.e., for the surveillance of modern semiconductor processes.

Great strides have been made over the past few years in the development of techniques for probing the mechanical properties of materials on the submicron scale. Nanoscale film characteristics such as topography, hardness, adhesion, elasticity, friction, and wear are becoming crucial to applications being developed by a broad range of industries. This leads to an increased reliance on the Atomic Force Microscope (AFM) in research and development, and failure testing, due to its ability to perform both the nanomechanical tests and to image the resulting topographical structures in a technique called nanoindentation.

The nanoindentation test can be used to determine hardness and Young's elastic modulus as a function of depth, at a single point. This is achieved by producing a series of load-unload hysteresis curves with progressively increasing load, where the indenter remains in contact with the point of interest throughout. During reloading, the depth versus load data is essentially superimposed on the previous unloading curve until the additional load increment is applied when further plastic deformation takes place.

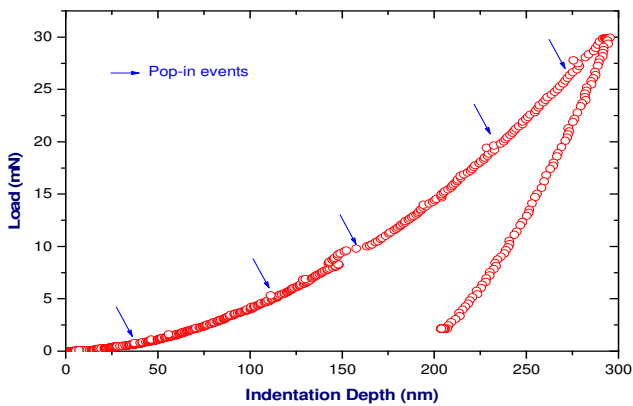


Fig. 1. Load-displacement curve

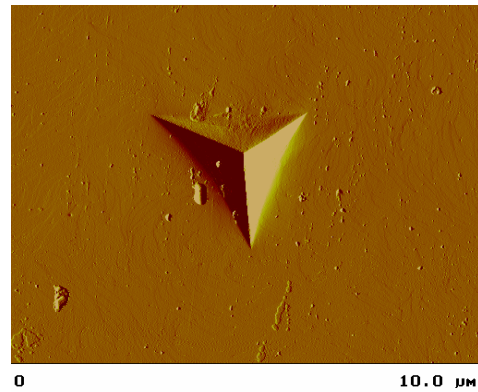


Fig.2. Residual impression (AFM)

Herein, the nanoindentation studies were performed for wide bandgap semiconductors such GaN and ZnO epitaxial thin films. The nanoindentation studies conducted for different thicknesses of the samples and their mechanical properties such as hardness, Young's modulus and fracture toughness were obtained at the nanoscale range. Very interestingly, the so called “pop-in” events were observed for the samples which were directly correlated with the defects distribution inside films. A possible mechanism has been discussed in combination with theoretical modelling. Furthermore, the AFM studies were performed on the post-indented samples to investigate the topological behaviour at nanoscale level.

The deformation of the epitaxial GaN and ZnO thin films were investigated by using nanoindentation studies. Multi ‘pop-in’ events have been observed in the load-indentation depth curve (Fig. 1). The critical stress produced beneath the Berkovich indenter was main criterion for the first ‘pop-in’ event at very shallow depths in the GaN thin film. The physical mechanism responsible for the multi ‘pop-in’ events were explained by the collision of the deformed region, produced by the indenter tip, with the top edge of the threading dislocation at the corresponding depths in the GaN thin film. In addition, we note that the critical depth for the first ‘pop-in’ to occur depends on the lattice mismatch of the film. AFM studies on residual impression did not show any micro-cracks in and around the indentation region (Fig. 2). Finally, indentation below the critical depth showed that the surface flexes elastically and beyond which interaction with threading dislocation causing plastic deformation.

IT-14

Formation mechanism of twin boundary and fabrication of periodically-twinned structure in borate crystal

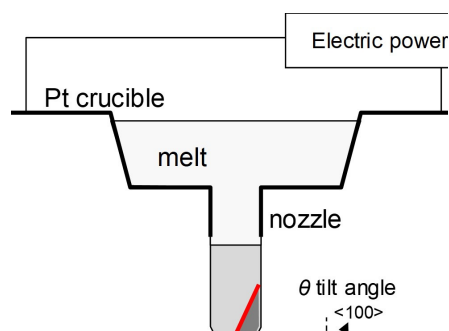
Kensaku Maeda*, Kozo Fujiwara, Satoshi Uda,
Institute for materials research, Tohoku University, Japan

*E-mail: kensaku@imr.tohoku.ac.jp,

We produced a periodically-twinned lithium tetra borate crystal that is non-ferroelectric and transparent to vacuum-UV light. Periodic structure was formed during melt growth process by using twin boundary formation mechanism. Twin boundary orientation depends on crystal growth direction. It was demonstrated that the periodically-twinned crystal can function as a wavelength conversion device, and the second-harmonic light of Nd:YAG laser was generated.

The development of an all-solid-state vacuum-UV (wavelength $< 200\text{nm}$) light source is required for achieving ultrafine laser processing. Such as an all solid state laser light source must be both stable and inexpensive. Devices with QPM (quasi-phase-matching) structure, where the sign of the nonlinear optical coefficient is periodically reversed, can reduce the incoming wavelength by half. Conventional QPM devices were formed in ferroelectric oxide crystals by applying an external electric field. However, ferroelectric oxide (LiTaO_3 , LiNbO_3 etc.) is opaque to vacuum-UV. Therefore, it is quite difficult to make a QPM device for VUV light source. Lithium tetraborate ($\text{Li}_2\text{B}_4\text{O}_7$; referred to as LB4) is a transparent to VUV light and has a high nonlinear optical coefficient ($d_{33} = 0.93 \text{ pm/V}$). However, poling method using electric field cannot apply to this because of non-ferroelectric. Instead of this, twinning can be occurred, which accompanies the reverse of the c-axis and the sign of the nonlinear optical coefficient d_{33} . Twinned crystal can be formed during only crystal growth process from the melt. In the case of quartz crystal, which is non-ferroelectric, twinned crystal forms by applying stress. And a hot-pressing method was proposed to make QPM device and conversion to 193 nm wavelength light was succeeded [1]. However, this method also cannot apply to Lithium tetraborate because of crystallographic symmetry. Therefore, we focused on crystal growth process of twinned lithium tetraborate. In other words, to clarify the twin boundary (TB) formation mechanism is our target. And we try to developed a method for fabrication of periodically-twinned lithium tetraborate, and to generate second-harmonic light of Nd:YAG laser

Fig. 1. Micro-pulling down method.



Twinned LB4 crystals were grown by the micro-pulling down (m-PD) method (Fig.1). A large thermal gradient was generated at solid/liquid interface. The solid/liquid interface was planar, and crystal growth direction was maintained by rotation angle of a twinned seed crystal. When the growth direction was $\langle 100 \rangle$, (010) TB formed in grown crystal. Similarly, when the growth direction was $\langle 010 \rangle$, (100) TB formed in grown crystal. Critical growth direction between (010) and (100) TB formation is $\langle 110 \rangle$ [2].

Periodically twinned structure can be fabricated by using above mechanism which means TB orientation is defined by crystal growth direction [3]. Fig. 2 shows control method of TB formation. A plate-like twinned crystal and a movable platinum wire heater are prepared. A Pt wire, which is resistive heated, melts surrounding crystal. Crystal melts and grows according to the wire heater movement. When a wire heater moves to c^- -axis crystal region from (100) TB, c^+ -axis crystal forms in c^- -axis crystal region. Periodic structure can be formed by repeating this process. Fig. 3 shows an etched surface of fabricated 100- μm -interval twinned crystal. Periodic interval of twinning depends on the size of melted area and repeating interval. Although this crystal was a plate-like shape, a bulk periodically twinned crystal can be grown by directional growth using this plate-like crystal as a seed (Fig. 4).

A fabricated bulk crystal includes 100 μm interval twin boundaries and second-harmonic generation (SHG) of this crystal was measured using a Q-switched neodymium-doped yttrium aluminum garnet (Nd:YAG; $\lambda = 1064 \text{ nm}$) laser. This periodic twin crystal will function as a 5th-ordered QPM structure for a SHG of Nd:YAG laser, because coherence length at 1064 nm laser is 20 μm . The output SHG energy was 3.8 $\mu\text{J/pulse}$ when the input energy was 130 mJ/pulse. The SHG light from the single crystal is less than 0.1 $\mu\text{J/pulse}$, which is the lowest detection limit. Thus, it is demonstrated that the periodically twinned crystal can function as a QPM device. A finer periodically twinned crystal would be required to tune in shorter phase-matching wavelengths.

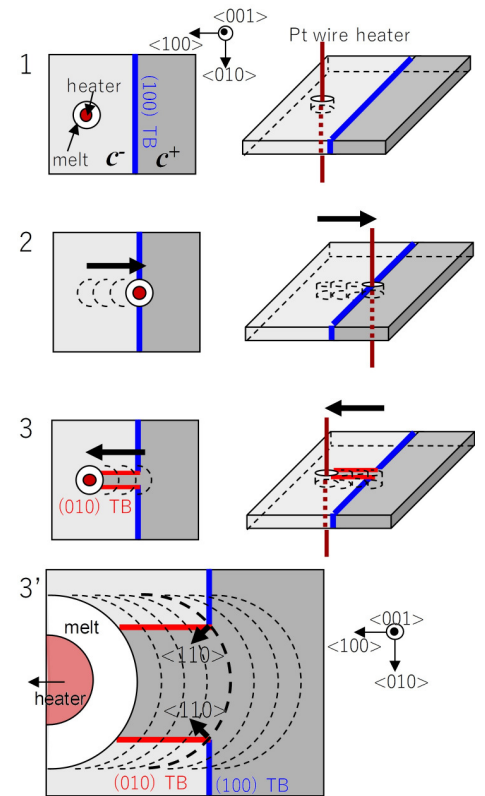


Fig. 2. Twin boundary control

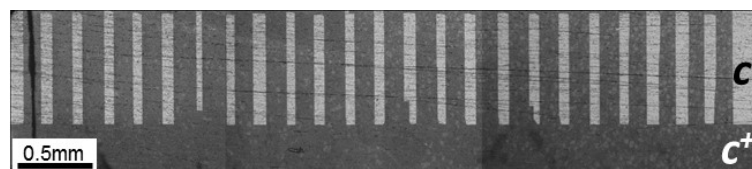


Fig. 3. 100- μm -interval twinned crystal.

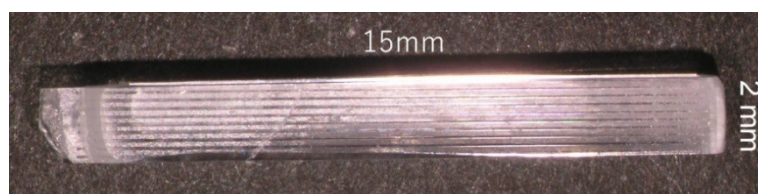


Fig. 4. Bulk periodically twinned crystal.

References

- [1] S. Kurimura *et al.*, *Optical Materials Express*, **1** (2011) 1367-1375.
- [2] K. Maeda *et al.*, *Journal of Crystal Growth*, **331** (2011) 78-82.
- [3] K. Maeda *et al.*, *Applied Physics Express*, **6** (2013) 015501.

IT-15

Role of Thermal Hydraulics on the Crystal Growth by Chemical Vapor Deposition

P. K. Mollick and M. Krishnan*

Materials Group, Bhabha Atomic Research Centre, Mumbai- 400085

Chemical Vapour Deposition (CVD) is a thermo-chemical process by which deposition of solid crystals takes place over a targeted substrate surface. Cracking of precursor molecule at a desired temperature is considered to be the first step followed by homogeneous and heterogeneous chemical reactions resulting in the deposition of solid crystal. Therefore, the CVD essentially takes place inside a reaction chamber/ reactor at a reasonably high temperature. Precursor(s) in the gaseous form are majorly feed through one of its inlet of the reactor which is practically a small size orifice in many of the cases. Thus the gaseous phase containing unconverted precursor and converted intermediates travels along the path till the substrate surface is reached for the deposition reaction to take place.

It is therefore very much anticipated that the temperature and the flow pattern of gaseous streams inside the reactor as well as near the substrate surface can influence the reaction kinetics by large which in turn will change the size of the primary crystal. In the present talk, two case studies will be discussed from the fundamental chemistry to the droplet formation mechanism of CVD to result in different shape and size of primary crystals over a substrate surface.

The first case study will focus on the formation of thermal and viscous boundary layers and their effects on the size and shape of the primary crystal. Thickness of the thermal and the viscous boundary layer depends on the fluid velocity and the temperature of a given system. Therefore the thickness of the layers was calculated using Reynolds and Prandtl numbers.

Fig. 1 is showing the schematic and simulated plot of formation of boundary layers close to the substrate surface. The primary grain containing the pyrolytic carbon crystal is believed to form within a certain thickness of the boundary layer beyond which it cant get adsorbed on the surface. Therefore, the chemical reactions with the necessary temperature can only be accomplished if the thickness of the thermal boundary layer favours.

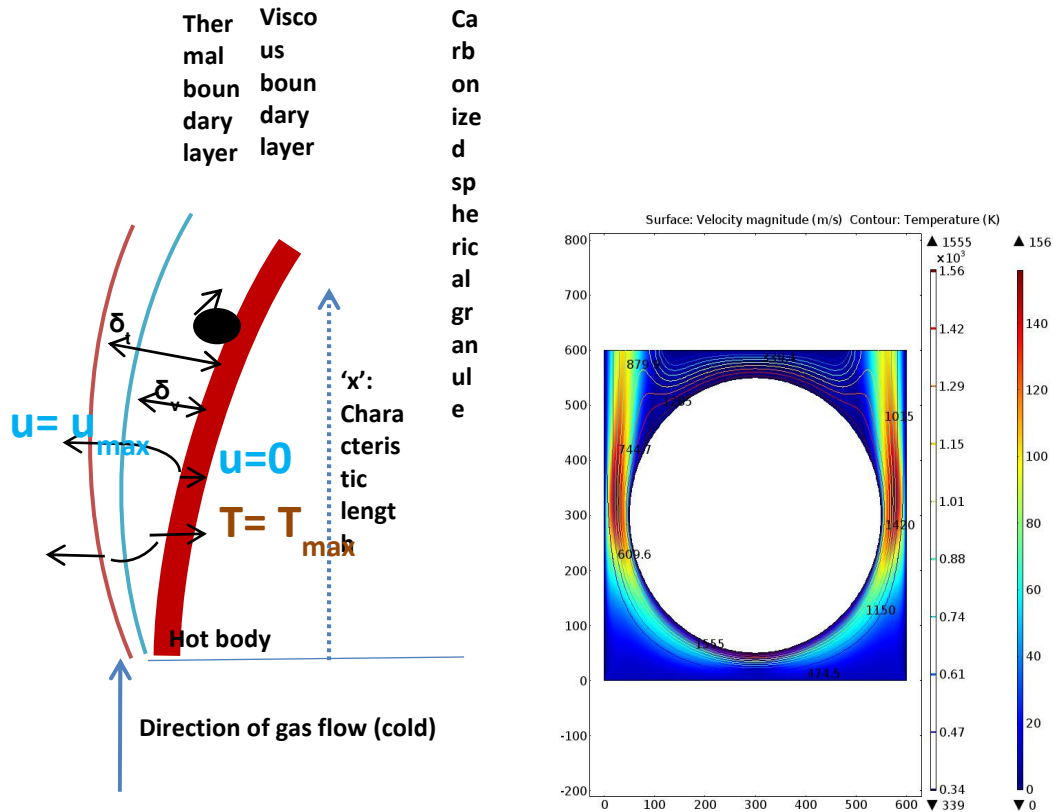


Fig. 1. Schematic and simulated plot showing formation of boundary layers near the surface subjected for CVD

Scanning Electron Microscopy (SEM) image of the deposited pyrocarbon layer over a spherical microsphere is shown in Fig 2. And the corresponding Small Angle Neutron Study (SANS) was carried out in order to approximate the average size of the primary crystal and which is shown in Fig. 3 for different process conditions.

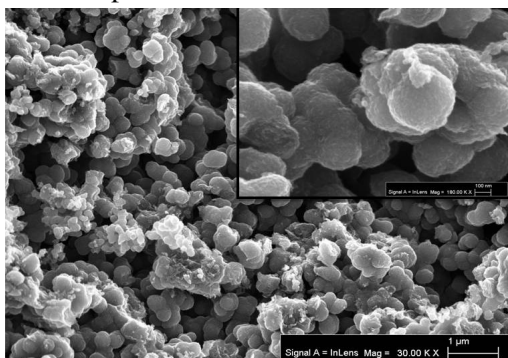


Fig. 2. SEM image of PyC coated surface

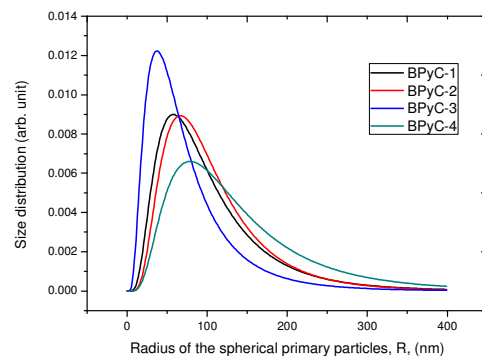


Fig. 3. SANS profile of PyC grain size

The second case study shows the effect of the operating parameters such as gas flow rate, temperature, sample position, sample dimensions, sample orientation on the deposition of crystal by CVD. Fig. 4 shows velocity magnitude and the temperature contour across the substrate surface when kept in various orientations in different widths and corner chamfered.

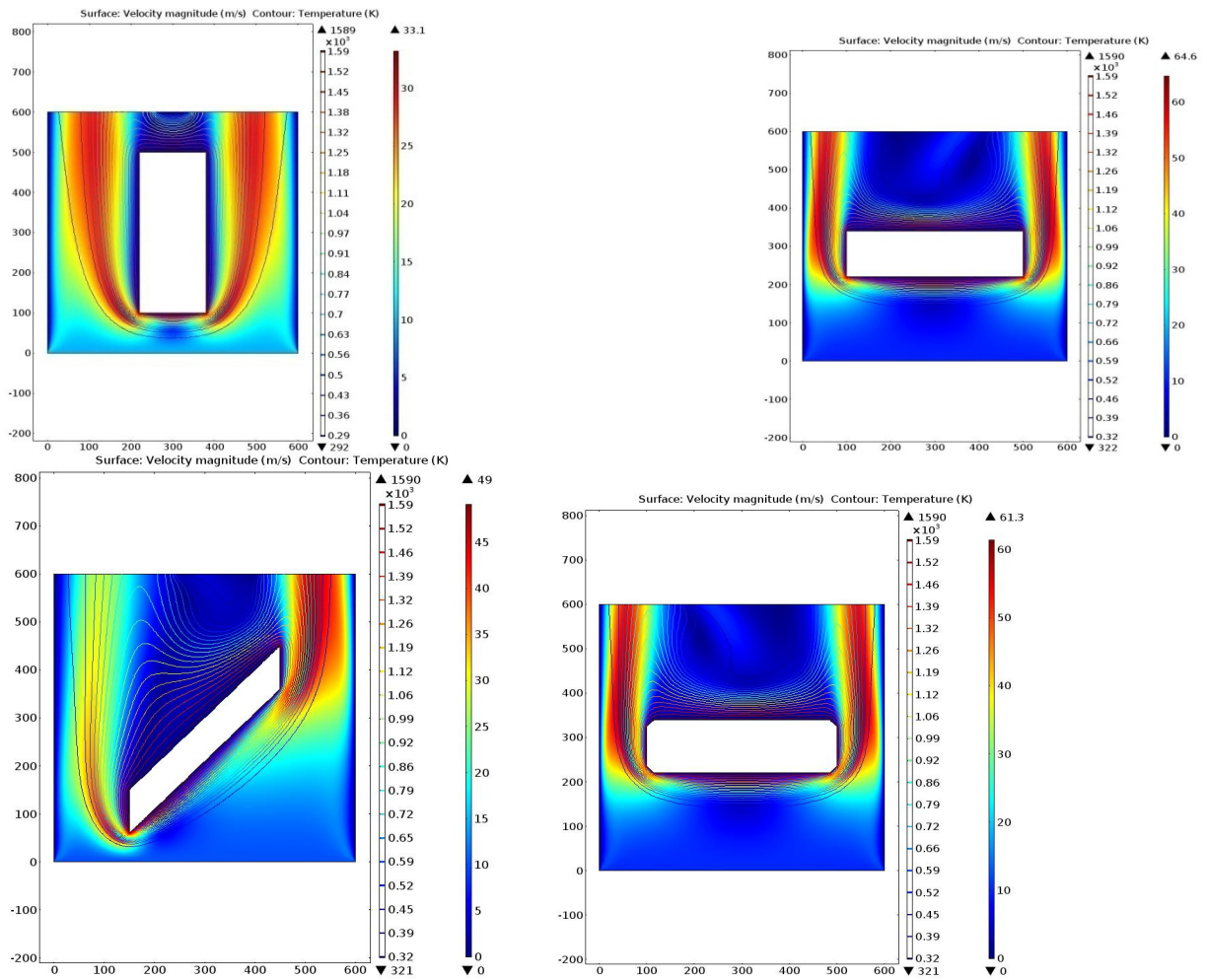


Fig. 4. Velocity magnitude and temperature contour past a substrate surface subjected to CVD. The talk will cover aspects of fluid dynamics and temperature profile during a successful and desired coating of crystals by CVD method.

IT-16

Understanding Structural Stability and Electronic Properties of Carbon Based Nanocomposites for Lithium Ion Battery Applications by First Principles Density Functional Calculations

P. Murugan

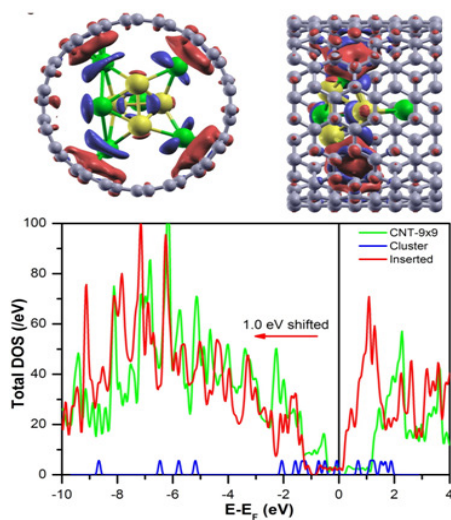
Functional Materials Division, CSIR Central Electrochemical Research Institute Karaikudi – 630 003, Tamil Nadu, India

Recently, Lithium-Ion Battery (LIB) contributes a major chunk of the power source for various portable electronic and electrical devices. On comparing that of conventional battery systems, this battery has following salient features; 1) compact size, 2) high energy density, 3) superior operating voltage, 4) long cycle life, and 5) less columbic efficiency. In order to meet faster growth in developing the portable electrical devices, such as, electrical vehicles and hand held electronic devices, further improvement in LIB is essentially required. The performance of LIBs mainly depends upon the nature of electrode and electrolyte materials. The electrode materials, particularly cathode, such as layered LiMO_2 ($M = \text{Co}, \text{Ni}, \text{Al}$) compounds are widely studied. However, while usage of it as the cathode of LIB, each compound has experiencing own disadvantages, such as, specific capacity fading, lower operating voltage, cost of those materials, and difficulty in synthesis procedure. In order to overcome these issues, combining two or more compounds are mixed together forming alloy or composites with appropriate ratios, that are ideal for employing them as the efficient electrode for LIB. The optimizing the proper ratio of composite or alloy is required tedious job by doing experiment. Also, there is not much understanding the structural stability and bonding nature of optimized alloy or composite. By employing density functional based first principles calculations, originated from quantum mechanics, we can optimize the composition or alloy ratio and also, this calculations provide to useful insight about atomic structure, structural stability, and electronic properties of those system. Further, it can be performed without experimental inputs and understanding the origin of structural and electronic stability of those composites or alloys.

By employing DFT calculations, we studied the structural stability and electrochemical properties of alloys made from layered LiMO_2 ($M = \text{Co}, \text{Ni}, \text{Al}$) compounds. The calculated results show that the formation stability and electrochemical properties of Ni based compounds are improved by introducing Co atoms into the lattice matrix. Also, the introduction of the small amount of Al provides the improved structural stability of alloy. By performing the various compositions, we also optimized suitable compositions of alloy as the cathode of LIB.

On the other hand, the carbon-based materials are commercially used for anode of LIBs,. However, graphite exhibits only low theoretical specific capacity (372 mAh/g), hence it cannot be used for high power devices. Other elements from group-IV (carbon family) were also observed to have a large theoretical capacity (maximum of 4200 mAh/g for Si). However, unlike carbon, these materials undergo large volume expansion during the cycling processes, which leads to pulverization of the electrode material and ultimately results in poor cycling performance. In addition, the inter-particle electronic conductivity of these materials is not so impressive. This also impedes the usage of alloying materials for LIB applications. However, to overcome these challenges, several strategies are so far adopted, such as, synthesizing the nanoparticle of the aforesaid materials, making porous structures of the active materials, and making a composite with a carbon matrix. On comparing to the bulk phase, nanomaterials have several advantages, such as, higher resistance towards mechanical strain, larger surface area and providing

a shorter path for Li ion diffusion. In general, it has been observed that the capacity of the carbon-based composite anode materials is higher since the added carbon matrix is also contributing towards the total energy density of the anode by capturing more number of Li ions, thus increases the overall capacity of the anode. In addition, they can also provide steady cycling performance due to the higher stability of the composite towards reversible lithiation-delithiation reaction.



We studied the atomic structures of Carbon based nanocomposites, made up of CNT or graphene, Si/Ge/Sn nanoclusters. The composition stability was understood by employing DFT calculations. Our results show that the cation- π interaction mediates the stability of composites. The calculated charge transfer and electronic structures also support the increase of stability of lithiated cluster inserted CNTs. This composite can be potentially used as anode of LIB.

IT-17

Single Crystal, Spectral and Electronic Transition Studies on (E)-N-(3-Ethoxy-4-Hydroxybenzylidene)-4-Nitrobenzohydrazide

*C Meganathan S. Subaschandraboze**

Central Institute of Plastics Engineering & Technolog, Guindy, Chennai- 32a

Centre for Research & Development, PRIST University, Vallam, Thanjavur-613403, Tamil Nadu, India

Investigation of organic optical materials is playing a major role in recent research. Organic optical materials are widely used in optoelectronics, photonics, optical switching, telecommunications, modulator, optical computing and integrated optical circuit applications [1,2] since most of the optical materials constituted by weak Van der Waals and hydrogen bonds with conjugated π -electrons [3]. The compounds having hydrazide (CH -N -C= O) and π -electrons possess enhanced optical activity [4]. Moreover, the organic single crystals exhibiting photoconductive, photovoltaic and photocatalytic activities [5]. The conjugative electron systems in the compound display extremely larger second-order optical nonlinearities [6]. The aim of the present study is, obtain the single crystal structure and study the vibrational and electronic spectra; in addition, Density Functional Theory (DFT) and Time Dependant-DFT calculations were performed to investigate the molecular orbitals, excited electronic states and natural atomic-orbitals of the title compound.

The single crystal of (E)-N-(3-ethoxy-4-hydroxybenzylidene)-4-nitrobenzohydrazide.H₂O (EHBNB) was grown by a slow evaporation method. The crystal structure was determined by single crystal x-ray diffraction method. The FT-IR (4000-400cm⁻¹) and FT-Raman (3500-50 cm⁻¹) spectra were recorded to study the vibrational behavior of EHBNB molecule. To explore the electronic transition of EHBNB, the UV absorbance spectrum was recorded in the range of 200-800nm. Furthermore, the Density functional theory (DFT) and Time-dependent DFT (TD-DFT) calculations were performed to investigate the molecular geometry, vibrational behavior, electronic excitation and inter-intermolecular charge transfers within the molecule. The singlet (S) and Triplet (T) electronic excited states (n state=6) of EHBNB were examined, in which, the electron spin density (s), excitation energy (ΔE_{1-6}), oscillator strength (f) and electric dipole moment (μ) were examined. The frontier molecular orbitals (FMOs) were studied to find the band gap of FMOs.

The natural atomic orbitals (NAO) and natural localized molecular orbitals (NLMO) of EHBNB were analyzed and the pictorial of orbital distribution was obtained. Since the presence of H₂O in a crystalline environment the topology and bond critical points (BCP) were analyzed due to the presence of H₂O, but there is no deformation in aromaticity of phenyl rings but a bit distraction in hydrazide link. This compound has very good first order hyperpolarizability (β_0) coefficient. Finally, the intermolecular interactions and electron densities were analyzed using Hirshfeld surface and fingerprint analysis.

Keywords: FT-IR; FT-Raman; FMOs; NAO; TD-DFT;

*Corresponding author

References

[1] D.S. Chemla, J. Zyss, Nonlinear Optical Properties of Organic Molecules and Crystals, Academic Press, New York, 1987

IT-18

Modelling for Organic Solids via *Ab Initio* Crystal Structure Predication and Quantum Chemical Methods

P. Srinivasan¹ and A. David stephen²

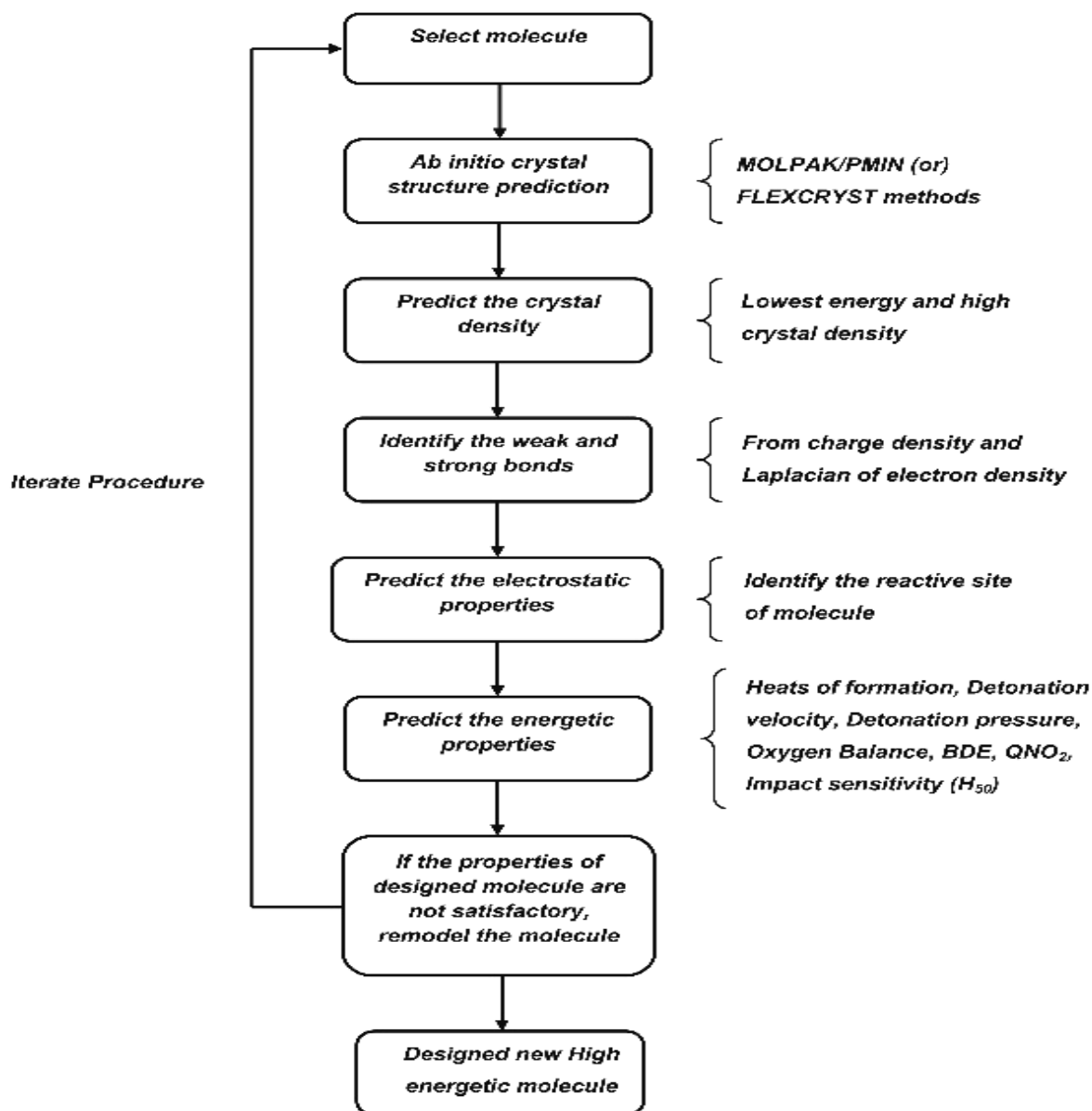
¹*PG & Research Department of Physics, Chikkaiah Naicker College, Erode, India*

²*Department of Physics, Sri Shakthi Institute of Engineering and Technology, Coimbatore, India*

Email: sriniscience@gmail.com

Computational modelling and quantum chemical methods are enable the definition of a large number of molecular quantities characterizing the reactivity, shape, electron density and binding properties of a complete molecule as well as of molecular fragments and substituent's. The *ab initio* crystal structure prediction method lies in the application area where a successful prediction method can give a good understanding of the crystallisation process, and also the prediction of highly energetic molecules might decrease the level of experimental risks. The computed theoretical parameters are gives two main features: firstly, the compounds and their various fragments and substituent's can be directly characterized on the basis of their molecular structure only; and secondly, the proposed mechanism of action can be directly accounted for in terms of the chemical reactivity of the compounds under study. Quantum chemically derived parameters are fundamentally different from experimentally measured quantities. In using quantum chemistry-based parameters with a series of related compounds, the computational error is considered to be approximately constant throughout the series. Further, the quantum chemical methods reduce the number of experiments required and allow one to do more intelligent experiments. The computational material design via molecular modelling and *ab initio* quantum chemical methods viable routes prior to the synthesis of new organic solids with desired properties.

The main advantage of predicting the crystal structure of high energetic materials are: firstly, it gives the exact density of the energetic materials which is not possible to determine accurately by other theoretical methods, secondly, it largely simplifies the search for high density energetic materials from trial synthesis of large number of compounds to design potential explosive/propellant molecules. Generally, the explosive power of a energetic material largely depends on density of material. Further, the strength of bonds in the molecule needs to be checked, as it is directly related to initiation of detonation and it decides part of the sensitivity of the molecule. In this context, the bond topological characterization allows to understand the bond strength (strong and weak bonds) of molecules at electronic level. Hence, the inclusion of charge density distribution along with the structural information and relation between bond charge depletion and bond sensitivity may be appropriate for the material design. The sensitivity of an energetic material for the external stimuli is also one of the key properties of energetic materials and it has potential application in handling the explosive materials. Below figure shows the new computational strategy for high energetic materials design.



Keywords: Crystal structure prediction, DFT, MOLPAK, Gaussian and ESP

IT-19

Designing Potent Inhibitors of Influenza A Virus - A Quantum Chemical and Spectroscopic Study

M. Prasath

Department of Physics, Periyar University PG Extension Centre, Dharmapuri – 636701

*E-mail id: sanprasath2006@gmail.com

Influenza A virus is a rapidly contagious virus, causing acute to chronic respiratory disease in humans, and it has been responsible for several global outbreaks. The virus is also a zoonotic pathogen infecting swine, avian, horse, and other species. The swine have been recognized as a primary influenza virus mixing vessel because they are susceptible to infection by both human and avian influenza viruses, facilitating re-assortment among different influenza virus strains. The neuraminidase (NA) enzyme of influenza A virus is a potential target to develop antiviral drugs. NA is an enzyme; it cleaves sialic acid groups from glycoproteins, which is required for flu viral infection replication. So far, three neuraminidase inhibitors have been approved for the treatment of flu infection, namely, zanamivir, oseltamivir and peramivir. In recent years the researchers are developing plant derivative drugs for treating influenza virus.

In the present context, the plant derivative drugs like Liquiritigenin, Liquiritin, Luteolin, Vitexin, Ononin, Corylin, Licocoumarone and Roseoside are taken for further calculations. The structure of the molecules was optimized and their values are compared with docked values. The experimental data of FT-IR, FT-Raman vibrational frequencies and UV-Vis spectra was recorded and their values are good agreement with computational results. The molecular orbital contributions were studied by using the total (TDOS), partial (PDOS), and overlap population (OPDOS) density of states. The molecules obeys the properties of Lipinski's rule of five, hence the molecules exhibit good bioactive score. A molecular docking analysis of molecules was carried out with neuraminidase enzyme. The docking result shows the lowest binding affinity and inhibition constant of the molecule present in the active site, which is considered to be a better inhibitor.

The HOMO-LUMO reveals the good kinetic stability and less toxicity of the molecules in active site. The dipole moment is an important molecular parameter to study the orientation of the dipole vector and intermolecular interactions of the molecule such as dipole-dipole interactions of non-bonded type. The natural bond orbitals, Fukui functions and molecular electrostatic potential (MEP) shows the chemical selectivity and reactivity site of the molecules. The above mentioned calculations are executed for molecules such as Liquiritigenin, Liquiritin, Luteolin, Vitexin, Ononin, Corylin, Licocoumarone and Roseoside. The results for all molecules are compared with each other and shows which one is better candidate for influenza A virus.

References

Tumpey TM, Garcia-Sastre A, Taubenberger JK, Palese P, Swayne DE, Basler CF. 2004. Pathogenicity and immunogenicity of influenza viruses with genes from the 1918 pandemic virus. Proc. Natl. Acad. Sci. U. S. A. 101:3166–317

ORAL PRESENTATIONS

OP-1

Surface Stress and Surface Reconstruction: an Ab initio Study on the Polar GaN (0001) Surface

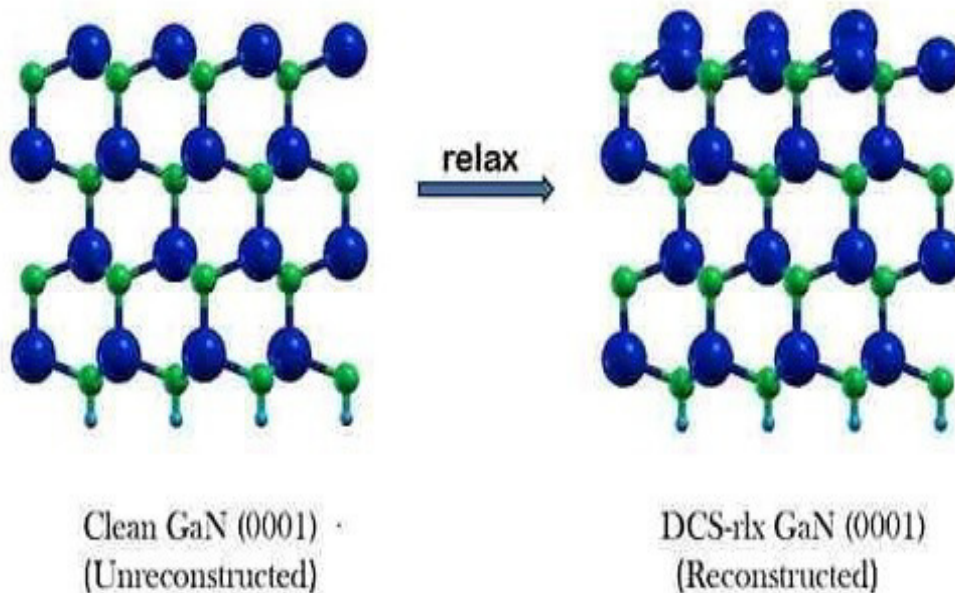
Razia¹ and Madhav Ranganathan*¹

Department of Chemistry, Indian Institute of Technology Kanpur, Kanpur 208016, India

Email: madhavr@iitk.ac.in

A detailed understanding of surface properties is important to many technologies, including material synthesis, nanomaterials, as well as in understanding the bulk and thin film growth of crystal. Wurtzite Gallium Nitride (GaN) is a semiconductor that is widely used in fabrication of blue light emitting diodes (LED). These LEDs are usually fabricated on (0001) surface of GaN, a polar surface having alternate Ga and N layers. However, computation of surface properties for polar surfaces is challenging, due to the absence of reflection symmetry along the polar direction. Through quantum mechanical calculations using periodic density functional theory (DFT), it has been shown that the clean GaN (0001) surface is characterized by the presence of lattice distortions and can be said to be reconstructed [1,2]. Surface stress is

a quantity that can be used to understand the origin of these reconstructions, however, it is not straightforward to calculate this for a polar surface. Here, we propose a method to estimate surface stress using a sequence of DFT calculations of carefully chosen configurations and calculating their corresponding supercell stress [3]. These stress calculations were correlated with the energetics of reconstructed and unreconstructed surfaces.



Schematic diagram showing different configuration for GaN (0001)

References

- [1] P. Kempisty, P. Strąk, S. Krukowski, Surf. Sci. 605 (2011) 695.
- [2] M. Chugh and M. Ranganathan, J. Phys. Chem. C 120 (2016) 8076.
- [3] O.H. Nielsen and R. M. Martin, Phys. Rev. B 32 (1985) 3780.

OP-2

Influence of additional Heat Exchanger Block on Directional Solidification System for growing Good Quality multi-crystalline Silicon Ingot – A Simulation Investigation

*Nagarajan S G¹, Srinivasan M¹ and Ramasamy P*¹*

SSN Research Centre, SSN College of Engineering, Kalavakkam-603110, Chennai, Tamilnadu

Email: ramasamp@ssn.edu.in

Transient simulation has been carried out for analyzing the heat transfer properties of Directional Solidification (DS) furnace. The simulation results revealed that the additional heat exchanger block under the bottom insulation on the DS furnace has enhanced the control of solidification of the silicon melt. Controlled Heat extraction rate during the solidification of silicon melt is requisite for growing good quality ingots which has been achieved by the additional heat exchanger block. As an additional heat exchanger block, the water circulating plate has been placed under the bottom insulation. The heat flux analysis of DS system and the temperature distribution studies of grown ingot confirm that the established additional heat exchanger block on the DS system gives additional benefit to the mc-Si ingot.

OP-3

Coupled Growth of Tin-Zinc Eutectic Crystals during Directional Solidification and Influence of Solid-Solid Interface Anisotropy in Morphological Evolution

*Aramanda Shanmukha Kiran¹, Salapaka Sai Kiran¹, Kamania Chattopadhyay² and Abhik Choudhury*¹*
Department of Materials Engineering, Indian Institute of Science, Bangalore, India

Email: askiran131@gmail.com

Directional solidification of binary eutectic alloys show various types of microstructural features. Solidification process is influenced by control (solid-liquid interfacial velocity V , fixed thermal gradient G across the solid-liquid interface) and material (phase diagram, concentration, interfacial energies and their anisotropies, solute diffusion in the liquid) parameters. One of the major factors influencing morphological evolution is the volume percent of two crystal phases. Generally, in a coupled eutectic system low volume percent (minority phase) phase will adopt a rod-like morphology, while the other phase (majority phase) forms a continuous matrix. However, Sn-Zn alloy is exception to this idea. Solidification experiments of Sn-Zn eutectic alloy indicate that the microstructure can be lamellar over large areas, despite the minority phase (zinc phase) having a volume fraction of less than 10%. In addition, the interphase boundaries in the solid keep a well-defined orientation during growth. We hypothesise that this biasing both in terms of the rod to lamellar transition and lamellar orientation results from an effect of the anisotropy of the free energy of the interphase boundary. In support of this theory we present both theoretical arguments as well as results obtained from experimental characterization techniques (using SEM/Electron diffraction).

OP-4

Heteroepitaxial Quantum Dots on Patterned Substrates

Monika Dhankhar¹ and Madhav Ranganathan^{1*}

Department of Chemistry, Indian Institute of Technology Kanpur, Kanpur 208016, India

Email: dmonika@iitk.ac.in

Quantum dots are very small crystals with typical size ranging from 1 nm to 100 nm. In heteroepitaxial growth, the elastic strain due to the lattice mismatch leads to spontaneous quantum dot formation. However, these dots, such as the silicon-germanium quantum dots on a flat Si(001) substrate, exhibit a large size distribution and spatial disorder. One approach to direct the size and organization of the quantum dot arrays in these systems is to use pre-patterned substrates as a template for growth. We construct a theoretical framework based on continuum mechanics to study the growth of quantum dots on patterned substrates. The corresponding numerical resolution is performed using a small slope approximation and a pseudospectral method to resolve the elastic problem[1-3]. The competition between the length scale of the pattern and the intrinsic quantum dot size leads to a rich behaviour where localization of dots can be modified with respect to the features of the patterns. In cubic elastic materials such as silicon and germanium, the alignment tendency due to the elastic anisotropy also changes the location of the quantum dots. In our work we show that, indeed, this elastic anisotropy is crucial in order to reproduce the key experimental results on quantum dot formation on substrates that has Gaussian pit-like patterns[4].

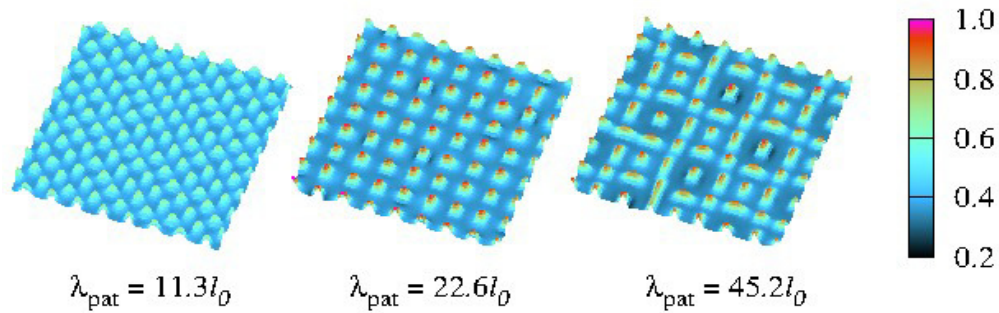


Fig. 1. Snapshot showing quantum dot growth starting with different pattern wavelengths (λ_{pat}) indicated. The color bar refers to the height of the film in units of the l_0 ($l_0 = 8.8$ nm). The system size is 128×128 in units of l_0 and the initial thickness of the film above the patterned substrate is ~ 8 ML or 2.19 nm.

References

- [1] J.-N. Aqua, X. Xu, Surf. Sci. 639 (2015) 20.
- [2] G.K. Dixit, M. Ranganathan, J. Phys. Condens. Matter 29 (2017) 375001.
- [3] G.K. Dixit, M. Ranganathan, Nanotechnology 29 (2018) 365305.
- [4] J. M. Amatya, J. A. Floro, Appl. Phys. Kett. 109 (2016) 193112.

OP-5

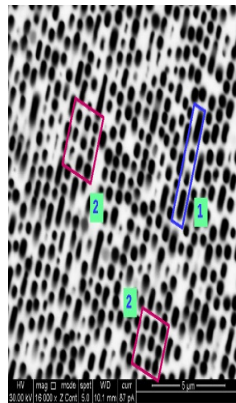
Phase Field Modeling of Microstructure Evolution in Sn-Zn Eutectic Alloy under Directional Solidification Conditions

*Sumeet Khanna¹, Abhik Choudhury*¹*

Department of Materials Engineering, Indian Institute of Science, Bangalore, India

Email: sumeet92k@gmail.com

The Sn-Zn eutectic system is considered as a potential substitute to Pb based alloys in solder applications. One of the factors that determine the strength and stability of the interconnect region in a device is the microstructure at the solder joint. Here, we simulate the growth of Sn-Zn eutectic alloy under conditions of directional solidification using the phase field method [1]. The microstructure obtained during directional growth depends upon the thermodynamic properties and physical parameters of the alloy such as the composition, phase fraction of the solidifying phases, interfacial surface energies between the phases, and process parameters like the growth velocity and the imposed temperature gradient. It is experimentally observed that the Sn-Zn eutectic shows a range of microstructures under different processing conditions, which can be broadly characterized as broken lamellar, hexagonally arranged Zn rods and rectangularly arranged Zn fibres. In this study, we explore the role of interfacial surface energy anisotropy between the solid phases on morphology selection. Depending upon the strength and orientation of interfacial anisotropy, we obtain simulated microstructures similar to the experimental ones. Thus, using the phase field method, we explain the interface dynamics in solidification and the microstructural stability in the Sn-Zn eutectic alloy.



Legend:

- 1: Lamellar/ Broken- Lamellar Zn phase
- 2: Rectangular arrangement of Zn fibers

Figure 1: Experimental Sn-Zn eutectic microstructure (Zn phase = black), from Kiran

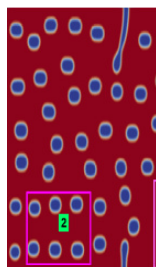


Figure 2: Simulated Sn-Zn eutectic microstructure (Zn phase = blue)

OP-6

Growth and Characterization of L-Tartaric Acid Lead Acetate Single Crystals
Jagadeesh M. R¹, Suresh Kumar H. M^{*1}

^a Department of Physics, Jain Institute of Technology, Davangere-577 005, India

^b Department of Physics, Siddaganga Institute of Technology, Tumkur-572 103, India

E-mail address: jmrshyagale@gmail.com

New nonlinear optical (NLO) semiorganic crystals of L-tartaric acid lead acetate (LTALA) were grown from aqueous solution using slow evaporation method. The grown crystals were subjected to different characterizations viz, X-ray diffraction, FTIR, UV, TGA, and NLO studies. XRD study reveals that the crystal belongs to triclinic system with the space group P1. The vibrational frequencies of various functional groups have been derived from FTIR spectrum. Thermal stability of the grown crystal was investigated by TG-DTA studies and it is observed that the title compound is thermally stable up to 230°C. Optical absorption study has been carried out and a good transparency in the entire visible region is observed with the lower cutoff wavelength of 225 nm. Kurtz powder method was employed to explore the NLO characteristics of the grown crystal. Further, the comparative studies were made for optically active L-tartaric acid derivatives.

Keywords: L-Tartaric acid, Semiorganic, Slow evaporation, TG-DTA, NLO Crystal,

OP-7

Synthesis, Theoretical And Docking Studies, Antibacterial Activities Of Hydrazone Derivative

*K. Ananthi¹, *Dr. H. Anandalakshmi², Dr. S. Senthilkumar³,*

Department of Chemistry, Annamalai University

Email: ananthikumar13@gmail.com

The newly synthesized compound of 3-methoxy-N'-(3,4-dimethoxybenzylidene)benzohydrazide derivative was characterized by elemental analysis like Mass, FT-IR, H¹ NMR and C¹³ NMR and single crystal X-ray diffraction techniques. The first order hyperpolarizability and dipole moment also calculated. The experimental FT-IR and Raman wave numbers were compared with the respective theoretical values obtained from DFT calculations and found to agree well with the theoretical values. The HOMO-LUMO analysis used to determine the charge transfer within the molecule. All theoretical calculations were performed on the basis of B3LYP/6-311++G (d,p) level of theory using DFT methods. Further the synthesized compound were screened for their in vitro antibacterial and antifungal strains. The compounds displayed higher antifungal potential as compared to antibacterial potential. The most antimicrobial potent derivatives were also investigated for their cytostatic and cytotoxic properties against three cell lines. Finally, molecular docking study had been performed by *in silico* method to analyse their anti-tuberculosis aspect against InhA, the enoyl acyl carrier protein reductase (ENR) from Mycobacterium tuberculosis and using 2NSD protein.

Keywords: Benzohydrazide, IR, NMR, Mass, DFT method.

OP-8

Investigation of Electron Density, Impact Sensitivity and Electrostatic Properties of Highly Energetic Benzexodiazol Derivatives via DFT and AIM Analysis

L. Sathya¹, P. Srinivasan^{1*}, B.Gnanavel¹ And A. David Stephen²

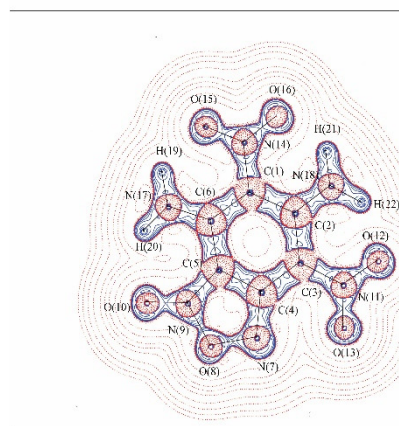
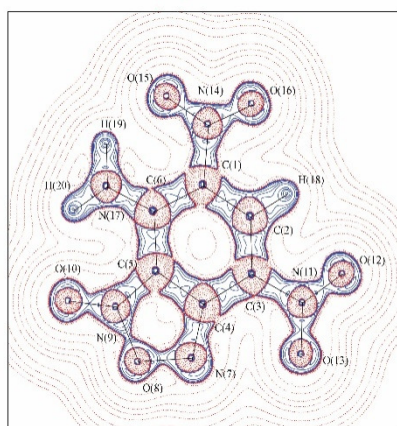
¹Department of Physics, Chikkaiah Naicker College, Erode, India

²Department of Physics, Sri Shakthi Institute of Engineering and Technology, Coimbatore, India

*E-mail: sriniscience@gmail.com

A charge density study on high energetic molecules, 5,7 dinitro-2,1,3-benzexodiazol 4-amine 3-oxide (C₆H₃N₅O₆) and 5,7 dinitro-2,1,3-benzexodiazol 4,6-diamine 3-oxide (C₆H₄N₆O₆) has been carried out by using Density Functional Theory (DFT) with HF/6-311G**, B3LYP/6-311G** and B3LYP/aug-cc-PVDZ basic sets. The optimized geometrical parameters such as bond lengths, bond angle and dihedral angles are calculated and compared with the similar types of molecules. Interestingly, the HOMO and LUMO electronic transition occurs in the molecule (I) and molecule (II) are 3.45 eV and 3.28eV respectively. The DFT method predicts that the electron density $\rho(r)$ of the molecule (I), ring N-O bonds is $\sim 3.37 \text{ e}\text{\AA}^{-5}$ and the corresponding Laplacian $\nabla^2\rho(r)$ is $\sim -24.75 \text{ e}\text{\AA}^{-5}$. A large electronegative potential is found in the vicinity of the -NO₂ group, and a small electropositive region is rest of the molecules.

Keywords: DFT, HOMO, LUMO, ESP and AIM



The Laplacian of electron density maps from B3LYP/6311G**

OP-9

Effect of Crucible Dimension in the Directional Solidification Process

G. Aravindan¹, M. Srinivasan¹ and P. Ramasamy^{*1}

SSN Research Centre, SSN College of Engineering, Kalavakkam, Chennai 603 110.

World population is increasing day by day with energy requirement. Currently energy technology has been turning to the renewable energy side, because of long term requirement. In renewable energy

sources solar energy is crucial one. Installed renewable power grids (excluding large hydro) in India (Up to Feb 2016): Wind power is 29,151 MW (59.8 %), Solar power is 9,566 MW (18.6 %), Bio mass power is 8,182 MW (15.9 %), Small hydro power is 4,346 MW (8.5 %) and Waste-to-power is 114 MW (0.2 %). Percentage of wind power in the renewable energy power production is very high but it has drawbacks compared to solar panels such as maintenance cost and lower efficiency after the life time of 20 years (wind energy is 66% and solar panel is 80 %). In the PV market 60 % of solar panels are occupied by the mc-Si solar cells, it is produced by DS process. Efficiency of mc-Si wafer is less than the mono-Si wafers but it has low cost, simple operating process and high mass production compared to mono-Si wafer production. During the mc-Si growth process stress and dislocation reduction is important because it will affect the conversion efficiency of mc-Si wafer solar cells.

We have numerically simulated two 6.90 Kg mc-Si ingot directional solidification (DS) systems (Different crucible dimension: DSS-1 and DSS-2) by using Finite Volume Method (FVM). DSS-1 crucible size is 200 mm * 200 mm * 280 mm and DSS-2 crucible size is 158 mm * 158 mm * 340 mm. The temperature distribution, melt-crystal (m-c) interface shape, vertical temperature gradient and melt flow velocity have been investigated. DSS-1 has convex m-c interface shape and DSS-2 has concave interface shape. Lower vertical temperature gradient and lower melt flow velocity are obtained for DSS-1 compared to DSS-2.

OP-10

Quantum Chemical and Docking Studies on Piperidine Derivatives via DFT and Autodock Methods

P. Periyannan¹, P. Srinivasan², A. David Stephen³ and K. Ravichandran^{1}*

¹*Department of Physics, Kandaswami Kandar's College, Velur, Namakkal (Dt), India.*

²*PG&Research Department of Physics, Chikkaiah Naicker College, Erode, India.*

³*Department of Physics, SriShakthi Institute of Engineering and Technology, Coimbatore, India.*

* E-mail: kravichandran05@gmail.com

The piperidine derivatives have large biological activities like antimicrobials, anti inflammatory, antiviral, anti malarial etc. Here, present computational investigation of 1-Chloroacetyl-3-isopropyl-r-2,c-6-diphenylpiperidin-4-one (CID) and 1-Formyl-c-3,t-3-dimethyl-r-2,c-6-diphenylpiperidin-4-one (FDP) Piperidine derivatives undergone by quantum chemical calculation using Gaussian09 program package. Notably, the optimized geometrical parameters obtained by B3LYP/6311G** and HF/6311G** methods are shows good agreement with experimental X-ray data. The bond topological analysis of electron density at the bond critical points (bcp) of the also been calculated. The atomic charges of the molecules have been compared with AIM, MPA and NPA charges. Interestingly, the electrostatic potential map gives a large electronegative region at the vicinity of the oxygen atom and electropositive region around the piperidine ring. Also highest occupied molecular orbital (HOMO) and lowest unoccupied molecular orbital (LUMO) energy levels of frontier orbital were obtained.

Keywords: DFT, AIM, MPA, NPA, HLG, ESP.

OP-11

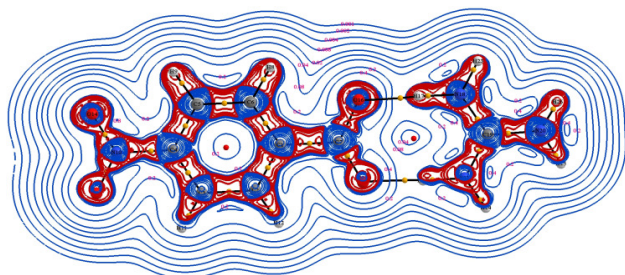
Atoms in Molecule Analysis and Third-Order Nonlinear Optical Absorption Properties of Guanidinium 4-nitrobenzoate

Sasikala V.^{*1}, D. Sajan¹

^aCentre for Advanced Functional Materials, DST-FIST & KSCSTE SARD Supported Postgraduate and Research Department of Physics, Bishop Moore College, Mavelikara, Alappuzha, Kerala-690110, India.

*E-mail: sasikala1986@gmail.com

The atoms in molecule analysis shows that the equilibrium geometry of Guanidinium 4-nitrobenzoate (GPNB) molecule consists of topological rings; due to the benzene ring and the other due to an eight membered ring which is formed from the carboxylate carbon atom, intramolecular N-H...O bonds and the carbon atom of the guanidinium group of the molecular system and the later ring is found with low values of topological characteristics of the electron density relative to the former topological ring which is indicating the strong electron density accumulation at the benzene ring with respect to the ring formed by the intramolecular H-bonding junction of the molecule. The contour lines showing the negative Laplacian of electron density distribution along the plane of the oxygen and nitrogen atoms of the equilibrium geometry of the molecule is shown in Figure. The two-photon assisted reverse saturable absorption mechanism and the optical limiting characteristics of the ethanol solution of GPNB were studied using the open-aperture Z-scan technique. The microscopic non-linear optical behaviour of GPNB



has been investigated by DFT/B3LYP/c-pVTZ theory method. The static as well as the dynamic dependence of linear polarizabilities, first-hyperpolarizabilities and second hyperpolarizabilities for various NLO processes have been theoretically estimated from the optimized geometry of the molecule. The nuclear relaxation

contribution to the vibrational polarizabilities and the first-hyperpolarizabilities for each mode of vibrations of GPNB has been numerically estimated. The theoretically predicted values for vibrational and electronic NLO response contributions of the molecule have showed their better NLO property compared to urea molecule. The open-aperture Z-scan study suggested the potentiality of the material in optical limiting applications.

HIGHLIGHTS

The nonlinear absorption behaviour and the optical limiting property of GPNB were discussed.

The microscopic optical nonlinearities of GPNB have been theoretically investigated.

The nuclear relaxation contributions to the vibrational polarizabilities were analyzed for each mode of vibrations.

The atoms in molecules analysis have been performed for the molecule.

OP-12

The Electrical Conductivity of Methylene-Methyliminomethyl Formamidinium Molecular Nanowire via DFT and QTAIM Theory

S. Palanisamy¹, P. Jayalakshmi¹, P. Srinivasan², A. David Stephen³ and K. Selvaraju*¹

^aDepartment of Physics, Kandaswami Kandar's College, Velur-638182, Namakkal (Dt) India

^bDepartment of Physics, Chikkaiah Naicker College, Erode-638004, Erode (Dt), India

^cDepartment of Physics, Sri Shakthi Institute of Engineering and Technology, Coimbatore-641062, India

* E-mail: physicsselvaraj@gmail.com

In the present computational study, Structural and the electrical characteristics of Au and thiol substituted methylene-methyliminomethyl formamidinium (MMF) molecular nano wire have been carried out with density functional theory (DFT) by adding polarization and diffuse function with the basis set LANL2DZ using Gaussian09 program. The applied electric field of various values on the molecule altered the geometrical parameters (such as, Bond length, Bond angle and Torsion angle) also calculated. The electrostatic and transport properties of the molecule have been analyzed for the same external field. The bond topological analysis based on the AIM theory shows the difference of charge distribution in all bonds. The variation in the atomic charges (MPA, NPA) of the molecule for the various applied electric fields has been analyzed. The HOMO-LUMO gap (HLG) of the molecule for zero bias is 1.90 eV, as the field increases this gap decrease to 0.27 eV, which has been compared to the density of states (DOS) spectrum. The spatial redistribution of the frontier orbitals (HLG) shows that all the atoms of MMF molecule between the two thiol atoms are not delocalized. The applied electric field polarizes the molecule, in consequence of that the dipole moment of the molecule increases from 6.46 Debye to 9.65 Debye. Hence, although the molecular wire exhibit small HLG, there is no possibility of electrical conduction and it acts as an insulating wire. Further, the movement of ESP regions in the ESP map of the molecule for applied potential clearly shows the charged regions and the effect of substitution. This observation gives an insight on this kind of lengthy molecules, which are may be useful to synthesise insulating layers.

Keywords: DFT, AIM, HLG, DOS, ESP



Figure shows the HOMO-LUMO Gap of Au and S substituted methylene-methyliminomethyl formamidinium molecule

OP-13

Theoretical Investigation of Electrical and Optical Properties of Sodium Succinate Hexahydrate (B Phase) Single Crystal: A Potential Third Order NLO Material

S. Anitha¹, P.S. Latha Mageshwari¹, R. Priya^{*1}

¹Department of Physics, T. J. S. Engineering College, Peruvoyal, 601 206, India,

^{*2}Department of Physics, R. M. D. Engineering College, Kavaraipettai, 601 206, India, 9444765290, 044 - 3330 3030

³Department of Physics, R. M. K. Engineering College, Kavaraipettai, 601 206, India,

*Email: rmdpriya29@gmail.com

Single crystals of third order nonlinear optical Sodium Succinate Hexahydrate (SSH) (β phase) has been synthesized using aqueous solution at room temperature by slow evaporation technique. Single crystal X-ray diffraction analysis confirmed that grown crystal crystallizes in centrosymmetric monoclinic system with space group $P2_1/c$. The sample of thickness 1mm was used for recording the optical transmittance in the wavelength range from 200 to 2000 nm and the cut-off wavelength was found to 296 nm. Good optical transmittance was found in the sample in the region of conductivity, electrical susceptibility and optical conductivity, were determined. Using dielectric visible wavelength and the theoretical calculation of optical constants, such as reflectance, refractive index, electrical studies, the ac, dc conductivity and activation energy of the title compound for various frequencies at different temperatures was evaluated and results were discussed in detail.

Table 1 Crystallography data

Parameters	A	B	C	β	Volume
Reported data	8.9033Å	6.3000Å	10.717Å	102.614	586.60Å ³
Grown crystal data	8.9300Å	6.3200Å	10.760Å	102.57	593.00Å ³

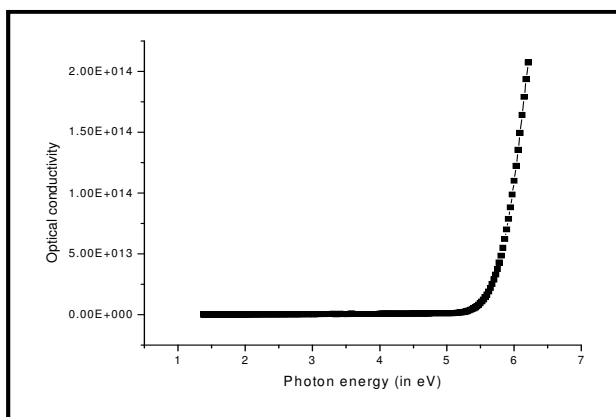


Fig. 1. Variation of Optical Conductivity with Conductivity wit Photon energy

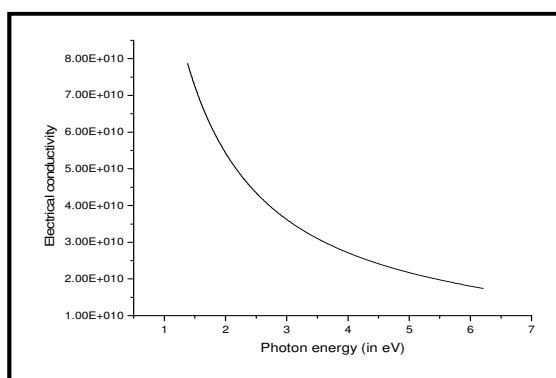


Fig. 2. Variation of electrical Photon energy

OP-14

Performance Analysis of Hybrid Bulk Junctionless Transistors Using Numerical Simulation

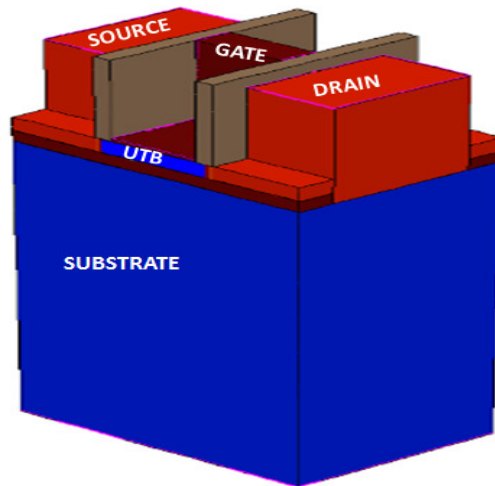
A.Nisha Justeena¹ and R.Srinivasan^{*1}

Department of IT, SSN college of Engineering Kalavakkam, Chennai

*Email: nishaarockiam@gmail.com

In this manuscript, we propose Hybrid Bulk Junctionless devices. Hybrid devices combine two different device structures. MOSFET and FinFET devices sitting on SOI substrate has been proposed in [1]. In this work, we combine the SOI junctionless MOSFET and bulk junctionless trigate device to be called as hybrid junctionless trigate FET. The design and characteristics of the proposed device are done using commercial 3D TCAD simulator. Three different gate dielectric materials, SiO₂, Si₃N₄ and HfO₂ are explored. The results are compared against the regular junctionless trigate device using their I_{ON}, I_{OFF}, $\frac{I_{ON}}{I_{OFF}}$, DIBL, Subthreshold slope, Transconductance, and unity gain frequency. The adjacent figure shows the 3D device structure, and the following table gives some of the properties of the proposed device. The proposed device shows better $\frac{I_{ON}}{I_{OFF}}$, DIBL, and f_T performance.

Parameters	Hybrid Bulk Junctionless device			Bulk Junctionless device (ref [2])
	SiO ₂ (3.9)	Si ₃ N ₄ (7.5)	HfO ₂ (25)	HfO ₂ (25)
I _{on} /I _{off}	3x10 ⁵	1x10 ⁶	3.5x10 ⁷	10 ⁵
DIBL(mv/V)	36	33.3	29	40
f _T (GHz)	427	450	485	432



[1]. K.P. Pradhan, Priyanka, Mallikarjunarao, P.K. Sahu, " Exploration of symmetric high-k spacer (SHS) hybrid FinFET for high performance application" Superlattices and Microstructures 90 (2016) 191-197.
 [2].M. H. Han, C. Y. Chang, H. Bin Chen, J. J. Wu, Y. C. Cheng, and Y. C. Wu, "Performance comparison between bulk and SOI Junctionless transistors," *IEEE Electron Device Lett.*, vol. 34, no. 2, pp. 169–171, 2013 .

OP-15

Band Gap Engineering of Cu₂-II-IV-VI₄ Quaternary Semiconductors Using PBE-GGA, TB-mBJ and mBJ+U Potentials.

*J. Bhavani*¹, Rita John¹*

¹*Ethiraj College for women, Chennai*

²*Department of Theoretical Physics, University of Madras, Chennai 600 025*

*E-mail: bhavanishiva24@gmail.com

The chalcogenide quaternary semiconductor series, I₂-II-IV-VI₄ are known to have potential applications such as photovoltaic absorbers, optoelectronic, and thermoelectric materials. Unfortunately, accurate theoretical understanding of the electronic properties of these materials is hindered by the involvement of Cu *d* electrons. Density Functional Theory (DFT) based calculations using the Local Density Approximation (LDA) or Generalized Gradient Approximation (GGA) often underestimates the electronic properties of these materials, especially for narrow-gap systems. The modified Becke-Johnson exchange potential (TB-mBJ), is used to calculate the electronic properties of Cu based quaternary semiconductors Cu₂ZnGeX₄ (X = S, Se & Te) which includes band structure and other electronic properties such as TDOS and PDOS are analyzed in detail, in particular to have a better understanding of the procedure which leads to improved results with the TB-mBJ potential. Also the results obtained using TB-mBJ potential are compared with PBE-GGA. Even though the comparison of results with the experimental and other theoretical calculations show that the results obtained by TB-mBJ are much superior to other theoretical techniques but are still underestimating when compared to experimental results. This explains the inadequacy of mBJ potential for semiconductors with strongly delocalized *d* electrons. Thus in this paper the screened Coulomb interactions of localized electrons, often treated as adjustable parameters in constructing model Hamiltonians are important quantities for studying strongly correlated materials are used to study the electronic properties of Cu based quaternary semiconductors. The on-site Coulomb *U* is incorporated within mBJ potential (mBJ + *U*) which leads to a better description of the *pd* hybridisation and therefore the resultant band gap is very much comparable with the experimental results.

Keywords: Cu₂-II-IV-VI₄ (X = S, Se & Te), Band Structure, TB-mBJ potential, mBJ+U, Cu-based semiconductor, importance of *d*-orbitals. On-site Coulomb *U*

OP-16

Engineering Sub Wavelength Scale 3D Focal Structures Using Annular Walsh Filter

D. Thiruarul¹, K.B. Rajesh^{1}*

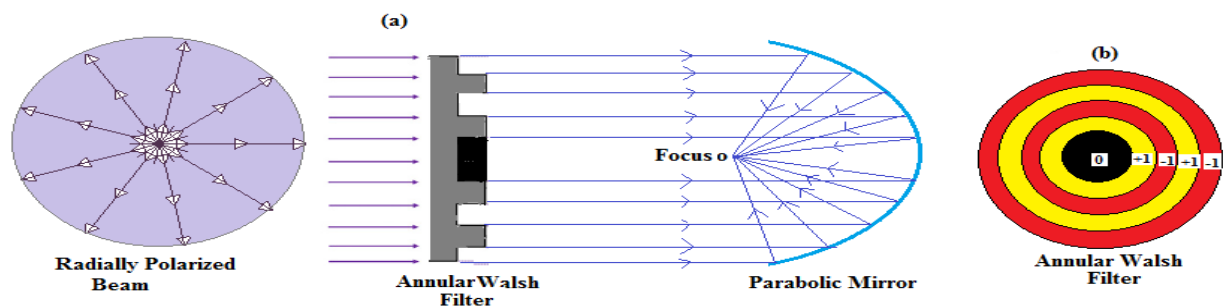
Department of Physics, Chikkanna Government Arts College, Tiruppur, Tamilnadu, India

*E-mail: rajeshkb@gmail.com

Based on vector diffraction Theory, the tight focusing properties of radially polarized Bessel Gaussian vortex beam (BGVB), phase modulated by annular Walsh function filters and focused by a high

NA parabolic mirror system is studied numerically. The annular Walsh filter derived from the annular Walsh functions forms a complete set of orthogonal phase filters that takes values of either 0 or π phase corresponding to +1 or -1 over the domain specified by the inner and outer radii of the annulus. Numerical results show that properly modulating the annular obstruction of Walsh filter, pupil to beam ratio and topological charge of the input Bessel BGVB one can generate many novel focal patterns such as three dimensional multiple focal spot segments, sub wavelength optical needle etc., We expect that such three dimensional focal structures are useful for nano-lithography, particle trapping and transportation, as well as confocal and STED microscopy, optical super-resolution, optical micro-manipulation, optical tomography, microstructure fabrication and so on.

Keywords: Annular Walsh Filters, Self-Similarity, High NA Parabolic Mirror



A schematic of the proposed system is shown in figure

OP-17

Effect of Heat Exchanger Block Thickness on Grown Multi-Crystalline Silicon Ingot by Directional Solidification Process

*M. Thiagarajan¹, S.G. Nagarajan¹, M.Srinivasan*¹, and P. Ramasamy²*
SSN Research centre, SSN College of Engineering, Chennai, India-603110

Numerical investigation was carried out for analyzing the von-Mises stress of multi-crystalline silicon ingot during the Directional Solidification Process. DS furnace with Various thickness of heat exchanger block 10 mm, 20 mm, 30 mm, 40 mm, 50 mm, 100 mm, 150 mm, 180 mm, 200 mm, 220 mm, and 250 mm has been simulated and their response to solidification process has been analyzed. The axial and radial temperature, maximum principal stress, maximum shear stress study has been carried out for analyzing the von Mises stress distribution. By varying the thickness of the heat exchanger block the axial temperature distribution has been altered. From simulation results, we concluded that there should be a match with the axial and radial temperature gradient for getting the lower von-Mises stress. Here we have optimized the axial temperature distribution which is optimal to the radial temperature distribution for obtaining minimum von-Mises stress by changing the thickness of the heat exchanger block.

Key words

Solar cell, simulation, Directional solidification, Silicon, Thermal stress, Heat exchanger block thickness, Temperature gradient.

OP-18

First Principles Calculation on the Electronic and Optical Properties of AA-Stacked Two-Dimensional Graphene, Silicene, Germanene, and Stanene

*Benita Merlin¹ and Rita John^{*1}*

University of Madras, India, ²Alpha Arts and Science College, India

Email: ritajohn.r@gmail.com

Graphene and its 2D analogues: silicene, germanene, and stanene exhibit exotic properties due to the presence of Dirac cone in the electronic band structure. The absence of the band gap at the Dirac point abstains their direct application in the semiconductor industry which could be surmounted by functionalization, edge effect, and stacking. In this study, we have analyzed the electronic band structure and optical properties of AA-stacked bilayer graphene and its 2D analogues and compared the results with single layers. The calculations have been done using Density Functional Theory with Generalized Gradient Approximation as exchange correlation potential as in CASTEP. The study on electronic band structure shows the splitting of valence and conduction bands. Among different stacking, AA-stacked bilayer produces a band gap of 0.342eV in graphene and an infinitesimally small gap in other 2D materials. The band gap is due to the capping of p_z Orbitals between the two layers. All materials exhibit excellent optical properties throughout the optical region. Optical properties like absorption, reflectivity, conductivity, and the electron loss function are studied along both polarization directions. Inferences from the study of optical properties: The static dielectric constant of each material is found to be increased from single layer to AA-stacked bilayer along both polarization directions. Unlike the single layer, all materials exhibit plasma frequency along both polarization directions. The study on the refractive index brings out the birefringence characteristics and the anisotropic behaviour. The intensity of absorption increases from single layer to bilayer. Absorption peaks shift from ultraviolet to infrared from graphene to stanene along both polarization directions. All materials exhibit reflectivity mainly in the UV region along the perpendicular polarization direction. Electron loss function exhibits three peaks along the parallel polarization direction corresponding to germanene and stanene like the single layer while silicene shows only one peak. The peaks due to π plasmons are weaker than the peaks due to $\pi + \sigma$ plasmons. The further study brings out greater inferences towards their direct application in the optical industry through a wide range of the optical spectrum.

Keywords: DFT, GGA, Band structure, graphene, silicene, germanene, stanene, optical properties

OP-19

Liquid like Nucleation in Nanoscale Thin Films

*Pooja Rani , Arun Kumar , B. Vishwanadh , Kawsar Ali , A. Arya , R. Tewari and Anandh Subramaniam I**

*Materials Science and Engineering, Indian Institute of Technology Kanpur, Kanpur-208016, India.
Materials Science Division, Bhabha Atomic Research Centre, Trombay, Mumbai-400085, India.*

* Email: anandh@iitk.ac.in

The concept of critical nucleus size (r^*) is of pivotal importance in phase transformation involving nucleation and growth. Above this size, it is favorable for the product phase to grow; while, 'embryos' smaller than this size tend to revert to the parent phase. The current investigation pertains to crystallization in nanoscale thin films and study of the same using high resolution lattice fringe imaging (HRLFI) and finite element simulations. Using CuZrAl bulk metallic glass system as a model system for this study, we demonstrate liquid like nucleation behaviour in thin solid films on heating. The r^* for the formation of the $\text{Cu}_{10}\text{Zr}_7$ phase in thin films of decreasing thickness, approaches that of the r^* for the formation of the crystal from the liquid (i.e. $r_{\text{thin film}}^* \rightarrow r_{\text{liquid}}^*$). Working in the nucleation dominant regime, we determine the position of the nuclei (along z-direction) from lattice fringe images– an information which is usually absent in such images. The TEM sample is used as a free-standing thin film, crystallite sizes are measured using HRLFI, thickness of the film is determined by electron energy loss spectroscopy and strain energy of the system is computed using finite element computations.

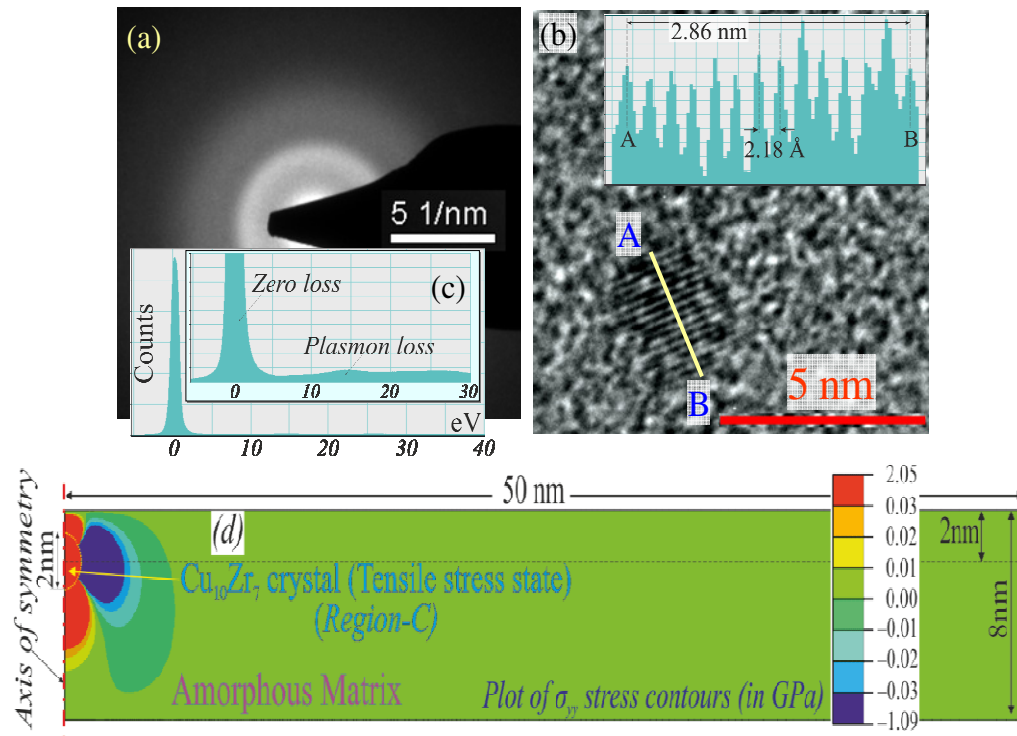


Figure 1: (a) Selected area diffraction (SAD) pattern showing the formation of an amorphous structure on suction casting the $(\text{Cu}_{64}\text{Zr}_{36})_{96}\text{Al}_4$ alloy. (b) HRLFI from a crystallite ($2r = 2.86$ nm) embedded in an amorphous matrix. (c) A typical EELS spectrum acquired from region of diameter 10 nm, which is used in the computation of the thickness of the specimen. (d) FEM simulation of the stress state in the presence of a crystalline in an amorphous matrix.

OP-20

Effect Of Zinc Sulphate on Growth, Characterisation and Applications of L Lysine Single Crystals

*P. Sagunthala*¹, P.Yasotha²*

Department of Physics, Sri Vasavi College, Erode, Tamil Nadu, India.

E-mail: saguphy@gmail.com

Single crystals of the L lysine acid added zinc sulphate (LLZS) have been grown by slow-evaporation method. The crystal structure is confirmed by X-ray powder diffraction and single crystal diffraction methods. When L lysine was added with zinc sulphate monohydrate, the grown crystal crystallizes in monoclinic system with space group $C_{2/c}$. The modes of vibrations of different molecular groups present in the crystals have been identified by spectral analyses. The thermal stability and decomposition of the samples have been studied by thermal analysis. The antibacterial and anti cancerous activities of the grown crystals have been tested with select bacteria and human cervical cancer cell line respectively. The grown LLZS crystals were found to be good antibacterial and anti cancerous agents and they may be considered for pharmacological applications.

OP-21

Structural and Spectroscopic (Ft-IR, ¹³c and ¹h Nmr) Investigation, Molecular Orbital Calculation and Nlo Properties of Novel Piperidine Derivative By Quantum Chemical Calculation

*Akumtoshi Aier¹, P. Samuel Asirvatham¹, M. Krishna Priya³, T. Ramila⁴, B. K. Revathi*¹*

Department of Physics, Madras Christian College (A), Chennai-59, India

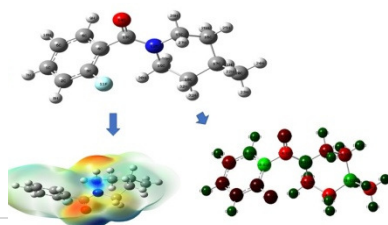
PG and Research Department of Physics, Queen Mary's College(A), Chennai-04, India

E-mail: revathibkrishnan@yahoo.com

The theoretical calculations of (2-fluorophenyl)(4-methylpiperidin-1-yl)methanone (2FMPPM) have been investigated with density functional theory based at the B3LYP level and 6-311++G(d,p) basis set using Gaussian 09W. The geometrical parameters, FT-IR, ¹³C and ¹H NMR(GIAO method) have been calculated for confirming the structure of the molecule. The electronic properties such as the HOMO-LUMO energy gap, mapped molecular electrostatic potential surfaces(MEP), mulliken charges. The thermodynamical and NLO properties were also calculated for 2FMPPM.

Keywords: Geometrical parameters, FT-IR, ¹³C and ¹H NMR, HOMO-LUMO, Mulliken, MEP and NLO.

Graphical Abstract



OP-22

Spectral Investigations (FT-IR, FT-Raman, UV-Visible), NBO, NLO, Molecular geometry, Mulliken charges, HOMO-LUMO, MEP calculations of 1-[(2R, 4S, 5S)-4-azido-5-(hydroxyl methyl) oxolan-2-yl]-5-methylpyrimidine-2, 4-dione [1] by DFT method

Thanmayalaxmi. D,^{1*} Suvitha. A,² Ravishankar. K,³

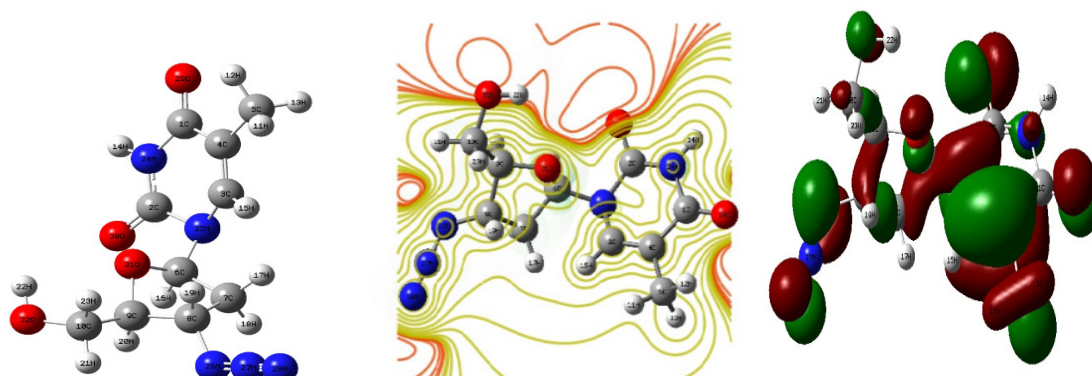
¹ CMR Institute of Technology, Bangalore, India

² CMR Institute of Technology, Bangalore, India

³ B.M.S college of Engineering, Bangalore, India

*E-mail:dthanmaya@gmail.com

Our work is based on DFT calculations on Zidovudine molecule, the only approved antiviral for the treatment of HIV infection. We have reported the theoretical and experimental analysis on FT-IR, FT-Raman, UV spectrum. The DFT calculations were performed by using B3LYP/6-311++ basis set using Gaussian 09 software. The sample of spectroscopic grade was purchased and the FT-IR and FT-Raman spectrum of the compound is recorded using Bruker IFS spectrometer. The ultraviolet visible spectrum of zidovudine dissolved in methanol was recorded using a UV-Vis spectrophotometer in 200–400 nm range at room temperature. The HOMO-LUMO energy gap determines the chemical reactivity, kinetic stability, optical polarizabilities, chemical hardness, softness of the molecule. The MEP diagram gives the vital idea about the size, shape and importantly, its neutral, positive, negative electrostatic potentials are expressed in the form of color coding. Besides, Mulliken atomic charges, frontier molecular orbital (FMO), MEP, NLO activity, Natural Bond-Orbital analysis(NBO) of the title molecule were also performed.



OP-23

Modification on Coumarin Based Groups toward for Highly Efficient organic Dye-Sensitized Solar Cells: A DFT Study

A. Arunkumar¹ and P. M. Anbarasan^{1*}

Department of Physics, Periyar University, Salem - 636 011, India.

Email: anbarasanpm@gmail.com

In this work, we screen a series of coumarin based (NKX-2311) dye sensitizers, namely (D1-D4) are investigated for use in dye-sensitized solar cells (DSSCs) application. Organic dye sensitizers containing coumarin unit as donor, prop-1-ene as spacer and 2-cyanoacrylic acid an electron acceptor based on donor- π -spacer-acceptor (D- π -A) structure. The modified effect on the electronic and photovoltaic (PV) properties have been investigated by the combination of density functional theory (DFT) and time-dependent DFT (TD-DFT) methods. Solvent effects have been examined by conductor-like polarizable continuum model (C-PCM). In general, different exchange-correlation (XC) functional's for calculating the first singlet excited-state NKX-2311 dye were analyzed. Accordingly, TD-B3LYP functional and 6-31G(d) basis set were matched with reference value. Therefore, absorption spectra of D1-D4 dye molecules have been conducted by TD-B3LYP/6-31G(d) method. As a results, D1 and D3 dyes was strongly modified groups for smaller energy gap, red-shifts and electron injected into semiconductors successfully. It is expected to provide theoretical guidance on designing photosensitive with new organic dyes for application in DSSCs yielding highly efficient performance.

Keywords: Organic Dyes, DFT, TD-DFT, UV-Vis and B3LYP.

OP-24

Single-Crystal Neutron Diffraction Study of the Strong O-H \cdots O Hydrogen Bond in 2-picolinic perchloric acid

R.S. Arun Raj, D.Sajan^{*}, Rajul Ranjan Choudhury and R. Chitra

Centre for Advanced Functional Materials, Department of Physics,

Bishop Moore College, Mavelikara, Alappuzha, Kerala 690110, India

Solid State Physics Division, Bhabha Atomic Research Center, Trombay, Mumbai 400085, India

*E-mail: drsajanbmc@gmail.com

Hydrogen bond is an important interatomic interaction, because it is very abundant in biological systems responsible for the molecular and macroscopic properties of materials, molecular recognition, protein folding and function, proton transport in proton conductors, and crystal engineering and supramolecular structure. Investigation of the neutron structure of 2-picolinic perchloric acid (2PPA) could accurately tell us about the mechanisms of the migration of the proton through the hydrogen bond's center. The presence of N-H \cdots O and O-H \cdots O interactions are identified for designing the supramolecular arrangement of this material. N-H \cdots O and O-H \cdots O intramolecular interactions performs an important role

in the present structure, since it is favoured by the six-membered hydrogen-bonded ring. The pattern of the hydrogen bonding and the packing of the molecules in the crystal are shown in Fig. 1a and 1b. It is observed that there is very strong O-H...O hydrogen bond between the carboxyl oxygen of 2PPA symmetry related molecule. In fact this hydrogen bond is found to be symmetric in nature with both O-H and H...O distance being 1.231Å, and this bond is found to be bent with O-H..O angle to be 156°. It is important note that the hydrogen atom in this very strong O-H..O hydrogen bond is not disorderd as concluded from the shape of its thermal ellipsoid. Hence the 2PPA molecule exists in dimmeric form in these crystals with the center of inversion lying at the Hydrogen atom of the O-H..O hydrogen bond connecting the monomers(Figure -1a). It is observed that the perchlorate moieties are placed between the two 2PPA molecules and interact through C-H..O hydrogen bonds

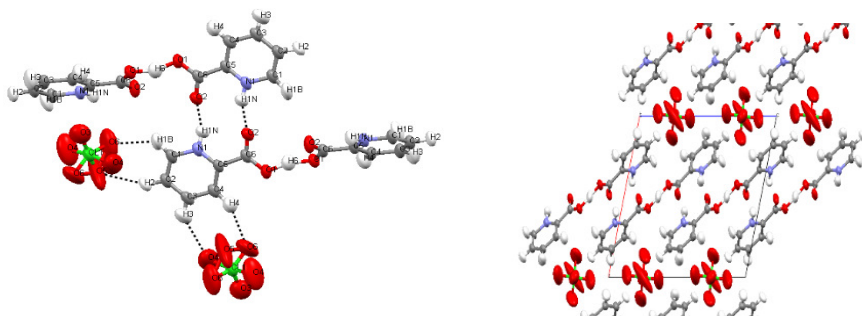


Fig. 1a & 1b A plot of 2PPA molecules from the neutron data

OP-25

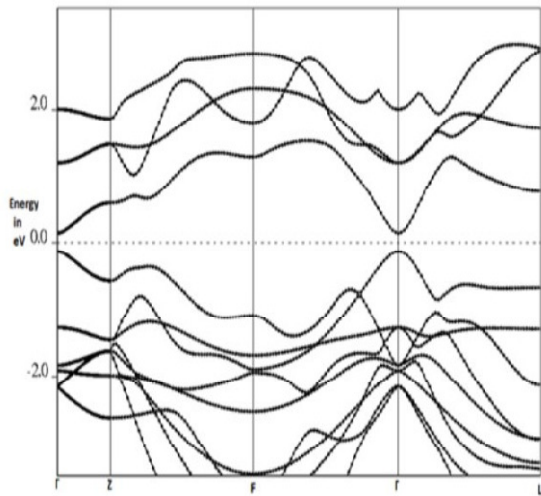
Effect of Spin-Orbit Coupling in Topological Insulator Bi₂Se₃ Using DFT as a Tool

Umamaheshwari¹ M & Rita John^{1*}

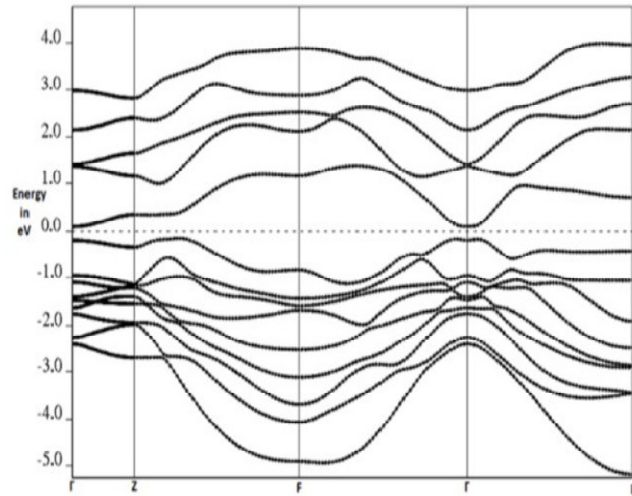
Department of Theoretical Physics, University of Madras

Email: ritajohn.r@gmail.com

The compound Bi₂Se₃ is a fascinating topological insulator consisting of surface states with single Dirac-cone at the Γ point [1] with a relatively larger energy gap in the insulating phase owing to room temperature applications. The current study explores the effect of spin-orbit coupling (SOC) in this time-reversal symmetry protected compound. Using quantum espresso-DFT as a tool we performed first-principles electronic study of Bi₂Se₃ with and without the inclusion of spin-orbit coupling. Due to the presence of the bismuth element, the large spin-orbit coupling of the compound is reflected on the band structure. Further we make use of band parity analysis at the time-reversal invariant points as suggested by Fu and Kane[2] and confirm the compound to be a strong topological insulator only upon including the spin-orbit coupling. The computational results thus help us to understand the importance of spin-orbit coupling for the topological nature of the compound.



Band structure of Bi₂Se₃ without SOC



Band structure of Bi₂Se₃ with SOC

Keywords: spin-orbit coupling, band parity analysis, DFT calculation, Bismuth Selenide

References:

- [1] Topological insulators in Bi₂Se₃, Bi₂Te₃ and Sb₂Te₃ with a single Dirac cone on the surface *Nature Physics* volume 5, pages 438–442 (2009)
- [2] Topological insulators with inversion symmetry. *Phys. Rev. B* 76, 045302 (2007)

OP-26

Experimental and Theoretical Investigation of Structural and Magnetic Properties of YbFe₂As₂ Crystal

S. Santhosh Raj¹, P. Iyyappa Rajan², Nilotpal Ghosh³, S. Mahalakshmi², R. Navamathavan^{1*}

¹Division of Physics, School of Advanced Sciences, Vellore Institute of Technology (VIT), Chennai Campus, Vandalur – Kelambakkam Road, Chennai 600127, India

²Chemistry Division, School of Advanced Sciences, Vellore Institute of Technology (VIT), Chennai Campus, Vandalur – Kelambakkam Road, Chennai 600127, India

³Science and Engineering Research Board, Department of Science and Technology, Vasant Kunj, New Delhi - 110070, India

Email: navamathavan.r@vit.ac.in

We report the structural and magnetic characteristics, resistivity behaviour and electronic structure of a new compound YbFe₂As₂ based on combined experimental and spin polarized density functional theory (DFT) methods. The Rietveld refinement of crushed single crystals of YbFe₂As₂ shows monoclinic unit cell structure. The electronic structure was calculated from the experimental input structural solution obtained from the Rietveld refinement of melt growth assisted synthesized single crystal YbFe₂As₂ [1] and our calculations adopted the Perdew-Burke Ernzerhof method (PBE+U) to treat the strong correlation effects of 3d and 4f electrons of Fe and Yb atoms. The hybridization between Yb (4f) – Fe (3d) states revealed a strong electron-correlation phenomenon between Yb and Fe states revealed

from partial density of states could be a plausible reason for breaking of antiferromagnetic (AFM) structure into small ferromagnetic moments of Fe atoms which is in agreement with magnetic measurements of YbFe_2As_2 single crystal sample. The density of states (DOS) reveals the metallic behaviour which is in agreement with resistivity measurements of YbFe_2As_2 . There is a spin splitting between up and down spin Fe 3d states and tends to produce a pseudo gap at the Fermi level. The electronic band structure for YbFe_2As_2 depicts that in addition to high dispersion bands in the conduction band region, there are flat bands present at the Fermi region which is composed of As 4p states and Fe 3d electronic states contribution. A possible correlation has been made between the calculated electronic structure of YbFe_2As_2 and measured physical properties.

Keywords: YbFe_2As_2 , electronic structure, structural refinement, pseudo gap.

Reference

[1] S. Santhosh Raj *et al.*, Mater. Res. Exp. 4(8), p.086101 (2017)

OP-27

Population Balance Modelling of Crystal Growth Behaviour in A Batch Crystallizer

Lister H Falleiro,¹ B. Ashraf Ali*¹

Department of Chemical Engineering National Institute of Technology Karnataka, Surathkal, 575025, India

*E-mail: ashrafmchem@gmail.com,

The scale-up of crystallization processes is one of the most complex tasks in process engineering. Several target quantities have to be kept within narrow boundaries, such as crystal size and size distribution, yield, purity (Mersmann, 2001). In this sense, seeding is one of the most critical steps in optimizing crystallization behaviour and ensuring the final CSD. Seed crystals with the correct initial particle size, mass and crystal form must be introduced at the right time and in the right position. Optimal seeding can change a poorly behaved, inconsistent crystallization process, to one that is repeatable and produces particles with the required particle size (Doki et al., 1999). A seeding step provides the opportunity to add in a controlled manner the same mass, size and polymorphic form of seed crystals at the same temperature, position and time point in a batch process (Doki et al., 2001).

The effect of seed injection location is investigated by coupling CFD with discrete phase modelling (DPM). KDP crystals are injected at four locations in the batch crystalliser, and after an injection time of 5s, the number of a particle entering the agitation domain is calculated. Based on the frequency of the crystals entering the agitation domain the probability of secondary nucleation is higher since it is reported in the literature that the secondary nucleation is mainly due to crystal and impeller blade collisions. It is found that the probability of some particles entering the rotating domain is least at location IV.

Seeding is a useful technique to suppress spontaneous nucleation and enhances the crystal growth. Thus it allows targeting crystal size distribution and yield. The quantitative information on seeding is

limited in determining the quantity and size of the seed crystals. Seeds should be introduced into a crystallizer to get the desired product size of the crystalline product. There is no methodology available for this purpose so far.

In this paper we investigate the crystal dynamics in such a batch crystallizer, CFD coupled with population balance model. Euler-Granular model is used to model the multiphase system, and the Gidaspow model is used to predict the solid particles interactions. The growth rate of KDP crystals is investigated by varying seed loading for and initial seed size of 500 microns and keeping the other operating parameters constant. To describe the hydrodynamics of particles and the growth process fully, the kinetics model of particle growth is incorporated into the coupled model by using a user-defined function (UDF) using the growth parameters previously estimated experimentally by Temmel et al. (2016).
Keywords: CFD, Population balance modelling, crystal growth, seeding, Sauter mean diameter.

References:

- Doki, N., Kubota, N., Sato, A., Yokota, M., 2001. Effect of cooling mode on product crystal size in seeded batch crystallization of potassium alum. *Chemical Engineering Journal* 81, 313–316. [https://doi.org/10.1016/S1385-8947\(00\)00172-8](https://doi.org/10.1016/S1385-8947(00)00172-8)
- Doki, N., Kubota, N., Sato, A., Yokota, M., Hamada, O., Masumi, F., 1999. Scaleup experiments on seeded batch cooling crystallization of potassium alum. *AIChE Journal* 45, 2527–2533. <https://doi.org/10.1002/aic.690451208>
- Mersmann, A., 2001. *Crystallization Technology Handbook - Second Edition Revised and Expanded*, Marcel Dekker Inc.
- Temmel, E., Eisenschmidt, H., Lorenz, H., Sundmacher, K., Seidel-Morgenstern, A., 2016. A Short-Cut Method for the Quantification of Crystallization Kinetics. 1. Method Development. *Crystal Growth & Design* 16, 6743–6755. <https://doi.org/10.1021/acs.cgd.6b00787>

OP-28

Vibrational (FTIR & FT-Raman spectra), electronic (UV-vis) analysis and molecular docking evaluation of Mangiferin in neuraminidase enzyme using DFT stimulations

B. Sathya¹ M. Prasath^{1}*

Department of Physics, Periyar University PG Extension Centre, Dharmapuri – 636701

E-mail id: sanprasath2006@gmail.com

Influenza (flu) is an infectious viral disease which causes severe illness by RNA virus and capable for morbidity and mortality in annual epidemics. The flu affects the respiratory systems and damages the tissues easily. The elder people affected by flu virus and it causes leading sudden death. The flu unevenly spherical and embraced by a lipid membrane it contains two glycoproteins namely Hemagglutinin (HA) and Neuraminidase (NA) which are fundamental for flu viral disease. The simulation has turned into a purpose for the plan of anti-influenza drugs. The structure of Mangiferin was optimized using DFT method with basis set 6-311G(d,p) to find the minimum energy of the molecule and the optimized geometry is compared with the experimental values this study insights the molecular flexibility. The experimental data of FT-IR, FT-Raman vibrational frequencies and UV-Vis spectra was recorded and their values are in good agreement with the computational results. A molecular docking analysis of

Mangiferin is carried out with neuraminidase enzyme. The docking result shows the binding affinity and inhibition constant of the molecule present in the active site. The HOMO-LUMO reveals the good kinetic stability and less toxicity of the Mangiferin molecule. The molecular orbital contributions were studied by using the total (TDOS), partial (PDOS), and overlap population (OPDOS) density of states. This implies that the title molecule enhances the good candidate for anti- influenza drugs.

OP-29

Intermolecular Interaction, Charge Density Distribution and Electrostatic Properties of Kaempferol in the Active Site of Ache via Docking and Quantum Chemical Calculations.

Dr. Renuga Parameswari Azhagesan¹, Dr. Kumaradhas Poomani*

¹Department of Physics, Laxminarayana College of Arts and Science for women, Dharmapuri.

*Department of Physics, Periyar University, Salem-636 011, India

A high level *ab initio* and Density functional calculations were performed for kaempferol molecule in gas phase (I) and for the same molecule lifted from the active site of AChE receptor (II). This quantum chemical study has been carried out to understand the conformational modification, charge redistribution, changes in the bond topological and electrostatic properties of (II), at the active site of AChE. The dipole moment of the kaempferol (1.56D) has been increased (2.47D), when the molecule enters into the active site. The minimum docked energy of the kaempferol molecule in the active site of Kaempferol-AChE is -8.82 kcal/mol. The interactions of kaempferol with AChE residue atoms confirm that kaempferol interacts with the choline binding site-Trp84. This leads kaempferol to inhibit AChE. The molecular electrostatic form differentiates the difference of ESP between the two forms. A large negative region is found at the vicinity of O atoms.

Keywords: Kaempferol, Acetylcholinesterase, Quantum chemical calculations; charge density; Dipole moment; Electrostatic potential.

OP-30

Optical and Spectral Characterization of Tartaric Acid Doped Lsmh Crystal

Anithalakshmi M,¹ Robert R*²

¹Department of Physics, Adhiyaman Arts and Science College for Women, Uthangarai, Krishnagiri

²Department of Physics, Government Arts College for Men, Krishnagiri – 635 001

*E-mail: robertosur@yahoo.co.in

Enormous effort has been put on the growth and perfection of crystals of different materials with regard to their applications [1]. The development in the growth of highly efficient NLO crystals for visible and ultraviolet regions is important for both Laser spectroscopy and laser processing. They have wide applications in the field of telecommunication and optical information storage devices [2,3]. In this present work, optical and spectral properties of tartaric acid doped lithium sulphate monohydrate crystals grown by slow evaporation method have been studied. The grown crystals were subjected to various characterization studies such as EDAX, PXRD, Photo luminescence, FTIR and Raman spectral and UV Visible Analyses. The Energy Dispersive Spectroscopy analysis gives the resultant component present in compositions.

POSTER PRESENTATIONS

PP-1

Heater Modification on Directional Solidification System by Numerical Investigation

G. Anbu¹, M. Srinivasan^{1} and P. Ramasamy¹*

SSN Research Centre, SSN College of Engineering, Kalavakkam-603110, Chennai, Tamilnadu

Email: srinivasanm@ssn.edu.in

Directional Solidification method is the simplest technique compared to Cz technique. DS method is like casting method in which the solidification takes place in single direction. Poly-Silicon feed is melted in square shaped quartz crucible which is coated with the Silicon Nitride for avoiding the sticking problem. During the melting process the hot zone is fully covered by the thick insulation layers for avoiding the heat loss. In order to start the solidification process, the bottom side insulation layer is opened at elevated velocity. Hence the crystal will start to grow from the bottom of the crucible. The controlled growth rate about 1 cm/hr is established by adjusting the heaters power and by the controlled opening rate of bottom insulation. Keeping the convex melt-crystal interface during the growth process is essential for getting good quality crystal which can be employed by the heater power adjustment. During the crystal growth process the impurities are introduced from the crucible/coating materials. The level of impurities, mainly B, P, and Al, is about several ppm. Heaters provide heat for the hot zone and are an important factor in controlling the thermal field. With increased ingot size, multiple heaters were in control of the thermal field in the furnace. Relatively flat growth interface could be obtained by optimizing the powers of the top and side heater.

We have modified the geometry of the heater and studied its influence on the solidification process. The heater modified in the conventional DS furnace has been modified. The effect of modified hot zone on the thermal stress, maximum shear stress and dislocation density has been studied. The modified heater results lower in thermal stress, shear stress and dislocation density in the grown silicon ingot.

PP-2

Physical properties of tin chalcogenide crystals for solar cell applications

A G Kunjomana^{1} and Bibin John¹*

CHRIST (Deemed to be University), Department of Physics and Electronics, Bangalore-29

E-mail: kunjomana.ag@christuniversity.in

The swiftly increasing demands for energy together with more concern about the environment, force the human kind to seek sustainable energy resources and the clean energy extraction technology. Hence, photovoltaics received immense attention in the past years. In order to reduce the synthesis cost of solar cell, the inorganic semiconducting materials especially group IV-VI compound materials have received special attention due to the non-toxicity, good stability, high electrical and optical properties, and

low cost. Among them tin monoselenide (SnSe) binary compound has many advantages. SnSe is a *p*-type material with orthorhombic crystal structure. It has a direct energy bandgap of 1.30 eV and absorption coefficient, 10^5 cm^{-1} , which is earth abundant and non-toxic compared to other binary semiconducting materials like GaAs, CdTe, PbTe etc. The phase control of Sn-Se system is less tedious than ternary and quaternary semiconducting materials. Hence, in the present research work, SnSe polycrystalline charge was prepared by constant temperature muffle furnace attached with rotation mechanism. The obtained charge was powdered and then transferred in to the high pure quartz ampoule of length 10 cm and diameter 15 cm and sealed under high vacuum $\sim 10^{-6}$ mbar to prevent contaminations. The sealed ampoule was kept for melt growth for the production of bulk single crystals of SnSe by employing indigenously fabricated furnace. The harvested crystals using the Bridgman-Stockbarger technique were cleaved under liquid nitrogen temperature and subjected for various characterizations to analyze the crystal structure, defects, surface morphology, stoichiometry, band gap and absorption coefficient by the sophisticated characterization tools such as, X-ray diffraction, optical and scanning electron microscopy, energy dispersive analysis by X-rays and UV-Vis-NIR spectroscopy. The obtained results prove that the tin monoselenide material is an efficient candidate for the absorber layer in the solar cell devices.

PP-3

Exploring the Structure, Electron density and HOMO-LUMO analysis of Tetrathiafulvalene (TTF) molecule (Superconducting) via DFT and AIM analysis

P. Gnanamozi¹, V. Pandiyan¹, A. David Stephen² and P. Srinivasan^{1}*

Department of Physics, Nehru memorial College, Puthanampatti – 621 007

Department of Physics, Sri Shakthi institute of Engineering Technology, Coimbatore – 641 062

PG & Research Department of Physics, Chikkaiah Naicker College, Erode, India

*E-mail: sriniscience@gmail.com

The bond topological and electrostatic properties of the energetic TTF molecule was carefully evaluated by *ab initio* (HF) and density functional theory (B3LYP) calculations. The optimized (HF/6-311G** and B3LYP/6-311G**) geometric parameters are in excellent agreement with the similar type experimental data. For both levels of calculation, the C–S and C≡N bonds have low charge accumulation at the bond critical point, which indicates that the charges of the bonds are highly depleted compared with all other bonds in the molecule. The bond topological analysis based on the AIM theory shows the difference of charge distribution in all bonds. The molecular conductive properties are solely related to the ESP of the entire system as expected to a little ESP across the system compared with electrode as it has large ESP. For, a good conducting molecule the ESP's are expected to see little along the molecule. The ionization potential gives the very good information of conductivity. These observations give an insight on this kind of super conducting material, which are useful to design navel electronic devices.

PP-4

Effect of shock waves on dielectric properties of KDP crystal

A.Sivakumar¹, S.A.Martin Britto Dhas^{1}*

Department of Physics, Abraham Panampara Research Center, Sacred Heart College, Tirupattur, Tamilnadu, India- 635 601

*E-mail: brittodhas@gmail.com

An alternative non-destructive approach is proposed and demonstrated for modifying electrical properties of crystal using shock-waves. The method alters dielectric properties of a potassium dihydrogen phosphate (KDP) crystal by loading shock-waves generated by a table-top shock tube. The experiment involves launching the shock-waves perpendicular to the (100) plane of the crystal using a pressure driven table-top shock tube with Mach number 1.9. Electrical properties of dielectric constant, dielectric loss, permittivity, impedance, AC conductivity, DC conductivity and capacitance as a function of spectrum of frequency from 1 Hz to 1 MHz are reported for both pre- and post shock wave loaded conditions of the KDP crystal. The experimental results reveal that dielectric constant of KDP crystal is sensitive to the shock waves such that the value decreases for the shock-loaded KDP sample from 158 to 147. The advantage of the proposed approach is that it is an alternative to the conventional doping process for tailoring dielectric properties of this type of crystal.

Key Words: Shock Waves, KDP Crystal, Dielectric constant

PP-5

Applications of Nanofluids in Heat Pipe Solar Collector - A Review

N. Jayanthi^a, M. Venkatesh^{b,} and R. Suresh Kumar^c*

^aDepartment of Physics, R.M.K.College of Engineering & Technology, Chennai

^bDepartment of Physics, K.S.Rangasamy College of Arts and Science (Autonomous), Tiruchengode.

^cDepartment of Physics, R.M.K.Engineering College, Chennai

*E-mail: venky8086@gmail.com

Nowadays, solar energy is considered as clean, free and renewable energy with minimum environmental effects. Solar energy is the most sustainable form of energy among other renewable energy sources. Due to increased demand of energy, limited availability of fossil fuels, more attention is given to solar energy applications. Nanofluids can be defined as a solid-liquid composite materials consisting of nanometer sized solid particles, fibers, rods or tubes suspended in different base fluids. Choi from Argonne National Laboratory observed experimentally that the addition of high thermal conductivity metallic nano-particles into the base fluid was increased the thermal conductivity of these fluids and improve their overall heat transfer capability. Nanofluids have good properties of radiation, absorption, high thermal conductivity, high specific surface area and low pumping power. Solar energy collectors are a special kind of heat exchangers that transform solar radiation energy to an internal energy of the transport medium. The major component of any solar system is the solar collector. It is a device which absorbs the incoming solar radiation, converts it into heat, and transfers this heat to a fluid flowing through the collector. The performance of the solar collector depends upon the properties of the working

fluid which are used to maximize the solar energy absorption in the solar collector. The heat pipe solar collector consists of a heat pipe inside a vacuum – sealed tube. It has significant advantages over the flat-plate solar collector in terms of the heat loss. The major challenge is how to enhance the efficiency of the device to convert the solar energy into thermal energy. This drawback was overcome by using nanofluids in heat pipes. The solar collector using nanofluids had much better thermal performance than that using water only. Nanofluids exhibited a better thermal conductivity and convection coefficient in comparison to the pure fluid.

PP-6

Growth and characterization of a promising NLO 2,4- dinitrophenylhydrazone crystal

R. Gnanadeepam¹ A. Senthil^{1}*

Department of Physics, SRM University, Ramapuram, Chennai-89, India.

*E-mail: gnanadeepamaj@gmail.com

Single crystals of 2,4- dinitrophenylhydrazone (2,4-DNPH) a organic nonlinear (NLO) material have been successfully grown by slow evaporation technique. Solubility curve of 2,4-DNPH has been determined in the solvent Acetone. . The crystals were characterized by employing UV-VIS spectrum, FTIR and X-ray diffraction methods.

Keywords: 2,4- dinitrophenylhydrazone, Solution growth, Characterization studies.

PP-7

Experimental and theoretical investigation on piperazinium hexachloro stannous trihydrate single crystal for second harmonic generation applications

Radhakrishnan Anbarasan¹ and Jeyaperumal Kalyana Sundar^{1}*

Materials Science Laboratory, Department of Physics, Periyar University, Salem- 636 011, Tamil Nadu, India.

* E-mail: jksundar50@gmail.com

A novel metal-organic piperazinium hexachloro stannous trihydrate single crystal properties are explored through combined form of experimental and density functional theory. The single crystal of piperazinium hexachloro stannous trihydrate was grown by solvent evaporation method. All the theoretical calculations are carried out using hybrid basis set B3LYP/6-31 G(d,p)/LANL2DZ with effective core potential (ECP). The structural and lattice parameters are confirmed from the X-ray diffraction. The functional group vibrational assignments are theoretically calculated and well correlated with experimental spectra. The material has 60% transmission in the entire visible region, and lower cut off wavelength is 271 nm and the possible electronic transition is n- σ^* . The initial thermal decomposition is started at 60 °C, and the decomposition stages are investigated by thermal analysis. The intermolecular charge transfer and highest occupied molecular orbital and lowest unoccupied molecular orbital energy, chemical reactivity descriptors are calculated from the frontier molecular orbital analysis. The H \cdots Cl/Cl-H (60%) intermolecular hydrogen bond interactions have the predominant role to determine

molecular property and crystal packing arrangements. The distinct atom to atom intermolecular interactions are explored through fingerprint plots. The second harmonic efficiency of title crystal is 1.8 times greater than of typical KDP material. The dipole moment, polarizability and first-order hyperpolarizability are 23.89 D, -2.29 esu and 3.26 esu respectively are calculated from density functional theory. The obtained results show that piperazinium hexachloro stannous trihydrate crystal can be delighted as a good candidate for nonlinear optical applications.

Keywords: metal-organic crystal; DFT; Hirshfeld surface; Thermal studies; Hyperpolarizability

PP-8

Theoretical with Experimental Comparison of Optical and Electrochemical Properties on Ethyl-2-Cyano 3-(4-(Dimethylamino) Phenyl) Acrylate Single Crystal

S. Kotteswaran and P. Ramasamy*

SSN Research Centre, SSN College of Engineering, Chennai-603 110, Tamilnadu, India

Ethyl-2-cyano 3-(4-dimethylaminophenyl) acrylate crystals were grown by slow cooling method by the condensation reaction of 4-dimethylaminobenzaldehyde and methylcyanoacetate. The molecular structure of the crystal was confirmed by single crystal X-ray diffraction, ^1H Nuclear Magnetic Resonance (^1H NMR), ^{13}C Nuclear Magnetic Resonance (^{13}C NMR) and Mass spectrum. The single crystal X-ray diffraction study revealed that the crystal belongs to the triclinic crystal system with space group P. The functional groups of the crystal were confirmed by Fourier transform infrared spectrum (FTIR). The absorption properties of the crystal were analyzed by Ultraviolet-Visible (UV) absorption spectrum. The Molar extinction coefficient of the crystal was also calculated using Beer Lamberts law. The emission behavior of the compound was analyzed by Photoluminescence (PL) spectrum. Cyclic voltammetry of the compound was analyzed through three electrode system at the scan rate of 100 mV/sec and HOMO-LUMO of the crystal was calculated by cyclic voltammetry. Optical and electrochemical properties of the Ethyl-2-cyano 3-(4-dimethylaminophenyl) acrylate crystals were calculated using TD-DFT. The thermal behavior of the crystal was analysed by Thermal gravimetric and differential thermal analysis (TG-DTA). The photo conductivity of the crystal was measured and the result shows that the crystal exhibits the positive conductivity.

PP-9

Synthesis and Characterization of Cds Quantum Dots (Qds) Using Fruit Extract As an Organic Capping Agent

K. Kandasamy¹, M. Venkatesh^{2}, S.P. Rajasingh³*

Department of Chemistry, K. S. R. College of Arts and Science for Women, Tiruchengode – 637 215, Tamilnadu, India.

²Department of Physics, K.S. Rangasamy College of Arts and Science (Autonomous), Tiruchengode – 637 215, Tamilnadu, India.

³Department of Chemistry, Chikkanna Government Arts College, Tiruppur – 641 002, Tamilnadu, India.

*E-mail: *venky8086@gmail.com*

An organic capping and stabilizing agent is a main role of size and shape controller in Nano synthetic methodology. Most of the articles reported fruit pulp contains 94.4% Water, 29% Glucose, 24% Fructose, 199 m/100g of Potassium, huge number of phenolic, flavonoid, alkaloid compounds which can act as organic capping and stabilizing agents. Low dimensional semiconductor quantum dots (<5 nm) have received great attention for potential use in biomedical and device applications. Therefore, CdS Quantum Dot (QDs) synthesized for one step process through the green synthesis that used juice of fruit pulp act as a capping and stability agent. Synthesized CdS QDs were characterized using UV-visible spectrophotometer, Fourier transform infrared spectroscopy, Raman spectroscopy, X-ray diffraction, High-resolution microscopy with selected area electron diffraction pattern, Energy Dispersive X-Ray Analysis. From UV-Visible DRS report, we found the very low band gap energy. FT-IR indicated organic functional groups and CdS metal atoms. Raman scattering offers high specificity in molecular identification. XRD studies (JCPDS Card No. 10-0454) showed the formation of (111), (220) and (311) planes of cubic nature. HR-TEM followed by SAED analysis indicated the formation of spherical, crystalline, CdS of diameter ranging from 3-5 nm. EDAX analysis confirmed the presence of Cd and S in nanospher.

Keywords: CdS, quantum dots, Organic capping agent, Green synthesis.

PP-10

Growth and characterisation of pure and L-Methionine doped Sulphamic Acid single crystal

M.Selvapandiyan^{1} and J.Arumugam¹*

¹*Department of Physics, Periyar University PG Extension center, Dharmapuri- 636 705, Tamil Nadu,*

²*Department of Physics, Sri Vidya Mandir Arts & Science College, Uthangarai- 636902, Tamil Nadu*

³*Department of Physics, Periyar University, Salem- 636 011, Tamil Nadu, India*

Email: mselvapandiyan@rediffmail.com

The nonlinear optical materials play crucial role in optical communication and optoelectronics field. Single crystals of inorganic nonlinear optical material of pure and L-methionine doped sulphamic acid were grown by solvent evaporation technique at room temperature. The grown crystals were subjected to Single crystal X ray diffraction, UV visible absorption, Microhardness and Photoconductivity studies. The grown crystal was characterized by single crystal X ray diffraction to determine the cell parameters. The optical absorption spectra recorded in the wavelength was ranged from 190 nm to 800 nm and its energy gap for both pure and L-methionine doped sulphamic acid crystals are 5.77 eV and 5.06 eV. The mechanical strength of the grown crystal was found from Vicker's hardness measurements. Work hardening coefficient values of grown crystals are 1.65 and 2.61. It showed that pure and L-methionine doped Sulphamic acid crystals are soft in nature. Photoconductivity studies revealed that grown crystals exhibit negative photoconductivity nature of the material.

Keywords: Slow evaporation, nonlinear optical material, photoconductivity,

PP-11

Numerical investigation on mc-silicon growth process for Photovoltaic applications

V. Kesavan¹, M. Srinivasan¹ and P. Ramasamy^{1}*

SSN Research centre, SSN College of Engineering, Chennai-603110, India.

The numerical simulations of heat and mass transport have been carried out. The heater design has been modified to analyse the melt convection and reduction of oxygen impurities. The simulation has been made for conventional and modified heater design using directional solidification (DS) furnace. The results were compared and analyzed. The better heater design was used to control the oxygen impurities in the mc-Si ingot. The reduced melt convection in the silicon melt is obtained due to the modified heater design. The modified heater design reduces the oxygen impurities in the crystal. The modified heater design improves the melt-crystal (m-c) interface shape. It gives less concave interface shape in the periphery region near the crucible wall. The m-c interface is mainly affected by flow pattern and intensity of the melt convection. The numerical results are very useful for better understanding of thermal effect and melt convection in the DS system for reduction of oxygen impurities in the mc-Si ingots.

Keywords: Directional solidification, Solar cells, oxygen Impurities, Numerical simulation, melt convection and Thermal effect.

PP-12

Numerical Simulation and Global Heat Transfer Computations of Reduction in thermal Stress Maxima of CZ Grown Silicon Crystal

M. Avinash Kumar¹, M. Srinivasan^{1}, P. Ramasamy²*

¹SSN Research Centre, SSN College of Engineering, Chennai-603110, India.

Numerical simulation is one of the important tools in the investigation and optimization of the single-crystal silicon growth by the Czochralski (Cz) method. In the present work, numerical simulation has been done for the growth of CZ-grown silicon single crystal throughout the growth process at a certain crystal position of about 100mm and 300mm. In Cz growth process, thermal stress is a major factor responsible for the dislocation generation. Thermal stress in Czochralski-grown silicon single-crystals is determined with a 2D axisymmetric approach which is axisymmetric due to axisymmetric boundary conditions. This 2D numerical simulation accounting for heat and mass transfer within the melt predicts physical phenomena inside the CZ furnace. The variation and reduction in thermal stress maxima for various crystal and counter crucible rotations are studied. A commercial crystal growth simulation software CGSim (Crystal Growth Simulator) has been used for all computations. A global heat transfer computations were performed for the investigation of thermal stress in a Czochralski (CZ) silicon crystal. The temperature distribution, thermal stress properties including maximum shear stress and von Mises stress distributions at two different axial crystal positions have been investigated with the help of heat transfer simulations. By analysing the obtained results, the stress maxima during the growth process in a crystal can be controlled by applying optimal crystal and counter crucible rotations. From the computational results, the thermal stress distribution along grown crystal and the possible reason for dislocation formation in the Czochralski-grown single-crystal silicon are determined.

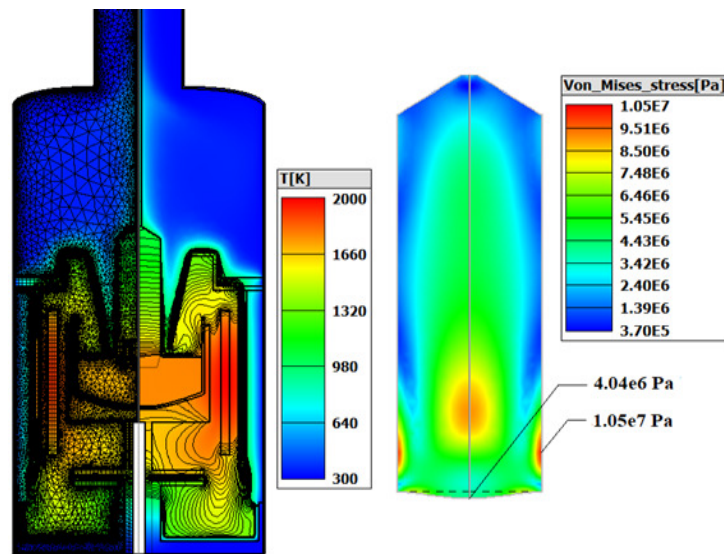


Fig. 1. Simulated temperature distribution and grid structures of CZ growth furnace and the simulated thermal stress for 300mm crystal for optimal crystal and counter crucible rotation.

References

- V. V. Kalaev, I. Yu. Evstratov, Yu. N. Makarav, Journal of Crystal Growth 249, 87-99 (2003).
 O. V. Smirnova, N. V. Durnev, K. E. Shandrakov, E. L. Mizitov, V. D. Soklakov, Journal of Crystal Growth 310, 2185–2191 (2008).
 B. Gao, K. Kakimoto, Journal of Crystal Growth 384, 13–20 (2013).

PP-13

Structural, Optical and Dielectrical properties of chalcone derivative crystal grown by VASR technique.

*N.Madhavan, S.A. Martin Britto Dhas**

PG and Research Department of Physics, Sacred Heart College, Tirupattur- Vlr-Dt. 635681

Chalcone derivative crystal BMC were grown by Vacuum Assisted SR technique using acetone as a solvent. The grown crystal were subjected to various characterization studies like Powder XRD analysis to determine the crystalline nature and FTIR analysis to investigate the functional group present in the material. The optical properties like optical band gap, absorption coefficient, excitation coefficient, dielectric constant for real and imaginary part, electrical conductivity, optical conductivity, refractive index of the crystals were analyzed using UV-Vis spectrophotometer. Dielectrical analysis like dielectric constant, dielectric loss, resistivity, ac and dc conductivity etc was carried out at different temperatures like 30, 50 75 °C in the frequency ranging from 1 Hz – 10MHz. The temperature dependent dielectric parameters such as dielectric loss and dielectric constant decreases with increasing applied frequency. The results will be discussed during the conference.

Keywords: FTIR, UV-Vis, Di electrical analysis, Chalcone crystal, etc.

PP-14

The Structural and Magnetic Properties of Gadolinium Doped Of Nickel Nanoferrite Using Microwave Combustion Method

K. Poovarasu^a, M. Vanitha Sri^b and M. Venkatesh^{a}*

^a*Department of Physics, K.S.Rangasamy College of Arts and Science (Autonomous), Tiruchengode*

^b*Department of Chemistry, Government Arts College for Women, Salem- 636 008*

*E-mail: venky8086@gmail.com

Nanophase ferrites are a class of magnetic materials that have been the most attractive area of the research. Ferrites nanoparticles are usually prepared by various physical and chemical methods like mechanical milling, inert gas condensation, hydrothermal reaction, ceramic method, sol gel and co precipitation technique etc. Influence of rare earth ions on spinel ferrite causes structural disorder and lattice strain, thereby increasing the electrical and magnetic properties. The concentration of rare earth doping in the ferrites is important in describing the properties of ferrites. Therefore, we used microwave combustion method to prepare nickel ferrite nanoplatelets under the influence of Gadolinium rare Earth iron with the aid of uric acid as fuel.

Keywords: Nanoplatelets, rare Earth doped Nickel ferrite, Microwave synthesis, Magnetic materials

References

M. Venkatesh, G. Suresh Kumar, S. Viji, S. Karthi, E.K. Girija, Microwave assisted combustion synthesis and characterization of nickel ferrite nanoplatelets, *Modern Electronic Materials* 2 (2016) 74–78.

PP-15

Microwave Assisted Combustion Synthesis and Characterization of Nickel Ferrite Nanoplatelets Doped Effects on Rare-Earth Irons

D. Koushika^a, M. Vanitha Sri^b and M. Venkatesh^{a}*

^a*Department of Physics, K.S.Rangasamy College of Arts and Science (Autonomous), Tiruchengode*

^b*Department of Chemistry, Government Arts College for Women, Salem – 636 008*

*E-mail: venky8086@gmail.com

Magnetic ferrites are a group of technologically important magnetic materials. Synthesis of nanocrystalline spinel ferrite has been investigated intensively in recent years due to their potential applications in high density magnetic recording, microwave devices and magnetic fluids. Nickel, catalysis, gas sensors, lithium ion batteries and even in biomedicine. Nickel ferrite is a ferrimagnetic material and it exhibits an inverse spinel cubic structure. In particular, the materials containing 3d transition metals, the magnetism carriers are the electrons from the 3d shell that are considered to migrate from one atom to another. In rare earth (RE) metals, the magnetism carriers are the 4f electrons which are protected by the

5s² 5p⁶ shells, so their magnetic ferrite has received much attention because it is widely used in spintronics, microwave absorption moments are well localized at individual atoms. Small amounts of rare Earth element can affect the magnetic properties and the magnetic coercivity etc. Recently, nickel ferrite nanoparticles with various particle sizes, surface areas, and morphologies have been prepared by many methods. However, most of the methods employ complicated procedures, high reaction temperatures, long reaction times, toxic reagents, and sophisticated processing. There are several plenty of developed methods, microwave synthesise have special attention for the preparation of nickel ferrite nanoparticles because of many advantages like rapid heating, shorter time, fast reaction, easy reproducibility, particle size and shape control, high yield, high purity, efficient energy transformation and volume heating. However there are serious challenges in developing facile method to obtain pure, ultrafine and homogeneous nickel ferrite nanostructures. To the best of our knowledge, there is no report on the preparation of rare Earth doped nickel ferrite nanoplatelets via microwave combustion method. Here we report a rapid and facile microwave combustion method to prepare nickel ferrite nanoplatelets under the influence of rare Earth iron with the aid of trisodium citrate as fuel.

Keywords: Nanoplatelets, rare Earth doped Nickel ferrite, Microwave synthesis, Magnetic materials

PP-16

Growth and Characterization of L Lysine Added Single Crystals

P.Yasotha, P.Sagunthala
Sri Vasavi college, Erode,

* E-mail: yasophysics12@gmail.com

The organic-inorganic (semi-organic) crystal not only possesses the high optical non-linearity of a purely organic compound but also the favorable thermal and mechanical properties of an inorganic compound . The organic material L lysine, along with the inorganic materials potassium chloride and potassium nitrate were selected to grow crystals by solution growth technique at room temperature. L lysine added single crystals salts of potassium (LLPC and LLPN) were grown using saturated solutions of organic [L lysine] and inorganic [KCl and KNO₃] materials in 1:3 ratio adopting slow evaporation technique. The grown crystals were characterized by various characterization techniques to know their structural, functional, optical, mechanical and thermal properties, and dielectric behaviour. Crystalline nature was verified with PXRD analysis for each of the successfully developed crystals and reflections were duly indexed. The lattice parameters were determined by single crystal XRD. Both LLPC and LLPN crystals had monoclinic crystal. Various functional groups present in the grown crystals were identified by FTIR analysis and they are in line with the findings of XRD. This analysis proved the presence of both the parent materials in the grown crystals. The optical study revealed that the developed crystals had lower cut-off wavelength and relatively higher transparency range. The grown crystals, therefore, can be used in the optoelectronics and photonics device fabrication fields. Vicker's micro hardness analysis identified the grown crystals as soft materials based on indentation analysis since their n values are greater than 1.6. The stiffness constant C11 for different applied loads were determined and found to be as expected. Thermal analysis proved the thermal stability of the grown crystals LLPC and LLPN as 255 and 255 °C respectively. Hence the grown crystals can be recommended for their application in high temperature

region. Low values of dielectric constant and dielectric loss of the grown crystals at high frequency guaranteed their potential application in the fields of ferroelectrics, optoelectronics and photonics.

PP-17

Reduction of Oxygen Impurities by Titanium Carbide heat exchanger block and retort in mc-Silicon: Numerical modelling

M. Vishnuwaran, M. Srinivasan, V. Kesavan, and P.Ramasamy*
SSN Research Center, SSN College of Engineering, Chennai-6030110.

*Email: srinivasanm@ssn.edu.in

Directional solidification (DS) is one of the mainstream techniques for production of the mc-silicon ingot. Reduction of non-metal impurities in DS silicon ingots is a challenge in the solar cells production and strong contamination comes from the graphite parts. In our present work, we changed the material as titanium carbide (TiC) instead of graphite for heat exchanger block and retort. The numerical simulation of oxygen impurity transport has been investigated by using Titanium Carbide as heat exchanger block and retort in the DS furnace. The simulation results were compared and analysed. The performance of TiC relative to graphite was observed, it gives lower oxygen impurities and uniform impurity distribution in the ingot. It also reduces the SiO segregation in argon gas domain. It gives better results than the graphite based system.

PP-18

Photocatalytic Performance of the Biologically Synthesized Titanium dioxide (TiO₂) Nanoparticles using Lemon Leaf Extract

*Vishali D¹, Manikandan B¹, K R Murali² and Rita John*¹*
Department of Theoretical Physics, University of Madras

*E-mail: ritajohn.r@gmail.com

Biosynthesis of nanoparticles is a cost effective and environmental benign method. It also serves as an alternative approach for production of metal oxide nanoparticles which is non-toxic. In the present work, we studied photocatalytic activity of synthesized TiO₂ nanoparticles and observed the degradation rate of the Methylene Blue (MB) under UV light. Titanium dioxide (TiO₂) nanoparticles are synthesized by green approach using Citrus aurantifolia (lemon leaf extract) as a reducing agent. We used distilled water as a solvent for leaf extract and ethanol to dissolve Titanium Tetraisopropoxide (TTIP). The synthesized TiO₂ nanoparticles are characterized using XRD, SEM, and UV- visible spectroscopy. The formation of TiO₂ nanoparticles is confirmed by the above characterization techniques. The Average crystallite size of the synthesized TiO₂ nanoparticles from Scherrer's equation is found to be 25 nm. The degradation percentage of 95% is achieved for dye load 20 mg/L at pH 11 in 60 min. And also the effect of pH, initial concentration of dye, photocatalyst dosage on the dye degradation are studied and their rate

constant, half-life time are compared. The present work is compared with other reported results and is found to be in good agreement.

Reference:

- 1) Mahalingam Sundrarajan, S.Gowri – ‘Green synthesis of titanium dioxide nanoparticles using *Nyctanthes arbor-tristis* leaves extract’, *Chalcogenide Letters* 8(8) 2011.
- 2) Nasikhudin et al.,- Study on photocatalytic properties of TiO₂ nanoparticle in various pH condition, *J.Phy.:Conf.ser.*1011 012069.

PP-19

Role of Copper Chloride on the Growth, Optical and Antibacterial Properties of Γ -Glycine Single Crystal

V.Vijayalakshmi¹ and P.Dhanasekaran^{1}*

Crystal Growth Laboratory, Department of Physics, Erode Sengunthar Engineering College, Erode

² Department of Physics, Bharathiar University Arts and Science College, Modakkurichi- 638104, India.

E-mail: dhanasekaranp1@gmail.com

In this paper, we report the successful growth of copper chloride added glycine single crystal by using slow solvent evaporation method. The incorporation of copper chloride on glycine was confirmed by the Powder X-Ray Diffraction (PXRD) and Fourier transform infrared (FTIR) studies. UV-Visible transmittance spectrum confirmed that the grown crystals have wide optical transparency window in the entire visible and near infrared region. The antibacterial activities of the title compound were performed by agar disc diffusion method against the ACDP declared harmful bacteria's such as *Bacillus cereus*, *Proteus*, *Staphylococcus aureus*, *Streptococcus aureus*, *Klebsiella* and *shigella*.

PP-20

Vibrational Spectroscopy (FT-IR and FT-R) Investigation and Computational (DFT) Analysis on the Structure of 2,7 dihydroxy Naphthalene

M. Vennila¹, R. Rathikha², S. Muthu³, A. Senthil⁴

¹Department of Physics, P.M.R. Engineering College, Maduravoyal, Chennai-96

²Department of Physics, Presidency College, Chepauk, Chennai-05.

³Department of Physics, Aringnar Anna Arts and Science College, Kanchipuram.

⁴Department of Physics, SRM Institute of Science and Technology, Ramapuram Campus, Chennai-89.

E.mail: tasenthil@gmail.com

In this work, the experimental and theoretical vibrational spectra of 2,7-dihydroxy naphthalene were studied. The FT-IR and FT-R spectra were recorded in the region 4000-600 and 4000-100 cm⁻¹

¹respectively. The structural and spectroscopic data of the molecule in the ground state were calculated by using density functional method (B3LYP) with the 6-31 +G(d,p) and 6-31 ++(d,p) basis sets . The observed and calculated values are found to be in good agreement. The predicted first hyperpolarizability shows that the molecule has good nonlinear optical (NLO) behaviour. The calculated HOMO-LUMO energy gap reveals that charge transfer occurs within the molecule. On the basis of the thermodynamic properties at different temperatures have been calculated.

PP-21

Spectroscopic investigation, FT-IR, FT-Raman,HOMO -LUMO and natural bond orbital analysis on 4-(2-Hydroxyethyl)morpholine

K. venkateswaran, M. Karnan and R. Muthukumar, K. venkateswaran PG & Research Department of Physics, Srimad Andavan Arts and Science College, Tiruchirappalli 620005, India*

*E-mail: venkateshauroville@yahoo.co.in

The study was done experimentally by the Fourier transform infrared spectrum (FT-IR) and Fourier transform Raman spectroscopy (FT - Raman) of 4-(2-Hydroxyethyl)morpholine. In this work, experimental and theoretical study on the molecular structure, quantum chemical calculations of energies and vibrational wavenumbers is presented. The vibrational frequencies of the title compound were obtained theoretically by DFT/B3LYP calculations employing the standard 6-311++G(d,p) basis set for optimized geometry and were compared with FTIR and FT - Raman spectrum. Complete vibrational assignments, analysis and correlation of the fundamental modes for the title compound were carried out. The vibrational harmonic frequencies were scaled using scale factor, yielding a good agreement between the experimentally recorded and the theoretically calculated values. The study is extended to calculate the HOMO–LUMO energy gap, mapped molecular electrostatic potential (MEP) surfaces, polarizability, Mulliken charges, Natural bond orbital analysis and thermodynamic properties of the title compound.

Keywords: 4-(2-Hydroxyethyl)morpholine, FT-IR, FT-Raman, DFT studies, Vibrational spectra, HOMO–LUMO, MEP surface, NBO

PP-22

Defects Investigation Probed by Powder X – Ray Diffraction Technique on Pure and Doped Transition Metal Vanadate

*P. Vasantha Kumar¹ and S. Rajashabala*¹*

Department of Theoretical Physics, School of Physics, Madurai Kamaraj University, Madurai, Tamilnadu, India, 625021

*E-mail: rajashabala@yahoo.com

The effect of Ni doping on the crystalline structure, growth orientation, dislocation density and crystallite size of hydrothermally synthesised Copper Vanadate Nanoparticles were characterized by

Powder X – Ray Diffraction Technique. From the XRD pattern of Copper Vanadate, all the diffraction peaks were well matched with JCPDS Card Number: 73 - 1032 and confirmed the formation of Copper Vanadate Nanoparticles in monoclinic structure with polycrystalline nature. The sharp peaks at (200) and (022) indicate the good crystalline nature of the prepared Copper Vanadate. Moreover the pure Copper Vanadate Nanoparticles prefer to grow along (200) direction. These two prominent diffraction peaks are slightly shifted to higher angle region due to the smaller ionic radius of Ni²⁺ than Cu²⁺ when 2M% of Ni dopant was added. Further increase of Ni concentration suppresses the (200) peak intensity and hence the preferential growth direction is shifted to (022) plane instead of (200). The FWHM, measures the defects formed in the surface states, of the plane increases with increase of dopant concentration. The average crystallite size of Copper Vanadate Nanoparticles decreases with increase of Ni concentration, where as the dislocation density increases, due to the lattice defects presents in the surface of the Copper Vanadate Nanoparticles. The decrease in crystallite size increases the surface area of 2 M% of Ni doped Copper Vanadate Nanoparticles, which could resulted in more active sites at the surface and lattice disorder like oxygen defects.

Keywords: Copper Vanadate nanoparticles, defects, crystallite size and dislocation density.

References:

- M. Hartmann & W. Schwinger, Chemical Society Reviews, (2016) 45(12) 3311–3312.
C. Zhang & J. Lin, Chemical Society Reviews, (2012) 41(23) 7938.

PP-23

Molecular Engineering on Carbazole Donor Based Metal-Free Organic Dyes For Dye Sensitized Solar Cells

*V. Mohankumar¹, P. Pounraj¹, M. Senthil Pandian², P. Ramasamy*¹*

SSN Research Centre, SSN College of Engineering, Chennai - 603 110, Tamil Nadu, India

*Email: ramasamyp@ssn.edu.in

A series of metal free organic sensitizers have been designed and their optoelectronic properties for DSSC applications have been systematically investigated using density functional theory (DFT) and time dependent density functional theory (TD-DFT) methods. The optical and electronic properties of the dyes were tuned by structural modifications. In the present investigation series of modified carbazole donor based metal free dyes were studied. The optimized geometry, frontier molecular orbitals, energy levels and electronic absorption spectrum were studied. The electronic structures suggest that the intramolecular charges are transferred from the donor to the acceptor. The Natural Bond Orbital analysis (NBO) gives the net electron transfer from the donor to acceptor. The electrochemical properties and light harvesting efficiency of the designed dye sensitizers were calculated. Increase of the π spacer was induced red shift of the absorption peak. The theoretical calculations help to design effective dye molecules for DSSC application.

PP-24

Synthesis, Growth, Structural and Optical Characterization of the Organic Nonlinear Optical Thiosemicarbazide 5- Sulfosalicylate (T5ss) Single Crystals

R.Usha¹, D.Jayalakshmi¹

a Department of Physics, Saveetha School of Engineering, Saveetha Institute of Medical and Technical Sciences, Thandalum, Chennai 602 105

b Queen Mary's College, Chennai, PG and Research Department of Physics, Chennai, India

Pure Thiosemicarbazide 5-Sulfosalicylate crystals (T5SS) have been grown by slow evaporation technique. The lattice parameters of the grown crystal are determined by X-ray diffraction and it reveals that the crystal belongs to monoclinic system. The various functional groups present in the crystal are confirmed by FT-IR spectral analysis. UV-Vis-NIR spectrum showed the absence of absorption in the wavelength region of 367–800 nm and UV cut-off wavelength of T5SS occurs at 367 nm. Furthermore, the third order nonlinear optical properties were investigated by the z-scan technique using continuous wave Nd-YAG laser.

PP-25

Generation of Ultra-Long Pure Magnetization Needle by Azimuthally Polarized Beam with a Ternary Optical Element

M.Udhayakumar¹, K.Prabakaran², K.B. Rajesh^{1}*

Department of Physics, Chikkanna Government Arts College, Tiruppur, Tamilnadu, India

²Department of Physics, Mahendra Arts and Science College (Autonomous), Namakkal, Tamilnadu, India

*Email: rajeskb@gmail.com

Based on the vector diffraction theory and Inverse Faraday Effect, the light induced magnetization needle is generated by tightly focusing a azimuthally polarized beam that is modulated by a self-designed ternary hybrid (phase/amplitude) filter (THF). Both the phase and the amplitude patterns of THF are judiciously optimized by the versatile particle swarm optimization (PSO) searching algorithm. It is noted that by optimizing to produce an ultra-long pure magnetization needle with lateral sub-wavelength scale and a super-long spherical magnetization chain with three-dimensional super resolution. The present work regarding these super-resolution magnetization patterns is of great value in high density all-optical magnetic recording, atomic trapping as well as confocal and magnetic resonance microscopy.

Keywords: Super-Resolution, Diffractive Optical Element, azimuthally polarized beam.

Acknowledgment

This work is supported by the Department of Science and Technology (DST), India under project SERB-YSS (F. No. 2015/001852).

PP-26

An Investigation on Thermal Diffusivity and Dielectrical Properties of Sulfanilic Acid Nonlinear Optical Single Crystal

J. Thirupathy¹, S.A. Martin Britto Dhas^{*1}

Department of Physics, Abraham Panampara Research Centre,
Sacred Heart College, Tirupattur- 635601, India

Email: brittodhas@gmail.com

Sulfanilic acid (SA) crystal is known to be an excellent material for applications such as photonic, electro-optical and harmonic generation in non linear optics (NLO). In this present article, good quality SA single crystal has been grown by slow evaporation solution technique (SEST). After the growth period of 95 days, a transparent SA single crystal is collected with the dimension of $9 \times 9 \times 2 \text{ mm}^3$. The grown SA crystal was subjected to photoacoustic spectroscopy (PAS), dielectric and impedance analysis (IA). The study of PAS was utilized to find out thermal transport property of thermal diffusivity and the outstanding result makes it suitable for lasers and thermal related applications. Impedance analysis has been implemented for the grown SA crystal for various values of temperature and it comes out with good results so that it could be a candidate for few applications in the field of microelectronic and electro – optical industries.

Keywords: Crystal growth, Photoacoustic spectroscopy, Impedance analysis

PP-27

Crystallographic and Computational Studies on N-Acetylglycine Single Crystal

V.J.Thanigaiarasu¹, N.Kanagathara^{1*}, M.K.Marchewka²

¹ Department of Physics, Jaya College of Arts and Science, Thiruninravur, Chennai 602 024

² Department of Physics, Saveetha School of Engineering, Saveetha Institute of Medical and Technical Sciences, Thandalam, Chennai 602 105

³ Institute of Low temperature and Structure Research, Polish Academy of Sciences, 50-950, Wroclaw -2, P.O.Box 937, Poland

*E-mail: kanagathara23275@gmail.com

Single crystals of N-acetylglycine were obtained by the slow evaporation technique at room temperature. Single crystal X-ray diffraction analysis reveals that the crystal belongs to monoclinic system with centro symmetric space group $P2_1/c$. The lattice parameters are calculated to be $a=4.8410(10) \text{ \AA}$, $b=11.512(2) \text{ \AA}$, $c=9.810(2) \text{ \AA}$, $\alpha=90^\circ$, $\beta=97.02(3)^\circ$, $\gamma=90^\circ$ and $V=542.61 (\text{ \AA})^3$. Vibrational spectroscopic analysis is reported on the basis of FT-IR and FT-Raman spectra recorded at room temperature. Quantum chemical studies have been carried out by using B3LYP/6-311++G(d,p) basis set. Hydrogen bonded network present in the crystal gives notable vibrational effect. DSC has also been performed for the crystal shows no phase transition in the studied temperature range (113-293 K).

Keywords: Hydrogen bond, structure, FT-IR, FT-Raman, DSC

PP-28

Heterogeneous Nucleation and Vapor Growth of Antimony Telluride Crystals

Thankamma George¹, Ajayakumar¹ C J and A G Kunjomana*¹
Jyoti Nivas College, Department of Physics, Bangalore-95

E-mail: thankamchavelil@rediffmail.com

The growth of bulk crystals of Sb₂Te₃ semiconductor has been paid special attention due to their diverse properties, which provide boundless scope to develop innovative approaches towards the development of thermoelectric devices. Conventional melt methods were used to grow bulk Sb₂Te₃ crystals where non-stoichiometry, polycrystallinity and multi-phase formation pose challenges with regard to the quality of grown samples. Hence, the present work adopts the effective sublimation process to grow stoichiometric Sb₂Te₃ crystals with the aid of an indigenously fabricated dual zone furnace. The compound charge of Sb₂Te₃ was prepared by melting high pure (99.999%) elements of Sb and Te in an evacuated (~10⁻³ mbar) quartz ampoule (length 10 cm and diameter 1 cm), with the aid of a muffle furnace. The ampoules were developed cracks and the presence of oxygen was consistently detected as a contaminant in the bulk samples. In order to avoid off-stoichiometry, the vacuum has been raised to ~10⁻⁶ mbar and the temperature was increased at a rate of 20 °C/h, for attaining the set temperature of 700 °C. After systematic trials and slow cooling, chemically homogeneous shiny ingots were successfully synthesized. Powdered charge was transferred to an ampoule and sealed under high vacuum which was kept for the growth of crystals due to controlled heterogeneous nucleation. Energy dispersive analysis was done on the grown crystals and the data was used to find the quantitative estimation of the elemental percentages of antimony and tellurium. The weight % of Sb:Te was found to be in concurrence with the standard value of 38.88 : 61.12. As the temperature difference ΔT enhanced, the size of the crystals was found to be increased such that the crystals were evolved with all their six sides, under optimum supersaturation. The crystals exhibited the diffraction pattern corresponding to the hexagonal unit cell, with lattice parameters $a = b = 4.2634 \text{ \AA}$ and $c = 30.4441 \text{ \AA}$. The layer stacking of atomic arrangement with low surface roughness was confirmed by AFM. The value of microhardness is equal to 154 kg/mm² for pure Sb₂Te₃ crystals at an applied load of 25 g. Vapor grown Sb₂Te₃ crystals were found to possess good mechanical strength, smooth surfaces, less substructure and imperfections than those reported by chemical as well as melt methods.

PP-29

Synthesis of Perfect CuSnZr Cubic Thin Film by Simple Successive Ionic Layer Adsorption and Reaction Method

M. Balaji^{1,*}, T.R.K. Priyadarzini², R. Daphine²

¹ Department of Physics, Sourashtra College, Madurai - 625 004, Tamil Nadu, India

² Department of Physics, The American College, Madurai – 625 002, Tamil Nadu, India.

*E-mail: balajimsu@gmail.com

In this work, we synthesize and report perfect cubic shape CuSnZr thin film prepared by a simple successive ionic layer adsorption and reaction method on glass substrate with equal concentrations (1:1) of

cationic and anionic solutions. To identify the critical thickness of the film, films are prepared at three different concentrations at 0.05, 0.1 and 0.15 M with different annealing temperatures. The morphology and crystalline structure of the films are identified by High-Resolution Scanning Electron Microscopy (HR-SEM) and X-ray diffraction (XRD) analysis respectively. The thickness of the film increased linearly with increasing concentration of the material content. In which, the middle (0.1 M) concentration of the film shows the small spherical particles with the perfect cubes of average edge length 1247 nm with sharp edges and corners under a precise synthesis condition of 0.1 M of Copper, Tin and Zirconium at 300 °C for 3 hours. Transmission electron microscopy analysis of the film also supports the HR-SEM analysis. A sharp and prominent peak is observed in XRD pattern which depicts the cubic structure and the calculated crystallite size is found to be 45 nm.

PP-30

Structural and Optical Characterization of Potassium Bromide Doped L-Histidine Single Crystal Sweatha.L¹, Robert. R*¹

*PG & Research department of physics, Govt Arts College for Men,
Krishnagiri – 635 001, Tamilnadu, India*

E mail: roberthosur@yahoo.co.in

Nonlinear optical crystals find applications in the thrust areas of lasers, signal processing, data storage and second harmonic generation. Though there are a large number of nonlinear optical crystals available, their use in technological applications is hindered due to lack of certain physical and chemical properties[1]. Recently, amino acids are displaying high NLO properties due to its zwitter ionic nature[2]. Many authors have grown and reported the properties of NLO crystals by adding amino acids with inorganic compounds. The amino acid L- Histidine having an imidazole group as well as amino carboxylate groups can display high NLO properties. In this present work, Potassium Bromide doped L-Histidine single crystal were grown by slow evaporation technique at room temperature. The grown crystals were characterized Powder X-ray diffraction analysis ensures that the grown crystal is in P21/n space group and monoclinic system. Photoluminescence studies confirmed the electrical and optical conductivity of the photons present in the grown crystal. FTIR Spectral analyses were performed to identify the presence of various functional groups in the crystal. UV-Vis spectral analysis has been carried out to find the transparency of the grown crystal. Energy Dispersive X-ray spectroscopy (EDAX) analysis indicates the elements presented in the crystal. The electrical properties were investigated by impedance analysis and the results of various studies of the grown crystal were discussed.

Keywords: L-histidine, Potassium Bromide, slow evaporation method, powder X-ray diffraction and optical studies.

Reference

1. M. Krishnamohan, S.Ponnusamy, C.Muthamizhchelvan, Applied surface science 499 (2018) 92.
2. R.Dhanjayan, N.Sivakumar, Materials letters 196 (2017) 74-77.

PP-31

X-Ray and NMR Spectral Investigation, DFT Calculations, Molecular Dynamics, Physicochemical Descriptors, ADME Parameters, Pharmacokinetic Bioactivity Report On 1-[(2R, 4S, 5S)-4-Azido-5-(Hydroxyl Methyl) Oxolan-2-Yl]-5-Methylpyrimidine-2, 4-Dione [1]

Suvitha. A,^{1*} Thanmayalaxmi. D,² Ravishankar. K,³

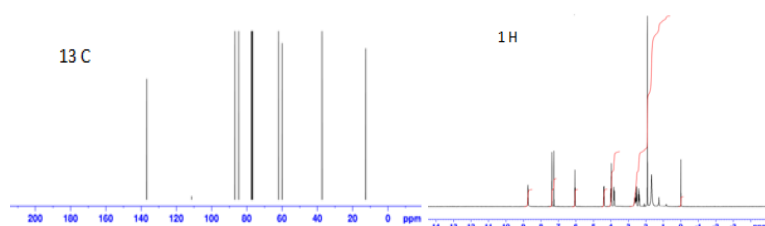
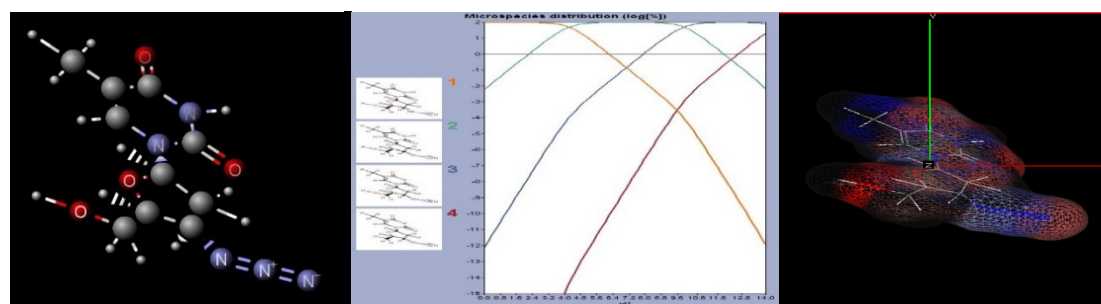
¹ CMR Institute of Technology, Bangalore, India

² CMR Institute of Technology, Bangalore, India

³ B.M.S college of Engineering, Bangalore, India

*E-mail: suvidanam@gmail.com

The compound was established to prevent and treat HIV/AIDS activity. A powder sample characterized by NMR spectra and X-ray diffraction. ¹H NMR and ¹³C nuclear magnetic resonance (NMR) chemical shifts of the molecule were recorded by Bruker Avance III NMR spectrometer with frequency 400.13 MHz and were calculated by gauge independent atomic orbital (GIAO) method and compared with experimental chemical shift. Powder XRD was recorded for the sample using Bruker D2 with Cu Kalpha radiation. A computational study on the molecule was performed by time independent DFT approach. The calculations was performed at B3LYP/6-311G++(d,p) level, then the theoretical spectral studies were performed and compared with the experimental values. In addition, Marvin Sketch, Swiss ADME, were used to compute physicochemical descriptors as well as to predict Molecular dynamics, ADME parameters, pharmacokinetic properties, pH value, drug like nature and medicinal chemistry friendliness of small molecule. All these properties were analyzed by Computer Aided Drug Designing approach (CADD) to support drug discovery.



PP-32

Controlled Growth of Hydroxyapatite Micro/Nanostructures Using Edta Under Microwave Irradiation

G. Suresh Kumar^{1,*}, E.K. Girija²

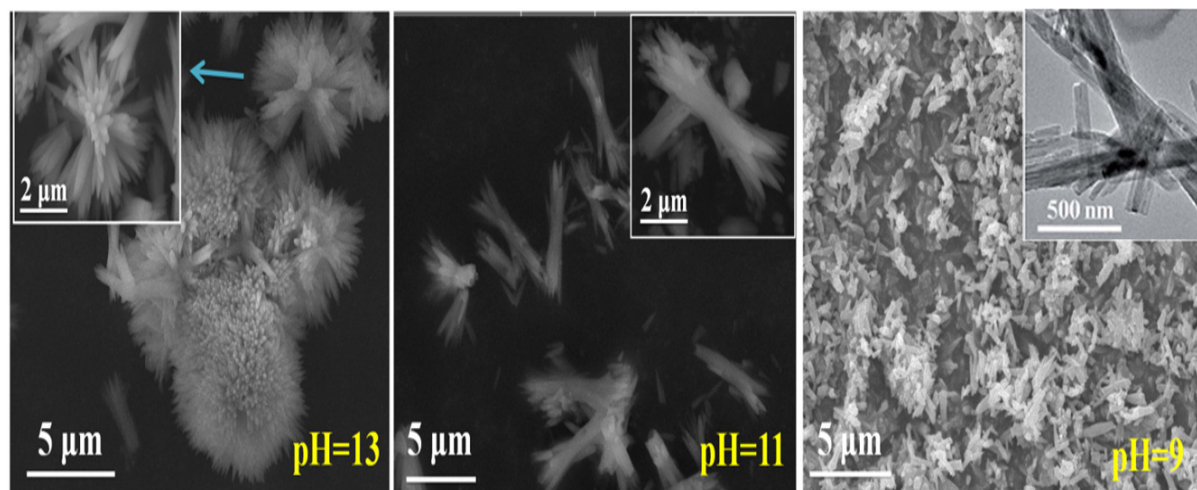
¹Department of Physics, K.S. Rangasamy College of Arts and Science (Autonomous), Tiruchengode

²Department of Physics, Periyar University, Salem 636 011, India.

*E-mail: gsureshkumar1986@gmail.com

Hydroxyapatite (HAp) is one of the calcium phosphate ceramics with Ca/P=1.67 and chemical formula $\text{Ca}_{10}(\text{PO}_4)_6\text{OH}_2$. It has received great interest for its use in various biomedical applications such as bone fillers, bone tissue engineering scaffolds, bioactive coatings and drug/protein delivery systems due to its excellent biocompatibility, bioactivity, osteoconductivity and similarity with the mineral component of calcified tissues. Applications of HAp are significantly influenced by size and shape of the nanoparticles.

We synthesized rod-like, bowknot-like and flower-like HAp micro/nanocrystals using EDTA as a regulator under microwave irradiation. It is found that the pH value and the complex reagent EDTA play the important roles in controlled growth HAp micro/nanostructures. The possible mechanism is proposed for the formation of rod-like, bowknot-like and flower-like HAp micro/nanostructures under microwave irradiation in the presence of EDTA. The prepared micro/nanostructures with different sizes and morphologies can be the potential materials for developing tunable drug delivery carriers towards healthcare applications.



PP-33

Spectral Investigation of FT-IR, FT-Raman , UV-Visible and NMR studies of 4-Methoxyphenylboronic acid using DFT method

*S.Sundari*¹ and S.Chandra¹*

Department of Physics, Annamalai University, Annamalai Nagar, Chidambaram – 608002

¹Assistant Professor, Department of Physics, Arignar Anna Govt Arts College, Attur- 636121

E-mail: sundarisadayappansks@gmail.com

The FT-IR and FT-Raman spectra of 4-Methoxyphenylboronic acid (4MPBA) have been recorded in the range 4000-400 cm⁻¹ and 4000-100 cm⁻¹ separately. Additionally, the UV spectra of 4MPBA have been recorded and analyzed. The molecular structures, fundamental vibrational frequencies and intensity of the vibrational bands are investigated and interpreted theoretically with the use of structural optimization and normal coordinate factor filled calculations based on density functional theory (DFT) with basis set 6-311++G(d,p). The hyper conjugative interaction energy E(2) and electron densities of the donor(i) and acceptor(j) bonds were calculated using NBO analysis. The energy gap of the molecule was found using HOMO – LUMO calculations. The UV-Visible analysis of the 2MPBA with their basis set. The ¹H and ¹³C NMR chemical shift values of 4MPBA in the ground state for B3LYP/6-311++G(d,p) basis set were also calculated using GIAO method.

Keywords

2MPBA, FT-IR, FT-Raman, UV-Visible Analysis, NMR and HOMO-LUMO

PP-34

Imine Based Propeller-Shaped Architectural Macrocyclic Synthons.

S.Sriam^{1}, Suresh Madhu¹, D.Velmurugan^{1*}, Gunasekaran^{2*} G. J. Sanjayan^{2*}*

^aDepartment of Crystallography and Biophysics, University of Madras, Chennai, India.

^bDivision of Organic Chemistry, CSIR-National Chemical Laboratory, Dr. Homi Bhabha Road, Pune 411 008, India

Email: hypowergravity@gmail.com

Self-assembling macrocyclic cages is quite intriguing relating to the formation of stable organisation. The basis of such structural assembly is of few atoms growing into large assembly. Macrocyclic synthons having favourable physicochemical properties having wide applications. Surface area of macrocyclic cages has advantage over Metal organic Framework (MOF). Conformational elasticity of the macrocyclic crystals has further implicational advantages than their fragile crystals counterpart. The macrocyclic synthons can be engineered to possess particular physicochemical properties. Imine induced gem-dimethyl have tendency to form a higher order macrocyclic cage as molecular basis. Imine Induced

gem-dimethyl has unique combination of progressive σ and π orbital localization. Gem-dimethyl assembly is orthogonally packed to induce elasticity in crystals. This investigation tries to understand the structural architecture of six different gem-dimethyl imine based macrocyclic cage and physicochemical descriptor of the six synthons. The molecular surface descriptor has been understood. The Hirschfield analysis was done to understand the isotropic packing of six gem-dimethyl macrocyclic cages along with intermolecular contacts. The specifically adaptability of imine induced gem-dimethyl synthons makes it more adaptable. The Thermo-physical properties of the imine induced gem-dimethyl synthons were analysed. The elastic constant with respect to orthorhombic system has been calculated to understand the elasticity of the imine induced gem-dimethyl macrocyclic cages.

PP-35

Hubbard-U – A correction to DFT A comparative study on the Electronic structure of FeO using LDA and GGA With & without Hubbard- U

Singaravelan T R and Rita John

Department of Theoretical Physics, University of Madras.

*E-mail: ritajohn.r@gmail.com

In nature, metal oxides are ubiquitous and so as their applications. But some of them show unusual fascinating properties which pave a way for the discovery of many new physical phenomena like High- T_c superconductivity, Mott insulators, Colossal Magneto Resistance (CMR). It is due to the fact that the valence electrons in these materials have strong Coulomb interaction giving rise to unique properties. One such material is antiferromagnetic FeO (wustite) which is a semiconductor by nature but Density Functional Theory (DFT) predicts it to be a metal as shown in Fig.2.2(a) because DFT doesn't take into account the on site Coulomb interaction. To overcome this limitation, we use DFT + U approach where U is Hubbard correction for the on site Coulomb interaction as shown in Fig.2.2(b).

Crystal structure of FeO: The unit cell shown in Fig.2.1 consists of four atoms of which the two Fe atoms have opposite spins with rhombohedral structure (space group R-3m,166).

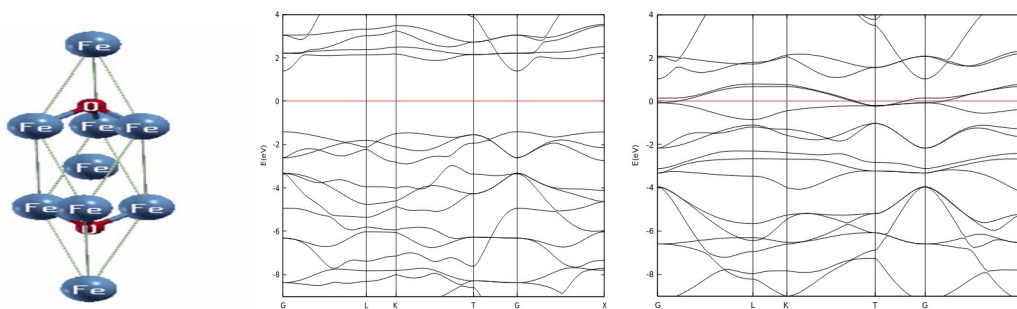


Fig. 2.1 FeO unit cell Fig. 2.2(a) and 2.2(b) Band structure of FeO without and with Hubbard- U

References

- [1] Hohenberg P., Kohn W. 1964. Phys. Rev 136, p.B864
- [2] Cococcioni M., de Gironoli S. 2005. Phys. Rev B 71, p.035105

Fig. 2.1 FeO unit cell Fig. 2.2(a) and 2.2(b) Band structure of FeO without and with Hubbard- U

PP-36

Investigation on the Synthesis, Growth and Physiochemical Properties of Creatininium Nitrate Single Crystal for Third Order Nonlinear Optical Applications

Sindhusha S^{a,b}, Padma C M^{b}*

^aDepartment of Physics, Nesamony Memorial Christian College, Manonmaniam Sundaranar University, Abishekapatti, Tirunelveli 627 012, Tamilnadu, India.

^{b, b}Department of Physics & Research centre, Women's Christian College, Manonmaniam Sundaranar University, Abishekapatti, Tirunelveli 627 012, Tamilnadu, India.*

Email: ssindhu25@gmail.com

The aim of this work is to investigate the synthesis, growth and physiochemical properties of third order non linear optical semi organic Creatininium nitrate single crystal. Optically transparent and defect free crystal was grown from aqueous solution by slow evaporation technique at room temperature. Single crystal X-ray diffraction (SXRDXRD) study reveals that the crystal is orthorhombic with space group P_{bca} and the calculated lattice parameter are $a=16.6509\text{\AA}$, $b=9.7336\text{\AA}$, $c=8.9989\text{\AA}$ and $V=1458.48\text{\AA}^3$. Fourier Transform Infrared Spectral analysis was used to investigate the functional groups present in the grown crystal. The optical absorption of Creatininium nitrate single crystal was recorded using UV-Visible spectral analysis and linear constants such as the absorption coefficient, band gap, extinction coefficient, refractive index and reflectance were calculated. Thermal stability of the crystal was analyzed by TG/DTA studies. Mechanical strength of the grown crystal was found out by using Vickers microhardness test. Third order non linear optical property was studied in detail by using Z- scan technique.

Key words: SXRDXRD, lattice parameters, band gap, optical property.

Reference

1. Robert Boyd W, Nonlinear Optics, Third Edition, Elsevier, USA, 2008.
2. Mitewa M, Gencheva G, Bontchev P R, Angelova O, Polyhedron, 1988, 7, 1273-1278.
3. Muralidharan S, Nagaraja K S, Udupa M R, Polyhedron, 1984, 3, 619-621
4. Fedila Berrah, Hanane Lamraoui, Nourredine Benali-Cherif, 2005, E61, 0210-0212.
5. Moghimi A, Khavassi H R, Dashedani F, Maddah B, Moradi S, J Iran Chem Soc, 2007, 4(4), 418-430.
6. Mythili P, Kanakasekaran P, Gopalakrishnan R, Ramasamy P, J Crystal Growth, 2008, 310, 1760-1764

PP-37

Enhancement in SHG, LDT and Thermal Properties Of Zn^{2+} Doped L-Alanine Acetate (LAA) Single Crystals

*Silviya M¹, Robert R^{*1}*

PG & Research Department of Physics

Govt. Arts College for Men, Krishnagiri-635 001, Tamil Nadu, India.

*E-mail: robertosur@yahoo.co.in

Crystals belonging to amino acids are promising candidates for NLO applications due to their chiral symmetry and non centrosymmetric space groups[1]. L-Alanine molecule exists as a zwitterion, where the carboxyl group is dissociated and amino group is protonated and if it is mixed with different organic and inorganic acids to form novel materials it is expected to get improved NLO properties [2]. Group II B metals (Zn, Cd & Hg) compounds have high transparency in UV region, because of their closed d^{10} shell.

Transparent single crystals of Zn^{2+} doped L-Alanine Acetate (LAA) have been grown from slow evaporation technique. Effect on SHG, LDT and thermal property due to Zn^{2+} doping in L-Alanine Acetate (LAA) single crystals have been investigated. SHG test using Nd-YAG laser confirms the dopant has improved the NLO property. TGA/DTA analysis shows that the metal dopant has not altered the thermal stability of molecules. LDT analysis reveals the suitability of Zn^{2+} doped L-Alanine Acetate (LAA) crystals for high energy laser photonic devices.

Key Words: Zn^{2+} , L-Alanine Acetate, slow evaporation, SHG, TGA/DTA, LDT.

References:

B. Uma, R. Samuel Selvaraj Optik 125(2014) 651-656.

A.S.J.LuciaRose Materials Chemistry and Physics 130(2011) 950-955.

PP-38

Crystal growth and optical studies on lithium hydrogen oxalate monohydrate single crystal

Senthilkumar Chandran^a P. Ramasamy^a

Department of Physics, SSN College of Engineering, Kalavakkam, Tamilnadu- 603 110

*E-mail: senthilkumarchandran89@gmail.com

Semi-organic lithium hydrogen oxalate monohydrate non-linear optical single crystals have been grown by slow evaporation solution technique at 40° C. The nucleation parameters such as critical radius, interfacial tension, and critical free energy change have been evaluated using the experimental data. The solubility and the nucleation curve of the crystal at different temperatures have been analyzed. The crystal has a positive temperature coefficient of solubility. The metastable zone width and induction period have been determined for the aqueous solution growth of lithium hydrogen oxalate monohydrate. The UV-Vis-NIR spectrum showed this crystal has high transparency. The photoconductivity studies indicate lithium hydrogen oxalate monohydrate has positive photoconductivity behaviour. The low etch pit density observed on (0 0 1) crystal surface and the high resolution x-ray diffraction analysis indicate the good quality of the grown crystals.

PP-39

Unidirectional growth of <100> Directed Sodium Di (L-Malato) Borate Single Crystal and Its Characterization

A.Senthil, and P. Ramasamy¹

Department of physics, SRM University, Ramapuarum Campus, Chennai-600089

¹SSNRC, SSN College of Engineering, Kalavakkam-603110, Chennai

*Email: tasenthil@gmail.com

Optically good quality, bulk single crystal of <100> directional Sodium Di (L-Malato) Borate (NaDMB) was successfully grown by Sankaranarayanan-Ramasamy (SR) method. The solubility and metastable zone width of NaDMB was estimated for water solvent. NaDMB has a positive gradient of solubility. The metastable zone width decreases with increasing temperature. The UV-vis-NIR spectrum reveals that the crystal is transparent between 245- 1100 nm and the lower cutoff is found to be around 240 nm. The crystalline perfection of the grown crystal has been analyzed by high-resolution X-ray diffraction rocking curve measurements and chemical etching studies. Electrical properties of grown crystals were studied by dielectric measurements. Vickers microhardness was calculated in order to understand the mechanical stability of the grown crystals.

PP-40

Structural Analysis of 1,3 Diamino Propane With Arsenic Acid Complex

K.Senthil Kumar¹, N.Kanagathara^{1}, G.Anbalagan², M.K.Marchewka³*

¹ Department of Physics, Rajalakshmi Engineering College, Rajalakshmi Nagar, Thandalam, Chennai 602 105

² Department of Physics, Saveetha School of Engineering, Saveetha Institute of Medical and Technical Sciences, Thandalam, Chennai 602 105

³ Department of Nuclear Physics, University of Madras, Guindy Campus, Chennai 600 025.

⁴ Institute of Low temperature and Structure Research, Polish Academy of Sciences, 50-950, Wroclaw -2, P.O.Box 937, Poland

*Email: kanagathara23275@gmail.com

The crystals of 1,3 diamino propane with arsenic acid crystalline product were obtained by the slow evaporation technique at room temperature. Single crystal X-ray diffraction analysis reveals that the crystal belongs to monoclinic system with centro symmetric space group C2/c. The lattice parameters are calculated to be $a=19.0121(18)$ Å, $b=4.6666(4)$ Å, $c =15.0943(13)$ Å, $\alpha=90^\circ$, $\beta=127.083(3)^\circ$, $\gamma=90^\circ$ and $V=1068.36$ (Å)³. Vibrational spectroscopic analysis is reported on the basis of FT-IR and FT-Raman spectra recorded at room temperature. Density functional theoretical calculations have been carried out by using B3LYP/6-311++G(d,p) basis set. Hydrogen bonded network present in the crystal gives notable vibrational effect.

PP-41

Synthesis and Characterization of Semi-Organic Nonlinear Optical Material: Potassium Doped Sodium Para-Nitrophenolate Crystal

M. Selvapandiyan and R. Sathyanarayanan*

Department of Physics, Periyar University P.G Extension centre, Dharmapuri, Tamil Nadu, India-636 701

*E-mail: mselvapandiyan@rediffmail.com

Single crystal of Potassium doped Sodium para-nitrophenolate crystal was grown using slow evaporation solution growth method. The structure of the Sodium para-nitrophenol crystal was examined by X-ray diffraction and the functional groups present in the compound were identified using FT-IR. The UV-Vis-NIR absorption spectrum revealed that the UV lower cutoff wavelength and the optical band gap of the crystal. The thermal stability of the materials was determined by the TG-DTA curves. The mechanical behaviour of the grown crystal was studied using Vickers micro hardness. Dielectric constant and dielectric loss were also measured as a function of frequency and temperature. The NLO parameters such as intensity dependence nonlinear refractive index (n_2), nonlinear absorption coefficient (β) and third-order susceptibility were calculated using Z-scan technique.

Keywords: Slow evaporation, X-ray, FT-IR, FT-Raman, UV, TG-DTA, Z-Scan

References:

1. M. Jose, R. Uthrakumar, A. Jeya Rajendran, S. Jerome Das *Spectrochimica Acta* **2012**,495
2. M. Jose G.Bhagavannarayana,K.Sugandhi,S.JeromeDas*Materials Letters*,**(2010)**,1369
3. B. Milton Boaz, J. Mary Linet, Babu Varghese, M. Palanichamy, S. Jerome Das*Journal of Crystal Growth*, **(2005)**, 448.

PP-42

Different Characterizations of Silver Aluminium Oxide Thin Films by Spray Pyrolysis Technique

Dr.P. Saritha

Assistant Professor, Department of Physics, Govt. College of Engineering, Thanjavur.

*E-mail:psarithaau@yahoo.com

$Ag_2Al_2O_3$ thin films were deposited on glass substrates by spray pyrolysis technique of silver-aluminium in reactive oxide mixtures. The reactive sputtering was done at varying power, oxygen flow rate and deposition temperature to study the influence of these parameters on the deposition of $Ag_2Al_2O_3$ films. The film structure was determined by X-ray diffraction, the optical properties were examined by spectrophotometer (UV-vis-NIR) and photoluminescence. Further, the film thickness and resistivity were measured by tactile profilometry and four probes. Additional mobility, resistivity and charge carrier

density by Hall Effect measurements were done. The optical transmittance and photoluminescence spectra of films deposited with these parameters indicate several band gaps, a direct one of around 2.3 eV. Electrical characterization reveals that the charge carrier concentrations and mobility were analyzed.

Keywords: Deposition technique; Electrical properties; Mobility Optical properties; Spray pyrolysis; Silver aluminium oxides.

PP-43

Morphology and Size Controlled Synthesis of Zinc Oxide Nanostructures

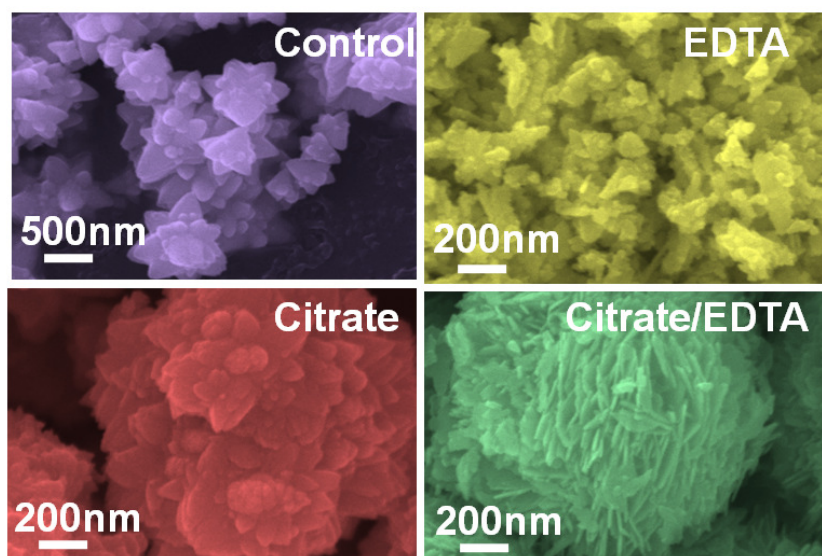
T. Saravanan¹, G. Suresh Kumar^{1,*}, E.K. Girija²

¹Department of Physics, K.S. Rangasamy College of Arts and Science (Autonomous), Tiruchengode 637 215, India

²Department of Physics, Periyar University, Salem 636 011, India.

*E-mail: gsureshkumar1986@gmail.com

Zinc oxide (ZnO) is one of attractive II–VI compound semiconductor material. Owing to its unique chemical and physical characteristics, ZnO is widely used in various applications such as gas sensors, light emitting diodes, field effect transistors, ultraviolet lasers, photodetectors, solar cells, photocatalysts, and so on. The physical and chemical characteristics of ZnO nanoparticles are significantly influenced by size and morphology and they plays an important role on the above mentioned applications. We report the synthesis of novel ZnO nanostructures with different sizes and morphologies by a rapid microwave assisted synthesis using ethylenediaminetetraacetic acid (EDTA) and/or trisodium citrate as chelating agents and their characterization. The obtained ZnO nanostructures having hexagonal Wurtzite structure with different morphologies such as flowers, flakes, solid spheres and porous spheres. The prepared ZnO nanostructures exhibit band gap between 3.270-3.374 eV due potential fluctuations in electronic band structure of ZnO owing to surface-related defects and/or adsorbed species. The proposed approach can be potential method to prepare novel ZnO nanostructures for photocatalytic and optoelectronic applications.



PP-44

Experimental and Theoretical Investigation of Structural and Magnetic Properties of YbFe₂As₂ Crystal

S. Santhosh Raj¹, P. Iyyappa Rajan², Nilotpal Ghosh³, S. Mahalakshmi², R. Navamathavan^{1}*

¹*Division of Physics, School of Advanced Sciences, Vellore Institute of Technology (VIT), Chennai Campus, Vandalur – Kelambakkam Road, Chennai 600127, India*

²*Chemistry Division, School of Advanced Sciences, Vellore Institute of Technology (VIT), Chennai Campus, Vandalur – Kelambakkam Road, Chennai 600127, India*

³*Science and Engineering Research Board, Department of Science and Technology, Vasant Kunj, New Delhi - 110070, India*

*E-mail: navamathavan.r@vit.ac.in

We report the structural and magnetic characteristics, resistivity behaviour and electronic structure of a new compound YbFe₂As₂ based on combined experimental and spin polarized density functional theory (DFT) methods. The Rietveld refinement of crushed single crystals of YbFe₂As₂ shows monoclinic unit cell structure. The electronic structure was calculated from the experimental input structural solution obtained from the Rietveld refinement of melt growth assisted synthesized single crystal YbFe₂As₂ [1] and our calculations adopted the Perdew-Burke Ernzerhof method (PBE+U) to treat the strong correlation effects of 3d and 4f electrons of Fe and Yb atoms. The hybridization between Yb (4f) – Fe (3d) states revealed a strong electron-correlation phenomenon between Yb and Fe states revealed from partial density of states could be a plausible reason for breaking of antiferromagnetic (AFM) structure into small ferromagnetic moments of Fe atoms which is in agreement with magnetic measurements of YbFe₂As₂ single crystal sample. The density of states (DOS) reveals the metallic behaviour which is in agreement with resistivity measurements of YbFe₂As₂. There is a spin splitting between up and down spin Fe 3d states and tends to produce a pseudo gap at the Fermi level. The electronic band structure for YbFe₂As₂ depicts that in addition to high dispersion bands in the conduction band region, there are flat bands present at the Fermi region which is composed of As 4p states and Fe 3d electronic states contribution. A possible correlation has been made between the calculated electronic structure of YbFe₂As₂ and measured physical properties.

Keywords: YbFe₂As₂, electronic structure, structural refinement, pseudo gap.

Reference

[1] S. Santhosh Raj *et al.*, Mater. Res. Exp. 4(8), p.086101 (2017)

PP-45

Growth, Optical, Thermal and Third-order Non-linear optical properties of Potassium Trihydrogen Succinate: A potential material with Self-defocusing Applications

 P.S. Latha Mageshwari¹, A.Chamundeeswari¹, S. Jerome Das^{*1}

Department of Physics, R. M. K. Engineering College, Kavaraipettai, 601206, India

²Department of Physics, Loyola College, Chennai 600034,

^{*3}Department of Physics, Loyola College, Chennai 600034, India.

The brisk growth in photonics, bio-photonics and optoelectronics fields in the recent decades have made scientists, and young researchers to ponder on many new materials that show signs of implausible nonlinear optical properties like second and third-order harmonics with substantial hyperpolarizabilities [1-2]. A peculiar third-order nonlinear optical (TONLO) single crystal super-acid salt potassium trihydrogen di-succinate (PTHS) is prolifically grown by slow evaporation solvent technique (SEST) at room temperature. The third-order nonlinear optical parameters such as absorption coefficient, nonlinear refraction, absolute value of susceptibility, number of molecules per unit volume in cm^3 and hyperpolarizability are derived by employing Z-scan technique. FTIR analysis was used to assess the subsistence of functional groups in the material whereas the optical absorption study substantiates the low absorption in the entire visible region and ICP-OES analysis authenticates the prevalence of alkali metal potassium. The overall outcome of PTHS crystal shows the optical limiting behavior and hence most appropriate for fabricating optical limiting and photonic devices.

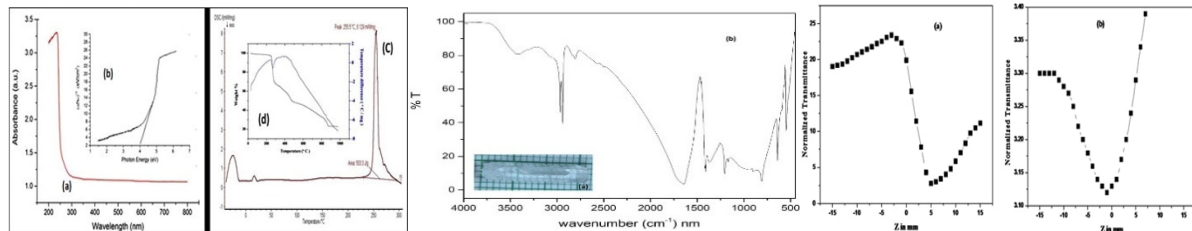


Fig. 1(a) (a) UV-vis-NIR spectra of PTHS, (b) Plot of $(\alpha h\nu)^{1/2}$ versus photon energy, (c) DSC trace of PTHS, (d) TGA/DTA curve of PTHS Photograph of as-grown PTHS crystal, (e) FTIR spectra of PTHS

Fig. 2(a) Photograph of as-grown PTHS crystal, (b) FTIR spectra of PTHS

Fig. 3(a) Plot of Normalized Transmittance versus Z (mm) (Closed aperture), (b) Plot of Normalized Transmittance versus Z (mm) (Open aperture)

Table 1. Crystallography data of PTHS

Parameters	Grown crystal data	Reported data
<i>a</i>	7.47 Å	7.404 Å
<i>b</i>	18.37 Å	18.437 Å
<i>c</i>	9.06 Å	9.006 Å
<i>B</i>	109.75	109.6
Volume	1170 Å ³	1170 Å ³
Space group	P2 ₁ /c	P2 ₁ /c
System	Monoclinic	Monoclinic

PP-46

Bio Synthesis and Characterization of CuO NanoParticles Using from *Ulva fasciata* Algae Extract

S.Ravi¹, R.Balasubramanian¹, B.Rajamannan² and R.Selvaraju³

^a*Engineering Physics Section, FEAT, Annamalai University.*

^b*Department of Physics, Annamalai University.
Tamilnadu, India. 608002.*

Bio- synthesis of CuO nanoparticles has been achieved using environmentally acceptable plant extract. It is observed that *Ulva fasciata* algae leaf extract can reduce Cu ions into CuO nanoparticles within 15 and 30 minutes of reaction time. Here the present study is carried out to establish the catalytic and antibacterial activity of synthesized CuO nanoparticles. The XRD data illustrated characteristic diffraction patterns of the elemental silver phases and the average size of the crystallites are estimated from the peak profiles by Scherrer method. FT-IR spectra of the leaf extract after the development of nanoparticles are determined to allow identification of possible functional groups responsible for the conversion of metal ions to metal nanoparticles. Catalytic activity of silver nanoparticles is analyzed using UV-Vis absorption spectra. The results were discussed.

Key Words: betel Leaf, XRD, antifungal activity

PP-47

Molecular Docking Studies and Density Functional Theory of Some Novel Ethyl 5-(1-Methyl-1H-Tetrazol-5-Ylthio)-4-Oxo-2,6-Substituted Diphenylpiperidine-3-Carboxylate Derivatives

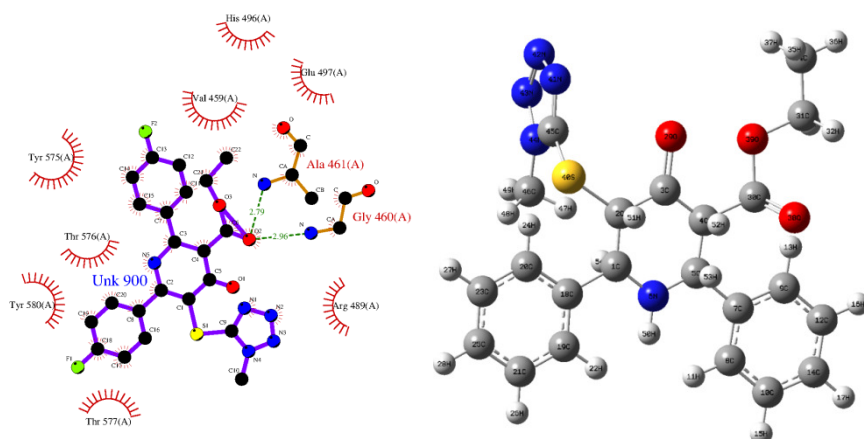
S. Ranjith^{1} and P. Sugumar¹*

^a*Department of Physics, SRM University, Ramapuram Campus, Chennai – 620 089, India.*

^b*Centre of Advanced Study in Crystallography & Biophysics, University of Madras, Guindy Campus, Chennai-600 025, India.*

E-mail: ranjith7784@yahoo.co.in

A wide variety of heterocyclic systems have been explored for the development of pharmaceutically important activities. Heterocycles form by far the largest of the classical divisions of organic chemistry. A new series of heterocyclic compounds containing both N-methylthiotetrazole (NMTT) and piperidine nuclei together, namely ethyl 5-(1-methyl-1H-tetrazol-5-ylthio)-4-oxo-2,6-substituted diphenylpiperidine-3-carboxylate derivatives, were synthesized by cyclocondensation of ethyl 4-(1-methyl-1H-tetrazol-5-ylthio)-3-oxobutanoate with ammonium acetate and substituted aromatic aldehydes. Molecular docking studies were performed on ethyl 5-(1-methyl-1H-tetrazol-5-ylthio)-4-oxo-2,6-substituted diphenylpiperidine-3-carboxylate derivatives with the targeted GTP binding protein, provides the binding modes of the docked compounds, and the hydrogen bond formation for enhancing the activity of this class of compounds can be highly advocated. Gaseous state (DFT) conformation was also evaluated for the synthesized compounds to find conformational preference in gaseous state. The aim of the study is to provide an overview of pharmacological activity associated with the presence or influence of tetrazole containing moiety in the piperidine nuclei.



PP-48

Mechanical and Dielectrical Properties of Dyes Doped Kdp Crystals for Non-Linear Optical Applications

S.Rajeshkumar¹, P.Kumaresan²

¹*P.G Department of Physics, King Nandhivarman College of Arts and Science, Thellar-604406, Tamil Nadu, India.*

²*P.G & Research Department of Physics, Thiru.A.Govindasamy Government Arts College, Tindivanam - 604 002. Tamil Nadu, India.*

Email: srk.ss82@gmail.com

The main aim of my research is to improve the NLO properties of KDP crystal by doping with organic impurities. KH_2PO_4 (KDP) crystal is widely used and thoroughly studied NLO crystals. The NLO and other properties of the crystal have been refined by doping of organic impurities. In the present investigation, Pure and dye Methyl Red doped KDP crystals were grown by slow evaporation technique at room temperature. Grown crystals have been characterized using single crystal X-ray diffraction, Fourier Transform Infrared Spectroscopy (FTIR), UV- visible spectroscopy and NLO studies. The presences of dyes were confirmed by FTIR and XRD spectra. Dye molecules possess π electron similar to conjugated polymers, but the molecules themselves are not very big. The analysis of single crystal XRD spectra confirms that all the doped samples have the perfect crystal properties. Their energy level structure shows the presence of bands containing many closely spaced levels corresponding to vibrational and rotational states. A variety of dyes for many laser operating wavelengths were employed in the past. The NLO reports of the samples are having high energy level comparing with pure KDP. Dyes embedded in KDP crystal and dye-doped crystal was also reported as useful non-linear optical media. The dielectric and mechanical properties of the materials are analyzed using LCRZ meter and Vicker's Microhardness Tester.

Key words: Crystal growth, KDP crystals, Dyes, FTIR Studies, NLO Studies, Dielectric studies.

PP-49

Studies of Urea Doped 4-Nitrobenzoyl Chloride Single Crystal

*R. Raja , S. Kanimozhi, S. Sudha, V.K. Mohanapriya, S.Kanimozhi
Department Of Physics, SCSVMV University, Enathur, Kanchipuram, Tamilnadu, India.*

*E-mail: kanisivaji01@gmail.com

The non linear optical single crystals of urea doped with 4-nitrobenzoyl chloride were grown by solution growth technique. The demand for high quality bulk sized organic crystals is continuously on the rise for the past few decades due to their large scale applications in the field of optical communication, photonics, optical computing, optical data storage and optical information processing so that these materials have become powerful candidates in getting the focus of crystal growers in the field of frontier research and technology. The lattice parameters of the grown urea doped with 4-nitrobenzoyl chloride crystal were studied using single crystal XRD analysis. FTIR analysis gives the detail of the functional groups present in the grown crystal. The thermal stability of the grown crystal was found by TGA/DTA analysis. The mechanical stability of the urea doped 4-nitrobenzoyl chloride crystal was studied by Vicker's Microhardness test. The SHG efficiency of the single crystal was tested to assess by using Kurtz-Perry powder method.

Key words: XRD, TGA/DTA, NLO

PP-50

Growth and Characterization of Dicoumarole Derivative Crystal

*S. K. Parmar^{*1}, H. K. Gohil², A. R. Zinzuvadia³, S. D. Hadiyal⁴, P. M. Vyas⁵ and A. H. Patel⁵*

¹Sarkari Madhyamik Shala, Kadbal, Jamjodhpur – 360530, Gujarat, India.

²Kalapi Vinay Mandir, Lathi – 365430, Gujarat, India

Department Of Chemistry, Saurashtra University, Rajkot – 360005, Gujarat, India

*E-mail: sanjay2706@gmail.com

Coumarins are fluorescent particles having great quantum yield and high photo stability. The coumarins are mostly colorless but substitutions at various positions bring out a red shift in absorption and emission and are utilized in the applications such as laser dyes, textile dyes, sensors as a optical brighteners, non-linear optical (NLO) materials and in biological labeling. The Dicoumarole derivative 4-amino-3-((4-amino-2-oxo-2H-chromen-3-yl)(3-(4-chlorophenyl)-1-phenyl-1H-pyrazol-4-yl)methyl)-2H-chromen-2-one obtained by slow solvent evaporation method. An approximate dimension of crystal is 0.630 x 0.400 x 0.310 mm. The Crystal where characterized using different characterization techniques like single crystal XRD, FT-IR, dielectric study and TG-DTA. Single crystal XRD was adopted for determination of lattice constant, space group and structure analysis. Single Crystal XRD suggests that the crystals are having triclinic crystal system P-1(#2) space group. FT – IR suggests O – H, C – H, C = O, C – Cl many more other bonds. Thermal study suggests that the crystal remains stable up to almost 200 °C. Results were discussed.

PP-51

Bulk Growth Of 3,4 – Diamino Benzophenone By Micro-Tube Czochralski Method

S. Usharani¹, J.Judes^{1*}, V. Natarajan², M. Arivanandhan³

¹University VOC College of Engineering, Anna University: Tuticorin campus, Tuticorin-628 008 India.

²Department of Physics, Dr. Sivanthi Aditanar College of Engineering, Tiruchendur 628215, India

³Centre for Nanoscience and Technology, Anna University, Chennai 600025, India

*E-mail: ushaponmuthu@gmail.com

Most of the optical applications require highly energetic laser radiation which is possible by frequency conversion through nonlinear optical (NLO) effect. Therefore, NLO materials are highly useful for generating green and blue lasers by doubling the low frequency laser radiations. The materials inherent with this significant property find its wide applications in second harmonic generation (SHG), frequency conversion, electro-optic modulation, optical parametric oscillation, optical bistability, photochemistry, biomedical research, optical windows and spectroscopy. Benzophenone and its derivatives are the potential organic NLO materials with good optical, mechanical properties and non-hygroscopic nature [1]. In the present work, bulk crystals of one of the benzophenone derivatives, 3, 4-diamino benzophenone (3,4DABP) are grown by Micro-tube Czochralski technique. In order to grow high-quality single crystals, different growth parameters like micro-tube diameter, length and temperature gradient of the furnace were optimized. The bulk single crystal of DABP was successfully grown under the optimized condition (Fig.1). The structural, optical, thermal properties of the grown crystals were investigated. The powder Kurtz method was employed to study the NLO properties of DABP crystals. The rest of the results will be discussed in detail.



Fig.1. Photograph of as grown DABP

References

- [1] Cockorham P, Frazier C.C, Guha S, Chauchard E.A, Appl.Phys.,1991,B53, 275.
- [2] Philip J.Cox, Abu T.MD, Anizzuman R, Howard Pryce –Jones, Graham G. Skellern, Alastair J.Florence, Norman Shankland, 1998,C54, 856-859.

PP-52

Investigation on Growth and Characteristics Glycine Sodium Fluoride (GSF) For Optoelectronic Applications

R. Ravisankar^{1*}, R. Vijayakumar¹, N.Harikrishnan¹, G.Senthilkumar² D. Rajendiran^{1,3}, J.Chandramohan⁴

¹Post Graduate and Research Department of Physics, Government Arts College, Thiruvannamalai – 606603, Tamilnadu

³Department of Physics, University College of Engineering Arni, Arni- 632317, Tamilnadu

³Post Graduate and Research Department of Physics, Shanmuga Industries Arts and Science College, Thiruvannamalai – 606603, Tamilnadu

⁴Department of Physics, **Sun Arts and Science College**, Keeranoor, Thiruvannamalai-606755, Tamilnadu,

* **E-mail:** ravisankarphysics@gmail.com

Glycine doped sodium fluoride (GSF) crystal has been grown by slow solution evaporation technique. The powder X-ray diffraction of the grown crystal was recorded and indexed. Functional groups present in the sample were identified by FTIR spectral analysis. The thermal characteristics of the grown crystal were determined by thermogravimetric and differential thermal analysis (TG/DTA), which show the thermal stability of the grown crystals. The optical transmittance window and lower cutoff wavelength have been identified by UV-absorption spectrum analysis. Second harmonic generation (SHG) efficiency measurement was carried out by powder Kurtz method. In order to analyze the mechanical properties of the grown crystal was subjected to Vicker's microhardness indentation analysis. The dielectric constant and loss factor of the samples were estimated at different frequencies and temperatures and the results are analyzed. The etching *studies* have been performed to investigate the surface quality of glycine doped sodium fluoride crystal.

Keywords: Glycine sodium fluoride, Non-Linear optical material

PP-53

Crystal Growth and Characterization of Glycine Potassium Iodide (GPI) For Nonlinear Optical Applications

R. Ravisankar^{1*}, D. Rajendiran^{1,2}, R. Vijayakumar¹, P. Jayaprakash³, K.M. Freny Joy⁴

¹Post Graduate and Research Department of Physics, Government Arts College, Thiruvannamalai

²Post Graduate and Research Department of Physics, Shanmuga Industries Arts and Science College

³Department of Physics, Annai Mira College of Engineering and Technology, Arapakkam, Vellore

⁴Department of Physics, Madras Christian College, Tambaram, Chennai – 600059, Tamilnadu

* **E-mail:** ravisankarphysics@gmail.com

Glycine Potassium Iodide (GPI) crystals have been grown by slow evaporation solution technique at room temperature. The functional groups and vibrational frequencies were identified using FTIR

spectral analysis. The cell parameters were determined from single crystal X-ray diffraction analysis. Thermogravimetric analysis (TGA) and differential thermal analysis (DTA) were used to study its thermal properties. The optical transmittance window and lower cutoff wavelength have been identified by UV-absorption spectrum analysis. Second harmonic generation (SHG) efficiency measurement was carried out by powder Kurtz method. The dielectric studies have been employed to examine the substantial improvement in dielectric constant and dielectric loss of glycine doped Potassium Iodide (GPI) crystal. The non linear optical absorption of the samples has been studied by Z-scan technique. The observed properties have confirmed that the grown crystal is suitable for nonlinear optical applications.

Keywords: Glycine Potassium Iodide, Characterization studies, NLO applications

PP-54

Structure and Intermolecular Interactions of Some Benzodiazepine Derivative Molecules with GABA-A Receptor: A Molecular Docking and Quantum Chemical Analysis

M. Prasath , B. Sathya and M. Ramaraj*

Department of Physics, Periyar University PG Extension centre, Dharmapuri-636701

*E-mail: sanprasath2006@gmail.com

Benzodiazepine is an antixyloptic agent, induce and maintain sleep, reduce seizures, and induce conscious sedation. It acts as a positive allosteric modulator of gamma-aminobutyric acid-A (GABA-A) receptor. Here some of the benzodiazepine derivative molecules like Halazepam, Ketazolam and Medazepam were evaluated using theory models.

In this context, the molecular geometric parameters were predicted by DFT method and the gas phase is compared with active site. A molecular docking, HOMO-LUMO and dipole moment have been carried out to understand the conformational change in the active site of GABA-A receptor. The nearest neighbours, shortest intermolecular contacts between the molecules and GABA receptor and the lowest binding energy of the molecules have been analysed from the docking method. Further, the electrostatic properties of the molecule also determined. The electrostatic potential (ESP) map of the molecules allows identifying the nucleophilic and electrophilic regions of the molecules. Stability of the molecules arising from hyper conjugative interactions, charge delocalization has been analysed using natural bond orbital (NBO) analysis. The Entropy of the molecules are also performed at B3LYP/6-311G(d,p) levels of theory. In addition, the thermodynamic properties of the compounds were calculated at different temperatures and corresponding relations between the properties and temperature were also studied.

PP-55

Synthesis, Structure Elucidation of a New Chalcone Derivative

T. Ramila, ¹B.K. Revathi, ²M. Krishna Priya, ¹AkumToshi Aier, ^{1}P. Samuel Asirvatham*

^{1, 1}Department of Physics, Madras Christian College, Chennai-59, India.*

²PG and Research Department of Physics, Queen Mary's College, Chennai-04, India.

*E-mail: ramilarami43@gmail.com

A new organic material was synthesized by slow evaporation method. The single crystal XRD study reveals that the compound crystallizes in monoclinic crystal system with space group C2/c and the lattice parameters are $a=28.4090(12)$, $b=3.9242(2)$, $c=37.5734(17)\text{\AA}$, $\beta=109.843(3)^\circ$ and $V=3940.1(3)\text{\AA}^3$. Structure of the compound was solved and refined with SHELXS97 and SHELXL14 programme. The translation symmetry molecules are connected through C-H...O type intermolecular interactions and forming a molecular ribbon and the ribbons are running parallel to "a" axis.

PP-56

Observation of Carbon Related New Donors in Cz-Silicon in the Temperature Range 450 °C to 510 °C Based On Ftir

*Rajeev Singh^{*1}, P. B. Nagabalsubramanian²*

^{1,2}Department of Physics, Arignar Anna Government Arts & Science College,

Karaikal (UT of Puducherry), India – 609605

*E-mail: bansalexam@gmail.com

In view of potential applications of Czochralski (CZ) silicon, it is still a primary material for electronic industry. The formation of carbon related new donors (NDs) has been studied at different temperatures in the range 450 °C to 510 °C for different annealing time. At the temperature 480 °C, the activation energy for oxygen is found 2.14 eV for less carbon concentration samples whereas it has relatively low value for high carbon concentration samples. It implies that the formation of NDs is not controlled only by the diffusion of oxygen interstitials but due to presence of other impurities like carbon, hydrogen etc. Carbon suppresses the formation of thermal donors but after 480 °C, it accelerates the formation of NDs [Fig.1]. The FTIR of sample shows the formation of carbon related donors at 480 °C. The peak at 669 cm^{-1} shows strong intensity at 495 °C but it is diminished at 510 °C.

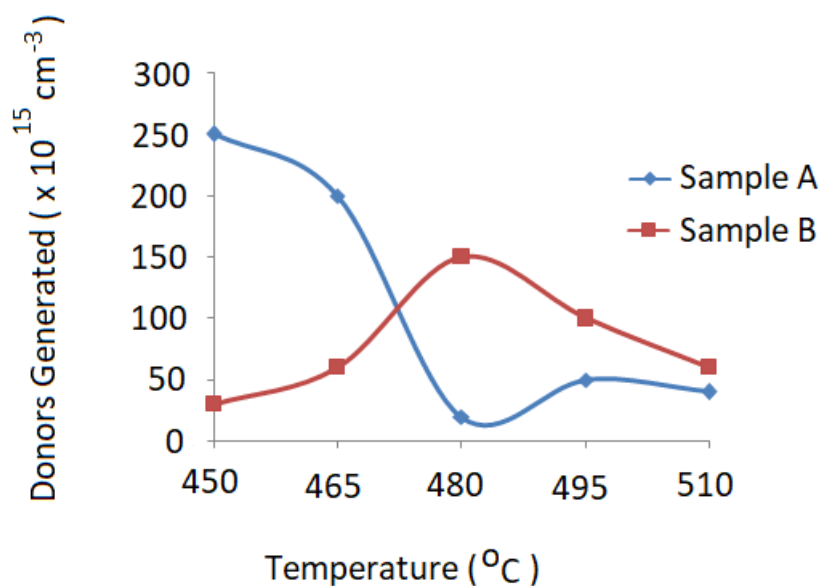


Fig. 1

PP-57**Mechanical Behaviour of Benzimidazole Derivative Single Crystals**

M. Rajalakshmi^{*1} and *R. Indirajith*²

¹*Department of Theoretical Physics, University of Madras, Guindy Campus, Chennai 25.*

²*Department of Physics, B. S. Abdur Rahman Crescent, Institute of Science & Technology, Chennai – 48.*

*E-mail: rajalakshmipuffin@gmail.com

Benzimidazole derivative were synthesised and grown by slow evaporation solution growth method. Good optical transparency crystal were harvested and subjected for Microhardness studies. Vickers microhardness study was carried out on the surface of the single crystal with various loads at room temperature with the indentation time as 5 s. Vickers hardness numbers H_v was calculated and it is found to increase with the applied load. Mayer's index number 'n' was calculated. The results are discussed in detail.

Hardness is a characteristic of a material, not a fundamental physical property. It is defined as the resistance to indentation and it is determined by measuring the permanent depth of the indentation. Superhard materials have attracted great attention because of their important industrial applications. In order to explore new superhard materials, the nature of hardness was extensively investigated, with numerous models proposed to predict the hardness of materials. Microhardness testing is one of the best methods for understanding the mechanical properties of materials such as elastic constants and fracture behaviour. Organic crystals were intensively investigated due to their high nonlinearities, high mechanical properties, rapid response in electro-optic effect and tailor made flexibility.

In the present work the mechanical behaviour of benzimidazole derivatives was studied using Vickers microhardness tester. Vickers microhardness study was carried out on the surface of the single crystal with

various loads at room temperature with the indentation time as 5 s. Vickers hardness number H_v was calculated and it is found to increase with the applied load. Mayer's index number 'n', crack length, elastic stiffness constant, yield strength, fracture toughness and Brittle index were calculated. Mechanical waves generated by piezoelectric crystals of composites are very valuable in determining the elastic properties of all solid materials. The results are discussed in detail.

PP-58

Growth and Characterization of Piperazine Doped Adipic Acid Single Crystal

R. Raja , S. Kanimozhi

Department Of Physics, SCSVMV University, Enathur, Kanchipuram, Tamilnadu, India.

**E-mail: kanisivaji01@gmail.com*

A single crystal of piperazine doped adipic acid has been grown using solution growth technique. The single crystals play a vital role take part in the development of electronic industry, solid state technology, laser and electro optical engineering, communication systems and computer industries. The lattice parameters of the grown piperazine doped with adipic acid crystal were studied using single crystal XRD analysis. FTIR analysis gives the detail of the functional groups present in the grown crystal. The thermal stability of the grown crystal was found by TGA/DTA analysis. The mechanical stability of the piperazine doped adipic acid crystal was studied by Vicker's Microhardness test. The SHG efficiency of the single crystal was tested to assess by using Kurtz-Perry powder method.

Key words: XRD, TGA/DTA, FTIR, NLO.

PP-59

Synthesis, Characterization and Application of Nickel Doped ZnO Nanocrystals for the Photocatalytic Degradation of Textile Dyeing Effluent

P. Logamani¹, R. Rajeswari², G. Poongodi^{1}*

1- Research Scholar, Research and Development Centre, Bharathiar University, Coimbatore - 641 046.

2-Department of Chemistry, Quaid-E-Millath Govt. College for Women, Chennai - 600 002.

3-Department of Physics, Quaid-E-Millath Govt. College for Women, Chennai - 600 002.

**Email: srpoongodi@gmail.com*

Nickel doped ZnO nanocrystals were synthesized by hydrothermal method. X-ray diffraction (XRD) and Field Emission Scanning Electron Microscopy (FESEM) with Energy dispersive X-ray spectroscopy (EDAX) were used to assess the structure and morphological properties of the catalyst prepared. The XRD diffraction peak confirms that the synthesized Ni doped ZnO has highly crystalline hexagonal wurtzite structure. FE-SEM images established the nanorod morphology of the sample. The photocatalytic activity of pure and Ni doped ZnO nanocrystals were tested with Amaranth dye using

visible light (365nm) in an annular photo reactor. The reaction parameters such as pH, catalyst dosage and dye concentration were optimized. Degradation study revealed that doping has distinct influence on the photocatalytic behaviour of ZnO. With the optimized conditions, Decolourisation was 96% and the Degradation was 74% at the end of 180 min. The present research study shows that Ni doped ZnO nanocrystals could be used as an effective photocatalyst for the removal of dyes in textile effluents in a suitably designed photocatalytic reactor.

Keywords: Photocatalysis, Ni doped ZnO, FESEM, Amaranth dye

PP-60

Synthesis, Growth, Spectral and Optical Properties of L-Alaninium P- Hydroxybenzoate Nonlinear Optical Single Crystal

*G. Parvathy, R. Kaliammal, K. Velsankar, S. Sudhahar**

Department of physics, Alagappa University, Karaikudi-03

E-mail: parvathyphysics@gmail.com

Organic nonlinear optical crystal of l-alaninium p- hydroxybenzoate have been grown by slow evaporation solution growth method at room temperature using as ethanol:water mixed solvent. The crystal system, space group, various planes of reflections and crystal perfections were identified by single crystal and powder X-ray diffraction analyses. The presence of functional groups in the synthesized compound was identified by FTIR spectral analysis. Thermal behaviour and thermal stability of LAPH were studied by TG-DTA analyses. The lower cut-off wavelength at 340 nm were determined by UV-Visible spectra. UV-Vis transmission studies reveal that the grown crystal was optically transparent through visible range making it suitable for NLO applications. The photoluminescence spectra give the qualitative and quantitative analyses of grown LAPH crystal, the excitation wavelength at 360 nm. The Kurtz-Perry powder second harmonic generation technique confirms the nonlinear optical property of the grown crystal.



PP-61

Synthesis Growth Structural Spectroscopic and Optical Properties of L-Lysine Monohydro Chloride Ammonium Chloride Non Linear Optical Single Crystals

R.Ragavendiran¹, M. Selvapandiyan^{2}, C. Govindaraj³*

¹Department of Physics, Government Arts and Science College for Women, Bargur, Tamil Nadu, India

²Department of Physics, Periyar University PG Extension Centre, Dharmapuri - 636701, Tamil Nadu, India

³ Department of Chemistry, Sri Vidya Mandir Arts and Science College, Uthangarai, Tamil Nadu, India.

*Email: mselvapandiyan@rediffmail.com

Semi-organic non linear optical material of L-Lysine monohydro chloride Ammonium chloride were grown by slow evaporation technique at room temperature in the ratio of 1:1. Single crystal XRD was carried out to examine the crystal system and unit cell parameters. Powder XRD patterns confirm the basic structure of materials and the functional groups are identified by using FTIR spectrum. TG/DTA analysis is confirms that the thermal stability of grown crystals. The transparency of grown crystals was analysed by UV-VIS-NIR. The second harmonic generation (SHG) conversion efficiency has been estimated and the output power of the crystal was determined by using Kurtz powder technique.

Key words;

Crystal growth; slow evaporation technique-Lysine monohydro chloride doped Ammonium chloride

PP-62

Thermal and Spectroscopic Analysis of Idol Making Rocks

R.Jayaprakash^{1}, P.Rajkumar², S.Rajesh kumar²*

^{1,2}Department of Physics, King Nandhivarman college of Arts & Science, Thellar-604406, Tamil Nadu, India

*E-mail: focusraj108@gmail.com

The present work is focused on the characterization study of idol making rocks shreds excavated recently from korakottai Thiruvannamali dist in India. The study is intended to identify the firing temperature, firing conditions and morphology of the idal making rocks samples. The samples were analyzed using FTIR, XRD and TG-DTA. FTIR and XRD studies were used in mineralogical characterization of rocks. The firing temperature and conditions were interpreted by studying the difference in mineral composition in the samples using FTIR and XRD. TG-DTA is considered the complementary technique to elucidate the firing temperature from the thermal characteristic reactions such as dehydration, decomposition and transformations of minerals in the course of controlled firing of the samples. The results showed that all the samples fired in a oxidizing condition and firing temperature also inferred.

PP-63

Comparative DFT Study and Vibrational Spectra of Hemiterpenes: A Study on A- And B-Furoic Acid Dimers

P.Rajkumar^{1}, S.Selvaraj¹, R.Suganya², D.Velmurugan³, S.Gunasekaran⁴, S.Kumaresan¹*

^{1*}*Spectrophysics Research laboratory-Department of Physics, Arignar Anna Government Arts College, Cheyyar, Tamil Nadu, India-604407.*

²*Department of Medical Physics, Anna University, Chennai, Tamil Nadu, India, 600025.*

³*CAS in Crystallography and Biophysics, University of Madras, Guindy Campus, Chennai, Tamil Nadu, India, 600025*

⁴ *Sophisticated Analytical Instrumentation Facility, St. Peter's Institute of Higher Education and Research, St.Peter's University, Avadi, Chennai-600054, Tamil Nadu, India.*

*E-mail: focusraj108@gmail.com

Characterization of α - and β -furoic acid (α FA & β FA) by spectral techniques has been performed with spectroscopic investigations like FT-IR, FT-Raman, UV and NMR techniques and quantum chemical computation. The structural and spectroscopic data of the molecule were obtained from HF and B3LYP with 6-311++G (d,p) levels using density functional theory (DFT). The detailed natural bond orbital (NBO) analysis and stability with intra-molecular charge transfer have analyzed. The charge transfer occurring in the molecule was verified and found to be stable from smaller energy-gap by HOMO-LUMO analysis. The first order hyperpolarizability of the investigated molecules has been studied theoretically. The calculated parameters were found to be in best agreement with experimental findings, there by confirming, the monomer and dimers structure. NLO and MEP surfaces properties have been calculated and analyzed.

Keywords: FTIR, FT-Raman, NMR, DFT, NLO, MEP

PP-64

Modelling for Organic Solids via *Ab Initio* Crystal Structure Predication And Quantum Chemical Methods

P. Srinivasan¹ and A. David stephen²

¹*PG & Research Department of Physics, Chikkaiah Naicker College, Erode, India*

²*Department of Physics, Sri Shakthi Institute of Engineering and Technology, Coimbatore, India*

*Email: sriniscience@gmail.com

Computational modelling and quantum chemical methods are enable the definition of a large number of molecular quantities characterizing the reactivity, shape, electron density and binding properties of a complete molecule as well as of molecular fragments and substituent's. The ab initio crystal structure prediction method lies in the application area where a successful prediction method can give a good understanding of the crystallisation process, and also the prediction of highly energetic

molecules might decrease the level of experimental risks. The computed theoretical parameters are gives two main features: firstly, the compounds and their various fragments and substituent's can be directly characterized on the basis of their molecular structure only; and secondly, the proposed mechanism of action can be directly accounted for in terms of the chemical reactivity of the compounds under study. Quantum chemically derived parameters are fundamentally different from experimentally measured quantities. In using quantum chemistry-based parameters with a series of related compounds, the computational error is considered to be approximately constant throughout the series. Further, the quantum chemical methods reduce the number of experiments required and allow one to do more intelligent experiments. The computational material design via molecular modelling and ab initio quantum chemical methods viable routes prior to the synthesis of new organic solids with desired properties.

Keywords: Crystal structure prediction, DFT, MOLPAK, Gaussian and ESP

PP-65

Computational, Spectral And Structural Studies Of A New Organic NLO Crystal: 2-Amino 5-Methyl Pyridinium Succinate For Nonlinear Optical Applications

*S. Nithya¹, B. Chandra Shekar², K.R. Aranganayagam³, K. Boopathi^{*4}*

¹ *Department of Physics, Kumaraguru College of Technology, Coimbatore- 641049*

² *Department of Physics, Kongunadu Arts and Science College, Coimbatore- 641029*

³ *Department of Chemistry, Kumaraguru College of Technology, Coimbatore- 641049*

⁴ *Department of Inorganic Chemistry, School of Chemical Science, University of Madras (Guindy Campus), Chennai-600025*

*E-mail: boopathi.chemist@gmail.com

A new organic charge transfer complex, 2-amino 5-methyl pyridinium succinate (2A5MPS) have been synthesized and good quality was successfully grown by the slow evaporation method. The ¹H and ¹³C NMR spectral studies further confirm the molecular structure of the grown crystal. The various functional groups present in the title compound have been identified by Fourier transform infrared spectroscopy. Single crystal X-ray diffraction study confirms that the 2A5MPS crystallizes in orthorhombic crystal system with space group P2₁2₁2₁. Optical properties of 2A5MPS were ascertained by UV absorbance and reflectance spectra. The band gap of the title compound is found to be 4.73 eV. Thermal stability of the grown crystal was evaluated by thermogravimetric (TG) and differential thermal analysis. The nonlinear optical (NLO) activity test using a Q-switched and pulsed Nd: YAG laser confirms the generation of second harmonics. Computational studies that include optimization of molecular geometry, natural bond analysis (NBO), Mulliken population analysis and HOMO-LUMO analysis were performed using Gaussian 09 software by B3LYP method at 6-31g basis set level.

PP-66

Sensitivity Enhancement of Copper with the Use of Transition Metal Dichalcogenides (Tmdcs) In Surface Plasmon Resonance Biosensor

A. Nisha¹, P.M. Anbarasan¹, P.Maheswari³, K.B. Rajesh^{2}*

¹*Department of physics, Periyar University, Salem, Tamil Nadu, India*

¹*Department of physics, Periyar University, Salem, Tamil Nadu, India*

³*Department of physics, PSGR Krishnammal College for Women, Coimbatore.*

^{2*}*Department of Physics, Chikkanna Government Arts College, Tirupur, Tamil Nadu, India.*

*Email: rajeskb@gmail.com

In this work we designed and investigated the Surface Plasmon Resonance biosensor, with various 2D materials called Transition Metal Dichalcogenides (Black Phosphorous, Graphene, MoS₂, WS₂ and MoSe₂) is over coated on the base of copper. Here the TMDCs are introduced for the enhancement of sensitivity and better absorbance of biomolecules. The proposed configurations of various TMDCs increases the sensitivity with increasing the No. of layers, the higher sensitivity are obtained for all TMDCs notably 315°/RIU and shows sensitivity for all refractive index of the sensing mediums from 1.30 to 1.40. These higher sensitivity materials are better for further device applications.

Keywords: Surface Plasmon Resonance, Biosensor, Transition Metal Dichalcogenides, Copper.

PP-67

Screening Effect Of Various Acceptor Groups In The Perylenemonoimide Based D- II -A Architecture Of Dye Sensitized Solar Cells: A Theoretical Study

M. Prasath and D. Nicksonsebastin

Department of Physics, Periyar University PG Extension Centre, Dharmapuri-636701

*E-mail: sanprasath2006@gmail.com

The designed metal –free organic dyes have interrogated by density functional theory and Time Dependent DFT to evaluate ground state and excited state geometries of seven different acceptor organic sensitizers. Optoelectronic properties of seven different acceptor dye sensitizers, namely A1 to A7 were studied. The various acceptor groups are cyanoacrylic acid, dicyanovinylcarboxylic acid, dicyanovinyl sulfonic acid, pyridine, benzotriazole, phthalimide and quinoxaline then thiophene and perylenemonoimide acts as π spacer and donor groups were studied. Energy band modulation has been performed by these dyes with same electron donating and dissimilar electron withdrawing group. The efficiency of the designed dye molecules was analyzed using various parameters. Such as the HOMO-LUMO energy gap, Absorption spectra, exciton binding energy (E_b), light harvesting efficiency (LHE), Excited state lifetime (τ) and free energy for electron injection. A good photovoltaic performance based on the optimized geometry, the relative position of the frontier molecular orbital energy levels and the absorption maximum of the dye were proposed for offering a remarkable response.

Keywords: Dye Sensitizer, DSSC, DFT, UV-Visible Absorption Spectra, Excited state lifetime Electron injection.

PP-68

Synthesis, Growth, Structure, Characterization and Anti Microbial Activities of L-Isoleucinium-P-Toluenesulfonate Monohydrate (Liptsa)

Dr. P.Nagapandiselvi and Dr. M. Muralidharan

Department of Physics, SSN College of Engineering, Kalavakkam, Kanchipuram

Department of Physics, Anna University, Chennai-25

*Email.id: nagapandiselvip@ssn.edu.in

Amino acids based single crystals are fascinating materials for nonlinear optical and medical applications. This report presents the synthesis, growth, crystal structure determination, characterization and antimicrobial activities of L-Isoleucinium-p-toluenesulfonate monohydrate (LIPTSA). LIPTSA was synthesised and their single crystals were grown by slow evaporation solution growth technique. The crystal structure was elucidated by single crystal X-ray diffraction at 293 K. It was in monoclinic crystal system with a space group of $P2_1$ ($Z=2$) and lattice parameters: $a = 10.1903(3) \text{ \AA}$, $b = 6.5741(3) \text{ \AA}$ and $c = 12.7642(4) \text{ \AA}$, $\alpha = 90^\circ$, $\beta = 104.389(2)^\circ$, $\gamma = 90^\circ$, $V = 828.28(5) \text{ \AA}^3$. L-Isoleucinium-p-toluenesulfonate monohydrate was characterized by FT-IR, FT Raman, and UV-Visible spectral analysis. Thermal analysis showed that the material is thermally stable up to 120°C . SHG intensity of the title compound was recorded and compared with that of KDP by Kurtz – Perry powder technique. The antibacterial activities of the title compound were performed by disk diffusion method against the bacteria's: *Staphylococcus aureus*, *Aeromonas spp.*, *Salmonella typhi*, *Pseudomonas aeruginosa*, *E. coli*, *Shigella spp*, *Klebsiella pneumoniae*, *Vibrio cholerae*, *Proteus spp* and *Bacillus subtilis* for pharmaceutical applications,

PP-69

Structural, Vibrational, Electronic and Molecular docking dynamics of 2-benzyloxy 3-methoxybenzaldehyde – An experimental and quantum approach

P.B.Nagabalasubramanian^{a}, K. Manivannane^b T. Prabu^b, S. Periandy^c, Rajeev Singh^a*

^aDepartment of Physics, Arignar Anna Govt. Arts & Science College, Karaikal, Puducherry, India.

^bDepartment of Physics, A.V.C. College (autonomous), Mayiladuthurai, Tamilnadu, India.

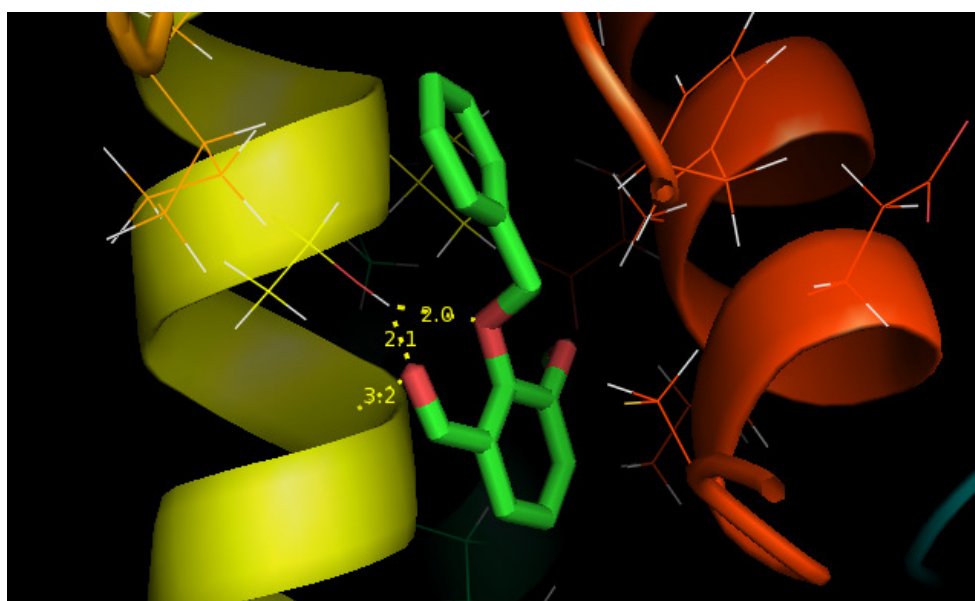
^cDepartment of Physics, Kanchi Mamunivar Centre for Postgraduate Studies, Puducherry, India.

*Email: nagaphysics1975@gmail.com

An anti-proliferative agent 2-benzyloxy-3-methoxybenzaldehyde(Benzyl-o-vanillin) abbreviated as 2B3MB was comprehensively recorded by FT-IR, FT-Raman, UV, as well as ^1H and ^{13}C spectroscopic

techniques. The observed absorption and scattering spectral sequence were analyzed to predict the molecular property. The Gaussian computational calculations such as vibrational frequencies, Mulliken and NBO charges, UV-Vis, NMR (GIGO technique) are carried out by hybrid DFT/B3LYP method with 6-311++G(d,p) basis set. The corresponding results obtained from computational calculations were verified with experimental data. The chemical shifts obtained by GIGO technique were linked to TMS were compared. A detailed study on the electronic and optical properties; absorption wavelengths, excitation energy, dipole moment and frontier molecular orbital energies were carried out. Molecular electrostatic potential (MEP) were generated and tried to predict the drug activity of the compound by observing FMO interaction profile. To understand more insight on the drug activity, the molecular docking study was conducted, and results of the docking study identified that the title molecule has high potential ligand-receptor property with the protein CYP2B5 substrate.

Key words: FT-IR, FT-Raman, NMR, Benzyl-o-vanillin, CYP2B5 substrate, Molecular Docking.



2-

benzyloxy-3-methoxy benzaldehyde (Benzyl-o-vanillin) with protein **CYP2B5 substrate (Protein ID : 2PG5)** form ligand-receptor interactions & makes binding free energy (ΔG in kcal/mol) of 2.0, 2.1 and 3.2

PP-70

Synthesis and Spectroscopic Investigation of 4-(Benzylideneamino) Benzenesulfonamide

*R.Muthukumar¹, M. Karnan¹ and K.Venkateswaran², R.Muthukumar*¹*

PG & Research Department of Physics, Srimad Andavan Arts and Science College, Tiruchirappalli 620005, India

*E-mail: muthur@andavacollege.ac.in

The compound, 4-(benzylideneamino)benzenesulfonamide derivative was synthesized by chemical method. The molecular structure confirmation was done experimentally by the Fourier transform infrared spectrum (FT-IR) and Fourier transform Raman spectroscopy (FT - Raman). In this work, experimental and theoretical study on the molecular structure, quantum chemical calculations of

energies and vibrational wavenumbers is presented. The vibrational frequencies of the title compound were obtained theoretically by DFT/B3LYP calculations employing the standard 6-311+G(d,p) and 6-311++G(d,p) basis set for optimized geometry and were compared with FTIR and FT - Raman spectrum. Complete vibrational assignments, analysis and correlation of the fundamental modes for the title compound were carried out. The vibrational harmonic frequencies were scaled using scale factor, yielding a good agreement between the experimentally recorded and the theoretically calculated values. The study is extended to calculate the HOMO–LUMO energy gap, mapped molecular electrostatic potential (MEP) surfaces, polarizability, Mulliken charges and thermodynamic properties of the title compound.

Keywords: 4-(benzylideneamino) benzenesulfonamide, Vibrational spectra, HOMO–LUMO, MEP surface

PP-71

Growth, Structure and Characterization of NLO Active 4-Methylpyridinium Picrate

S. Sivaraman¹, R. Markkandan^{1}, R. Selvaraju² and SP. Meenakshisundaram³*

^aDepartment of Chemistry, Annamalai University, Tamilnadu, India

^bThiru A Govindasamy Government Arts College, Tindivanam, India

^cDepartment of physics (FEAT), Annamalai University, Tamilnadu, India

*Email: rmark29@gmail.com

Crystal structure of single crystals of 4-methylpyridinium picrate (MPP) grown by slow evaporation solution growth method was elucidated by single crystal X-ray diffraction analysis and it belongs to monoclinic system with noncentrosymmetric space group $P2_1$. The crystallinity of the material was confirmed by powder X-ray diffraction which agrees well with the simulated pattern with varied intensities. The functional groups present in the molecule are identified by FT-IR analysis and the band gap energy was estimated using diffuse reflectance data by the application of Kubelka-Munk algorithm. The thermal stability of the compound was investigated by carrying out TG-DTA analysis. Photoluminescence studies were also carried out for the grown MPP crystal. The second harmonic generation efficiency (SHG) is estimated using the Kurtz and Perry powder technique and it reveals NLO (nonlinear optical) character.

PP-72

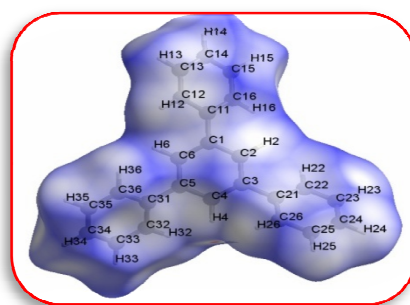
Crystal Growth, Spectral, Optical, Thermal Analysis and Quantum Chemical Calculation of the Organic Single Crystal

M. Manikandan¹, P. Rajesh^{1}, P. Ramasamy¹*

Centre for Crystal Growth, Department of Physics, SSN College of Engineering, Kalavakkam, Tamilnadu, India - 603 110.

Email: rajeshp@ssn.edu.in

The organic nonlinear optical materials are most important in the area of second harmonic generators, electro-optic modulators, optical data storage, optical signal processing, frequency conversion, and so on. In the present work, an organic single crystal Triphenylbenzene (TPB) was grown by low-temperature slow evaporation solution growth method. The crystal system and cell parameters determined are single crystal X-ray diffraction. The crystalline nature of the grown crystal was confirmed using powder X-ray diffraction analysis. The different functional groups were identified using FTIR and FT-Raman analyses and compared with theoretical values. The UV-VIS NIR analysis shows that the grown crystal possesses good transparency in the entire visible region with lower cut-off wavelength. The desire cut-off wavelength and good transparency in the visible and near IR region are a very important factor for materials to be used for many optical applications [1]. Thermal stability of the crystals was tested from the thermogravimetric and differential thermal analysis (TG/DTA). The nonlinear optical properties such as dipole moment (μ), polarizability (α) and first-order hyperpolarizability are calculated. The determined first-order polarizability (β) was found as 5.521×10^{-30} esu. The molecular Hirshfeld surface analysis is an effective tool to provide a summary of intermolecular interactions, molecular shape in crystals, which helps to analyze and visualize the d_{norm} , surface contributions, and 2D finger plots [2]. Intermolecular interactions of the TPB crystal have been executed through Hirshfeld surface analysis.



Rajesh, P. and Ramasamy, P., Mater. Lett. **2009**, 63, 2260-2262.

Mamatha, S.V., Naveen, S., Mohammed, Y.H.E., Lokanath, N.K. and Khanum, S.A., Chem Data Collections, **2017**, 11.

PP-73

Growth and Characterization of Alanine Doped Urea Thiourea Magnesium Chloride (Autmc) Single Crystals

P.Malliga

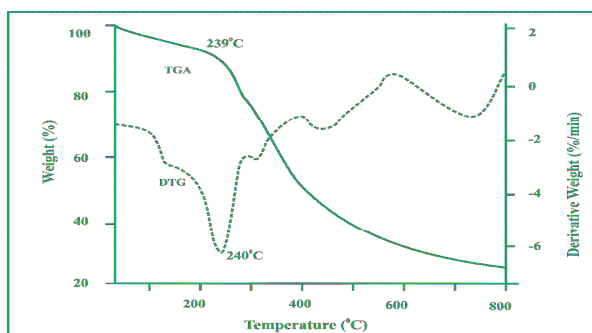
Department of Physics, Sathyabama Institute of Science and Technology Tamilnadu, Chennai: 600 119,

*Email:calltomp@gmail.com

A novel semiorganic optical material, L-alanine doped urea thiourea magnesium chloride (AUTMC) single crystals was grown successfully by slow solvent evaporation method at room temperature of 34 °C. The crystal structure and lattice parameters were determined by single crystal X-ray

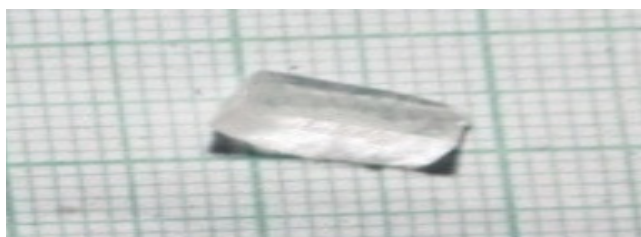
diffraction analysis .XRD data of crystals AUTMC crystals show a slight change in the values of lattice parameters and volume in comparison with the pure urea thiourea magnesium chloride (UTMC) crystal indicating the inclusion of dopant alanine. FT-IR studies confirm the presence of functional groups and the modes of vibration. Minimum optical absorption is observed in the wavelength region 292 –1000 nm. Also, it is observed that the lower cut-off wavelength is not much altered in the case of alanine doping. The emission of green radiation is observed which confirms the NLO property. The TG/DTA analyses show that the thermal stability is considerably increased with the addition of alanine dopant in the pure UTMC

Thermogravimetric trace of



UTMC crystals

alanine doped



As grown crystal of alanine doped UTMC crystals

PP-74

Sensitivity Enhancement Of Surface Plasmon Resonance Optical Biosensor Based On Graphene Structure With Nanocomposite Layer

P.Maheswari¹, V.Ravi¹, A.Nisha³, K.B.Rajesh^{2}*

¹*Department of physics, PSGR Krishnammal College for Women, Coimbatore.*

¹*Department of physics, Government Arts College ,Salem-7.*

³*Department of physics, Periyar University, Salem, Tamil Nadu, India.*

^{2*}*Department of Physics, Chikkanna Government Arts College, Tirupur, Tamil Nadu, India.*

*Email id: rajeskb@gmail.com

In this paper a new configuration of surface plasmon resonance (SPR) sensor based on graphene structure with nanocomposite layer is analysed theoretically based on N- layered matrix method for kretschmann configuration. A nanocomposite layer containing the nickel nanoparticles and ZnO as host

dielectric. The performance parameters of proposed sensors are investigated in terms of sensitivity, detection accuracy and quality factor at the operating wavelength of 633nm. The influence of the refractive index of the coupling prism, the thickness of the nanocomposite layer, the constituent components of the nanocomposite layer and the number of the graphene layer is investigated and the optimal value is calculated for the maximum sensitivity. The observed numerical results showed higher sensitivity when increasing the number of graphene layers. It is clearly observed that using graphene layer, the proposed biosensor exhibits simultaneously high sensitivity of 321.02 deg/RIU, detection accuracy of 0.0034 and quality factor of 38.58RIU⁻¹ with nanocomposite layer of thickness 70nm. Compared with existing biosensors, the proposed biosensor exhibits higher sensitivity, lower FWHM and better performance in the quality factor of the sensor which would make our design have more applications in the field of biosensor.

Keywords: surface plasmon resonance, graphene, nanocomposite, sensitivity.

PP-75

Crystal Growth, Structural, Vibrational, Optical, Thermal and Mechanical Properties of Semi Organic Piperazinium Tetrachlorozincate Monohydrate(PTCZ) Single Crystal for Nonlinear Optical Applications

M. Magesh^{1}, P. Karuppasamy¹, M. Senthil Pandian², P. Ramasamy³*

^aSaveetha Institute of Medical and technical Sciences, Chennai-602 117, Tamilnadu, India.

^bSSN Research Centre, SSN College of Engineering, Chennai-603 110, Tamilnadu, India

*Email: mage.radha@gmail.com

The semi-organic single crystals of piperazinium tetrachlorozincate monohydrate (PTCZ) were successfully grown by slow evaporation solution technique (SEST). The grown crystal was subjected to the single crystal XRD studies for confirming the cell parameters. The various functional groups of the grown crystal were confirmed by the FTIR analysis. The optical quality of the grown crystal was identified by the UV-Vis NIR spectral analysis and also calculated the optical band gap energy. The photoconductivity study discloses that the grown crystal has positive photoconductive nature. The thermal behavior of the PTCZ single crystal was investigated by thermogravimetric and differential thermal analysis (TG-DTA). The grown crystal was subjected to Vicker's micro hardness study and observed mechanical stability of grown crystal. The third-order nonlinear optical properties such as nonlinear refractive index (n_2), absorption co-efficient (β) and susceptibility ($\chi^{(3)}$) were studied by Z-scan technique using solid state laser (640 nm).

Keyword: Crystal growth, Single crystal X-ray diffraction, Optical transmittance, Photoconductivity, TG-DTA, Mechanical, Z-scan technique.

PP-76

Structural, Optical and Dielectrical Properties of Chalcone Derivative Crystal Grown by VASR Technique.

*N.Madhavan, S.A¹. Martin Britto Dhas*¹*

PG and Research Department of Physics, Sacred Heart College, Tirupattur- Vlr-Dt. 635681

*E-mail: martinbritto@shcpt.edu

Chalcone derivative crystal BMC were grown by Vacuum Assisted SR technique using acetone as a solvent. The grown crystal were subjected to various characterization studies like Powder XRD analysis to determine the crystalline nature and FTIR analysis to investigate the functional group present in the material. The optical properties like optical band gap, absorption coefficient, excitation coefficient, dielectric constant for real and imaginary part, electrical conductivity, optical conductivity, refractive index of the crystals were analyzed using UV-Vis spectrophotometer. Dielectrical analysis like dielectric constant, dielectric loss, resistivity, ac and dc conductivity etc was carried out at different temperatures like 30, 50 75 °C in the frequency ranging from 1 Hz – 10MHz. The temperature dependent dielectric parameters such as dielectric loss and dielectric constant decreases with increasing applied frequency. The results will be discussed during the conference.

Keywords: FTIR, UV-Vis, Dielectrical analysis, Chalcone crystal, etc.

PP-77

Correlation between Magnetization and Cell Volume in Mn²⁺ Substituted Copper Ferrite Nanocomposites

*M. Balaji**

Department of Physics, Sourashtra College, Madurai - 625 004, Tamil Nadu, India

Magnetic Mn_(1-x)Cu_(x)Fe₂O₄ (where $x = 0.0, 0.2, 0.4, 0.6, 0.8$ and 1.0) spinel ferrite nanocomposites were successfully synthesized by chemical co-precipitation method. The XRD patterns of all the prepared samples have the face centered cubic spinel ferrite structure. The average crystallite size is in the range between 18-20 nm. The room temperature magnetic (VSM) measurement confirms the superparamagnetic behavior of the samples, which depicts the nano crystalline nature. The saturation magnetization value increases with increase in concentration of copper ions. The crystallographic parameters were calculated by UNIT CELL software, which attributes the decrease in cell volume is the main contribution to enhance the magnetization value.

PP-78

**Growth of High Quality Organic Single Crystal by Rotational Sankaranarayanan–Ramasamy (Rsr)
– A Novel Method**

P. Karuppasamy,^{1} T. Kamalesh,¹ Muthu Senthil Pandian,¹ P. Ramasamy,¹ Sunil Verma,^{2,3}*

¹*SSN Research Centre, SSN College of Engineering, Chennai-603110, Tamil Nadu,*

²*Laser Materials Development and Devices Division, Raja Ramanna Centre for Advanced Technology (RRCAT), Department of Atomic Energy (DAE), Indore-452013, Madhya Pradesh,*

³*Homi Bhabha National Institute (HBNI), Anushakti Nagar, Mumbai - 400094, Maharashtra,*

*E-mail: karuppasamp75@gmail.com

The optically high quality 2-aminopyridinium 4-nitrophenolate 4-nitrophenol (2AP4N) single crystals have been grown by (i) Sankaranarayanan–Ramasamy (SR) method and (ii) Rotational Sankaranarayanan–Ramasamy (RSR) method. The effect of rotation on unidirectional crystal growth method (RSR) has been reported for the first time. The apparatus was specially designed and developed for the growth of high quality crystals by slow cooling under several rotational conditions. The high-quality crystals have been achieved under forced convection and the quality of the crystal is high compared to the crystals grown under free convection conditions. The crystal structure was analyzed by single crystal X-ray diffraction (SXRD) measurement. The grown crystal was subjected to the powder X-ray diffraction (PXRD) analysis to confirm the growth plane along (001) plane. The optical quality of the grown crystals has been analyzed by UV-Vis NIR spectrophotometer. It confirms that the grown crystal is highly transparent in the visible and near IR region. The photoluminescence behaviour was recorded in the wavelength region between 450 - 700 nm. The photoconductivity measurement was analysed and it has a positive photoconductivity nature. The grown crystal has less dislocation densities as confirmed by chemical etching analysis. The mechanical strength of the grown crystals was investigated by Vickers microhardness tester. The frequency dependent dielectric properties (permittivity and loss) of the crystals were carried out. The laser damage threshold (LDT) was measured for both SR and RSR method grown crystals. The full-width at half maximum (FWHM) of high-resolution X-ray diffraction (HRXRD) curves indicate that the RSR method grown crystal has high crystalline perfection. The results obtained from the SR and RSR method grown 2AP4N crystals were compared. The RSR method grown crystal has higher optical transparency, higher photoluminescence, higher photoconductivity, higher mechanical strength, higher laser damage threshold, higher crystalline perfection, less dislocation density, low dielectric loss and low full width at half maximum (FWHM). The second harmonic generation (SHG) of 2AP4N was analyzed by Kurtz-Perry powder technique. The SHG efficiency was found to be 4.5 times that of reference KDP material. The above studies reveal that the RSR method grown crystals are more useful for practical device applications.



SR and RSR method grown 2AP4N single crystals

Acknowledgement:

The authors gratefully acknowledge DAE-BRNS, Government of India for the financial support (Ref. no. 34/14/06/2016-BRNS/34032).

PP-79

Structural, Morphological and Mechanical Properties of Doped Chalcogenide Materials

*Karthikeyan R¹, Jeffrey Jose¹, Bibin John² and Kunjomana A G*¹
CHRIST (Deemed to be University), Department of Physics and Electronics, Bangalore-29*

*E-mail: kunjomana.ag@christuniversity.in

In the recent past, the growing demand for energy has created a need to investigate the harvesting of alternate sources as conventional natural resources are exhaustible. Solar energy harvesting undoubtedly is a major aspect of renewable energy. Compound semiconductor crystals have gained widespread attention as a credible substitute for silicon in terms of device applications owing to their excellent optical, mechanical, thermal and electrical properties. The IV-VI compound semiconductor family, especially chalcogenides has earned the interest of many researchers owing to their versatility and favorable properties. Doping is a convenient and easy method to enhance the properties of a compound. In this work, sulphur (S) doped tin monoselenide (SnSe) bulk crystals have been grown using vapour deposition method through an indigenously fabricated furnace. The specially designed quartz ampoules were cleaned thoroughly and the stoichiometric sample was filled followed by vacuum sealing to make sure that no other unwanted foreign elements were present and no undesirable oxidation occurred. The growth conditions were maintained systematically in order to achieve good quality crystals. The obtained samples were subjected to various characterization techniques to determine the structure, morphological and optical properties of the harvested crystals. SEM analysis revealed the sample to be free of defects. EDAX profiles shows that the grown samples were chemically pure and the presence of no other undesirable element was found. The harvested crystal has good mechanical stability which was investigated using the microhardness tester. The optical properties of the crystal was found using UV-Vis-NIR spectroscopy.

PP-80

A Role of Temperature on the Properties of Lanthanum Oxide Nanoparticles by Reflux Routes

*S. Karthikeyan¹, M. Selvapandiyan^{*1}*

Department of Physics, Periyar University PG Extension Centre, Dharmapuri -636701.

* E-mail: skarthiphysics@gmail.com

Recently young researchers are concentrating on the morphology controlled synthesis of La_2O_3 for their widespread application in the fields of semiconductors, photo diode, thermoelectric devices, super capacitors and etc. In this work, nanostructured La_2O_3 has been synthesized by reflux method. The band gap of the as-prepared and calcined samples as 5.7 eV and 5.8 eV respectively. The morphology and particle size of the calcined sample was slightly altered than that of as prepared sample was confirmed by scanning electron microscopy (SEM). The as-prepared and calcined products were characterized by X-ray diffraction (XRD) and it reveals that the prepared nanoparticles belong to the system of Hexagonal. Fourier transform infrared (FT-IR) was disclosed the presence functional groups and modes of vibrations in the prepared Lanthanum Oxide nanoparticles.

Key words: La_2O_3 nanoplates, Reflux method, Optical band gap.

PP-81

Growth, Optical and Laser Damage Threshold Properties Of 4-Dimethylaminopyridinium 4-Nitrophenolate 4-Nitrophenol (Dmapnp) For Nlo Applications

T. Kamalesh^{1}, P. Karuppasamy¹, Muthu Senthil Pandian¹, P. Ramasamy¹, Sunil Verma^{2,3}*

¹SSN Research Centre, SSN College of Engineering, Chennai-603110, Tamil Nadu.

²Laser Materials Development and Devices Division, RRCAT, Indore-452013, Madhya Pradesh.

³Homi Bhabha National Institute, Anushakti Nagar, Mumbai-400094, Maharashtra.

*E-mail: kamaleshkamal918@gmail.com

The optically transparent organic single crystals of 4-dimethylaminopyridinium 4-nitrophenolate 4-nitrophenol (DMAPNP) were grown by slow evaporation solution technique (SEST) using acetone as a solvent [1-2]. The cell parameters of the grown crystal were analyzed by single crystal X-ray diffraction (SXRD) analysis. Different type functional groups were confirmed by FTIR and FT-Raman analysis. Optical transmittance, band gap and cut-off wavelength of the DMAPNP crystal were determined by UV-Vis NIR spectral analysis. The photoconductivity studies reveal that the DMAPNP crystal has negative photoconductivity nature. The thermal stability of the DMAPNP crystal was carried out by thermogravimetric and differential thermal analysis (TG-DTA). The laser damage threshold (LDT) was studied for the DMAPNP crystal by using Nd: YAG laser (532 nm). The second harmonic generation (SHG) efficiency of DMAPNP crystal was measured by Kurtz-Perry powder technique.

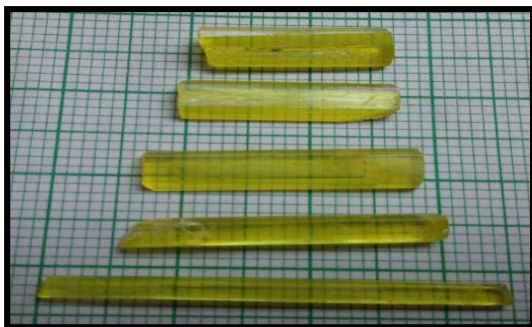


Figure 1. As grown DMAPNP crystal

References

- P. Srinivasan, T. Kanagasekaran, N. Vijayan, G. Bhagavannarayana, R. Gopalakrishnan and P. Ramasamy Opt. Mater, 30, 553 (2007).
C.C. Evans, M. B. Beucher, R. Masse and J. F Nicoud, Chem Mater, 10, 847(1998).

PP-82

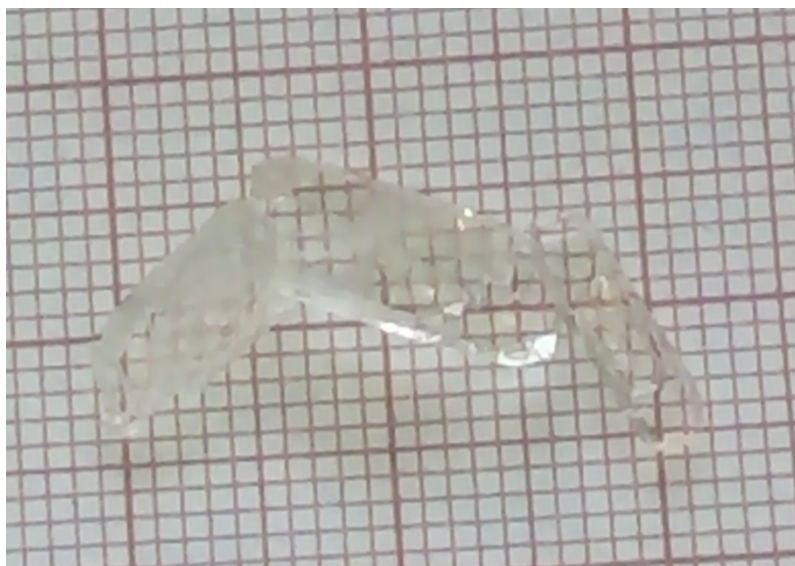
Crystal Growth and Characterization of 2-Amino 6-Methylpyridinium 3,4 Dimethoxybenzoate Organic Nonlinear Optical Single Crystal

R.Kaliammal^a, G.Parvathy^a, G.Maheswaran^a, S.Sudhakar^{a}*

^aDepartment of Physics, Alagappa University, Karaikudi-630003.

*E-mail: raveenarec@gmail.com

Organic nonlinear optical crystals of 2-amino 6-methylpyridinium 3,4 dimethoxybenzoate nonlinear optical single crystal were grown by slow evaporation solution growth technique using ethanol: distilled water as mixed solvent. The crystal structure, lattice parameters and crystalline perfection were confirmed by single crystal and powder X-ray diffraction analysis. The functional groups and chemical composition of grown 2ADMB crystal was confirmed by FTIR analysis. UV-Vis spectra study showed that grown crystal has high transparency in the entire visible region and the cut off wavelength at 320 nm. It exhibits the grown crystal suitable for NLO applications. PL spectra study of grown 2ADMB showed an intense emission peak at 360 nm for an excitation wavelength at 340 nm. The SHG technique confirms the nonlinear optical property of the grown crystal. The grown crystal of 2ADMB thermal analysis was also observed by TG-DTA analysis.



PP-83

Vibrational, NBO, Fukui Function, DOS, Thermodynamical and Molecular Docking Analyses of P-Chlorophenacyl Bromide Using Hartree Fock And B3LYP Methods

G. John James^{1,}, Senthilkumar Chandran², M. Arivazhagan¹*

¹Department of Physics, Government Arts College, Tiruchirappalli, Tamilnadu-620022

²Department of Physics, Research Centre, SSN College of Engineering, Kalavakkam, Chennai, Tamilnadu-603110

*E-mail: jamesgnanapragasam@gmail.com

The molecular structure of p-chlorophenacyl bromide was optimized using DFT/ B3LYP and Hartree Fock (HF) functions with 6-311+G(d,p) basis set. The P-CPB belongs to C_1 point group symmetry. The vibrational studies were carried out by FT-IR and FT-Raman and experimental values are compared with theoretical values. The whole vibrational assignments were done on the basis of potential energy distribution. The chemical shifts are computed from NMR analysis by Gauge-including atomic orbital approach. The electronic properties of the p-chlorophenacyl bromide were calculated based on the HOMO and LUMO energies. The hyper-conjugative interaction of the P-CPB was analyzed by NBO analysis. The first order hyperpolarizability of the title molecule was theoretically determined and it shows that the P-CPB has good NLO behavior. Molecular electrostatic potential shows the high positive and negative reactivity site of the molecule. Fukui functions and atomic charge are calculated. The electronic band structure of P-CPB was studied by density of states. The thermodynamics properties of the title molecule were computed in the gas phase. Inhibitory activity of P-CPB was confirmed by molecular docking analysis.

PP-84

N-hexylcarbazole donor substituted triphenylamine compound based sensitizers for dye sensitized solar cells application - theoretical investigation

*P. Pounraj¹, V. Mohankumar¹, M. Senthil Pandian², P. Ramasamy^{*1}*

SSN Research Centre, SSN College of Engineering, Chennai - 603 110, Tamil Nadu, India

*E-mail: ramasamyp@ssn.edu.in,

Triphenylamine donor based dyes are investigated theoretically as potential sensitizer for dye sensitized solar cell (DSSC). Thiophene and cyanovinyl groups are used as π -spacers with different configuration. Cyanoacrylic acid is used as an anchoring group and all the dyes are bi-anchored dyes. N-hexylcarbazole donor group is substituted in the third para position, leads to D-D-(π -A)₂ structure. The eight N-hexylcarbazole donor substituted triphenylamine based dyes are designed with different π -spacers configuration for the dye in DSSC application. The optimized molecular structure, minimum energy, dipole moment and polarizability of the dye structure were computed using Density functional theory (DFT). The vertical electron excitation energy, maximum absorption wavelength, oscillator strength, light harvesting efficiency and free energy changes for electron injection and dye regeneration of the dyes are predicted by the Time Dependent Density Functional Theory (TD-DFT) calculations. Increasing the conjugation length by the addition of π -spacers in the D-D-(π -A)₂ dyes resulted in narrow bandgap, higher molar extinction coefficient, red-shift in the absorption spectra, intramolecular charge transfer and increase in Light Harvesting Efficiency. Also the different π -spacers configuration affects the electronic and optical property of the dyes. Hence, this study confirms that N-Hexylcarbazole donor substituted triphenylamine compound based dye can be used as a photosensitizer for DSSC applications.

PP-85

Synthesis and Characterization of Ni_{0.5-x} Mg_xCu_{0.5} Fe₂O₄ Sintered Spinel Ferrite System

J.Jeyabunaveswari¹, Dr. S.Aravazhi^{}*

¹Assistant professor in physics, CK College of engineering & technology, Cuddalore.

² professor in physics, St. Joseph's college of Arts and Science, Cuddalore.

*E-mail: jeyabunaveswari@gmail.com

A new class of ferrites are attracted considerable attention in the recent years Several workers have since investigated the Ni_{0.5-x} Mg_xCu_{0.5} Fe₂O₄ system . The sample of Ni_{0.5-x} Mg_xCu_{0.5} Fe₂O₄ system was synthesized by doping Mg²⁺ ions in some of the sites of Ni²⁺ ions in Ni-Cu mixed ferrite system and analyze the porosity, molecular density and particle size. Synthesis of the compound Ni_{0.5-x} Mg_xCu_{0.5} Fe₂O₄ (x=0.0-0.5) was attempted by sintering the sample at 1100° C for 20 hrs resulting the formation of Ni_{0.5-x} Mg_xCu_{0.5} Fe₂O₄ Sintered Spinel Ferrite System. Characterization was done by x-ray diffraction. Results suggest that the samples were well prepared under ideal conditions ,from low value of % of porosity it can be depicted that the samples have well compaction. From the decreasing trend of lattice constant with concentration (x) it can presume that the Mg²⁺ ions exactly goes in to the lattice site

PP-86

Growth, Spectral, Optical, Thermal, Dielectric And Mechanical Studies On Urea Potassium Iodide Single Crystal

Hareeshkumar M. R.¹, Jagadeesh M. R.², G. J. Shankaramurthy^{3,}*

¹*Department of Physics, GM Institute of Technology, Davangere-577 006, India*

²*Department of Physics, Jain Institute of Technology, Davangere-577 003, India*

³*Department of Physics, UBDTCE College, Davangere-577 004, India*

*E-mail address: hari.melgiri@gmail.com

Single crystals of urea potassium iodide (UPI) have been grown from aqueous solution by slow evaporation method up to a dimension of 12x12x3 mm³ over a period of 25-30 days. Characterizations were carried out to study the structural, optical, thermal, mechanical, dielectric properties of the grown crystals. The structural study was carried out by powder XRD. The vibrational frequencies of various functional groups have been derived from Fourier transform infrared (FTIR) spectrum. Thermal stability of the grown crystal was investigated by TG-DTA analyses. The thermogram reveals that the grown crystal has very good thermal stability. Optical absorption studies have been carried out and a good transparency in the UV-Visible region is observed with the lower cutoff wavelength of 335 nm. Dielectric study was carried out as a function of frequency and the normal dielectric behavior was observed. The Vickers microhardness test was carried out to study the mechanical properties of the grown crystal.

Keywords: Urea Potassium Iodide, UV, TG-DTA, Dielectric, Microhardness

PP-87

Growth and Characterization of Cadmium Doped Zinc Tris Thiourea Sulphate Crystal (Cd-ZTSC) by Gel Growth Technique

H. K. Gohil^{*1}, S. K. Parmar², A. R. Zinzuvadia³, P. M. Vyas⁴ and A. H. Patel⁴

¹*Kalpiti Vinay Mandir, Lathi – 365430, Gujarat, India*

²*Sarkari Madhyamik Shala, Kadbal, Jamjodhpur – 360530, Gujarat, India.*

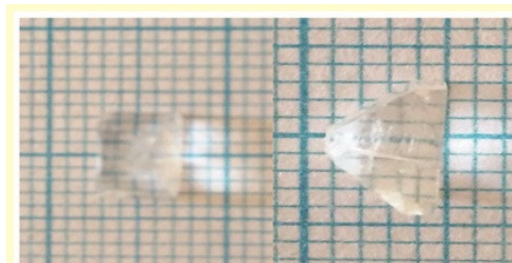
³*Kamalshi High School, Babra-36542,1 Gujarat, India*

⁴*Physics Department, Kamani Science & Prataprai Arts College, Amreli – 365601, Gujarat, India*

*E-mail: hkgohilphysics@yahoo.com

Zinc Tris (Thourea) Sulfate (ZTS) is well known non-linear optical crystal which combines both organic and inorganic materials. ZTS crystals frequently grown by solution growth method and many more but very few try has been take place to grow this crystal by using single diffusion gel growth technique. Cadmium is well known for its electrical properties and Photovoltaic Devices Properties. Cadmium doped zinc tris thiourea sulphate crystals (Cd-ZTSC) were transparent and colorless. Powder XRD of Cd-ZTSC confirms the crystalline nature of the material. Cd-ZTSC crystals shows orthorhombic crystalline systems with unit cell parameters $a = 11.126 \text{ \AA}$, $b = 7.773 \text{ \AA}$ and $c = 15.491 \text{ \AA}$. FT-IR shows

the presence of O-H Stretching, N-H Stretching, C=C Stretching, O-H Stretching, C=C Stretching, Metal-Oxygen Bonding bonds. Thermal studies shows that the crystal remains stable up to 210°C. Dielectric studies shows that as the frequency increases dielectric constant decreases.



PP-88

Identification of novel NAD (P) H dehydrogenase [Quinone] 1 antagonist using computational approaches

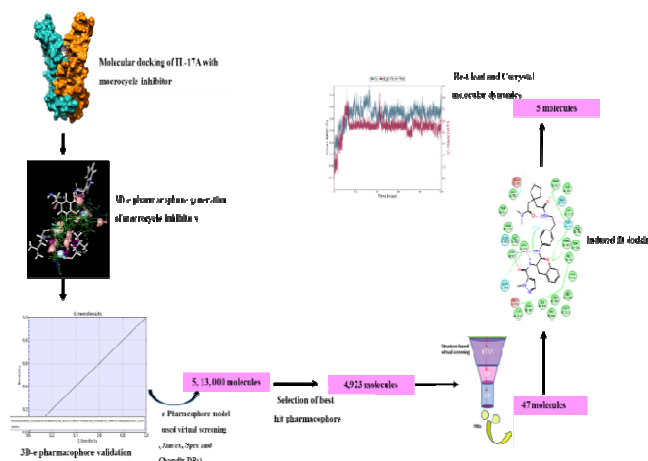
Anantha Krishnan Dhanabalan^a, Rajendran Selvakumar^a, Devadasan Velmurugan^a and Krishnasamy Gunasekaran^{a,b*}

^aCAS in Crystallography and Biophysics, University of Madras, Guindy Campus, Chennai-600025, Tamilnadu, India.

^bBioinformatics Infrastructure Facility, University of Madras, Guindy Campus, Chennai-600025, Tamilnadu, India.

*E-Mail: krishavc92@gmail.com

NAD (P) H: quinone oxidoreductase 1 (NQO1) inhibitors are proved as promising therapeutic agents against cancer. This study is to determine potent NAD (P) H dependent NQO1 inhibitors with new scaffold. Pharmacophore-based 3D QSAR model has been built based on 45 NQO1 inhibitors reported in the literature. The structure-function correlation coefficient graph represents the relationship between phase activity and phase predicted activity for training and test sets. A QSAR model statistics shows the excellent correlation of the generated model. Pharmacophore hypothesis (AARR) yielded a statistically significant 3D QSASR model with a correlation coefficient of $r^2 = 0.99$ as well as an excellent predictive power. From the analysis of pharmacophore-based virtual screening using by SPEC database, 4093 hits were obtained and were further filtered using virtual screening filters (HTVS, SP, XP) through structure based molecular docking. Based on glide energy and docking score, seven lead compounds show better binding affinity compared to the co-crystal inhibitor. The results of Induced Fit Docking and Prime/MM-GBSA suggest that leads AN-153/J117103 and AT-138/KB09997 binding with the catalytic site. Further, to understanding the stability of identified lead compounds MD simulations were done. The lead AN-153/J117103 showed the strong binding stable of the protein-ligand complex. Also the computed drug likeness reveals potential of this compound to treat cancer.



Reference:

Ahmed Atia, Nadia Alrawaiq, A. A. (2014). A Review of NAD(P)H:Quinone Oxidoreductase 1 (NQO1); A Multifunctional Antioxidant Enzyme. *Journal of Applied Pharmaceutical Science*. <http://doi.org/10.7324/JAPS.2014.41220>

Arora, R., Issar, U., & Kakkar, R. (2018). Identification of novel urease inhibitors: pharmacophore modeling, virtual screening and molecular docking studies. *Journal of Biomolecular Structure and Dynamics*, 1–15. <http://doi.org/10.1080/07391102.2018.1546620>.

PP-89

Identification of Novel inhibitors for BACE1 using Pharmacophore based Virtual screening and Molecular Dynamics

Anantha Krishnan^{1*}, Manish Keshrwani², Krishnasamy Gunasekaran^{1, 2}
Devadasan Velmurugan²

¹ Bioinformatics Infrastructure Facility (BIF), University of Madras, Chennai-25

² CAS in Crystallography and Biophysics, University of Madras, Chennai-25

*Email id:krishavc92@gmail.com

The inhibition of β -Secretase (BACE1) has become a promising target for the treatment of Alzheimer’s disease (AD). Availability of BACE1 crystal structures in both Apo and complexed forms enables to find structure-based BACE1 inhibitors for AD. In order to understand the binding mechanism and structure–activity correlation of amidine containing BACE1 inhibitors, a combined molecular docking, pharmacophore and 3D-QSAR studies have been carried out with 34 amidine derivatives to develop a pharmacophore model. Pharmacophore based virtual screening (VS) has been performed against BACE1 (PDB ID: 4GMI), using three chemical databases (CoCoCo, Enamine, Zinc), which yielded 6000 hit list compounds. These compounds were further analyzed using structure based docking in hierarchical filtering approaches of Glide such as HTVS, SP and XP precision modes. The docking studies show the binding orientations of the inhibitors at active site amino acid residues of β -Secretase. Results from glide XP docking and induced fit docking showed that two compounds (Lead 1 and Lead 2) have good interactions with the target protein in comparison with co-crystal (MV078571 BACE inhibitor).

Further, molecular dynamics simulation has been carried out for these lead compounds to understand the stability and binding free energetics. The present study is thus a pharmacophore based screening followed by molecular dynamics which identified two new inhibitors in prospect of drug design for Alzheimer disease.

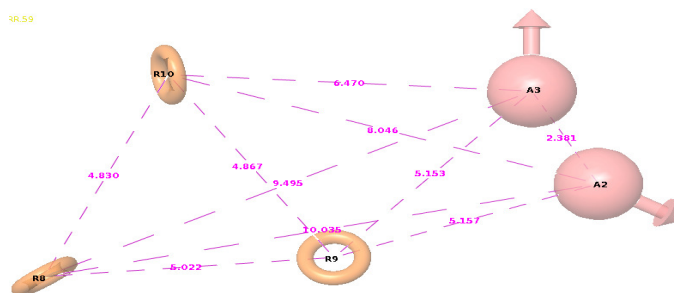


Figure: Convincing Pharmacophore Hypothesis (AARRR) with distance

PP-90

Investigation on 2-Methyl-5-(propan-2-yl) phenol an anticancer drug by Spectroscopic, *in vivo* and Molecular Docking Studies

M.Govindammal^{1*}, M.Prasath^{1*}, S.Kamaraj²

[#]Department of Physics, Periyar University PG Extension Centre, Dharmapuri-636701

[@]Department of Biotechnology, Periyar University PG Extension Centre, Dharmapuri-636701

*E-mail id: malathiphy3@gmail.com

The molecule 2-Methyl-5-(propan-2-yl) phenol (carvacrol) was optimized utilizing density functional theory (DFT) with B3LYP/6-311G(d,p) basis set. The vibrational frequencies and potential energy distribution (PED)% of carvacrol molecule were computed and it shows good agreement with experimental values. The reactivity nature of the molecule was analysed with various DFT methods such as local reactivity descriptors, Molecular Electrostatic Potential (MEP), Frontier Molecular orbitals (FMOs). Drug likeness and ADMET properties were analysed for the prediction of pharmacokinetic properties like Absorption, Distribution, Metabolism, Excretion and Toxicity. The molecular docking analysis reveals that inhibitory nature of the carvacrol molecule. Various signalling pathways are regulating the anti-cancer progression including PI3K/AKT. Interrupt this signalling pathway could be helps to discover the new drug derivatives. Hence, the present study reports the structural details, intermolecular interactions of PI3K and carvacrol, and also the toxicity study (*in vivo*) was analysed by inhibition of human lung cancer cells (A549) proliferation.

Keywords: anti-cancer, Molecular docking, Fukui function, carvacrol and PI3K/AKT.

PP-91

Growth and Characterization of Cadmium Doped Zinc Tris Thiourea Sulphate Crystal (Cd-ZTSC) by Gel Growth Technique

*H. K. Gohil^{*1}, S. K. Parmar², A. R. Zinzuvadia³, P. M. Vyas⁴ and A. H. Patel⁴*

¹ *Kalapi Vinay Mandir, Lathi – 365430, Gujarat, India*

² *Sarkari Madhyamik Shala, Kadbal, Jamjodhpur – 360530, Gujarat, India.*

³ *Kamalshi High School, Babra-36542,1 Gujarat, India*

⁴ *Physics Department, Kamani Science & Prataprai Arts College, Amreli – 365601, Gujarat, India*

*E-mail: hkgohilphysics@yahoo.com

Zinc Tris (Thiourea) Sulfate (ZTS) is well known non-linear optical crystal which combines both organic and inorganic materials. ZTS crystals frequently grown by solution growth method and many more but very few try has been take place to grow this crystal by using single diffusion gel growth technique. Cadmium is well known for its electrical properties and Photovoltaic Devices Properties. Cadmium doped zinc tris thiourea sulphate crystals (Cd-ZTSC) were transparent and colorless. Powder XRD of Cd-ZTSC confirms the crystalline nature of the material. Cd-ZTSC crystals shows orthorhombic crystalline systems with unit cell parameters $a = 11.126 \text{ \AA}$, $b = 7.773 \text{ \AA}$ and $c = 15.491 \text{ \AA}$. FT-IR shows the presence of O-H Stretching, N-H Stretching, C=C Stretching, O-H Stretching, C=C Stretching, Metal-Oxygen Bonding bonds. Thermal studies shows that the crystal remains stable up to 210°C. Dielectric studies shows that as the frequency increases dielectric constant decreases.

PP-92

Studies on Growth, Optical and Mechanical Properties of Semi-Organic Crystal – Bis (Thiosemicarbazide-S, N) Zinc (II) Dinitrate

*Redrothu Hanumantharao¹, S.Kalainathan^{*1}*

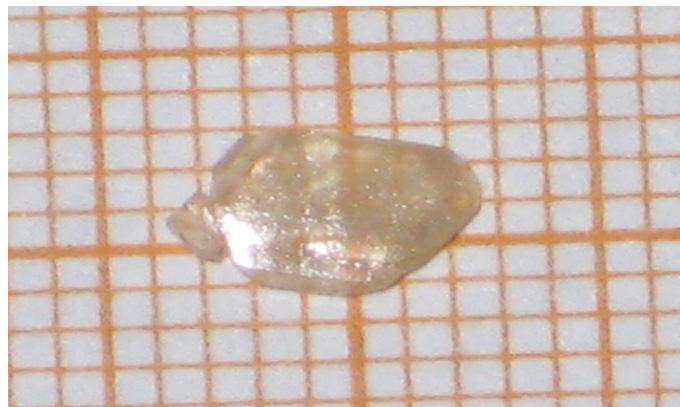
^a *Vignan Institute of Information Technology (VIIT), Visakhapatnam, Andhra Pradesh*

^b *Crystal research center, VIT University, Vellore, Tamilnadu – 632014, India*

*E-mail: skalainathan@gmail.com

Single crystals of Bis (thiosemicarbazide-S, N) zinc (II) dinitrate (BTZDN), a semi organic crystal, have been grown by slow solvent evaporation technique. Solubility studies are done for BTZDN crystal in the range of 30–50 ° C .The grown crystal has been characterized by Single crystal XRD, TGA-DTA and UV-Vis-NIR spectral analysis .Single crystal XRD revealed that material crystallized in monoclinic crystal system with space group $C2/c$. UV-Vis-NIR studies reveal that materials show good transmittance in visible region. Measuring transmittance of BTZDN permitted the calculation of the extinction coefficient K , Reflectance R as functions of photon energy. The optical band gap of BTZDN is 5.274 eV. Micro hardness studies were carried out on the grown crystal surface in the load range of 10-50 g.

Keywords: Organometallic compounds, crystal growth



PP-93

Synthesis, Spectral, DFT Studies on inorganic-organic hybrid material: Tetrabromo (piperazinium) zincate (II) (TBPZ)

K. Boopathi*¹, K. Muthu Krishnan¹, K.R.Aranganayam², P.Ramsamy³

¹Department of Inorganic Chemistry, School of Chemical Science, University of Madras (Guindy Campus), Chennai-600025

²Department of Chemistry, Kumaraguru College of Technology, Coimbatore- 641049

³SSN Research Centre, SSN College of Engineering, Kalavakkam-600 110

*E-mail: boopathi.chemist@gmail.com

A new inorganic-organic hybrid nonlinear optical crystal tetrabromo (piperazinium) zincate has been synthesized and its single crystal was grown by slow evaporation method. The grown crystal has been characterized by structural, spectral, density functional theory studies and nonlinear optical properties. Single crystal X-ray diffractions study reveals that grown crystal belongs to orthorhombic crystal system with space group $P2_12_12_1$. The H^1 and C^{13} NMR spectra was recorded to establish molecular structure of the compound. The presence of various vibration modes and functional groups in the synthesized compound was confirmed by FT-IR spectral analysis. In order to understand, Quantum chemical calculations DFT studies have been carried out (DFT) employing B3LYP functional, LanL2DZ as the basis set with the help of Gaussian 09W to optimize geometrical model, HOMO-LUMO calculations, first-order hyperpolarizability, and electrostatic potential calculations. The second order harmonic generation efficiency was measured using Kurtz and Perry technique and it was found to be 1.5 times that of KDP.

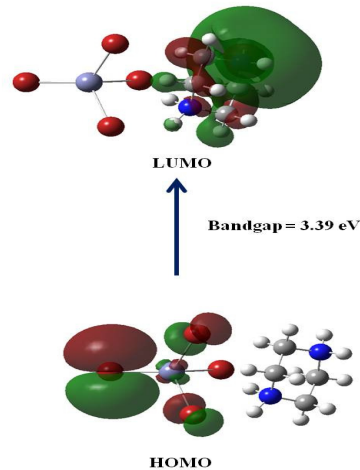


Fig.1. Frontier molecular orbitals (HOMO-LUMO) of TBPZ

PP-94

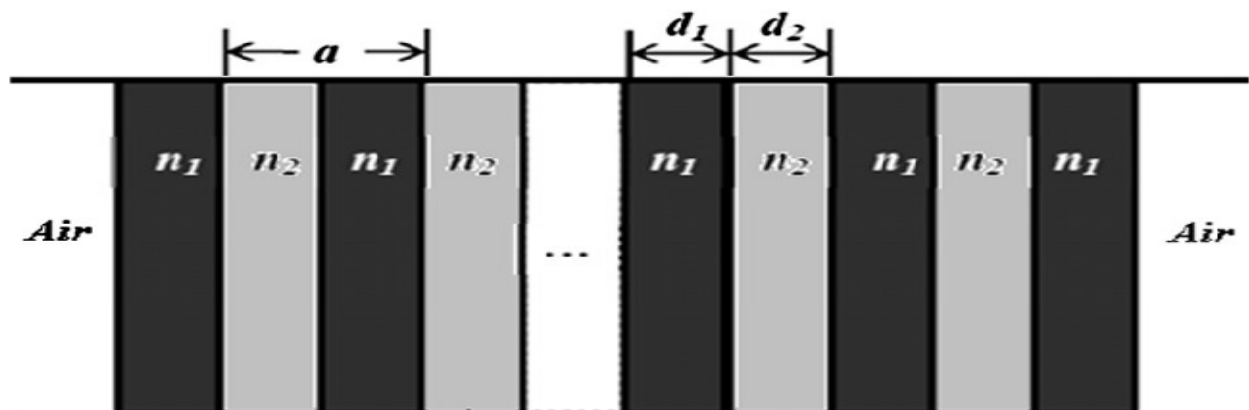
The Effect of Angle Of Incidence on Photonic Band Gap in Lithium Niobate with Silver Composite Based One Dimensional Photonic Crystal

*V.Doni Pon, K.S.Joseph Wilson**

Arul Anandar College, karumathur, Madurai, India-625514

*E-mail: wilsonpra@yahoo.co.in

The effect of angle of incidence on photonic band gaps (PBG) in a metal nanocomposite based one dimensional photonic crystal consisting of alternate layers of $\text{LiNbO}_3\text{-Ag}$ and air has been investigated. The PBG can be tuned by varying the radius of the geometry and by changing the angle of incidence. The propagation characteristics of the proposed structure are analyzed using transfer matrix method. It is found that PBG remains constant in a particular frequency region and also it is shifted to the higher frequency region with the angle of incidence.



PP-95

Studies on the Growth and Characterization of Organic 2-Amino-5-Nitropyridinium Dichloroacetate Non Linear Optical Single Crystal

David Willington T^a, Joema S E^b

^aDepartment of Physics, Nesamony Memorial Christian College, Manonmaniam Sundaranar University, Abishekapatti, Tirunelveli 627 012, Tamilnadu, India.

^bDepartment of Physics, Nesamony Memorial Christian College, Manonmaniam Sundaranar University, Abishekapatti, Tirunelveli 627 012, Tamilnadu, India.

*Email : david.willy00@gmail.com

Noncentrosymmetric organic non linear optical single crystals of 2-Amino-5-nitropyridinium Dichloroacetate (2A5NPDCA) was grown by slow evaporation technique at room temperature. The grown crystal structure was confirmed by Single Crystal X-ray diffraction analysis and it is revealed that the grown crystal crystallized in orthorhombic crystal system with space group P_{212121} . The various functional groups present in the grown crystal were confirmed by FTIR analysis. The transmittance ability of the grown crystal was studied by UV-Visible Spectral analysis. The non linear optical property of the grown 2A5NPDCA single crystals was confirmed by Kurtz Perry powder technique. The thermal stability of the synthesized material was analyzed by using TG/DTA studies. The mechanical strength, Meyer index, Yield strength and elastic stiffness of 2A5NPDCA were studied by using Vickers microhardness test.

Key words: crystal structure, FTIR, thermal stability, mechanical strength.

Reference

- 1.Chemla D S, J Nonlinear optical properties of Organic molecule and Crystals, Academic, NewYork, 1987.
- 2.Kumari R, Ramamurthi K, Vasuki.G, Bohai M.Y, Bhagavannarayana G, Spectrochim Act A, 2010, 76, 369-375.
- 3.Vijayan N, Ramesh Babu R, Guna Sekaran M, Gopala Krishnan R, Ramaswamy PT, J Cry. Growth, 2003, 256, 174-182.
4. Yvette Le Fur, Muriel Bagieu-Beucher, Rene Masse, Jean-Francois Nicoud, Jean-Pierre Levy, Chem. Mater. 1996, 8, 68-75.

PP-96

Enhanced Sensitivity of Cu-Mn Ferrite Gas Sensor By Incorporating SnO₂ Nanocomposites Towards Carbon Dioxide and Oxygen

M. Balaji^{1,*}, R. Daphine², T.R.K. Priyadarzini²

¹ Department of Physics, Sourashtra College, Madurai - 625 004, Tamil Nadu, India

² Department of Physics, The American College, Madurai – 625 002, Tamil Nadu, India.

*E-mail: balajimsu@gmail.com

SnO₂ combined Mn_(1-X)Cu_(X)Fe₂O₄ (X = 0, 0.5 and 1.0) nanocomposites are synthesized with equal weight percentages by co-precipitation method. XRD analysis of prepared samples confirmed the mixed spinel cubic polycrystalline nature of ferrites. Likewise the pure SnO₂ shows a tetragonal phase. Increase in crystallite size and decrease in strain value are found with the addition of SnO₂. From the morphological analysis ferrite sample shows agglomerated particle nature and the spherical particles are embedded on the surface due to the size and surface defect. In addition, the SnO₂ on Cu-Mn ferrite leads to increase in the particle size and dilute the magnetic property of the ferrite materials significantly. The sensitivity values of the gas sensor increases with the addition of SnO₂ in MnFe₂O₄ and Mn_{0.5}Cu_{0.5}Fe₂O₄ against Oxygen and Carbon dioxide. Whereas, SnO₂ - CuFe₂O₄ shows a weak sensitivity compare to its individual Cu-ferrite. The present study indicates that SnO₂-MnFe₂O₄ and SnO₂-Mn_{0.5}Cu_{0.5}Fe₂O₄ are highly sensitive to test gases, which corroborates that adsorbed/chemisorbed oxygen or surface lattice oxygen atoms plays a dominant role for the complete oxidation of molecule.

PP-97

Investigation of Anticorrosive and Antibacterial Efficacy of Copper Substituted Hydroxyapatite/Functionalized Multiwalled Carbon Nanotube Nanocomposite Fabricated 316L Stainless Steel

D. Sivaraj and K. Vijayalakshmi

Research Department of Physics, Bishop Heber College, Tiruchirappalli-17, Tamil Nadu, India.

Copper substituted hydroxyapatite/f-MWCNT nanocomposite were fabricated on 316L stainless steel (SS) implant by chemical spray pyrolysis technique. The fabricated film was characterized by Fourier transform infrared spectroscopy, powder X-ray diffraction, scanning electron microscopy and energy dispersive X-ray spectroscopy analysis. The results showed that pure and Cu substituted samples are in crystalline nature without any discernible crystalline impurity. Antimicrobial studies have demonstrated that all Cu-doped sample exhibit excellent antimicrobial activity in vitro against pathogens. FESEM micrographs of Cu doped sample showed reduced porosity with dense nature that Potentiodynamic polarisation test showed that the Cu-doped coating provided good barrier characteristics and achieved superior corrosion protection for 316L SS implant than hydroxyapatite/f-MWCNT nanocomposite coating.

Key Words: Hydroxyapatite, 316L stainless steel, Corrosion resistance, antimicrobial activity

Keyword: Hydroxyapatite; Bioactive: f-MWCNT; Corrosion resistance;

PP-98

Growth, Structural, Vibrational Analysis, Hirshfeld Surfaces, Quantum Chemical Studies, Uv-Vis Nir And Photoconductivity Studies Of The P- Toluidine P- Toluenesulfonate Single Crystal

S. Chinnasami¹, M. Manikandan¹, Senthilkumar Chandran², Rajesh Paulraj^{2*}, P. Ramasamy³

Centre for Crystal Growth, Department of Physics, SSN College of Engineering, Kalavakkam, Tamilnadu, India-603 110.

*E-mail: rajeshp@ssn.edu.in

A single crystal of p-toluidine p-toluenesulfonate (PTPT) has been grown by slow evaporation solution technique (SEST) at room temperature. Single crystal X-ray analysis confirms that grown crystal belongs to the monoclinic structure with space group P21 [1]. Intermolecular interactions and fingerprint plots of PTPT molecules are executed by Hirshfeld surface analysis. Quantum chemical calculations of the title compound (PTPT) were carried out using density functional theory (DFT) with Becke-3-Lee-Yang-Parr (B3LYP) functional combined with standard 6-311G(d,p) basis set using GAUSSIAN 09W program package without any constraint on the geometry. The characteristic absorption band occurs at below 290 nm. The functional groups were identified using FTIR and FT-Raman analyses and compared with theoretical values. The title molecule contains fourteen C–H bonds and three O–H bonds. The calculated HOMO and LUMO energy values are -6.125 eV and -1.157 eV, respectively [2]. The strongest interaction energy is calculated for the electron donating from the bonding to antibonding ($\sigma \rightarrow \sigma^*$) interaction, which is σ (N20 - C21) \rightarrow σ^* (N20 - O18) with the stabilization energy of 357.91 kcal mol⁻¹ [2]. First hyperpolarizability value of PTPT was found to be 12.5 times that of urea molecule. Photoconductivity studies have been done for the grown crystal. It is observed that the dark current is greater than photocurrent. It shows negative photoconductivity nature of PTPT crystal. The etching analysis was executed on (0 0 1) plane of PTPT crystal. It has rectangular shape etch pits patterns.

References

- R. Xu, 4-Methylanilinium p-toluenesulfonate. *Acta Cryst.* **2010**, 66, o1794.
S. Chinnasami, M. Manikandan, Senthilkumar Chandran, Rajesh Paulraj*, P. Ramasamy. *Spectrochimica Acta A.* **2019**, 206, 340-349.

PP-99

Structural and Optical Properties of Zn Doped TiO₂ Prepared by Sol-Gel Technique: For Photocatalysis and Dye Sensitized Solar Cell (DSSC) Applications.

B. Manikandan, K.R Murali and Rita John

Department of Theoretical Physics, University of Madras, Chennai-600 025.

*E-mail: ritajohn.r@gmail.com

In this work Zn doped TiO₂ nanoparticles were synthesized by the sol gel method. The prepared nanoparticles were characterized by X-ray diffraction (XRD), Fourier transform infrared spectroscopy (FTIR), UV-Visible spectroscopy (UV-Vis). The crystallite size was estimated using Scherrer formula. Micro strain, stress, energy density and crystallite size were analysed using Williamson-Hall model (W-H). The FTIR spectrum shows the characteristic bands of TiO₂ and the characteristic band of Zn-O were found with increasing Zn concentration. The absorption and optical band gap were obtained from UV-Visible spectroscopy. The prepared Zn doped TiO₂ shows excellent activity for photodegradation of methylene blue dye under UV light illumination, and enhanced current conversion efficiency in dye sensitized solar cells (DSSC).

Keywords: TiO₂; Anatase; Sol-Gel; XRD; FTIR; UV-Visible; W-H model; DSSC; Photocatalysis

PP-100

Suitability of Drinking Ground Water Using Water Quality Index

Dr.B.Kavitha¹ and Dr.S.Akilandeswari²

1.Lecturer in physics, Government Polytechnic College, Trichy-22.

2.Assistant professor, Department of physics, Govt.Arts and science college for women(Autonomous), Kumbakonam.

*Email: kavitharamadoss@gmail.com

Water is essential to sustain life of human beings and also living things. The human body loses about four litres of water every day. So it is necessary to replace their volume by drinking the water every day. Alternate in physical, chemical and biological characteristics of water may cause harmful effects on human and aquatic biota. Ground water samples were collected in ten different locations in and around Coimbatore. Physico chemical parameters for the collected were calculated and tabulated. The suitability of drinking ground water can be estimated by calculating water quality index. The results suggested that proper corrective measures should be taken for water samples to make the water suitable for drinking purposes.

Keywords: Ground water, water quality index, Coimbatore.

PP-101

DFT & TD-DFT Studies on 2,2'-Bipyridine-4,4'-Dicarboxylic Acid: Dye Sensitizers Solar Cell

B. Amudhavalli¹, M. Prasath^{1} and P. Srinivasan²*

¹ Department of Physics, Periyar University PG-Extension Centre, Dharmapuri- 636 705

² PG & Research Department of Physics, Chikkaiah Naicker College, Erode, India

*E-mail: sanprasath2006@gmail.com

Molecular geometries, electronic structures, and charge density were investigated using HF and density functional theory (DFT) at the 6-311G (d,p) levels for 2,2'-Bipyridine-4,4'-dicarboxylic Acid (BPDA) by gas phase method. The molecule exhibits C_1 chemical symmetry. Optimized geometrical parameters of the BPDA molecule have been calculated and compared with different methods. The electron densities at the bond critical point (BCP) of aromatic $C_{ar}-C_{ar}$ bonds are much stronger than the other bonds in the molecule. The calculated HOMO and LUMO energies show that charge transfer occurs within the molecule. The HOMO-LUMO gap calculated from quantum chemical calculations has been compared with the value calculated from the density of states. The MEP map shows that the negative potential sites are on electronegative atoms while the positive potential sites are around the hydrogen atoms. The results of this work suggest that 2,2'-Bipyridine-4,4'-dicarboxylic Acid (BPDA) based complexes might be effective sensitizers for next-generation dye-sensitized solar cells.

Keywords: DSSC, DFT, TD-DFT, HOMO-LUMO gap and Electron density

PP-102

Vibrational Spectroscopic Studies and Computational Study of 2,4-diamino-6-methyl-1,3,5-triazin-1-ium levulinate

K.Ayisha Begam^a, N.Kanagathara^{b}, G.Anbalagan^c, M.K.Marchewka^d*

^a *Department of Physics, Saveetha Engineering College, Thandalam, Chennai 602 105*

^b *Department of Physics, Saveetha School of Engineering, Saveetha Institute of Medical and Technical Sciences, Thandalam, Chennai 602 105, India*

^c *Department of Nuclear Physics, University of Madras, Guindy Campus, Chennai 600 025,*

^d *Institute of Low Temperature and Structure Research, Polish Academy of Sciences, 50-950 Wrocław, 2, P.O. Box 937, Poland.*

*E-mail: kanagathara23275@gmail.com

Crystals of 2,4-diamino-6-methyl-1,3,5-triazin-1-ium 4-levulinate crystallizes in monoclinic system with space group $P2_1/n$. The lattice parameters are calculated to be $a = 7.6580(11) \text{ \AA}$, $b = 17.598(2) \text{ \AA}$, $c = 10.8428(16) \text{ \AA}$, $V = 1370.6(3) \text{ \AA}^3$ and $Z = 4$. The geometrical parameters of the title compound are in agreement with XRD crystal structure data. The FT-IR and FT Raman spectrum of 2,4-diamino-6-methyl-1,3,5-triazin-1-ium levulinate was recorded and analyzed. The vibrational wavenumbers were computed using B3LYP/6-311++G(d,p) basis set. The data obtained from vibrational wavenumber calculations with potential energy distribution analysis are used to assign vibrational bands obtained in infrared and FT Raman spectroscopy of the studied molecule. Intense hydrogen-bonded network is present in the crystal structure of the complex with noticeable vibrational effects.

Keywords: DFT; FT-IR; FT Raman; XRD

PP-103

Growth, spectral, linear and nonlinear optical studies of a new Nitrophenol complex crystal

*R. Durgadevi and T. Arumanayagam**

PG and Research department of Physics, Pachaiyappa's College, Chennai-30.

*E-mail: arumai.tr@gmail.com

The Nonlinear optics single crystal of methenamine and 4-nitrophenol were synthesized and grown by the slow evaporation method from a mixture of methanol-water solvents in the ratio 1:1. The cell parameters of grown crystal were calculated by single crystal X-ray diffraction analysis. The FTIR spectral studies revealed that the presence of various vibration functional groups and mode of vibrations of the grown crystal. The Uv-vis spectrum shows that the crystal has highly transparent from 450 to 1100

nm. This extended transmission window will enable higher harmonic generation and wavelength extension by cascaded frequency conversion process. The optical band gap value of the HMPNP single crystal is 2.7 eV. The relative second harmonic generation efficiency of the HMPNP Crystal was found to be 2.3 times larger than that of reference urea crystal and the results were discussed in detail.

References:

- [1] Williams D J 1983 Nonlinear Optical Properties of Organic and Polymeric Materials (Washington: ACS)
- [2] Trask A V, Motherwell W D S and Jones W 2005 Cryst. Growth. Des. 5 1013
- [3] L.N. ang, X.Q.Wang, G.H.Zhang, X.T.Liu, Z.H.Sun, G.H.Sun, L.Wang , W.T.Yu, D.Xu, J. Cryst. Growth, **2011**, 327, 133-139.

PP-104

Magneto-transport studies on p-type $\text{Sb}_2\text{Te}_2\text{Se}$ Topological Insulators

Gopi Govindhan and Anandha babu Govindan

Department of Physics, SSN College of Engineering, Kalavakkam, Tamilnadu – 603110

**Email: anandcgc@gmail.com*

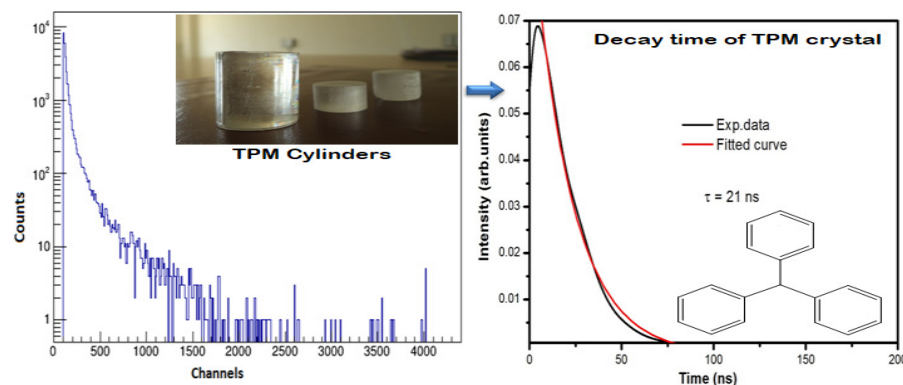
We report the magneto-transport characteristic of the metallic, *p*-type $\text{Sb}_2\text{Te}_2\text{Se}$ topological insulator (TI). Ternary chalcogenide TI system $\text{Sb}_2\text{Te}_2\text{Se}$ is unusual because it has a large bulk resistivity. A metallic behavior was observed in a recorded temperature dependent electrical resistivity $\rho(T)$ ranges from 300-0 K. The sample shows a high non-saturating magnetoresistance (MR) response. The magneto-conductance in low magnetic fields shows a cusp nature due to the WAL effect. In addition, Shubnikov-de Haas (SdH) oscillations observed in magnetoresistance (MR) between the magnetic field $B = 9-15$ T. The frequency of oscillations $F = 213$ T is calculated from Lifshitz-Kosevich (LK) analysis. These SdH oscillations were analysed using L-K fit. The transport characteristics of Topological surface states (TSS) are an important scenario in this work. The surface carrier density (n_s) and surface mobility (μ_s) are calculated to be $5.16 \times 10^{12} \text{ cm}^{-2}$ and $728 \text{ cm}^2/\text{V-s}$ respectively. Many topological Insulator (TI) materials, with good quality single crystals and high magneto-resistance response, could provide an excellent opportunity in fabricating novel high field magnetic sensors.

PP-105

Unidirectional Growth and Characterization of Triphenylmethane Single Crystals for Scintillator ApplicationV. Govindan¹, D. Joseph Daniel², H. J. Kim², K. Sankaranarayanan^{1*}¹Department of Physics, Alagappa University, Karaikudi-630 003, India.²Department of Physics, Kyungpook National University, Daegu 41566, South Korea.

Email: hhrsankar@yahoo.com

Organic scintillators have great impact in recent years due to detection of high energy particles in defective environment. In this aspect, the triphenylmethane has been crystallized unidirectionally by temperature gradient SR method with cylindrical dimension. Highly transparent large size (80 mm length and 15 mm diameter) single crystal was grown during the crystallization period of 25 days. The grown crystal cylinder was subjected to various physico-chemical investigations to establish its structural details both by X-ray diffraction and by infrared analysis, to study its thermal behaviour under gravimetric and calorimetric analyses, to record its photo response in the vicinity of UV-Visible wavelength and with the excitation wavelength of 385 nm and to explore the mechanical modulus by Vicker's microhardness test. The scintillation of the crystal cylinder under gamma radiation shows intense emission in the wavelength of interest and a decay time of 21 ns was noticed. These important results suggested the feasibility of this material for high energy radiation detection.

**Reference:**

V. Govindan, D. Joseph Daniel, H. J. Kim, K. Sankaranarayanan, "Unidirectional crystal growth, luminescence and Scintillation Characteristics of t-stilbene Single Crystals" *Dyes and Pigments*. 160 (2019) 848-852.

PP-106

Structural, Optical and Thermal Properties Of Organic 4,4'- Dimethylbenzophenone (Dmbp) Single Crystal Grown by Bridgman – Stockbarger MethodK. Ramachandran^{*1}, Arumugam Raja¹, V. Mohan Kumar¹, Muthu Senthil Pandian¹, P. Ramasamy¹¹SSN Research Centre, SSN College of Engineering, Chennai - 603 110, Tamilnadu, India

*E-mail: ramphy18@gmail.com

Bulk size, good quality and optically transparent 4,4'-dimethylbenzophenone (DMBP) single crystal was grown by Bridgman-Stockbarger method. The single crystal X-ray diffraction (SXRD) study reveals that the grown DMBP crystal belongs to orthorhombic crystal system with non-centrosymmetric space group of $P2_12_12_1$. The various functional groups were identified by using Fourier transform infrared (FTIR) spectrum analysis. The optical transmittance and cut off wavelength were analysed by using UV-Vis NIR spectrum. Thermal stability, melting and decomposition point of DMBP single crystal were carried out through thermogravimetric / differential thermal analysis (TG-DTA). The photoluminescence (PL) spectrum indicates that the maximum intensity peak is observed at 449 nm. The laser damage threshold of DMBP crystal was found to be 43.7 GW/cm^2 . The optimized molecular structure, first-order hyperpolarizability (β) and energy gap are calculated by using density functional theory (DFT). The molecular electrostatic potential (MEP) and natural bond orbital (NBO) analysis of DMBP molecule were calculated. The intermolecular interactions of crystal bonding system were elucidated from Hirshfeld surface (HS) plot analysis. The strongest intermolecular interaction of DMBP molecule is observed in the H...H (56 %) bonding interaction.

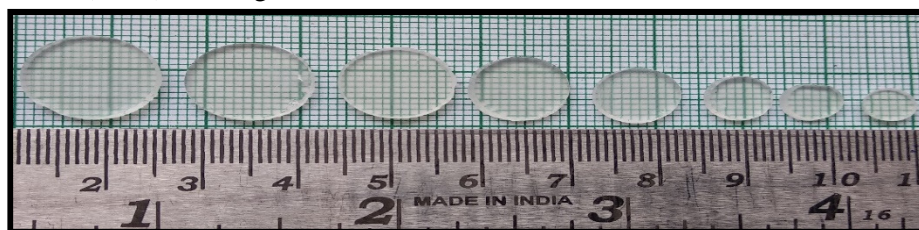


Fig. 1. Cut and polished wafers of DMBP crystal

References

- G. A. Babu, P. Ramasamy. *J. Cryst. Growth*, **2008**, 310, 3561-3567.
K. Ramachandran, P. Vijayakumar, A. Raja, V. Mohankumar, G. Vinitha, M. Senthil Pandian, P. Ramasamy. *J. Mater. Sci. - Mater. Electron*, **2018**, 29, 8571-8583.
M. Amalanathan, T.S. Xavier, I.H. Joe, V.K. Rastogi, *Spectrochim. Acta, Part A*, **2013**, 116, 574-583.

PP-107

Spectroscopic analysis (FT-IR and FT-Raman), NBO analysis, HOMO-LUMO and molecular docking studies on Cetirizine using DFT Simulations

N. Mani and M. Prasath*

Department of Physics, Periyar University PG Extension centre, Dharmapuri

* Email Id: sanprasath2006@gmail.com

Cetirizine ($C_{21}H_{25}ClN_2O_3$) molecule was optimized using density functional method (DFT) with 6-311G(d,p) basis set. Vibrational analysis of the Cetirizine compound was carried out using FT-IR and FT-Raman spectroscopic techniques ranges from $4000-450 \text{ cm}^{-1}$ and $4000-100 \text{ cm}^{-1}$ respectively. The molecular geometries and harmonic vibrational frequencies were calculated. A detailed interpretation of

the IR and Raman spectra, based on the potential energy distribution (PED) of the normal modes. The bond parameters such as bond lengths, bond angles and dihedral angles were calculated at the same level of theory. The calculated Highest Occupied Molecular Orbital (HOMO) and Lowest Unoccupied Molecular Orbital (LUMO) energies show that charge transfer occurs in the molecule. The electronic transition was studied using UV-Vis spectrum. The band gap energy, MEP map, Mulliken atomic charges were calculated using the same level of basis set. The molecular docking results suggest that the compound might exhibit inhibitory activity against ORM1-like 3 (ORMDL3) protein are associated with childhood asthma.

Keywords: DFT, FT-IR, FT- Raman, Molecular docking, ORMDL3

PP-108

Structural and Electrical properties of $(1-x)\text{Bi}_{1/2}\text{Na}_{1/2}\text{TiO}_3-x\text{BaTiO}_3$ Single Crystals Across the Morphotropic Phase Boundary by TSSG Method

*M. William Carry, G. Gopi, G. Anandha Babu**,

Department of Physics, SSN College of Engineering, Kalavakkam-603 110, Tamilnadu.

*Email: carrywilliam5234@gmail.com; anandhababug@ssn.edu.in

The piezoelectric solid solution $0.94(\text{Na}_{0.5}\text{Bi}_{0.5})\text{TiO}_3-0.06\text{BaTiO}_3$ (NBT-xBT) is a promising material to substitute for the environmentally undesired Pb-based piezoelectrics. Lead-free piezoelectric single crystals with a composition near the morphotropic phase boundary (MPB) have been grown by the Top seeded solution growth (TSSG) method. NBT-xBT ($x = 4, 5, 6, 7$) single crystal with different compositions, covering the rhombohedral to predominantly monoclinic phase and encompassing the morphotropic phase boundary (MPB), were grown by TSSG method. The Laue diffraction confirms the grown crystal as a single crystal with mosaic structure. Rietveld refinement studies revealed the presence of a phase boundary between monoclinic (Cc) and Rhombohedral (R3c) phases near MPB, where the dielectric and piezoelectric properties were enhanced. The dielectric, ferroelectric and piezoelectric properties along the $\langle 001 \rangle$ direction have been measured.



Figure. NBBT As grown Single crystal by TSSG method

PP-109

One-step synthesis and dual-luminescence properties of single phase fluoroperovskite $\text{KCaF}_3:\text{Eu}^{3+}$ Phosphors for White Light Emitting Diode and dosimetry Applications

Arumugam Raja^{*1}, *R. Nagaraj*¹, *K. Ramachandran*¹, *P. Ramasamy*¹

¹SSN Research Centre, SSN College of Engineering, Chennai-603110, Tamilnadu

*E-mail: rajaphy014@gmail.com

Europium activated Potassium Calcium Fluoride ($\text{KCaF}_3:\text{Eu}^{3+}$) phosphor was synthesized by conventional solid state reaction method. The crystalline structure and phase purity of the synthesized phosphor were analyzed by powder X-ray diffraction study. Molecule vibration activities were checked by Fourier Transform Infra-Red (FTIR) analysis. The surface morphology of KCaF_3 phosphors was characterized by Field Emission - Scanning Electron Microscopy analysis (FE-SEM). The $\text{KCaF}_3:\text{Eu}^{3+}$ phosphor was excited at 395 nm and five emission peaks were observed in visible region. Among these five peaks, the peak at 594 nm is dominant. The luminescence quantum efficiency was determined and the decay profile was obtained and analyzed. The Commission Internationale de l'Eclairage (CIE) chromaticity coordinates of Eu^{3+} activated KCaF_3 phosphors were calculated to be $x = 0.670$ and $y = 0.330$. The thermoluminescence property of Eu^{3+} activated KCaF_3 has been investigated for X-ray irradiation. Order of kinetics (b), activation energy (E), and frequency factor (s) were determined by peak shape method.

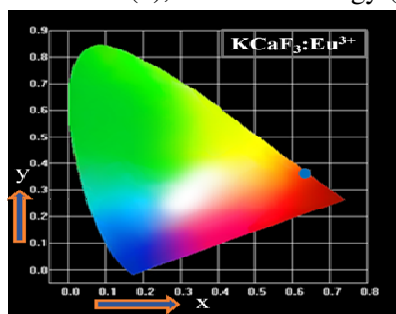


Figure: CIE color coordinates of $\text{KCaF}_3:0.06\text{Eu}^{3+}$ Phosphors

PP-110

Synthesis, growth and Characterization of 2-amino-5-nitropyridine 4-chlorobenzoic acid (1:1): a new D- π -A type Organic Single Crystal for Third-order nonlinear Optical (NLO) Applications

*V. Sivasubramani*¹, *Muthu Senthil Pandian*^{*1}, *P. Ramasamy*¹, *G. Vinitha*²

¹SSN Research Centre, SSN College of Engineering, Chennai-603110, Tamilnadu

²School of Advanced Sciences, VIT University, Chennai-600127, Tamilnadu

*E-mail: senthilpandianm@ssn.edu.in

Organic nonlinear optical (NLO) 2-amino-5-nitropyridine 4-chlorobenzoic acid (1:1) (2A5NP4CB) single crystals have been grown by slow evaporation solution technique (SEST) for the first time in the literature. The crystal structure was determined by single crystal X-ray diffraction (SXR) analysis. It crystallizes in the monoclinic crystal system with the centrosymmetric space group $P2_1/m$. The molecular weight and density of 2A5NP4CB crystal are found to be 295.68 g/mol and 1.538 Mg/m³. The crystallographic data was deposited in the Cambridge Crystallographic Data Centre (CCDC reference number-1511154). The presence of functional groups and its molecular structure have been confirmed by FTIR and NMR spectrum analysis, respectively. By employing unidirectional Sankaranarayanan-Ramasamy (SR) method, optically transparent 2A5NP4CB single crystal has been grown with the size of about 30 mm length and 10 mm diameter over a period of 60 days. The comparative investigations of 2A5NP4CB crystals grown by SEST and modified SR method have been investigated by HRXRD, UV-Vis NIR, chemical etching, Vickers microhardness and laser damage threshold analyses. The overall results show that the crystal grown by modified SR method possesses high quality compared to conventional SEST grown crystals. The electrical, thermal and photo sensing properties of the grown crystals were studied by dielectrics, TG-DTA and photoconductivity analysis, respectively. The Z-scan study shows that the grown crystal is highly nonlinear optical with saturable absorption, which makes it useful for optoelectronic applications. The optimized molecular structure, frontier molecular orbitals (FMOs), linear polarizability, first-order hyperpolarizability, Mulliken charge analysis and natural bond orbital (NBO) of 2A5NP4CB molecule were performed by density functional theory (DFT) method.



Figure. (a) ORTEP view of 2A5NP4CB with the atom numbering scheme, (b) SEST grown 2A5NP4CB single crystals and (c) SR method grown 2A5NP4CB single crystal

PP-111

Enhancement of the Growth Rate and Crystalline Perfection of Lithium Sulfate Monohydrate: An Efficient Negatively Soluble Piezoelectric Crystal

P. Rajesh, P. Ramasamy

Centre for Crystal Growth, Department of Physics, SSN College of Engineering, Kalavakkam 603110, Tamil Nadu, India

Lithium sulfate monohydrate (Li₂SO₄·H₂O) (LSMH) is an efficient ‘negatively soluble’ polar material, has good pyroelectric, piezoelectric and second harmonic generation (SHG) properties. In the trend for the development of single crystals for SHG and piezoelectric applications LSMH will undoubtedly attract more attention because of its good nonlinear optical, piezoelectric coefficient and

broad transparency in the range 180 nm - 1500 nm. Single crystals of Rochelle salt doped LSMH have been grown from aqueous solution by slow evaporation solution growth technique with the vision to improve the optical and electrical properties. The Rochelle salt is optically active, strongly piezoelectric due to presence of tartaric acid. The grown crystals have been subjected to various characterization studies to explore the various properties of the grown crystal. The crystalline perfection of the grown crystals has been assessed using rocking curve of HRXRD pattern. Small FWHM [13 arc-s] obtained from high-resolution X-ray diffraction spectrum shows that the grown crystal has good crystalline perfection and absence of low-angle grain boundaries. The mechanical behaviour has been analysed using Vickers microhardness measurements. The optical quality was assessed by recording UV-Vis-NIR transmission on the different sectors of the crystal. Piezoelectric studies are carried out on the (010) surface of the doped samples. The LSMH crystals grown from the solution containing Rochelle salt were found to have the good piezoelectric coefficient and will be useful for energy harvesting applications.

PP-112

Eu³⁺ Ions doped Boro-Phosphate Glasses for Photonic Applications

R. Nagaraj¹, K.Aravinth², P. Ramasamy², S. Ranjith¹

¹) Department of Physics, Ramapuram Campus, SRM University, Chennai – 600 089

²) SSN Research Centre, SSN College of Engineering, Kalavakkam, Chennai – 603 110

* E-mail: r.nagarajnaga16@gmail.com

Trivalent rare earth ions (RE³⁺) doped heavy metal Boro-Phosphate glasses have been studied extensively for the development of optoelectronic devices such as lasers, fiber amplifiers, light emitting diodes and color display devices. Among the RE³⁺ ions, Eu³⁺ ion emits narrow band, almost monochromatic with longer lifetime. Eu³⁺ ions doped Boro-Phosphate glasses with the chemical composition 40B₂O₃+(30-x)P₂O₅ +20ZnO +10Bi₂O₃ +xEu₂O₃ (where x=0.1, 0.5, 1.0, 2.0 and 3.0 in wt % labeled as ZBP0.1E, ZBP0.5E, ZBP1E, ZBP2E and ZBP3E glasses respectively) have been synthesized by conventional melt quenching method. The prepared glass samples were characterized through recording optical absorption, photoluminescence and decay spectral measurements in order to study their suitability for developing photonic devices. From the band positions of absorption spectra, the bonding parameters (δ) were calculated to explore the chemical bonding nature of the Eu³⁺ ions with its surrounding ligands. The luminescence spectra of titled glasses recorded by monitoring an excitation at 394 nm and all the spectra exhibit emission bands at 572, 586, 607, 649 and 703nm corresponding to ⁵D₀→⁷F₀, ⁵D₀→⁷F₁, ⁵D₀→⁷F₂, ⁵D₀→⁷F₃ and ⁵D₀→⁷F₄ transitions respectively. The Judd-Ofelt (JO) intensity parameters Ω_λ ($\lambda = 2, 4$ and 6) have been calculated from the emission bands to examine the symmetry and bonding of the ligand environment around Eu³⁺ ions site in the prepared glasses. The luminescence spectra were then characterized through CIE 1931 chromaticity diagram to explore the dominant emission color exhibited by the studied glasses for the suitable light emitting device (LED) applications. The radiative parameters such as transition probability (A), stimulated emission cross-section (σ_p^E), branching ratios (β_R) and radiative lifetime (τ_R) have been determined for the prominent emission transitions and among the prepared glasses, ZBP1E exhibits higher radiative parameters for the ⁵D₀→⁷F₂ transition and

hence the same can be suggested for the fabrication of photonic devices which include solid state lasers as well as optical amplifiers.

PP-113

Nucleation kinetics, crystal growth and characterization of ADP: KDP (85:15) mixed crystals for nonlinear optical applications

*Iyappan Gunasekaran¹, Rajesh Paulraj*¹, Ramasamy Perumalsamy¹*

¹*Department of Physics, SSN College of Engineering, Kalavakkam-603110, Tamil Nadu, India*

*E- mail: rajeshp@ssn.edu.in

Mixed crystals of Ammonium Dihydrogen Phosphate and Potassium Dihydrogen Phosphate were grown by temperature lowering seed rotation technique with the vision to improve the crystalline perfection. The grown mixed crystal shows positive temperature coefficient of solubility. Metastable zone width and induction period were determined. The lattice parameters of the grown mixed crystal were obtained using single crystal X-ray Diffraction studies. The optical transmission spectrum of the mixed crystal was recorded using Ultra Violet-Visible-NIR spectrum. Second harmonic generation studies were carried out for the pure ammonium dihydrogen phosphate, potassium dihydrogen phosphate and ammonium dihydrogen phosphate: potassium dihydrogen phosphate (85:15) mixed crystals. It was found that the second harmonic generation efficiency of the mixed crystal is higher than that of pure potassium dihydrogen phosphate crystals.

Keywords: Mixed crystals, Solution growth, Nucleation, Solubility, NLO materials.

PP-114

Ceramic/ Polymer Bio-Composite for Load-Bearing Application

J. Mobika^{1} and M.Raj Kumar¹*

¹*Department of Physics, PSG College of Arts and Science, Coimbatore, Tamil Nadu-641014*

*Email: mofikajayaraj@gmail.com

Load-bearing application particularly bone tissue regeneration has become one of the most focusing application in some decades. Because, millions of peoples across the world are affected by bone related diseases. Many composite materials have been widely used for load-bearing applications but to date have found only few of them are commercially successful, due to the many challenging problems like insufficient mechanical strength, biocompatibility and biodegradability. In this work, we are focusing to overcome this problem by design nanostructures that mimic bone's natural architecture. Mechanically strong and biodegradable silk fibroin (SF) is used as a polymer phase along with inorganic compound of natural bone namely, hydroxyapatite (HAP) as a ceramic phase to fabricate bio-composite by *in-situ* coprecipitation method. The chemical composition, phase analysis and morphology of prepared bio-composite was characterized by FTIR, XRD, EDX and FESEM analysis. In addition, the *in vitro* bioactivity of pure HAP and HAP/SF bio-composite was examined by soaking them in stimulated body

fluid for different period of time. Results showed that the formation and growth of bone like mineral on the surface of the product.

Keywords: Hydroxyapatite, Silk fibroin, Bio-composites, Load bearing application, Bone.

PP-115

Bulk Growth Of 3,4 – Diamino Benzophenone By Micro-Tube Czochralski Method

S. Usharani¹, J.Judes^{1}, V. Natarajan², M. Arivanandhan³*

¹*University VOC College of Engineering, Anna University: Tuticorin campus, Tuticorin-628 008 India.*

²*Department of Physics, Dr. Sivanthi Aditanar College of Engineering, Tiruchendur 628215, India*

³*Centre for Nanoscience and Technology, Anna University, Chennai 600025, India*

*E-mail: ushaponmuthu@gmail.com

Most of the optical applications require highly energetic laser radiation which is possible by frequency conversion through nonlinear optical (NLO) effect. Therefore, NLO materials are highly useful for generating green and blue lasers by doubling the low frequency laser radiations. The materials inherent with this significant property find its wide applications in second harmonic generation (SHG), frequency conversion, electro-optic modulation, optical parametric oscillation, optical bistability, photochemistry, biomedical research, optical windows and spectroscopy. Benzophenone and its derivatives are the potential organic NLO materials with good optical, mechanical properties and non-hygroscopic nature [1]. In the present work, bulk crystals of one of the benzophenone derivatives, 3, 4-diamino benzophenone (3,4DABP) are grown by Micro-tube Czochralski technique. In order to grow high-quality single crystals, different growth parameters like micro-tube diameter, length and temperature gradient of the furnace were optimized. The bulk single crystal of DABP was successfully grown under the optimized condition (Fig.1). The structural, optical, thermal properties of the grown crystals were investigated. The powder Kurtz method was employed to study the NLO properties of DABP crystals. The rest of the results will be discussed in detail.



Fig.1. Photograph of as grown DABP

References

[1] Cockorham P, Frazier C.C, Guha S, Chauchard E.A, Appl.Phys.,1991,B53, 275.

[2] Philip J.Cox, Abu T.MD, Anizzuman R, Howard Pryce –Jones, Graham G. Skellern, Alastair J.Florence, Norman Shankland, 1998,C54, 856-859.

PP-116

Antibacterial Efficiency of Chitosan Incorporated HAp nanocomposite Synthesized by Simple Co-precipitation Method

*L. Noor Ul Haq, K. Vijayalakshmi**

PG & Research Department of physics, Bishop Heber College, Tiruchirappali-17

*E-mail: xrdnoor@gmail.com

This present work portrays the Antibacterial efficiency of chitosan incorporated HAp nanocomposite by Simple co-precipitation Method. The resulted nanoparticles were characterized by X-ray diffraction (XRD), Fourier transform infrared spectroscopy (FTIR) energy dispersive X-ray spectroscopy (EDS) and scanning electron microscopy (SEM). The results established integration and similarity between Pure HAp and chitosan incorporated HAp nanocomposite. The XRD report revealed the structure of the material and it played a significant role to decrease the crystallinity and increase the surface area. The vibrational spectra shows significant shifts in the peaks with Chitosan addition. EDX analysis confirmed the composition rate of the Pure HAp and chitosan Incorporated HAp nanocomposite. SEM micrograph shows the transformation of morphology after Incorporated of Chitosan. The antibacterial activities were tested against Gram positive and Gram negative bacteria. The antibacterial results exhibits high toxicity potential for chitosan Incorporated HAp nanocomposite compared with Pure HAp.

PP-117

Growth, Physicochemical and Quantum Chemical Investigations on Hexamethylenetetraminium Di-Malate – An Organic Crystal for Optoelectronic Device Applications

M. Saravanakumar^a and J. Chandrasekaran^{a}*

^a Crystal Research Laboratory, Department of Physics, SRMV college of arts and science, Coimbatore - 20, Tamilnadu, India.

*E-mail:mskumarphy025@gmail.com

Organic nonlinear optical single crystals of Hexamethylenetetraminium di-malate (HMTM) were grown by a slow evaporation solution growth technique at room temperature using methanol as a solvent. The crystal structure and single crystalline phase characterizations were performed using single crystal X-ray diffraction (SXRD) and powder X-ray diffraction (PXRD) methods respectively. The crystal structure and various functional groups present in HMTM were confirmed by ¹H, ¹³C NMR, FTIR and FT-Raman analysis. The optical absorption and lower cutoff wavelength were identified by UV-Vis studies. The charge transport mechanism and photoconducting nature of HMTM were analyzed using dielectric and

photoconductivity studies. Powder SHG analysis was also carried out for powder samples using the Kurtz and Perry powder second harmonic generation (SHG) technique; the results were compared with KDP. In addition, the quantum computational studies, optimized geometry, vibrational studies, intra-molecular charge transfer interactions within the molecule using NBO studies, first and second order hyperpolarizability, HOMO-LUMO, natural population analysis and molecular electrostatic potential surface for HMTM have been investigated using Density function theory at B3LYP/6-311++G(d,p) level of theory. The vibrational spectral studies and NBO analysis were confirms the N-H...O intra-molecular hydrogen bonding. The intermolecular interactions and 2D finger print plots of HMTM were analyzed using Hirshfeld surface analysis.

PP-118

Structural and electrical properties of Lead-free (1-x) Na_{0.5} Bi_{0.5} TiO₃- xBaTiO₃ Solid Solutions

Rajesh Narayana Perumal^{*1(a,b)}, Venkatraj Athikesavan^{a,b)}

^{1a}Center for Radiation Environmental Science and Technology, SSN College of Engineering, Kalavakkam-603 110, India.

^b Department of Physics, SSN College of Engineering, Kalavakkam - 603 110, India.

*E-mail:rajeshnp@ssn.edu.in

The lead-free piezoelectric ceramic of (1-x) Bi_{0.5}Na_{0.5}TiO₃- x BaTiO₃ is synthesized using solid state reaction technique by varying the composition ranges of x to 0.00, 0.04, 0.06 and 0.08. When there is an addition of BaTiO₃ into Na_{0.5}Bi_{0.5}TiO₃, the ceramic exhibited strong piezoelectric property at the morphotropic phase boundary region. The sample is subjected to X-Ray diffraction (XRD) which revealed that the sample is homogeneous and has a rhombohedral structure with space group (R3c). Dielectric measurement was carried out for different composition at various temperatures. The maximum dielectric constant (ϵ_r) ~3233 was observed at 327°C. The sample was poled at a voltage of 3-5 kV. The remnant polarization of ferroelectric study gave a maximum value of (P_r) ~23.6 μ C/cm² at piezoelectric coefficient (d_{33}) ~ 139 pC/N which is obtained from the piezotest when x=0.04 for NBT-BT composition. Excellent dielectric, piezoelectric and ferroelectric properties suggested that x=0.04 is the actual MPB composition of the NBT-BT system which can be used in widespread applications such as sensor, actuator, etc.

PP-119

Effect of crystallization of Calcium oxalate crystals in the industrial area water on living organisms

R.Selvaraju¹, B.Anitha², K.Anandalakshmi³

¹ Engineering Physics, Annamalai University, Annamalainagar -608 002, Tamilnadu

²Department of Physics, CK College of Engineering & Technology, Cuddalore – 607 003, Tamilnadu³

Department of Physics, Periyar Government Arts College, Cuddalore – 607 001, Tamilnadu

*Email: drselvarajufetau@gmail.com

Water is one of the most essential things for all living organisms. It is polluted due to the wastage comes out from the different sources. Pollutants come from chemical industries cause harmful effect on industrial area water. The living organisms are affected by this polluted water. In this present work the samples are collected from the industrial area. The physicochemical properties are studied for the above samples. The effect of calcium content on living organisms is analyzed with the comparison of the desirable limit given by WHO. Using this water calcium oxalate crystals are grown by double diffusion gel technique method. After harvesting the crystals the FT-IR studies are carried out. The results are discussed.

PP-120

First principles study of structural and electronic properties of half Heusler compounds $ZrIrX$ ($X=As, Sb$ and Bi) using GGA and TB-mBJ

R. Anubama, Rita John

Department of Theoretical physics, University of Madras, Chennai-25

We have investigated the structural and electronic properties of half Heusler compounds $ZrIrX$ ($X = As, Sb, \text{ and } Bi$) using first principles calculation within Density Functional Theory (DFT). These properties are calculated using Full Potential Linearized Augmented Plane Wave (FP-LAPW) method within Generalized Gradient Approximation (GGA) and Tran–Blaha modified Becke–Johnson (TB-mBJ) exchange and correlation potentials. The structural parameters of $ZrIrX$ ($X = As, Sb, \text{ and } Bi$) compounds such as optimized lattice parameter (a_{opt}), bulk modulus (B) and their pressure derivative (B') are calculated using PBE-GGA. At optimized crystal structure, all three compounds are trivial semiconductors with a energy gap E_g . It is found that the topologically nontrivial state can be achieved in half Heusler alloys by tuning their hybridization strength, spin orbit strength and substitution etc. When spin orbit interaction is included, the compound $ZrIrBi$ shows semimetallic character with zero gap while the other two compounds show semiconducting behavior. We find that $ZrIrBi$ can exhibit a topological nontrivial phase by applying hydrostatic expansion by 1% causing band inversion with zero gap. While compression by 1% it shows normal semiconducting behavior with increase in band gap [1]. The band gaps of electronic structures of these compounds are improved by using TB-mBJ and it does not induce band inversion in these compounds causing no topological phase transition [2]. The present work is compared with other reported results and found to be in good agreement.

Key words: Density Functional Theory, half Heusler alloys, spin orbit interaction, topological nontrivial phase.

PP-121

Crystallographic, Spectroscopic and Hirshfeld Surface Analysis of Anilinium Arsenate

F.Mary Anjalin^a, N.Kanagathara^{a}, G.Anbalagan^b, M.K.Marchewka^c*

^aDepartment of Physics, Saveetha School of Engineering, Saveetha Institute of Medical and Technical Sciences, Thandalum, Chennai 602 105, India

^bDepartment of Nuclear Physics, University of Madras, Guindy Campus, Chennai 600 025,

^cInstitute of Low Temperature and Structure Research, Polish Academy of Sciences, 50-950 Wrocław, 2, P.O. Box 937, Poland.

*E-mail: kanagathara23275@gmail.com

In the present communication, aniline with arsenic acid molecular complex has been taken as the subject. The anilinium arsenate – a new crystalline product have been grown by slow evaporation technique at room temperature. Crystal X-ray diffraction study reveals that the grown crystal crystallizes in monoclinic system with centro symmetric space group P 21/c with primitives $a=9.872(2)\text{Å}$, $b=10.769(2)\text{Å}$, $c=8.223(2)\text{Å}$ and interfacial angles $\alpha=\gamma=90^\circ$ and $\beta=92.23(3)^\circ$. The strong hydrogen bond interactions between the singly protonated anilinium cation and single dissociated arsenate (1-) anions forms a three dimensional network. The crystallite size is calculated to be $14.089\ \mu\text{m}$ using Debye-Scherrer's formula. Room temperature powder infrared and Raman measurements for the aniline arsenic acid molecular complex (1:1) were carried out. The FT-IR and FT Raman spectra have been recorded and various vibrations of aniline as well as arsenate ions present in the grown crystal is identified and discussed in detail. Further the 3D Hirshfeld surface analysis and 2D fingerprint maps gives deep insight into the intermolecular interactions between the compound.

Key words: Crystal structure, hydrogen bond, XRD, FT- IR, FT-Raman

PP-122

Molecular Structure, Vibrational, Optical, Molecular Docking and Thermodynamics Properties of N, N-Dimethylnicotinamide

M. Arivazhagan¹, Senthilkumar Chandran²,

¹Department of Physics, Government Arts College, Tiruchirappalli, Tamilnadu-620022

²Department of Physics, Research Centre, SSN College of Engineering, Kalavakkam, Chennai, Tamilnadu-603110

*E-mail: jamesgnanapragasam@gmail.com

The experimental and computational analyze of the geometrical structure and vibrational frequency of N, N-dimethylnicotinamide is determined. The FTIR and FT-Raman spectra were carried out and vibrational frequencies are compared with the quantum chemical computational methods. The first-ordered hyperpolarizability and dipole moment values are calculated. The UV-Vis properties were carried out using UV-Vis-NIR analysis. Different thermodynamic properties are calculated and the results are compared with both methods (HF and B3LYP). The auto docking is also carried out for N, N-dimethylnicotinamide molecule.

Keywords: Molecular structure; Vibrational analysis; optical properties; Molecular docking.

PP-123

Crystal growth and characterization of glycine potassium Iodide (GPI) for nonlinear optical applications

R. Ravisankar^{1}, D. Rajendiran^{1,2}, R. Vijayakumar¹, P. Jayaprakash³, K.M. Freny Joy⁴*

¹*Post Graduate and Research Department of Physics, Government Arts College, Thiruvannamalai – 606603, Tamilnadu*

²*Post Graduate and Research Department of Physics, Shanmuga Industries Arts and Science College, Thiruvannamalai – 606603, Tamilnadu*

³*Department of Physics, Annai Mira College of Engineering and Technology, Arapakkam, Vellore – 632517, Tamilnadu*

⁴*Department of Physics, Madras Christian College, Tambaram, Chennai – 600059, Tamilnadu*

** E-mail: ravisankarphysics@gmail.com*

Glycine Potassium Iodide (GPI) crystals have been grown by slow evaporation solution technique at room temperature. The functional groups and vibrational frequencies were identified using FTIR spectral analysis. The cell parameters were determined from single crystal X-ray diffraction analysis. Thermogravimetric analysis (TGA) and differential thermal analysis (DTA) were used to study its thermal properties. The optical transmittance window and lower cutoff wavelength have been identified by UV-absorption spectrum analysis. Second harmonic generation (SHG) efficiency measurement was carried out by powder Kurtz method. The dielectric studies have been employed to examine the substantial improvement in dielectric constant and dielectric loss of glycine doped Potassium Iodide (GPI) crystal. The non linear optical absorption of the samples has been studied by Z-scan technique. The observed properties have confirmed that the grown crystal is suitable for nonlinear optical applications.

Keywords: Glycine Potassium Iodide, Characterization studies, NLO applications

PP-124

Molecular Structure and Electrostatic Properties of High Energetic 2,4,6-Trinitropyridine N-Oxide Molecule Via Quantum Chemical Calculations

L. Sathya¹, B. Gnanavel¹, A. David Stephen² and P. Srinivasan^{1}*

¹*PG & Research Department of Physics, Chikkaiah Naicker College, Erode – 638 004*

²*Department of Physics, Sri Shakthi institute of Engineering Technology, Coimbatore – 641 062*

**E-mail: sriniscience@gmail.com*

The TNPyO molecule has been optimized using quantum chemical methods (B3LYP/Aug-cc-PVDZ) in order to find the potential HEDMs. The predicted optimized structural parameters are in good agreement with experimental value. This quantum chemical calculation reveals that, the TNPyO molecule C–NO₂ and N–O (N-oxide) bonds are weak, which confirms that these bonds are the weakest bonds in the molecule. The simulated TNPyO molecule reveals negative oxygen balance (-0.86%) and its energy gap is 3.45 eV. The calculated impact sensitivity and imbalance parameters show very good agreement with already known explosives. These computational studies are the viable pathway and helpful for the experimental characterization and production of some of high energetic nitrogen rich molecules.

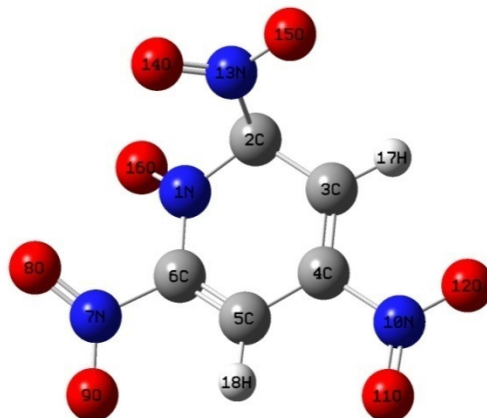


Figure shows the optimized structure of 2,4,6-trinitropyridine-1-oxide (TNPyO) molecule.

Keywords: Electron density, Explosives, Oxygen balance, Impact sensitivity and ESP

PP-125

Abundant and Multifunctional Materials for the electrochemical storage device applications

V. Vignesh¹, S. Bhagyashree², K. Subramani^{3,4}, M. Sathish^{3,4}, R. Navamathavan¹

¹Division of Physics, School of Advanced Sciences, VIT Chennai,
Vandalur - Kelambakkam Road, Chennai 600 127

²School of Electronics Engineering, VIT Chennai, Vandalur - Kelambakkam Road,
Chennai 600 127

³Functional materials division, ⁴Academy of Scientific and Innovative Research (AcSIR),
CSIR- Central Electrochemical Research Institute, Karaikudi- 630 003

*E-mail:navamathavan.r@vit.ac.in

Nowadays with the ever increasing population crisis, the less availability of conventional fuels has dramatically received very high demand. At this juncture, alternate sustainable sources of conventional/storage device application gadgets are of great importance. Even though, non-reliable nature of renewable sources such as solar, wind etc., due to their insufficient localized space and time of usability. In this connection, energy storage systems plays vital role to fulfill the needful due to their promising functionalities (for example batteries and supercapacitor). In this work, we report on a highly abundant and multifunctional nature of MnFe₂O₄ nanoparticles for electrochemical storage application in

lithium based electrolyte. From the electrochemical measurements of MnFe_2O_4 exhibits high operating potential with affordable capacitive performance. In a three-electrode system, a maximum specific capacitance of 430 F g^{-1} was attained in $1\text{M Li}_3\text{PO}_4$. Our results may pave the way for employing the low-cost co-precipitation method to fabricate advanced high energy storage and highly stable device with long cycle life. Having high energy, power and environmental benignity of energy stored device can meet these demands of uninterrupted power supply.

PP-126

Growth and Physical Investigation of $\text{AgIn}_{0.5}\text{Ga}_{0.5}\text{S}_2$ single crystal for Mid-IR Applications

N. Karunakaran and P. Ramasamy

Department of Physics, SRM Institute of Science and Technology, Chennai

²Center for crystal growth, SSN College of Engineering, Kalavallam-603110

Email: karthickkaruna@gmail.com

AgGaS_2 is one of the I-III-VI₂ ternary semiconducting compounds that crystallizes in the chalcopyrite structure which belongs to the $4\bar{2}m$ point group. AgGaS_2 has large nonlinear optical coefficients ($d_{36} = 39 \text{ pm/V}$) and excellent transmission in the mid-IR (1–18 μm) range [1]. It is one of the attractive IR nonlinear optical materials for device applications due to its unique properties, including large nonlinear optical devices such as optical parametric oscillators, different frequency conversions, second harmonic generators, etc. Silver Indium Gallium Sulfide ($\text{AgIn}_{0.5}\text{Ga}_{0.5}\text{S}_2$) belongs to the family of $\text{A}^{\text{I}}\text{B}^{\text{III}}\text{C}_2^{\text{VI}}$ ternary compound semiconductors which crystallize in the chalcopyrite structure. The growth of $\text{AgIn}_{0.5}\text{Ga}_{0.5}\text{S}_2$ single crystal is a two step process. Synthesis of the polycrystalline material from the starting elements is achieved using melt temperature oscillation method. The synthesized material is used to grow a single crystal. The $\text{AgIn}_{0.5}\text{Ga}_{0.5}\text{S}_2$ single crystals have been grown by the vertical Bridgman technique. The synthesized $\text{AgIn}_{0.5}\text{Ga}_{0.5}\text{S}_2$ polycrystalline charge was confirmed by powder XRD. The peak positions are in good agreement with the powder diffraction file. Thermal property was analyzed using TG-DTA technique. The melting point of the crystal is 896°C and freezing point is 862°C . The unit cell parameters were confirmed by single crystal X-ray. The grown crystal was subjected to IR transmission. The stoichiometric composition of $\text{AgIn}_{0.5}\text{Ga}_{0.5}\text{S}_2$ was measured using energy dispersive spectrometry (EDS).

PP-127

Synthesis and characterization of $\text{Zn}_{1-x}\text{Mg}_x\text{O}$ nanocrystals for thermoelectric applications

T.M.V.Muruguthiruvalluvan¹, V.Natarajan², M.Ramesh³, S.Pari³, R.Chandramohan⁴, P.Anandan⁵, M.Arivanandhan^{6}*

¹Department of Physics, Manonmaniam Sundaranar University, Tirunelveli, Tamil Nadu

²Department of Physics, Dr.Sivanthi Aditanar College of Engineering, Tiruchendur

³Department of Physics, National College, Tiruchirappalli, Tamil Nadu

⁴Department of Physics, Sree Sevugan Annamalai College, Devakottai, Tamil Nadu

⁵Department of Physics, Thiru Kolanjiappar Government Arts College, Virudhachalam

⁶Centre for Nanoscience and Technology, Anna University, Chennai

*E-mail: arivucz@gmail.com

Thermoelectrics (TE) is a promising technology to convert the waste heat into electric energy and thus CO₂ emission can be suppressed to some extent. The performance of a thermoelectric material can be determined by Figure of merit (ZT) which is directly proportional to electrical conductivity and inversely proportional to thermal conductivity of the material. ZnO is a promising oxide thermoelectric material especially at high temperature as it has high electrical conductivity. However, the main disadvantage of ZnO is that the thermal conductivity is also high and maintain the same at high temperature. The electrical and thermal conductivities of ZnO vary significantly with grain size and thereby the ZT of the material as well. The thermo power can be enhanced in nanocrystals compared to bulk material due to quantum confinement effect. Moreover, the phonons can get scattered in the nanostructures and thereby one can reduce the thermal conductivity of a material. Therefore, the nanomaterials are expected to have higher ZT than the bulk material. In the present work, pure and Mg added ZnO nanocrystals have been synthesised by sol-gel method with various Mg compositions. The structural and morphological properties of the prepared nanocrystals were analysed by XRD and SEM analysis. The XRD analysis confirmed the complete dissolution of Mg in ZnO lattice. The spherical morphology of the samples were observed in the SEM images. The electrical conductivity of the Zn_{1-x}Mg_xO nanocrystals decreased as the Mg concentration increased in the precursor solution due to widening of the bandgap. The Seebeck coefficients of the samples were measured as a function of temperature and the sample with a relatively high Mg content had a higher Seebeck coefficient compared with the other samples, especially at elevated temperatures. Zn_{0.9}Mg_{0.1}O had relatively high power factor compared with the other samples

PP-128

Synthesis and Characterisation of Nanostructured Bi_xCo_{1-x}O Material for Thermoelectric Applications

S. Alagar Nedunchezian¹, D.Sidharth¹, N. Yalini Devi¹, R.Rajkumar², G.Anbalagan², M. Arivanandhan^{1*}, R. Jayavel¹

¹Centre for Nanoscience and Technology, Anna University, Chennai 25.

²Department of Nuclear Physics, University of Madras, Guindy Campus, Chennai-25.

Thermoelectrics is a promising technology to convert waste heat into electricity. The performance of a thermoelectric material can be determined by its figure of merit (ZT) which is directionally proportional to electrical conductivity and inversely proportional to thermal conductivity. Therefore a material should have high electrical conductivity and low thermal conductivity for better thermoelectric performance. Nanostructuring is one of the promising ways to control the thermal conductivity by enhancing the phonon scattering. The oxide thermoelectric material shows the promising improvement in recent years. Moreover, the oxide materials are non-toxic, environmental friendly and ease to process as a device. The cobalt oxide based thermoelectric materials are more reliable and hence a series of Bi_xCo_{1-x}O nanocrystals are synthesized. The structural, morphological and compositional properties of the prepared materials are studied by XRD SEM and EDS analysis. Thermoelectric properties of the synthesized

materials are studied at various temperatures. The electrical conductivity is measured using the Hall measurement system and the seebeck coefficient is measured using indigenously fabricated Seebeck measurement system at various temperature. Using the measured data, the thermoelectric power factor ($S^2\sigma$, where S is seebeck coefficient and σ is electrical conductivity) is calculated for $\text{Bi}_x\text{Co}_{1-x}\text{O}$ samples (where X = 0%, 2.5%, 5%, 10%, and 20%) and the results are discussed in detail.

Keywords: Thermoelectrics, cobalt oxide, nanosturcturing, oxide thermoelectrics.

PP-129

Crystal Growth and Characterization of 4-Amino Benzophenone: A Promising Organic NLO Material

V. Natarajan^{1*}, S. Usharani¹, M. Arivanandhan², P. Anandan³, Y. Hayakawa⁴

¹Department of Physics, Dr. Sivanthi Aditanar College of Engineering, Tiruchendur 628215, India

²Center for Nanoscience and Technology, Anna University, Chennai, India

³Department of Physics, Kolanjiappar Arts College, Vridhachalam, India

⁴Research Institute of Electronics, Shizuoka University, Johoku 3-5-1, Naka-Ku., Hamamatsu 432-8011, Japan

The Non Linear Optical (NLO) materials are playing a vital role in generating the green and blue lasers through second harmonic generation (SHG) of low frequency laser radiations. Organic NLO crystals are attracted by the researchers due to their high NLO efficiency and fast response compared to the inorganic counter parts. The benzophenone and its derivatives are highly attractive materials due to their large NLO susceptibilities and lower cut-off wavelengths of about 400 nm. Although 4-aminobenzophenone (4-ABP) is a best derivative of benzophenone with 260 times higher SHG efficiency than that of Potassium Dihydrogen Phosphate (KDP), growth of high quality bulk crystal of 4-ABP still remains as a difficult task due to its photo-oxidation properties. In the present work, efforts were made to grow inclusion free 4-ABP single crystal by controlling the solvent evaporation. The structural, thermal and optical properties of 4-ABP crystals were studied. The enthalpy of 4-ABP melting process was estimated from differential thermal analysis. The optical transmission study shows that 4-ABP crystals grown from ethanol has high transparency compared to the ethyl acetate grown sample due to solvent inclusion in the later crystal.

PP-130

Comparitive Analysis of Synthesis and Electrochemical Characterizations of CeO_2/Rgo and $\text{CeO}_2/\text{Mos}_2$ Nanocomposites for Supercapacitor Application

M.Mohamed Ismail, P.Saraswathi devi, Prisilla Juliet, D.Mani, M. Arivanandhan*

Center for Nanoscience and Technology, Anna University, Chennai

*E-mail: arivucz@gmail.com

Supercapacitor is a promising energy storage device (ESD) for the future decades. 2D nanomaterials like rGO and MoS₂ are the suitable materials for electrical double layer capacitance (EDLC). In the present work, Graphene Oxide, CeO₂, MoS₂ were synthesized by modified Hummers method, modified Pechini method and hydrothermal method, respectively. The electrochemical behavior of rGO and MoS₂ were comparatively analyzed in a systematic way. The crystalline structure of the nanocomposites was examined by X-ray diffraction (XRD), and the peaks were well matched with the standard JCPDS data. Raman spectra analysis shows the CeO₂ F_{2g} vibration mode and D and G bands of GO and rGO nanosheets. Morphologies of the nano materials were characterized by the Scanning electron microscopy (SEM) and the images show the spherical shape morphology of CeO₂ nanoparticles, and sheet like morphologies of rGO and MoS₂. Electrochemical properties of the CeO₂/rGO, CeO₂/MoS₂ nanocomposite electrode materials were investigated by Cyclic Voltammetry (CV), chronopotentiometry (CP) and EIS analyses using three electrode systems. Presence of GO and MoS₂ prevent the aggregation and controlled the structure of CeO₂ nanocrystals. The specific capacitance of the CeO₂, CeO₂/rGO and CeO₂/MoS₂ were 616, 766, and 1100 F/g, respectively. Chronopotentiometry and EIS of pure CeO₂ and CeO₂/rGO, CeO₂/MoS₂ composite materials were investigated by their electrochemical performance. The CeO₂/rGO nanocomposite electrode material exhibits an enhanced supercapacitive performance due to the synergic effect of CeO₂ and GO compared to CeO₂ and CeO₂/MoS₂ nanocomposites.

PP-131

Theoretical, Biological and Insilico Studies of Pendant Armed Heteroleptic Nickel(II) Phenolate Complexes

P. Arthi, A. Kalilur Rahiman

Department of Chemistry, Srm Institute of Science and Technology, Ramapuram campus, Chennai, Tamilnadu

Post-Graduate and Research Department of Chemistry, The New College (Autonomous), Chennai-600 014, India

A new series of pendant-armed heteroleptic nickel(II) phenolate complexes of the type [NiL¹⁻³(diimine)] (1-6) have been synthesized by the reaction of pendant-armed ligand 2,2'-(benzoyliminodiethylene)bissalicylidene(H₂L¹), 2,2'-nitrobenzoyliminodiethylene)bissalicylidene(H₂L²) or 2,2'-(3,5-dinitrobenzoyliminodiethylene)bissalicylidene(H₂L³) with coligands (diimine; 2,2'-bipyridyl (bpy) or 1,10-phenanthroline (phen)) in the presence of Nickel(II) chloride, and characterized by spectroscopic techniques. The seven coordinated pentagonal-bipyramidal geometry around the nickel(II) center was inferred from the electronic spectra of the complexes. The bond length, bond angle and HOMO-LUMO energy gap calculations were carried out by DFT studies, using Gaussian 03 program. Electrochemical studies of the mononuclear complexes has been studied. Experimental and in silico molecular docking studies support groove mode of binding with DNA. Further, the molecular docking studies of complexes with B-DNA indicate the binding of the guanine-cytosine residues in the minor groove of the DNA. Molecular docking studies also revealed the interaction of complexes with protein ERK2 kinase and significant topoisomerase (Topo-I) inhibitory activity. All the complexes display pronounced cleavage activity against supercoiled pBR322 DNA in the presence of H₂O₂. In

vitro cytotoxicity of the complexes was tested against liver cancer cell line (HepG2) by MTT reduction assay.

Keywords: Pendant-armed complexes; DNA binding; DNA cleavage; Molecular docking.

PP-132

Kinetic Studies on the Phase Transfer Catalysed Free Radical Polymerization of Alkyl Methacrylate

Yoganand. K. S,

Department of Chemistry, SRM INSTITUTE OF SCIENCE & TECHNOLOGY

Ramapuram, Chennai – 600089, Tamil nadu. India.

*E-mail ; yoganand.ks@gmail.com

Phase Transfer Catalysis (PTC) is the technique which brings two mutually insoluble solvents in one phase in sufficient concentrations, so that the reaction can proceed rapidly. One of the earliest applications of phase transfer catalysis by quaternary ammonium salts is the synthesis of polymers through free radical mechanism. PTC which induces the regular arrangement of molecules, so crystalline polymers were formed. Our present research work deals with the kinetic experiments on phase transfer catalysed polymerization of methyl methacrylate initiated by water soluble initiators. A newly synthesized quaternary ammonium salt is used as the phase transfer catalyst and water soluble $K_2S_2O_8$ as the initiator and the polymerization was executed unstirred at 60 °C under nitrogen atmosphere. The effect of concentration of monomer, catalyst, initiator and solvent were evaluated. Also the rate of the reaction has been studied by varying the volume of the aqueous phase. Suitable kinetics also proposed for the polymerization process. The thermodynamic parameters have been evaluated by altering the temperature of the reaction from 50 °C to 65 °C. Molecular weight and its distribution were computed using gel permeation chromatography. Using the aforementioned values a suitable mechanism has been proposed. The formed polymer was characterized by FT-IR and NMR techniques.

Key words: PTC, PDS, MMA, PMMA

PP-133

Theoretical Investigations and Biological Studies of 4-Bromo-3-[N-(N-3,4-dimethoxyphenyl)ethyl-N-methylsulfamoyl]-5-methyl benzoic acid monohydrate

R.Kavipriya^a, Helen P. Kavitha^a, C.Suneel Manohar Babu^b, Jasmine P.Vennila^c

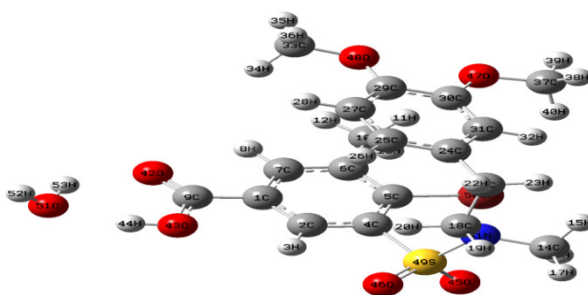
^aDepartment of Chemistry, SRM Institute of Science & Technology, Ramapuram, Chennai

^bAPI Group Manager, ASOLUTION Pharmaceutical Private Ltd, Mumbai

Department of Physics, Panimalar Institute of Technology, Chennai

In the present study, the molecular structure of 4-Bromo-3-[N-(N-3,4-dimethoxyphenyl)ethyl-N-methylsulfamoyl]-5-methyl benzoic acid monohydrate (DEMB) have been studied by density functional theory (DFT) calculation using B3LYP and standard basis set 6-31 G(d). The FT-IR and FT-Raman

spectra of DEMB were recorded and complete assignments of the observed vibrational frequencies have been proposed. Non-linear optical (NLO) behaviour of DEMB was investigated by determining the properties like electric dipole moment μ , polarizability α and hyperpolarizability β . The molecular properties, such as ionization potential, electro-negativity, chemical potential and chemical hardness have been deduced from HOMO-LUMO analysis. The calculated HOMO and LUMO energies showed that charge transfer occurs within the molecule. Natural bond analysis (NBO) study confirms the hyper conjugative interaction and charge delocalization. The comparison between the calculated and the observed vibrational spectra is done to understand the observed spectral features. DEMB was evaluated against pathogenic bacteria, such as Escherichia coli and Bacillus subtilis and fungi, such as Candida albicans and Aspergillus niger by Disc Diffusion Method. Docking studies were performed against antimicrobial protein beta-topoisomerase IV ATP inhibitor.



Optimized geometry of 4-Bromo-3-[N-(N-3,4-dimethoxyphenyl)ethyl-N-methylsulfamoyl]-5-methyl benzoic acid monohydrate

PP-134

Growth and Characterization with Molecular Modeling Studies of Benzotriazole Salicylic Acid (Bsa) Single Crystal

P.Sathya,

Department of physics, Anna university, Chennai – 25

***E-mail. sathyam.chawla@gmail.com**

In this study, Benzotriazole Salicylic acid (BSA) single crystal by slow evaporation solution growth method. The grown crystal was confirmed by single crystal X-ray diffraction analysis. The BSA compound crystallises in monoclinic system with space group P21/n which is recognized as centrosymmetric nature. The lattice parameters were obtained as $a = 13.80(7)\text{\AA}$, $b = 5.41(1)\text{\AA}$, $c = 16.66(2)\text{\AA}$, $\alpha = 90^\circ$, $\beta = 102.27(3)^\circ$, $\gamma = 90^\circ$, $V = 1216(4)\text{\AA}^3$. The vibrational spectroscopy (FT-IR and Raman spectra) of BSA compound has been studied under both theoretically and experimentally. The optimized geometrical parameters of BSA obtained by B3LYP/6-31g(d,p) density functional calculations. The HOMO and LUMO energy values were calculated along with their plot has been presented to understand the charge transfer occurring within the compound. Molecular electrostatic potential (MEP) surface map, hyperpolarisability and dipolemoment were calculated. Number of protons was identifying by 1H NMR

spectrum. Thermal study shows that material thermally stable up to 134°C and the compound starts to decompose at 216°C. The biological activities of BSA molecule have also been explored as a best potential inhibitor of *Bacillus cereus* bacteria. These findings may guide to design new triazole compounds with interesting biological activity.

ⁱ K. Mondal, U. K. Chatterjee and B. S. Murty, *Appl. Phys. Lett.*, 2003, **83**, 671–673.

ⁱⁱ A. Figini Albisetti, C. A. Biffi and A. Tuissi, *J. Alloys Compd.*, 2012, **544**, 42–45.

ⁱⁱⁱ K. Yamaguchi, Y. C. Song, T. Yoshida and K. Itagaki, *J. Alloys Compd.*, 2008, **452**, 73–79.

^{iv} A. Kumar, G. Kaur and A. Subramaniam, *Int. J. Mater. Res.*, 2013, **104**, 1171–1181.

PP-135

An unconventional spin-glass transition in ordered hexagonal DyMnO₃ single crystals

P. Aravinth Kumar,¹ G. Anandha Babu,^{*1} S. Ganesamoorthy² and P. Ramasamy¹

¹ Department of Physics, SSN College of Engineering, Kalavakkam 603110, India

² Materials Science Group, Indira Gandhi Centre for Atomic Research, Kalpakkam 603102, India

*E-mail: anandcgc@gmail.com,

The ferroelectric phase of the multiferroic hexagonal manganites (h-ReMnO₃) has been reported to undergo a series of magnetic transitions below room temperature involving long-range ordering/reorientation of 4fRe³⁺ and/or 3dMn³⁺ spins [1]. These transitions have attracted a lot of attention in recent years due to the geometrically frustrated nature of magnetic interactions [2]. We have revisited these transitions in high quality single crystals of h-DyMnO₃ using dc, ac susceptibility and magnetic relaxation measurements as a function of temperature (T), magnetic field (H) and frequency (ω). Taking h-DyMnO₃ as an example, we show that the Dy³⁺ spins below T_N~68K are in a superferrimagnetic (SFIM) state whereas they undergo spin-glass (SG) transition below T_{Dy³⁺}~7K. Our observations demonstrate that neither the Néel transition at T_N~68K nor the transition at T_{Dy³⁺}~7K is associated with long-range ordered states of Dy³⁺ spins as believed so far in the literature [3]. The SG state of h-DyMnO₃ is quite exotic as it occurs in an ordered compound purely due to geometrical frustration without any random disorder. It shows an interesting crossover from de Almeida-Thouless type exponent (m=2/3) to Gabay-Toulouse type (m=2) with increasing field [4-6]. Further, the time decay of the thermoremanent magnetization can be well described with the stretched exponential function

PP-136

Crystal and Electronic Structure Studies on Transparent Conducting Nitrides A_3N_2 ($A = \text{Mg, Zn and Sn}$) and Sn_3N_4

*T. Premkumar and R. Vidya**

Department of Medical Physics, Anna University, Sardar Patel Road, Chennai, India- 600025.

*E-mail: vidyar@annauniv.edu

Transparent conducting (TC) materials play an important role in the advancement of photovoltaic devices. Finding potential transparent conducting materials for photovoltaic applications is essential to reduce cost and enhance efficiency of such devices. Transparent conducting oxides (TCO) such as Indium Oxide, Indium doped Tin Oxide and Zinc Oxide are first generation TC materials because of their wide band gap and high electrical conductivity. Recently TC nitrides found to have good chemical stability and high refractive index over TCOs, which is advantage for high efficiency photovoltaic applications.

We have performed Density Functional Theory (DFT) calculations for novel nitrides of type A_3N_2 ($A = \text{Mg, Zn and Sn}$) and Sn_3N_4 to find the ground state crystal and electronic structure and bonding nature between the constituent atoms. The structural parameters optimized by our theoretical calculation are in good agreement with the experimental structural parameters [1, 2]. These optimized structural parameters are used for our further calculations. We have predicted a new synthetic route for Sn_3N_2 and Sn_3N_4 by treating Sn with ammonia. The studied nitrides exhibit semiconductor behavior with direct band gaps except Sn_3N_2 . Band gap of 1.7 eV is obtained for Mg_3N_2 from GGA calculation and band gaps of 0.24 eV and 0.7 eV are obtained for Sn_3N_4 using GGA and LDA calculations, respectively. On the other hand, GGA+ U was used to obtain the band gap in Zn_3N_2 and this elucidates the effect of strong correlation due to Zn $3d$ orbital. The bonding behavior is analyzed in detail by using charge density and electron localization function plots. In addition, Crystal Orbital Hamiltonian Population is utilized to retrieve bond strength values. Charge transfer from cation to anion decreases from Mg to Sn and correspondingly bond strength between the metal and Nitrogen atoms is also found to increase from Mg to Sn, which indicates increase in covalent nature of bonding from Mg to Sn. Zn_3N_2 is found to have the possibility for n -type as well as p -type doping because of the low effective mass of electrons and holes compared to other studied nitrides, which is very important for junction devices. Hence, Zn_3N_2 has suitable conductive properties and stability to be used as a photovoltaic material

PP-137

Numerical Investigation on Reduction of Thermal Stress and Dislocation Density in grown mc-Si Ingot for PV Applications

*S. Sanmugavel, P. Ramasamy**

Research Centre, SSN College of Engineering, Kalavakkam, Chennai – 603110

*E-mail: ramasamyp@ssn.edu.in

90% of the solar industries are using crystalline silicon. Cost wise the multi-crystalline silicon solar cells are better compared to mono crystalline silicon. But because of the presence of grain boundaries, dislocations and impurities, the efficiency of the multi-crystalline silicon solar cells is lower than that of mono crystalline silicon solar cells. By reducing the defect and dislocation we can achieve high conversion efficiency. The velocity of dislocation motion increases with stress. By annealing the grown ingot at proper temperature we can decrease the stress and dislocation. Our simulation results show that the value of stress and dislocation density is decreased by annealing the grown ingot at 1400K and the input parameters can be implemented in real system to grow a better mc-Si ingot for energy harvesting applications.

PP-138

Investigation of Growth and Characterization of Xylenol orange tetrasodium salt added KAP single crystal

G. Babu Rao, P. Rajesh and P. Ramasamy,*

Department of Physics, SSN College of Engineering, kallavakkam-603 110, Tamilnadu.

*Email: baburao87@gmail.com; rajeshp@ssn.edu.in

Dye inclusion crystals have attracted researchers in the context of crystal growth for applications in solid state lasers [1,2]. The effect of xylenol orange as dopant on the characteristic properties of KAP single crystal grown by conventional method was studied. From the powder XRD results show that the presence of dye has not altered the basic structure of KAP crystal. It is observed from the optical transmittance that the xylenol orange tetrasodium salt added KAP single crystal has slightly lower transmittance compared to pure KAP crystals. High intense luminescence at 610 nm is observed when excited with 440 nm for dye doped single crystals. From TG/DTA it is observed that, there is only one endothermic peak indicating decomposition point at 299 °C for dye doped KAP single crystals. The etch pit density of the pure and dye doped KAP single crystal is found as $2.33 \times 10^4 / \text{cm}^2$ and $0.95 \times 10^4 / \text{cm}^2$ respectively. The average laser

damage threshold obtained on the pure KAP was 4.3 Gw/cm^2 whereas a high damage threshold of 7.5 Gw/cm^2 was obtained from the dye doped KAP single crystal. From the mechanical study it is observed that dye doped KAP single crystal shows higher mechanical stability. The grown crystals of both pure and dye doped KAP single crystal are subjected to piezoelectric study. Higher d_{33} value observed for dye doped KAP may be due to the effective polar orientation of the ionic dye molecules in the KAP crystal lattice. Dye doped KAP single crystal shows high mechanical strength and good laser damage stability with low dislocation density which make it suitable for the device fabrication.

References:

- [1] B. Raju, A. Saritha, G. Bhagavannarayana, K.A. Hussain, J.Cryst. Growth 324 (2011)184.
- [2] I. Yu Velikhov, I. Pirutla, M. Ganina, V. Kolybayeva, A.N.L.Puzikov, Cryst. Res. Technol. 42 (2007) 27.

PP-139

Controlled Growth of 1D ZnO Nanorods on Flexible Substrate and their heterojunction properties

*Ganesh Kumar K, Arokiyadoss Rayerfrancis, Balaji C, Nafis A, Balaji Bhargav P**
Department of Physics, SSN College of Engineering, Kalavakkam -603110.

**E-mail: balajibhargavp@ssn.edu.in*

The synthesis of the well-aligned highly crystalline one dimensional ZnO nanorods on flexible substrates is demonstrated here. ZnO is a wide-bandgap semiconductor of the II-VI semiconductor group having large exciton binding energy at room temperature (60 meV). ZnO nanorods shown advantages in many applications such as electronics, sensors, piezoelectricity, etc. due to their large surface to volume ratio, high crystallinity and simple preparation methods. ZnO nanorods were grown with varying precursor solution concentration on seeded flexible stainless steel substrates by hydrothermal method. Nanorods were characterized for structural, morphological and optical properties. All the nanorods showed dominant orientation along the (002) direction, the intensity of the peak vary with the varying concentration of the precursor solution. FESEM images confirmed the vertically aligned structure of ZnO nanorods and the FTIR confirmed the formation of Zinc-oxygen bonding. Heterojunction studies are performed by coating p type organic polymer. Diode characteristics were analyzed by thermionic emission model.

Eurocon Instruments Pvt. Ltd.,

No.14, Murugan Nagar, Kundrathur road, Vazhuthalambedu,
Chennai - 600 044, Tamil Nadu, India. Phone: 044 2478 3019.

E-mail: euroconengg@gmail.com

Eurocon Offers a most comprehensive systems available in the market with complete support solutions depending on specific industry applications. Our Integrated approach helps us to evaluate clients current infrastructure and specifying the right mix of hardware and software required and training to meet project goals.

Our Esteemed Principles

Eurotherm.
by **Schneider Electric**



**MITSUBISHI
ELECTRIC**
FACTORY AUTOMATION

Honeywell
gas detection

LUMEL
EVERYTHING COUNTS

Our solutions



INDIGENOUSLY DEVELOPED CRYSTAL PULLER SYSTEM

SPECIFICATIONS

TRANSLATION UNIT

- Motor Torque: 5 Nm
- Pull length: 100 mm to 850 mm (Requirement Based)
- No Detectable Vibrations at Pull Speed
- Transportable Mass: 5 to 10 kg (Requirement Based)
- Electromagnetic Brakes: With & Without
- Drive system : Ball Screw
- Pull rate:



Normal Mode: 0.5 mm/day to 30mm/day & 0.1 mm/hr to 30mm/hr

Fast Forward Mode: Four speeds – 30 mm / 60mm / 90mm / 120mm per minute

Profile Mode: Used to read the Furnace profile

- The Speed is set using Keypad and Remote Handle for Easy Operation
- Fast Translation is mainly used for positioning the Seed Crystal inside the Furnace

ROTATIONAL UNIT

- Torque: 8 Nm
- Rotation Speed: 0.1 to 100 RPM (CW/CCW)
- ACRT Mode of Operation can be programmed with Saw Tooth, Triangular and Trapezoidal Wave Generation (Based on Customer Requirement)
- Settings is done using both Keypad and Manual Remote Handle
- Remote Handle has priority over the software

MEASUREMENT SYSTEM

'High Accuracy (0.01mm)' Smart Inductive System based Measuring Scale is fixed for the Movement Measurement

CONTROL CABINET

The Control Unit consists of Microcontroller and other electronic parts suitable for Communicating with the Driver & Display System. Settings are done using both Software and Manual Remote Handle. Translational & Rotation Motors are controlled using Modbus Control Driver Unit. A handheld Manual Remote Control for the Crystal Rotation/Translation Motor has been provided. Control Electronics, The Embedded Computing Mini Computer Model and Motor Driver are kept in the Control Cabinet.

FURNACE & TEMPERATURE CONTROL UNIT

- Construction: Outer Body - Mild Steel and Inner Body - Ceramic Muffle
- Chamber Size: Various Sizes as per the Customer Requirement
- Insulation: Special type of Ceramic Insulation
- Coil: Kanthal or Equivalent make coil for long lasting
- Temp Range: min - 400°C to max - 1500°C
- Accuracy: +/- .01 deg
- Temp Control: Eurotherm, PID Display to View & Set the Temperature
- Safety: A special type of Thermocouple that fuses to Protect Overheating
- Sensor: 'K' type Calibrated Sensor





Innovative Service Provider

DAS Instruments and solutions

No: 11, Block F2, Subham Shelters, Murugesan Nagar,
Okkiyam Thuraiyakkam, Chennai - 600097.

Email : dasinstruments@gmail.com

Phone: 8072441772

FOR HIGH QUALITY MEASURING INSTRUMENTS AND PROCESS CONTROLLERS

PROCESS CONTROL INSTRUMENTS WITH HIGH PRECISION/QUALITY/RELIABILITY

- **SINGLE LOOP, MULTI-LOOP PROGRAMMABLE PID TEMPERATURE CONTROLLERS.**
- **SINGLE PHASE/THREE PHASE THYRISTOR POWER REGULATORS FOR RESISTIVE AND TRANSFORMER LOADS**
- **ALL TYPES OF HIGH PRECISION THERMOCOUPLES, RTD AND OTHER SENSORS.**
- **ANALYTICAL INSTRUMENTS LIKE HPLC, UV-VIS SPECTROPHOTOMETER**
- **SAMPLE PREPARATION- GPC CLEANUP, EVAPORATOR, SOLID PHASE EXTRACTION.**
- **LABORATORY EQUIPMENTS-WATER CHILLER, REFRIGERATED/HEATING CIRCULATOR, HOTPLATE, ROTARY EVAPORATOR, VACUUM PUMP, VACUUM CONTROLLER, ETC.**
- **LABVIEW BASED CUSTIMAZATION PROJECTS ACCORDING TO CUSTOMERS APPLICATION.**
- **PLC BASED CUSTIMATATION PROJECT FOR AUTOMATION IN PROCESS CONTROL.**

PLUS MANY MORE.....

Eurotherm®

by **Schneider** Electric

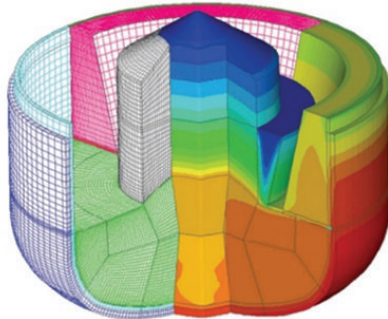




- ▶ Software licenses
- ▶ Simulation services
- ▶ Cooperation projects

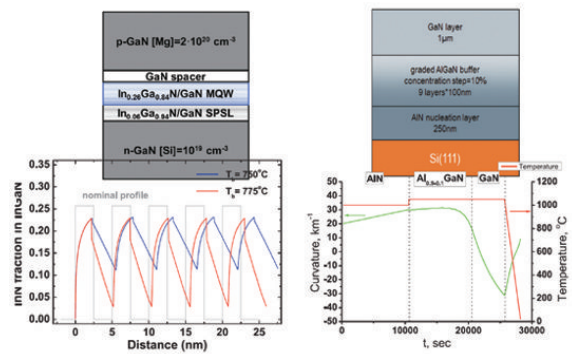
CGSim

Modeling of crystal growth from the melt and solution



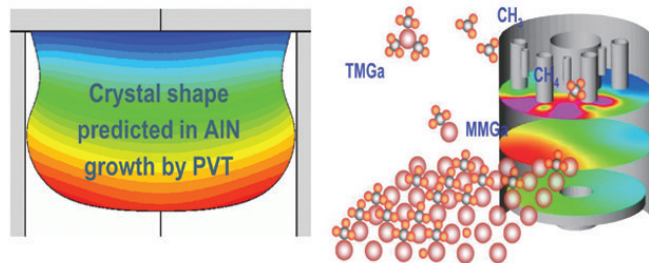
STREEM

Strain engineering in Electronic Materials



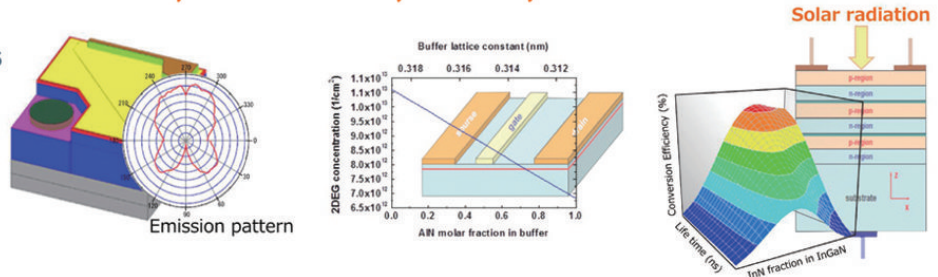
Virtual Reactor, CVDSim

- SiC and AlN growth by PVT
- InGaAlN, Arsenides, Phosphides, and Ga₂O₃ growth by MOCVD and HVPE
- SiC, ZnS, ZnSe, and Si growth by CVD



SimuLED, SimuLAMP, FETIS, PVcell

- LEDs, Laser Diodes
- HEMTs
- Solar cells
- Photodiodes



STR Group, Inc.

64 Bolshoi Sampsonievskii pr., Build. "E", Office 605, St. Petersburg, 194044, Russia
 Tel: +7-812-643-41-85 E-mail: str-info@str-soft.com
 www.str-soft.com